CHARACTERIZATION OF MUSASHI-2 IN HEMATOPOIETIC STEM CELLS

CHARACTERIZATION OF MUSASHI-2 IN HEMATOPOIETIC STEM CELL SELF-RENEWAL

By STEFAN RENTAS, M.Sc., B.Sc.

A Thesis Submitted to the School of Graduate Studies in Partial Fulfilment of the Requirements for Degree Doctor of Philosophy

McMaster University © Copyright by Stefan Rentas, July 2016

McMaster University DOCTOR OF PHILOSOPHY (2016) Hamilton, Ontario

(Biochemistry and Biomedical Sciences)

TITLE: The Characterization of Musashi-2 in Hematopoietic Stem Cell Self-Renewal

AUTHOR: Stefan Rentas, M.Sc., B.Sc. (McMaster University)

SUPERVISOR: Kristin Hope

NUMBER OF PAGES: xvii, 251

LAY ABSTRACT

The life-long production of new blood cells is enabled by blood stem and progenitor cells residing in the bone marrow. An understanding of the genes that control how stem and progenitor cells work to sustain the continued production of blood cells will enable new therapies to expand stem cells for life-saving transplantation purposes. The Musashi gene family has been implicated to control stem cell function in a variety of adult tissues (e.g. brain and gut) and emerging evidence using mice has defined Musashi-2 (Msi2) to be an essential regulator of blood stem and progenitor cells, yet no work to date has tested its function in the human system. Here I show that MSI2 is highly expressed in stem and progenitor cell populations of umbilical cord blood and that increased MSI2 protein levels greatly expands their number during culture as shown by their ability to engraft immunodeficient mice. I further found that MSI2 overexpression leads to significant downregulation of the aryl hydrocarbon signaling pathway, which has been shown when activated, promotes differentiation and loss of stem cells in culture. This work uncovered a new an import mechanism that controls stem cell expansion and could perhaps one day be leveraged for clinical use. For the second part of my thesis, I re-explored the role of Msi2 in the mouse hematopoietic system using a transgenic mouse that allows precise control over deleting this gene from the mouse genome. Using this technology I found the cells that were affected most by Msi2 deletion were early progenitor cells types. Altogether, my work provides novel insight in to the role of Musashi-2 in HSPC both human and mouse blood stem and progenitor cells.

ABSTRACT

The life-long production of blood cells is enabled by hematopoietic stem and progenitor cells (HSPC) residing in the bone marrow. An understanding of the genes that control how HSPCs work to sustain the continued production of blood cells will enable new therapies to expand them for life-saving transplantation therapies. The Musashi gene family of RNA binding proteins (RBP) has been implicated to control stem cell function in a variety of adult tissues (e.g. brain and gut) and emerging evidence in mice shows Musashi-2 (Msi2) to be an essential positive regulator of HSPCs, yet no work to date has tested its function in the human system. Here I show that MSI2 is highly expressed in cord blood (CB) HSPCs and that knockdown of MSI2 impairs HSC repopulation in xenotransplanted mice. Conversely, MSI2 overexpression yields multiple pro-self-renewal phenotypes, including 17-fold expansion of short-term repopulating cells as readout at an early post-transplant time point, and upon ex vivo culture, a net 23-fold expansion of long-term hematopoietic stem cells (LT-HSC). I further found that MSI2 overexpression post-transcriptionally downregulates the aryl hydrocarbon signalling pathway, which has been shown when repressed by a small molecule antagonist, greatly supports the expansion of human HSCs. Altogether, this work highlights RBPs and post-transcriptional control to have an integral role in controlling human HSC self-renewal. For the second part of my thesis, I re-explored the role of Msi2 in the mouse hematopoietic system using a newly generated tamoxifen inducible Msi2 knockout mouse. Using this approach I found Msi2 deletion significantly restricted repopulation in competitively transplanted mice and that this effect was due to depletion of early types of multipotent progenitors and not due to a loss of LT-HSCs. As there is currently a discrepancy as to which cells Msi2 precisely regulates in the mouse hematopoietic system, my work provides support that MPPs are the most affected cell type. Altogether, my thesis provides novel insight in to the role and mechanism of action of Musashi-2 in both human and mouse HSPCs.

ACKNOWLEDGEMENTS

I've had the pleasure to work in Kristin's lab from the beginning. In my first year I learned how to culture and transduce cord blood HSCs which soon led to the lab's first *in vivo* experiments. When it was time to analyze these transplanted mice, Kristin stayed late to see the results. We sat in the old, dimly lit flow room anxiously waiting to see results as tubes were put into the flow cytometer. Luckily, we soon found out the experiment worked! A couple years, a couple hundred mice, and a few dozen cord bloods later, we published the lab's first research paper, with many more on the way. As my time winds down in the Hope lab and change on the way (for me at least), I would be remiss to not start my thank you list with my terrific supervisor, Kristin! She's been such a great person to work with and I must thank her effusively for giving me the opportunity to be here from the beginning and have trust in me to not completely screw things up! There's been an incredible amount of support, positivity, and freedom to let me carry out ideas and experiments (some good, some not so much). You've helped me hone the art of writing, taught me the workings of stem cell/leukemia research, and most importantly, gave me an opportunity to be successful and trained me to be an independent researcher. So thanks for being such an awesome supervisor!

I am also deeply indebted to Muluken who helped on so many experiments (life lessons too) and as well a big thanks to Nick who worked earnestly on developing CLIP-seq for the lab, those efforts gave my work the boost it needed to get in to a good journal. I also need to thank our collaborators and in particular Veronique for carrying out all our requests for the RNA-seq analysis. Thanks as well to all the other graduate students (Laura, Michelle and Derek) and undergrads (Nensi, Ana and Jess) that have helped me along the way. I would like to thank my committee members Dr. Bhatia and Dr. Truant who have supported my efforts over the years and provided insightful feedback on my research. I'd also like to mention the many past and present institute members who I've become close friends with over the years and who made my time at Mac a lot of fun! Special mention goes out to Ryan, Allison, Lili, and Rami – a lot of good times were spent in and outside the lab together! Lastly I'd just like to acknowledge the unwavering support of my parents and family – despite my general absence and persistence to delay adulthood with graduate school, I know they're proud of what I've accomplished.

TABLE OF CONTENTS

Descriptive Note.....ii

Lay Abstract.....iii

Abstract.....iv

Acknowledgements.....vi

Table of Contents.....vii

List of Figures and Tables.....xi

List of Abbreviations and Symbols.....xiv

Declaration of Academic Achievement.....xvii

Chapter 1: Introduction.....1

- **1.0 Preamble**.....1
- **1.1 The discovery of hematopoietic stem cells**.....1
- **1.2 Characterization of primitive cells in the hematopoietic hierarchy**.....4
  - *1.2.1 New methods allow for prospective isolation of HSCs*.....4
  - *1.2.2 Common in vivo and in vitro assays to measure HSPC activity*.....6
- **1.3 HSC quiescence and homeostasis in hematopoiesis**.....8
  - *1.3.1 Novel molecular and genetic tools pave the way for modern HSC research*.....8
  - *1.3.2 Maintaining HSC quiescence through intrinsic and extrinsic control mechanisms*.....8
  - *1.3.3 Exiting quiescence, DNA damage and aging*.....10
  - *1.3.4 Contribution of LT-HSCs to steady-state hematopoiesis*.....11

1.3.5 HSC quiescence protects from oncogenesis...13

1.4 New models of lineage specification in the hematopoietic system...................14

1.5 Properties of HSC division and self-renewal..16

1.5.1 Asymmetric cell division...16

1.5.2 Cell division in HSPCs...17

1.6 Xenograft models and human HSCs...19

1.6.1 In vitro assays to model human hematopoieis...19

1.6.2 in vivo modeling of human hematopoiesis...20

1.6.3 The human hematopoietic hierarchy...21

1.6.4 A revised model of human lineage specification..24

1.6.5 Human HSC contribution to steady-state hematopoiesis.............................25

1.7 Expanding human HSCs for regenerative therapy...26

1.7.1 Using umbilical cord blood as a source of human HSCs for transplantation therapy...26

1.7.2 Factors that influence patient survival post-HSC transplantation..............28

1.7.3 Gene therapy, small molecules, and new culture methods lead the way...29

1.8 The role of Musashi-2 in murine hematopoiesis..31

1.8.1 The identification of Msi2 in mouse HSCs...31

1.8.2 Msi2 in mouse models of leukemia..33

1.8.3 Post transcriptional regulation by Musashi family RBPs............................34

1.8.4 Msi2 mechanism of actions in normal and malignant hematopoiesis..........35

Summary of Intent..37

Chapter 2..50

Musashi-2 Attenuates AHR Signaling to Expand Human Hematopoietic Stem Cells..50

Preamble...50

Abstract...52

Main..53

References...61

Methods...63

Chapter3..115

Post-transcriptional control by RNA binding proteins in hematopoietic stem cells...115

Preamble..115

Abstract..117

Introduction..118

Overview of RBPs and their control of translation...............................119

Distinct expression profiles of RBPs in normal human HSPCs...........121

RBPs regulating mRNA in HSCs...123

New methodologies to identify RBPs and their targets.........................127

Materials and Methods...130

References..130

Chapter 4..146

Musashi-2 maintains early hematopoietic multipotent progenitor cells.............146

Preamble..146

Abstract...148

Introduction..149

Results...151

Conditional deletion of Msi2 impairs competitive repopulation........................151

Msi2Δ/Δ in competitively transplanted mice have reduced numbers of MPPs..154

Conditional deletion of Msi2 in non-competitively transplanted mice reduces bone marrow cellularity and depletes early MPPs...156

Msi2 co-localization with RBPs and centers of RNA metabolism in HSPCs.......157

Discussion..161

Methods...165

References..169

Chapter 5: Discussion..188

5.0 Thesis overview..188

5.1 Intersection of AHR, MSI2 and HSC self-renewal...................................191

5.2 MSI2 OE to novel CB HSC expansion protocols......................................195

5.3 Msi2 regulation of MPPs mice...201

5.4 Post-transcriptional control in mouse HSPCs.......................................206

5.4 Concluding remarks...212

Bibliography..217

LISTS OF FIGURES AND TABLES

Chapter 1

Figure 1. Classic and revised mouse hematopoietic hierarchy..................................42

Figure 2. Transplantation kinetics of mouse HSPCS..44

Figure 3. Classic and revised human hematopoietic hierarchy..................................46

Figure 4. Musashi RNA binding mechanisms..48

Chapter 2

Figure 1. MSI2 OE enhances *in vitro* CB progenitor activity and increases numbers of STRCs...86

Figure 2. MSI2 OE expands LT-HSCs with ex vivo culture.....................................88

Figure 3. MSI2 OE in human HSPCs attenuates AHR signaling...............................90

Figure 4. MSI2 OE post-transcriptionally downregulates AHR pathway components...92

Extended Data Figure 1. MSI2 is highly expressed in human hematopoietic stem and progenitor cell populations..94

Extended Data Figure 2. MSI2 OE enhances *in vitro* culture of primitive CB cells...96

Extended Data Figure 3. MSI2 OE does not affect STRC lineage output and extends STRC-mediated engraftment...98

Extended Data Figure 4. MSI2 KD impairs secondary CFU replating potential and HSC engraftment capacity..100

Extended Data Figure 5. MSI2 OE confers an HSC gene expression signature......102

Extended Data Figure 6. MSI2 OE enhances HSC activity after ex vivo culture....104

Extended Data Figure 7. Predicted AHR targets and genes downregulated with SR1 and MSI2 OE are upregulated with MSI2 KD..106

Extended Data Figure 8. AHR antagonism with SR1 has redundant effects with MSI2 OE, and AHR activation with MSI2 OE results in a loss of HSPCs...............108

Extended Data Figure 9. MSI2 preferentially binds mature mRNA within the 3'UTR..110

Extended Data Figure 10. MSI2 OE represses CYP1B1 and HSP90 3'UTR Renilla Luciferase reporter activity..113

Chapter 3

Figure 1. A general model of post-transcriptional control by RBPs..........................140

Figure 2. Differential expression of RBPs across human HSPCs.............................142

Table 1. Top 30 RBPs in human HSPCs (Log2 expression)....................................144

Table 2. RBPs mediating HSC activity and leukemogenesis....................................145

Chapter 4

Figure 1. Conditional deletion of Msi2 significantly restricts HSPC reconstitution..174

Figure 2. Msi2 deletion promotes myeloid lineage bias and restricts lymphoid development...176

Figure 3. Msi2 deletion depletes MPPs in competitively transplanted mice............178

Figure 4. Conditional deletion of Msi2 in non-competitvely transplanted mice reduces bone marrow cellularity and depletes early MPPs..180

Figure 5. Msi2 has nuclear and cytoplasmic localization in HSPCs and does not strongly localize to mRNA decapping machinery..182

Figure 6. Tia1 is highly colocalized with Msi2 in HSPCs..184

Figure 7. Msi2 and HuR are differentially colocalized in subsets of HSPCs............186

Chapter 5

Figure 1. Summary of hematopoietic phenotypes between mouse and human with MSI2 OE and AHR deletion or inhibition with SR1...213

Figure 2. Transcript pathway analysis in CB HSPCs with MSI2 OE and KD...........215

LIST OF ABBREVIATIONS AND SYMBOLS

Acute myeloid leukemia	AML
Aryl hydrocarbon receptor	AHR
Bone marrow	BM
Blast crisis	BC
Blast-forming unit erythroid	BFU-E
Bromodeoxyuridine	BrdU
Cluster of differentiation	CD
Colony forming unit	CFU
Committed progenitor	CP
Common myeloid progenitor	CMP
Common lymphoid progenitor	CLP
Competitive repopulating unit	CRU
Cord Blood	CB
Cross-linking immunoprecipitation	CLIP-seq
Chromic myeloid leukemia	CML
Cytochrome P450 1B1 oxidase	CYP1B1
Day	D
Dimethyl sulfoxide	DMSO
Early T-cell precursor	ETP
Enhancer of mRNA decapping 3	Edc3
Erythroid progenitor	EP
Eukaryotic initiation factor	EIF
6-Formylindolo(3,2-b)carbazole	FICZ
FMS-like tyrosine kinase 3 ligand	FLT3-L
Fluorescence activated cell sorting	FACS
Granulocyte colony	CFU-G
Granulocyte-Erythroid-Macrophage-Megakaryocyte colony	GEMM-CFU

Granulocyte-Macrophage colony	CFU-GM
Granulocyte monocyte progenitor	GMP
Green fluorescent protein	GFP
Hematopoietic stem cell	HSC
Hematopoietic stem cell transplant	HCT
Hematopoietic stem progenitor cell	HSPC
High-throughput sequencing crosslinking immunoprecipitation	HITS-CLIP
Heat shock protein 90	HSP90
Human antigen R	HuR
Human leukocyte antigen	HLA
Interleukin	IL
Intermediate-term hematopoietic stem cell	IT-HSC
Knockdown	KD
Knockout	KO
Leukemic stem cell	LSC
Lineage$^-$ c-Kit$^+$ Sca-1$^+$	LSK
Limiting dilution assay	LDA
Long non-coding RNA	lncRNA
Long-term hematopoietic stem cell	LT-HSC
Long-term culture initiating cell	LTC-IC
Lymphoid primed multipotent progenitor	LMPP
Macrophage colony	CFU-M
Megakaryocyte erythrocyte progenitor	MEP
Messenger RNA	mRNA
microRNA	miRNA
Mononuclear cell	MNC
Multipotent progenitor	MPP
Multilymphoid progenitor	MLP
Musashi-2	MSI2

Myeloid dysplastic syndrome	MDS
Nuclear localization signal	NLS
Non-obese diabetic severe combined immune deficiency	NOD-Scid
Overexpression	OE
Poly-A binding protein	PABP
Precursor miRNA	pre-miRNA
Primary miRNA	pri-miRNA
Prostaglandin E2	PGE2
Reads Per Kilobase of transcript per Million mapped reads	RPKM
RNA binding protein	RBP
RNA immunoprecipitation polymerase chain reaction	RIP-PCR
RNA interference	RNAi
RNA-sequencing	RNA-seq
Short-term hematopoietic stem cell	ST-HSC
Short-term repopulating cell	STRC
Spleen colony forming unit	CFU-S
Stem cell antigen 1	Sca-1
Stem cell factor	SCF
Stem Regenin-1	SR1
(E)-2,3’,4,5’-Tetramethoxystilbene	TMS
T cell antigen 1	Tia1
Thrombopoietin	TPO
Transplant	Tx
Transforming growth factor-β	TGF-β
Total nucleated cells	TNC

DECLARATION OF ACADEMIC ACHIEVEMENT

I contributed to the design and execution of the research presented herein, as well as performed data analysis and writing of all sections of this thesis. Dr. Kristin Hope directed research projects, and aided in the analysis of data and editing of this thesis. Muluken Belew and Nicholas Holzapfel from the Hope lab performed experiments and contributed data; additional specific contributions by other lab members are noted in the manuscripts. Collaborators Veronique Voisin, Gary Bader, Brian Wilhelm, Gabriel Pratt and Gene Yeo helped perform bioinformatic analyses and specific contributions are also acknowledged in the manuscripts.

CHAPTER 1: INTRODUCTION

1.0 Preamble

This thesis presents research on novel molecular and genetic regulation of self-renewal in human and mouse hematopoietic stem cells (HSCs). The origin of this work stems from Hope et al. and the discovery of Musashi-2 (Msi2) as a novel regulator of mouse HSC self-renewal (Hope et al., 2010). The goal of this introductory chapter is to delve into the history of HSCs and to fast-forward to the latest developments in this field. In this thesis the term SCID repopulating cells (SRC) is used synonymously with HSC, despite the true readout of a human HSC is through transplantation in humans and not mice. Since research that comprises this thesis was performed using both mouse and human HSCs, this introduction will provide background on the basic biology of HSCs in both systems as well as provide clinical transplantation focus when discussing human HSCs. The chapter closes with the description of Msi2 in the mouse hematopoietic system, its varied biochemical activities and how it remains, until now, to be studied in humans.

1.1 The discovery of hematopoietic stem cells

Hematopoietic stem cells ultimately sustain the production of trillions of blood cells during a mammal's lifespan. These cells have the capacity to self-renew, a cell division that yields another HSC, or divide into increasingly lineage-restricted myeloid, erythroid and lymphoid intermediates which undergo massive proliferation and sequential differentiation to produce mature blood cells (Orkin and Zon, 2008; Seita and Weissman,

2010) (Figure 1A). The hierarchal organization of the hematopoietic system was postulated at least as early as 1909 by Russian histologist Alexander A. Maximow (Ramalho-Santos and Willenbring, 2007), and by the 1950s scientists were unknowingly using the properties of hematopoietic stem and progenitor cells (HSPCs) in their effort to treat bone marrow failure after radiation exposure (Jacobson et al., 1951; Lorenz et al., 1952). These early experiments demonstrated the efficacy of injecting irradiated mice with isogenic bone marrow and that survival was due to the proliferation of donor cells (Ford et al., 1956). While these experiments showed the hematopoietic system could be recovered through transplantation, they did not test whether the multiple hematopoietic lineages that arose occurred independently of each other or if all mature cells descended from a multipotent “ancestral” stem cell. This unresolved question set the stage for the groundbreaking research of James Till and Ernest McCulloch in the 1960s. Their initial work set out to quantify the number of transplanted cells necessary to provide radioresistance in mice (McCulloch and Till, 1960). These experiments quickly led to follow up studies where they found that transplanted bone marrow led to the formation of macroscopic hematopoietic colonies on the recipient mouse’s spleen (Till and McCulloch, 1961). Importantly, these spleen colony forming units (CFU-S) scaled in frequency with the number of bone marrow cells transplanted, and were multilineage, containing granulocytes, erythrocytes and megakaryocytes. Having developed an assay to readout donor cell engraftment, they next wanted to discern if these colonies originated from a single cell or from an aggregate of many transplanted cells. This important distinction was accomplished by providing a dose of ionizing radiation to donor cells which yielded gross chromosomal aberrations detectable by cytogenetic analysis. This showed many CFU-S were genetically distinct and homogeneous in their genetic marking, proving that the multilineage colonies were indeed clonal and thus derived from single cells (Becker et al., 1963). One of their last important findings of this period was to show that CFU-S, of which most were histologically composed of differentiated cells, had the capacity to remake new spleen colonies when transplanted in to secondary mice but that the frequency of cells capable of remaking these new CFU-S was variable, or "stochastic" in nature (Siminovitch et al., 1964; Till et al., 1963). This collection of work, all published in less than 5 years, provided the foundation for the proof of the existence of HSCs, operationally defined the requirements of a stem cell (multipotent and self-renewing) and invented the assays that would serve as a template for future work in the hematopoietic field (e.g. demonstration of self-renewal through serial transplantations). A note on this last point is that while not all of their methods have stood the test of time, for example better techniques for genetically marking HSCs was developed in the 1980s (Dick et al., 1985) and CFU-S were shown to unlikely be the product of HSCs (Spangrude et al., 1988), other aspects of their methods and analysis have remarkably held true. This includes Till and McCullochs' work examining the number of hematopoietic cells that offered mice survival post irradiation and formed CFU-S (McCulloch and Till, 1960; Till and McCulloch, 1961) as well as their work on quantifying the numbers of spleen cells that are capable of creating an immune response (Kennedy et al., 1966), formed the foundation of modern approaches to quantify stem cell frequency by limiting dilution assay (LDA) and Poisson statistics (Hu and Smyth, 2009;

Lefkovits and Waldmann, 1984; Spangrude et al., 1988; Szilvassy et al., 1990; Taswell, 1981). Altogether, it cannot be understated the lasting contribution Till and McCulloch had as among the earliest pioneers in stem cell research, their work not only provided the theoretical framework to study HSCs, but galvanized the prospect that development and maintenance of other post-natal tissues across multiple organs could proceed through a hierarchical stem cell model. Lastly, their work informed the development of the cancer stem cell model that arose during the 1990s, which predicts cancer is driven by identifiable malignant stem cells that guide a highly proliferative and abnormal caricature of their healthy tissue counterpart (Dick, 2008).

1.2 Characterization of primitive cells in the hematopoietic hierarchy

1.2.1 New methods allow for prospective isolation of HSCs

At the time Till and McCulloch discovered and defined the properties of stem cells, their assays, much like as they do today, depended on observing the outcome of HSC proliferation and differentiation after transplantation. They found early on that the CFU-S they studied were heterogeneous in the composition of cells that could re-make new colonies, since some contained cells that self-renewed and could propagate secondary colonies while others did not. This led to another profoundly insightful study by Till and McCulloch where they tested if the lack of self-renewal observed in some CFU-S was perhaps due to stem cells not all being equal in their intrinsic capacity for self-renewal. This was in comparison to the alternative hypothesis that all stem cells are intrinsically the same but randomly undergoing terminal differentiation and exhaustion during colony growth (Worton et al., 1969). A study by Worton et al. provided the first demonstration of the prospective isolation of different classes of early stem and progenitor cells, where they achieved by rudimentary density centrifugation methods, the isolation of distinct fractions of cells that upon transplantation gave rise to CFU-S with varying degrees of self-renewal. Over the next ten years two important techniques were developed that revolutionized the study of HSCs and the search to purify them from the milieu of cells in the bone marrow: fluorescently labeled monoclonal antibodies against cell surface antigens of immune cells (Kohler and Milstein, 1975) and the development of multi-parametric flow cytometry to analyze expression of surface markers on single cells (Hulett et al., 1969). Irving Weissman spearheaded this movement during the 1980s by combining these two powerful techniques. His group employed a method of negative selection which used newly discovered antibodies against B cells (B220), T cells (CD4 and CD8), macrophages (Mac-1) and granulocytes (Gr-1) to remove mature immune cells and enrich for primitive hematopoietic cells. The cells remaining were termed lineage negative (Lin^-). The second important breakthrough the Weissman group made was combining the negative selection protocol with a newly discovered antibody, E13 161-7, which enriched for progenitors of thymic lymphocytes (Aihara et al., 1986). They renamed this antibody stem cell antigen 1 (Sca-1) and performed the first isolation of highly purified mouse HSCs with the marker combination of Lin^- Sca^+ $Thy\text{-}1^{lo}$ (Spangrude et al., 1988). This kick-started nearly three decades worth of research across many laboratories to purify HSCs to near homogeneity through the iterative process of FACS purification and transplantation (Benveniste et al., 2010; Christensen and

Weissman, 2001; Kiel et al., 2005; Ogawa et al., 1991; Osawa et al., 1996; Yang et al., 2005). Figure 1A shows the classic model of the hematopoietic hierarchy including the surface marker phenotypes used to isolate each class of stem and progenitor cell. The most primitive cell in the mouse hematopoietic system that can be measured is now called a long-term HSC (LT-HSC), and expresses c-Kit, Sca-1, CD150, and is negative for lineage markers, CD34, CD48, Flt3, and CD41. Delineating classes of HSCs was an inevitable result upon comparing engraftment capabilities of different FACS purified populations. Thus LT-HSCs are defined by their ability to repopulate for at least 16 weeks after transplantation in primary mice and for their capacity for robust multilineage cell repopulation in secondary mice (Figure 1 B). LT-HSCs are thought to differentiate to short-term HSCs (ST-HSCs), which eventually give rise to multipotent progenitors (MPPs) and then lineage restricted committed progenitors (Seita and Weissman, 2010). Both ST-HSCs (Lin$^-$ c-Kit$^+$ Sca1$^+$ CD150$^+$ Flt3$^+$ CD34$^-$ CD41$^-$) and MPPs (Lin$^-$ c-Kit+ Sca1$^+$ CD34$^+$ Flt3$^+$ CD150$^-$) are capable of producing mature blood cells upon transplantation, but detection of mature cells in the peripheral blood and bone marrow from ST-HSCs declines after 12 weeks and from MPPs is less than 6 weeks (Figure 2). Therefore, self-renewal is now widely understood as a continuum in the capacity of isolated HSC populations to engraft and reconstitute blood cell lineages over varying periods of time.

1.2.2 Common in vivo and in vitro assays to measure HSPC activity

In order to quantify the number of actual functional LT-HSCs in a given population, LDA and competitive repopulating unit (CRU) assays were developed (Szilvassy et al., 1990).

These assays use lethally irradiated mice that are transplanted with limiting numbers of the target HSC population along with helper cells to facilitate early engraftment and hematopoiesis. 16–20 weeks post transplant, the chimera mouse is typically analyzed per target HSC dose for >1% repopulation and Poisson statistics is used to estimate the number of HSCs present in the original transplant. An important component of any transplant assay is ensuring the engrafted cells can be discerned from the recipient's cells. This is most often accomplished by retroviral or lentiviral introduction of a fluoresecent reporter protein into donor cells or by using donor congenic mouse strains that express different alleles for the pan leukocyte antigen CD45 (CD45.1 or CD45.2) than the recipient strain. Measurement of donor cells in the peripheral blood, spleen and bone marrow of recipient mice have for the most part replaced the CFU-S assay which only reads out the activity of progenitors.

Beyond the self-renewing HSC and MPP populations there is separation into the megakaryocyte, erythroid, myeloid and lymphoid branches of the hierarchy via progenitor populations that are committed to each of these lineages (Figure 1 A). *In vitro* colony forming unit (CFU) assays are widely used to assess frequency and function of committed myeloid and erythroid progenitor cells, including the most primitive colony type of granulocyte-erythrocyte-monocyte-megakaryocyte (CFU-GEMM), granulocyte-monocyte (CFU-GM), blast-forming erythroid (BFU-E), granulocyte (CFU-G), and monocyte (CFU-M). Throughout the 1980s and early 1990s extensive work was carried out to optimize the culture conditions for the hematopoietic CFU assay, such that today, the semi-solid methycellulose and cytokine components of the medium that is routinely used supports growth of all myelo-erythroid colony types (Humphries et al., 1979; Lemieux et al., 1995; Mayani et al., 1993).

1.3 HSC quiescence and homeostasis in hematopoiesis

1.3.1 Novel molecular and genetic tools pave the way for modern HSC research

During the 1990s, powerful molecular and genetic tools were developed allowing researchers to dissect how HSCs regulate the hematopoietic system. These advances include improvements in HSC purification protocols (Osawa et al., 1996), the development of genetically engineered mice (Capecchi, 1989), and evolution in retroviral and lentiviral gene therapies to overexpress and knockdown genes of interest directly in HSCs (Mulligan, 1993; Naldini et al., 1996; Root et al., 2006). In the years since those developments, various candidate gene and forward and reverse genetic screening approaches have shown that hundreds of genes, including protein coding (e.g. transcription factors) (Wilkinson and Gottgens, 2013), micoRNA (miRNA) and long non-coding RNA (lncRNA) (Jeong and Goodell, 2016) act to regulate HSC function. The nuanced complexity regulating quiescence and cell fate decisions in HSPCs is continuing to expand during the current “omics” era, since large scale next-generation sequencing and mass-cytometry methods have started to profile the transcriptome, meythlome and proteome status across all populations in the hematopoietic hierarchy at single cell level, for an unprecedented view of the molecular circuitry that defines each cell type (Cabezas-Wallscheid et al., 2014; Heng and Painter, 2008; Kowalczyk et al., 2015; Novershtern et al., 2011; Spitzer et al., 2015).

1.3.2 Maintaining HSC quiescence through intrinsic and extrinsic control mechanisms

So, what have we learned from over twenty years of studies about the biology of HSCs and the genetic mechanisms that control them? To start, HSCs are categorically defined by their general quiescence (Cheshier et al., 1999; Morrison and Weissman, 1994; Passegue et al., 2005; Wilson et al., 2008), which is maintained via intrinsic mechanisms such as inhibition of cell cycle progression through expression of p21 (Cheng et al., 2000), tumor suppressor genes like Pten (Yilmaz et al., 2006; Zhang et al., 2006a) and transcriptional repressors such as Gfi1 (Hock et al., 2004). Cell extrinsic mechanisms via ligand-receptor interactions with the bone marrow microenvironment, including mainly mesenchymal stem/stromal cells, megakaryocytes, and perivascular stromal cells, play an equally prominent role in maintaining HSC localization and quiescence (Boulais and Frenette, 2015; Morrison and Scadden, 2014). For example, signaling from Scf/c-Kit (Ding et al., 2012), Angiopoietin (Sacchetti et al., 2007), Thrombopoietin/MPL (Yoshihara et al., 2007), Leptin-receptor (Oguro et al., 2013; Zhou et al., 2014) and CXCR4/CXCL12 (Ding and Morrison, 2013; Greenbaum et al., 2013) have all been shown as vital HSC-bone marrow microenvironment interactions that control HSC G0 exit. While the original location of HSCs in bone marrow was found to be near the hypoxic interface with bone, regarded as the endoesteal niche (Calvi et al., 2003; Lo Celso et al., 2008), more recent studies by Sean Morrison’s group suggest HSCs prefer perivascular areas by sinusoids (Morrison and Scadden, 2014). They found that most LT-HSCs reside near perivascular structures through use of elegant conditional knockout mouse models that delete niche signaling molecules from specific cell types in the bone marrow (Ding and Morrison, 2013; Ding et al., 2012). Furthermore, they have recently corroborated these findings with deep imaging techniques (Dodt et al., 2007) and a novel GFP reporter of HSC activity (Acar et al., 2015). Perivascular localization of LT-HSCs has also been found by others by using a Hoxb5-GFP-reporter system to uniquely tag HSCs in the bone marrow (Chen et al., 2016). Altogether, these studies show that managing HSC quiescence occurs through multiple independent intrinsic and extrinsic control mechanisms.

1.3.3 Exiting quiescence, DNA damage and aging

Theories to the prevailing quiescence of HSCs has centered on the perceived cellular and genomic protection acquired from a largely non-replicative cell state. For instance, the dormant nature of HSCs (Foudi et al., 2009; Wilson et al., 2008) in a hypoxic perivascular niche (Acar et al., 2015; Parmar et al., 2007; Spencer et al., 2014) ensures energy metabolism occurs via anaerobic glycolysis which results in low ATP levels (Kohli and Passegue, 2014), attenuated protein synthesis and proteoxic stress (Buszczak et al., 2014; van Galen et al., 2014a), and a capacity to maintain low levels of potentially damaging reactive oxygen species (Ito et al., 2006; Takubo et al., 2010). Disrupting any of these processes in quiescent HSCs typically induces cycling, differentiation and decreased self-renewal potential (Buszczak et al., 2014; Kohli and Passegue, 2014). Perhaps unsurprisingly, aging eventually catches up to the cyto- and genoprotective measures quiescent HSCs undertake. For example, aged HSCs inevitably accumulate, yet tolerate, DNA damage (Rossi et al., 2007). Important work from the Milsom lab and others have gone on to show that young LT-HSCs, upon repeated exiting of quiescence with an immune stimulation, acquire DNA damage that is exacerbated with deletion of a Fanconi anemia related gene (involved in DNA repair pathway activity) resulting in hematopoietic failure in mice, thus recapitulating the disease seen in humans (Walter et al., 2015; Zhang et al., 2016). Therefore, repeated stressors that induce HSCs to exit G0, particularly over the course of many years, may explain why old HSCs accrue DNA damage (Beerman et al., 2014; Rossi et al., 2007). The source of this damage (if not from genotoxic agents or radiation) likely falls on deficiencies in the replication machinery which causes replication stress and DNA damage upon G0 exit (Flach et al., 2014). Interestingly, in the event of ionizing radiation, DNA damage is better managed in more proliferative progenitor subsets since they either undergo DNA repair via homologous recombination or programmed cell death, which compared to HSCs, are poised to survive damage and use more error-prone methods of DNA repair (Mohrin et al., 2010). While human hematopoiesis will be discussed in greater detail in following sections, human HSCs tend to respond differently to ionizing radiation such that they preferentially undergo apoptosis instead of attempting error-prone repair pathways (Milyavsky et al., 2010).

1.3.4 Contribution of LT-HSCs to steady-state hematopoiesis

A quiescent status also ensures an adequate supply of functioning HSCs (i.e. not undergone replicative/differentiative exhaustion) to replenish the progenitor pool over the course of an animal's lifespan. Evidence of this in humans comes from diseases like acquired aplastic anemia and Fanconi anemia, as both show loss of phenotypic HSCs coinciding with reduction of cells across all hematopoietic lineages, leading eventually to bone marrow failure (Brosh et al., 2016; Young, 2006). In these examples however, there is an obvious defect (genetic mutation or impaired immune system) and "stress" placed on HSCs leading to disease. So what role do normal LT-HSCs have during steady-state hematopoeisis? Do they actually replenish the progenitor pool over the course of an animal's life? What if there are no grave stresses as is the case for the life of a wild type, pathogen free laboratory mouse? These questions remain a contentious topic as several lines of evidence suggest that LT-HSCs do not in fact contribute very much to steady-state hematopoiesis, but instead are only activated during stress (e.g. immune activation and blood loss) (Trumpp et al., 2010). In support of HSCs not likely contributing to homeostatic hematopoietic processes, early BrdU pulse-chase label retaining cell experiments in mice showed LT-HSCs appear to divide only once every ~70 days (Cheshier et al., 1999; Kiel et al., 2007). Furthermore there is a sub-group of LT-HSCs that divide only up to 5 times in a mouse's lifetime (Wilson et al., 2008). These studies hint that LT-HSC contribution to daily hematopoiesis is likely minimal. Two important studies further support their limited role to maintain hematopoiesis during adulthood (Busch et al., 2015; Sun et al., 2014). These studies demonstrated through different lineage tracing experimental designs, that during homeostatic maintenance of hematopoiesis, MPPs and committed progenitors, typically understood to be non-self-renewing, persist for long periods of time and are responsible for the bulk of blood cell production. In the study by Busch et al. the investigators found after labeling HSCs with YFP, that there was a moderate percentage (30%) of predicted LT-HSCs contributing to the production of mature cells, however, the actual total output of cells from these LT-

HSCs across lineages was exceedingly small at <1%, a value that did not change over any period of time measured. Similarly in the study by Sun et al., fewer than 5% of LT-HSC clones were found in mature cell populations nearly one year after inducing genetic tagging (a laboratory mouse's lifespan is typically 2 years), whereas half of the MPP and myeloid progenitor clones contributed mature hematopoietic cells. Additionally Sun et al. found that 4 months after genetically marking cells (a time point they predicted should allow activation of HSCs) large and diverse changes were observed in the clonal contribution of hematopoietic populations, providing evidence that steady-state hematopoiesis is maintained by successive recruitment and proliferation (or waves) of many progenitors that are longer-lived than previously thought. Thus, the best evidence to date suggests that only during hematopoietic stress do HSCs provide meaningful support to re-establish equilibrium in hematopoiesis (Busch et al., 2015; Walter et al., 2015; Wilson et al., 2008; Zhang et al., 2016), as well as other highly proliferative events like aiding the initial development and establishment of the growing hematopoietic system during post-natal growth (Busch et al., 2015). This latter point is also in line with Fanconi anemia patients suffering bone marrow failure at a median age of 6 years old as fetal and post-natal HSCs proliferate more frequently earlier in life when growth is rapid but due to DNA repair defects these cells are eventually lost (Brosh et al., 2016).

1.3.5 HSC quiescence protects from oncogenesis

Given the proliferative potential of HSCs, their quiescence can also be seen as a means of protection from cancer initiation. This has been precisely demonstrated with loss of Pten in mouse HSCs, whereby not only is there depletion of normal stem cells through unchecked cycling and differentiation but the co-development of leukemia (Yilmaz et al., 2006). Interestingly, it was shown that loss of HSCs in Pten null mice is in part due to elevated levels of protein synthesis through activated mTORC1 signaling which is normally attenuated in quiescent HSCs (Signer et al., 2014). Reacquiring low protein synthesis levels by crossing with mice that have impaired ribosome activity ($Rpl24^{Bst/+}$ mutants) restored HSC function and delayed onset of leukemia. Thus gain of function mutations in oncogenes (including chromosomal translocations) (Krivtsov and Armstrong, 2007) or loss of function mutations in tumor suppressors in HSCs can induce HSC cycling and predispose to clonal outgrowth and cancer initiation, and in primary human leukemia such as AML, this typically occurs upon acquiring additional transforming mutations (Dick, 2008; Genovese et al., 2015; Greaves and Maley, 2012; Rentas et al., 2013).

1.4 New models of lineage specification in the hematopoietic system

A principal function of HSPCs is to undergo differentiation and lineage commitment to maintain normal output of mature blood cells. Two important bifurcation points exist in classic lineage specification models of hematopoiesis, including MPPs to common lymphoid progenitors (CLP) or common myeloid progenitors (CMP), and myeloid lineage bifurcation to megakaryocyte-erythroid progenitors (MEP) or granulocyte-monocyte progenitors (GMP) (Seita and Weissman, 2010). Bifurcation to committed MEP and GMP progenitors has been assumed for decades to be controlled by co-expression of antagonistic lineage specific transcription factors in CMPs, including

GATA-1 for MK-E and *PU.1* for GM specification (Orkin, 2000). The ensuing competition (Miyamoto et al., 2002) has even been onerously modeled mathematically (Roeder and Glauche, 2006), but there are multiple lines of evidence that now suggest individual cells do not significantly express multiple lineage-specific genes or transcription factors that regulate different fates (Paul et al., 2015). This new model instead shows that there is considerable cell-to-cell heterogeneity in previously identified CMP, GMP and MEP populations. The study by Paul et al. used single cell RNA-seq within these three myeloid progenitor subsets to identify 18 transcriptionally distinct subpopulations which are restricted to a particular differentiation program. A similar conclusion was reached by Perie et al.; their approach with transplanting barcoded progenitors and tracking mature cell output *in vivo* found CMPs almost always gave rise to either E or GM cell types (Perie et al., 2015). This was further extended to more primitive cells, where individual MPPs were largely committed to a single lineage. That most MPPs are "hardwired" or biased to a particular lineage was also found by the Passegué group through a novel sorting and transplantation approach (Pietras et al., 2015). Lineage biasing has also been shown in HSCs by way of single cell transplantation (Dykstra et al., 2007), and is a phenotype that can be prospectively isolated by specific combinatorial expression of SLAM family markers (Oguro et al., 2013). Thus, an alternative model to the classic hematopoietic hierarchy has been proposed (Figure 1B) to take in to account the single-cell heterogeneity that exists within primitive populations of the hematopoietic system. While these studies show an intrinsic lineage-primed differentiation program exists in HSPCs that guides their most likely cellular outcome, continuous live-cell imaging methods and standard *in vivo* modeling of HSC activity have shown cytokines such as macrophage colony stimulating factor (M-CSF), granulocyte colony stimulating factor (G-CSF) and chronic exposure to interleukin-1 (IL-1) instruct HSCs and progenitors to undergo differentiation to the myeloid lineage (Mossadegh-Keller et al., 2013; Pietras et al., 2016; Rieger et al., 2009). The high efficiency with which cytokines can induce myeloid lineage differentiation shows their capacity to direct cell fate outcomes and override the cell's "hardwired" program. This may provide an advantage to the immune system if release of cytokines during infection recruits HSPCs to respond and override their current lineage-biased state.

1.5 Properties of HSC division and self-renewal

1.5.1 Asymmetric cell division

Frequency of HSCs in the bone marrow remains unchanged until an animal has reached old age; here numbers increase but overall function declines (Jung et al., 2016). A type of replication event that could underpin maintenance of the HSC pool throughout the majority of life is asymmetric cell division (Neumüller and Knoblich, 2009). During this event a quiescent HSC would re-enter the cell cycle and divide into a daughter cell that self-renews and remains an HSC while the other daughter becomes progenitor fated. In this context, asymmetry is established at mitosis. If this replication event were to occur it is easy to appreciate how it could keep HSC numbers constant. Mechanisms for asymmetric cell division have been well studied in model systems such as *Drosophila* neural stem cells (neuroblasts) and *C. elegans* embryos (Gonczy, 2008). These models generally show an intrinsic axis of polarity that directs unequal partitioning of fate determinants (typically proteins or mRNA) during mitosis which influence downstream signaling pathways and gene expression programs to elicit fate changes in the recipient cell (Neumüller and Knoblich, 2009). Neurogenesis in drosophila therefore proceeds through apical-basal neuroblast cell divisions, where the cell dividing away from the neuroepithelium undergoes differentiation to a mature neuron (Knoblich, 2008). Null mutants for proteins that partition into the neuronal precursor cell and direct differentiation, such as Numb, result in unchecked cell division and tumour growth (Knoblich, 2008). Conversely loss of function mutants for proteins retained in neuroblasts, like the Par complex, exhibit neuroblast depletion (Knoblich, 2008). Thus, modulating the activity of genes that function in asymmetric cell division has a direct effect on stem cell numbers.

1.5.2 Cell division in HSPCs

There are very few examples of HSCs undergoing asymmetric division *in vitro* in the manner described above (unequal partitioning of fate determinants at mitosis) and no direct evidence of it occurring *in vivo*, although mathematical modelling of lineage tracing data from fluorescently tagged HSCs does favour the occurrence of asymmetric division (Busch et al., 2015). Support for *in vitro* asymmetric division in mouse HSPCs was provided with time-lapse imaging and a GFP reporter that indicates active Notch signaling. By tracking single cell divisions the Reya group found occurrences of HSPCs where one sister remained GFP$^+$ and the other GFP$^-$. This asymmetric activity in Notch signaling was attributed to unequal partitioning of Numb protein since its presence is known to suppress Notch (Gonczy, 2008). Tracking *in vitro* Numb segregation has been used in several additional studies to show whether knockdown/knockout or overexpression of a particular gene of interest impacts symmetric renewal (no daughters express Numb), symmetric differentiation (both daughters inherit Numb) and asymmetric division (one daughter gets Numb) in HSCs (Park et al., 2014; Will et al., 2013; Zimdahl et al., 2014). Whether the segregation pattern of Numb bears any significance on the downstream function of HSPCs appears unlikely since conditional deletion of Numb shows normal hematopoiesis at steady-state and during transplantation (Wilson et al., 2007); only in the study by Wu et al. did overexpression of Numb promote a loss of primitive cells during *in vitro* culture (Wu et al., 2007). To show Numb, or indeed any other protein segregates asymmetrically during HSC cell division in situ would require creation of a unique lineage tracing fluorescent reporter mouse that follows the pulse-chase paradigm developed to identify histone-label retaining dormant LT-HSCs (Wilson et al., 2008), however such a model has yet to be established. Aside from Numb, other proteins that have been shown to segregate asymmetrically in mouse HSPCs include Ap2a2 (Ting et al., 2011) and in the human system HSC markers CD133 and CD34 (Beckmann et al., 2007; Gorgens et al., 2014; Shin et al., 2014).

In summary, HSCs exiting quiescence and undergoing replication leads to one of 3 possibilities: symmetric renewal, symmetric differentiation or asymmetric division. Given these 3 division schemes (particularly symmetric renewal or symmetric differentiation), a gene whose loss or gain favors one outcome over the other, either during homeostasis or with transplantation stress, can be classified as one that influences HSC self-renewal. In these circumstances there is typically a numerical increase or decrease within the HSC pool. Since the focus of this thesis is primarily on genes controlling self-renewal in human HSCs, a brief survey of important mediators of self-renewal in the human context will be provided in later sections.

1.6 Xenograft models and human HSCs

1.6.1 In vitro assays to model human hematopoieis

The development of the CFU-S assay and congenic mice enabled the use of *in vivo* repopulating assays to measure mouse HSPC activity. The study of human HSPCs however suffered early on as complementary *in vivo* assays had not yet been created due to the biological constraints of grafting human cells in wild type mice. To circumvent these limitations, *in vitro* culture and colony-forming assays were developed to allow for the detection of primitive human bone marrow cells. These assays include the colony forming cell assay (CFC) as described in section 1.2.2 which are done over the course of 2 weeks in cytokine supplemented, semi-solid methylcellulose medium to readout progenitors (Broxmeyer, 1984) and long-term culture initiating cell (LTC-IC) assays which span a timeframe of several weeks and thus presumably readout the activity of more primitive self-renewing HSPCs (Coulombel, 2004). Historically, LTC-IC assays were performed on adherent bone marrow-derived mesenchymal cells (Dexter et al., 1977), however this evolved to more reproducible transformed mouse feeder cell lines that are easier to use (Sutherland et al., 1989). Measuring the output of LTC-ICs relied not just on the presence of cells surviving in culture after several weeks but also on the ability of those cells to form colonies with the standard CFC assay (Coulombel, 2004). The CFC and LTC-IC assay were instrumental for testing FACS-purified populations with enriched primitive cell activity (Baines et al., 1988; Civin et al., 1984; Sutherland et al., 1989; Terstappen et al., 1991). These studies would provide the starting point for prospective isolation of human cells within bone marrow, cord blood (CB), and fetal liver possessing *in vivo* repopulating capacity in immune deficient mice.

1.6.2 In vivo modeling of human hematopoiesis with immune deficient mice

The development of immune-deficient mice over 30 years ago was an essential development for allowing the modeling of human hematopoietic cells *in vivo*. The first generation of immune deprived mice had a severe combined immune deficiency (Scid) phenotype and lacked the capacity to make B and T cells (Bosma et al., 1983; Fulop and Phillips, 1990). Initial studies to engraft human hematopoietic cells in Scid mice used peripheral blood lymphocytes that produced antibodies to tetanus toxin (Mosier et al., 1988) and fetal liver cells to show sustained production of B and T cells which was indicative of engrafted human HSPCs (McCune et al., 1988). The first demonstration however of adult human HSC activity came from the Dick lab who performed transplantation of human bone marrow into Scid mice along with growth factors to support myeloid development and showed the capacity for ongoing donor myeloid and lymphoid development (Kamel-Reid and Dick, 1988). There have been multiple genetic alterations made to improve engraftment outcomes in the Scid mouse since its discovery, with the first major improvement being the use of the non-obese diabetic (NOD) mutation in combination with Scid (NOD-Scid) to impair both adaptive and innate immune cell function (Shultz et al., 1995). The problem with NOD-Scid mice however, was the formation of thymic lymphomas which hindered long-term studies. To overcome this challenge the Schultz group generated IL-2 receptor gamma null mice in the NOD-Scid background (NSG), leading to mice that had impaired innate immunity as well a complete lack of B, T and NK cells and no lymphoma generation (Shultz et al., 2007), thus supporting comparatively higher levels of multilineage human cell repopulation and the capacity to run experiments in excess of 6 months, which allows for a better approximation of stem cell activity. The latest generation of immunocompromised mice for reading out primitive human HSPC function has been engineered to express human cytokines in place of their mouse counterparts to allow for better support and reconstitution of the myeloid lineage, as NSG mice heavily bias human HSC development to B cell production and fail to produce meaningful numbers of neutrophils or maintain any trace of long-term erythrocyte or platelet production (Miller et al., 2013a).

1.6.3 The human hematopoietic hierarchy

The discovery of an antibody against the cell surface antigen CD34 was the first breakthrough in the positive selection of specific cells in human bone marrow enriched in CFCs and LTC-ICs (Civin et al., 1984). Shortly thereafter, lack of expression of CD45RA in combination with the presence of CD34 further improved identification of CFCs and LTC-ICs (Lansdorp et al., 1990). By using the Scid model, expression of both

Thy-1 (CD90) and CD34 allowed for further purification of *in vivo* repopulating HSPCs (Baum et al., 1992; Murray et al., 1995). This was followed by the demonstration of significant HSC enrichment in cells negative for CD38 but positive for CD34 expression, with the Dick group in particular denoting this population as NOD-Scid repopulating cells (SRC) (Bhatia et al., 1997). Thus by the end of the 1990s a clear definition was emerging on the collection of markers that could be used to enrich for human HSCs. Interestingly, these studies highlighted unique phenotypic attributes of the primitive human hematopoietic system as there was little evolutionary conservation in the marker expression profile of human HSCs when compared to mouse HSCs.

Ongoing work in the mouse system illustrated extensive heterogeneity in the engraftment kinetics, self-renewal, and differentiation biases of mouse bone marrow populations enriched for HSCs and progenitors. Since research in mice guided the studies with human cells, similar attempts were carried out to test the self-renewal and differentiation potential within subsets of CD34 marked cells. Here it was found that CD34+ CD38lo/+ cells were capable of generating transient myeloid biased grafts lasting up to 3 weeks before eventually exhausting (Glimm et al., 2001; Mazurier et al., 2003). These cells were termed short-term Scid repopulating cells (STRC) and are recognized today as consisting of committed progenitor populations including the classically defined CMP, GMP and MEP populations (Doulatov et al., 2010; Laurenti et al., 2013). Hierarchical organization within the human HSC compartment was later shown by Majeti et al. when they determined LT-HSCs were more highly enriched in the Lin- CD34+ CD38- CD45RA- Thy-1+ population and MPPs in Lin- CD34+ CD38- CD45RA- Thy-1- (Majeti et al., 2007). The MPPs discovered by Majeti et al. however still had serial transplantation capacity, which meant further refinement was needed to isolate human HSCs to near homogeneity. This work was carried out by Notta at el. by inclusion of the marker CD49f (Notta et al., 2011). The rationale for using CD49f was based on integrin-α2 (CD49b) expression on mouse HSCs demarcating cells with intermediate-term versus long-term self-renewal potential (Benveniste et al., 2010). LT-HSCs in humans are currently defined as Lin$^-$ CD34$^+$ CD38$^-$ Thy-1$^+$ CD45RA$^-$ CD49f$^+$ and ST-HSCs/MPPs as Lin$^-$ CD34$^+$ CD38$^-$ Thy-1$^-$ CD45RA$^-$ CD49f$^-$ (Figure 4A) (Notta et al., 2011). Limiting dilution analysis revealed ~10% of these LT-HSCs had long-term repopulating activity, defined by mature blood cells being detected >16 weeks after transplant, whereas mature cells from the MPP fraction were undetectable at 16 weeks (Notta et al., 2011). Additionally, LT-HSCs, unlike MPPs, were the only cells capable of robust secondary mouse engraftment. By using rhodamine dye efflux along with the combination of markers described above to enrich for human LT-HSCs, Notta el al. showed 28% of single cell transplants repopulated NSG mice, this was in spite of the inefficiencies of the xenotransplant system (e.g. the lack of human cytokine production). To complete the comparison of the primitive human hematopoietic cell compartment to what is observed in mice, the Dick lab showed a cell population existed that was analogous to lymphoid primed multipotent progentior (LMPP). Like mouse LMPPs, this population of early lymphoid progenitors were devoid of MK-E developmental potential but competent to make macrophages and granulocytes (Figure 3A). This population of cells was termed multilymphoid progenitors (MLP) and identified with the marker profile of Lin- CD34+ CD38- CD45RA+- Thy-1- (Doulatov et al., 2010). This work collectively shows human hematopoiesis faithfully mimics the developmental process originally characterized in mice (Doulatov et al., 2012).

1.6.4 A revised model of human lineage specification

Just as the classic model of mouse lineage specification was shown to be an aggregate of phenotypes from many lineage restricted cells captured in bulk populations identified by multi-colour flow cytometry (Paul et al., 2015; Perie et al., 2015; Pietras et al., 2015), so to was it recently revealed the underappreciated level of single-cell heterogeneity in differentiation potential that exists in human HSPCs (Notta et al., 2016). The work done by Notta et al. used a novel single cell culture assay to measure mature myeloid cell output from 9 populations of HSCs, MPPs, and committed progenitors from fetal, post-natal and adult bone marrow cells. Fetal liver had the highest proportion of multipotent progenitors with varying myeloid, E, and MK potentials and MK-E activity present throughout the hierarchy, however adult bone marrow progenitors were largely lineage restricted and to a lesser extent bi-potent whereas multipotency was restrained to the HSC compartment as was MK-E development. Therefore, what was previously identified as homogenous populations containing CMP, GMP and MEP contained a collection of single lineage restricted progenitors with very little MK-E developmental potential. The results from these single cell analyses describe an alternative 2-tier model in adult human hematopoiesis, where multipotency is restrained in the HSC fraction and progenitors are either uni- or bi-potent (Figure 3B) (Notta et al., 2016). It will be now be exciting to probe the transcriptome from single cells belonging to these 9 populations to confirm these findings and truly define the molecular underpinnings that determine lineage restriction.

1.6.5 Human HSC contribution to steady-state hematopoiesis

Within the past two years there have been significant advances to understanding steady-state hematopoiesis in mice using genetic marking or fluorescent protein lineage tracing methods (Busch et al., 2015; Sun et al., 2014). These studies showed that HSCs contribute minimally to homeostasis and most blood cell production is through long-lived progenitor populations. Similar studies however cannot be done in humans, thus testing the contribution of HSCs to maintaining the adult human hematopoietic system remains a challenge. By all accounts, hematopoiesis in healthy adults remains polyclonal (multiple HSCs and progenitors) as evidenced by a lack of skewing in inactivated X chromosomes in elderly women (Swierczek et al., 2012) and the finding that clonal hematopoiesis is a precursor to leukemia initiation (Genovese et al., 2015). However the only way to quantitatively track the polyclonal contribution of HSCs to hematopoieis is through analysis of peripheral blood and bone marrow of reconstituted mice or humans after myeloablative therapy. Xenotransplantation with lentiviral barcoded HSCs (Lu et al., 2011) showed long-term hematopoiesis is maintained in reconstituted mice by up to 30-50 HSCs. A similar finding was also demonstrated upon analysis of lentiviral insertion sites tracked in patients transplanted with gene corrected HSCs to treat Wiskott-Aldrich syndrome (WAS) (Biasco et al., 2016). In these patients, recovery of hematopoiesis occurred by a transient 3-6 month contribution of hematopoietic progenitors followed by pro-longed maintenance of the hematopoietic system by a second wave driven largely by

MPPs and HSCs. On average 1500 insertion sites (clones) were found in individuals after 3 years, however only a fraction of these were represented when they profiled bone marrow sampled HSC insertion sites. Here they found approximately 30% of HSC insertion sites were found in one or more lineages and almost all MPPs were represented. This finding is similar to what was described earlier (section 1.3.4) in the YFP HSC tagging of HSCs by Busch et al. Thus after transplantation a large majority of HSCs become quiescent and the continual production of blood cells appears to be maintained by committed progenitors, MPPs and some HSCs. Another important finding which validates to a large extent the new 2-tier model of lineage specification (Notta et al., 2016), was the demonstration that most lymphoid insertion sites are shared by myeloid cells and vice versa (indicating a prevailing multipotent progenitor), where as MK-E development insertion sites were typically distinct. Thus, human hematopoiesis appears to be highly polyclonal over long periods of time and is supported mainly by multipotent progenitors and to a lesser extent HSCs.

1.7 Expanding human HSCs for regenerative therapy

1.7.1 Using umbilical cord blood as a source of human HSCs for transplantation therapy

As HSCs present in transplanted bone marrow enable robust reconstitution of all blood cell lineages, their therapeutic potential is enormous to individuals who have congenital hematopoietic defects or are undergoing chemotherapy to treat leukemia. While HSC transplantation is the first and remains the most effective stem cell therapy in clinical use (Gratwohl et al., 2010), its efficacy is still limited by the rarity of stem cells retrieved from autologous (self, healthy bone marrow) or allogenic (donor, HLA matched) blood sources; for instance, only 30% of patients will have a sibling matched donor (Ballen et al., 2013). Furthermore, while over 20 million volunteers have volunteered in the American National Marrow Donor Program, patients particularly from different ethnic backgrounds are unlikely to find a suitable donor (Appelbaum, 2012). Thus alternative sources of HSCs such as from umbilical cord blood (CB) are needed to help alleviate these constraints. CB offers multiple advantages to bone marrow sources of HSCs, including rapid availability of cryopreserved samples, lower immunogenicity and rates and severity of graft versus host disease due to naïve immune cells, and comparatively greater proliferative and self-renewal capacity in HSPCs (Ballen et al., 2013; Miller et al., 2013b). Hal Broxmeyer's group pioneered the use of CB HSPCs (Broxmeyer et al., 1989) by performing the first transplant in a Fanconi anemia patient (Gluckman et al., 1989). Since then over 600,000 CB units have been registered for transplantation worldwide and over 30,000 CB HSPC transplants have been performed (Ballen et al., 2013).

Persistent use of CB in the clinic is challenged by the limited number of cells retrieved from a single CB unit leading to delayed engraftment and ensuing poor immune cell reconstitution. To circumvent the limited number of cells two CBs can be combined to facilitate transplantation in adults (Barker et al., 2003), the added difficulty here is finding HLA matches for the multiple CB units and patient. Finally, CB proportionally contains far fewer progenitors than what can be retrieved from adult bone marrow or mobilized peripheral blood, an issue that is compounded by the overall lack of total nucleated cells (Miller et al., 2013b). These difficulties highlight the growing need to enhance total numbers of HSPCs in CB transplants.

1.7.2 Factors that influence patient survival post-HSC transplantation

Patients receiving hematopoietic stem cell transplantation (HCT) are given myeloablative regimens such as chemotherapy and total body irradiation to induce death to circulating malignant or diseased cells and allow engraftment of healthy donor HSCs, the consequence of these conditioning regimes is collateral damage to the patient's immune system. Therefore a major impediment to the efficacy of HCT is the patient's susceptibility to infection and bleeding immediately following transplantation. Thus, treatment related mortality is often associated with insufficient reconstitution of neutrophils and platelets during the time immediately following the transplant. Shortened times to recovery of these critical cell types are key determinants of donor cell engraftment and successful patient outcome (Meldgaard Knudsen et al., 1999; Offner et al., 1996). Infusion of greater numbers of the more proliferative multipotent and committed myeloid progenitors would allow for rapid production of these necessary mature cell types and better patient recovery. Thus, expansion or enhanced activity of STRCs – a population containing committed myeloid progenitors – is of immense clinical significance to the reduction of patient mortality during HCT (Miller et al., 2013b). Taking in to consideration that long-term patient health relies heavily on sufficient numbers of stem cells to be transplanted and short-term survival on more differentiated multipotent and committed progenitors, an understanding of the genetic regulation of expansion and proliferation of both of these cell types will enhance HCT therapies.

1.7.3 Gene therapy, small molecules, and new culture methods lead the way

Infusing patients with as many genetically matched (or closely matched) HSPCs as possible will lead to the best patient outcome during HCT. Historically, methods to expand HSCs *in vitro* include using defined cytokine culture conditions, which includes factors such as SCF, TPO, Flt-3L, IL-3, IL-6 and G-CSF to stimulate proliferation (Conneally et al., 1997; Shpall et al., 2002) and co-culture on supportive stromal layers (Huang et al., 2007; Sutherland et al., 1991). A consistent challenge with *in vitro* culture systems is promoting HSPC proliferation without driving them to differentiate into mature cell types. To work around this limitation, many groups have tried overexpressing genes such as HOXB4 (Antonchuk et al., 2002) or NUP98-HOXA10 (Ohta et al., 2007) with retroviruses, and to great effect, have shown very high levels of murine HSC expansion. However, these findings have not translated particularly well to primate or human HSCs (Buske et al., 2002; Zhang et al., 2006b), suggesting that genetic regulation of self renewal is not precisely conserved from mice to humans. Additionally, the use of retroviruses has limited potential for clinical therapy since retroviral genome integration can result in oncogenic transformation. Thus effort has been directed towards the use of exogenously delivered recombinant proteins such as TAT-HOXB4 (Huang et al., 2010), TAT-NF-Ya (Domashenko et al., 2010) and Notch ligand (Delta$^{\text{ext-IgG}}$) (Delaney et al., 2010) to specifically stimulate HSC proliferation. Supplementing HSC growth medium with small molecules to enhance HSC proliferation without concomitant differentiation has perhaps seen the most success. Such small molecules include UM171 (Fares et al., 2014), Stem Reginin 1 (SR1), an aryl-hydrocarbon receptor (AHR) antagonist (Boitano et al., 2010), the copper chelator TEPA (Peled et al., 2005), the GSK-3β inhibitor BIO (Ko et al., 2011), prostaglandin E_2 derivatives ($dmPGE_2$) (North et al., 2007), and NR-101, a highly potent Thrombopoietin receptor agonist (Nishino et al., 2009). Altogether, each of these compounds or proteins offer varying degrees of effectiveness in achieving human HSC expansion, with SR1 and UM171 appearing to have the greatest promise based on the high frequency and total number of phenotypically marked primitive cells after 1 week of ex vivo expansion and their ability to provide robust long-term engraftment and secondary repopulation. Many of these molecules have begun clinical trial testing, including SR1 (Wagner et al., 2016), dmPGE2 (Cutler et al., 2013), and $\text{Delta}^{\text{ext-IgG}}$ (Milano et al., 2014). Each of these clinical trials has utilized a double CB transplant strategy whereby one CB is unmanipulated and identified by a unique HLA allele and the other differentially HLA marked CB undergoes the expansion protocol. SR1 appears to be the most promising to date as cells expanded in its presence robustly contributed long-term multilineage grafts in patients and improved early engraftment of progenitors that provide vital production of platelets and neutrophils to stave off hemorrhaging and infection in these highly immuno-compromised people (Wagner et al., 2016). The success of this study means moving to phase III trials where patients only receive expanded HSPCs.

Optimizing CB HSPC numbers has also been achieved by improving basic handling of samples and engineering new *in vitro* culture equipment to provide optimal conditions for growth (Csaszar et al., 2012; Mantel et al., 2015). The Broxmeyer group focused on eliminating CB exposure to oxygen and developed protocols to harvest samples in their native hypoxia, thus eliminating oxygen stress which induces p53-mediated ROS production via mitochondrial pore formation (Mantel et al., 2015). Peter Zandstra's group took an alternative approach to expanding CB HSPCs by developing a computer controlled fed-batch culturing method which continuously supplies growing HSPCs with fresh medium thus diluting differentiation secreted inhibitory feedback signals (Csaszar et al., 2012). The variety of approaches, including genetic, small molecule and novel cell culturing and handling methods shows the multitude of ways in which CB HSPCs can be enhanced for regenerative therapies and the continuing need to understand how these cells are regulated.

1.8 The role of Musashi-2 in murine hematopoiesis

1.8.1 The identification of Msi2 in mouse HSCs

In order to identify novel genetic regulators of HSC self-renewal an *in vivo* RNAi screen was performed that focused on knocking down genes with known roles in polarity and asymmetric cell division (Hope et al., 2010). Genes that typically regulate these processes have mostly been overlooked in HSC biology, even though they represent cellular mechanisms that are essential to the normal function of stem cells in model systems (Gonczy, 2008). One of the genes identified in this screen was the RNA binding protein (RBP) Musashi-2 (Msi2). Musashi gene family members regulate mRNA translation and were originally identified in *Drosophila* as regulators of asymmetric cell division and development of sensory bristles (Nakamura et al., 1994; Okabe et al., 2001). The homolog of Msi2, Msi1, has been studied extensively in the mammalian nervous system and is strongly expressed in fetal and adult neural stem cells where it promotes self renewal by maintaining Notch signaling through translational repression of Numb (Imai et al., 2001; Keyoung et al., 2001). Comparatively, much less is known about the function of Msi2 in hematopoiesis. Expression profiling of purified populations of mouse HSCs and progenitors showed *Msi2* is highly expressed in the most primitive HSC compartment, whereas expression of *Msi1* is essentially absent across all cell types (de Andrés-Aguayo et al., 2011; Hope et al., 2010; Kharas et al., 2010). Retroviral-mediated short-hairpin knockdown of Msi2 in mouse HSCs followed by transplantation into congenic mice results in a significant decrease in their repopulation capability compared to short-hairpin controls (Hope et al., 2010; Kharas et al., 2010). Interestingly, *in vitro* overexpression of Msi2 in primitive mouse hematopoietic cells followed by transplantation had the opposite effect of knockdown and led to an increase in repopulation (Hope et al., 2010). This latter finding of enhanced HSC activity with over expression of Msi2 is also supported by results from a retroviral insertion screen aimed at identifying novel regulators of mouse hematopoiesis (de Andrés-Aguayo et al., 2011). Based on the premise that retroviral integration can activate gene expression from nearby promoters, De Andres-Aguayo et al. showed clonal dominance of retrovirus integrated Msi2 over-expressing hematopoietic cells in transplanted mice. Importantly, regardless of the method of Msi2 overexpression-induction, in no case was leukemia observed as a result (Hope et al., 2010) (de Andrés-Aguayo et al., 2011). De Andres-Aguayo et al. also demonstrated that Msi2 gene-trap mice (truncation at the C-terminal RNA binding domain portion of the protein) have significant impairment in repopulation capability, due to a decrease in the proliferative capacity of short-term self renewing HSCs and multipotent non-self renewing progenitors (de Andrés-Aguayo et al., 2011). Additionally, a conditional knockout mouse model demonstrated Msi2 deletion promotes cycling and loss of long-term HSC quiescence leading to failure of HSC maintenance in adult mice and an inability for Msi2 deleted HSCs to engraft recipient mice (Park et al., 2014). Altogether, these data correlate with Msi2 knockdown and overexpression experiments (Hope et al., 2010; Kharas et al., 2010), and implicate Msi2 as being an important novel regulator of the murine HSC compartment.

1.8.2 Msi2 in mouse models of leukemia

Aside from the burgeoning role in maintaining normal murine HSC function, there are several studies that have implicated Msi2 in both primary human and mouse models of leukemia. *MSI2* was originally found in a novel chromosomal translocation with *HOXA9* in a cohort of acute myeloid leukemia (AML) patients (Barbouti et al., 2003). This spurred studies into exploring its role in mouse models of chronic myeloid leukemia (CML) where it was found to have a positive role in the progression to the acute and lethal blast crisis (BC) phase of the disease (Ito et al., 2010; Kharas et al., 2010). Mouse survival was significantly increased with *Msi2* knockdown in BC cells compared to control BC leukemia cells (Ito et al., 2010), and both Ito et al. and Kharas et al. showed that *MSI2* was highly expressed in human AML and BC-CML patient samples and elevated expression correlated with decreased patient survival (Ito et al., 2010; Kharas et al., 2010). Other studies support the positive effect Msi2 has on leukemia progression is not restricted to CML models, as loss of *Msi2* in a *MLL-AF9* driven mouse model of leukemia delays leukmogenesis by promoting differentiation and apoptosis and improves overall mouse survival (Park et al., 2015). Msi2 has further been shown to maintain a pre-leukemic state in a mouse model of myeloid dysplastic syndrome (MDS) (Taggart et al., 2016), since knocking out Msi2 eliminates MDS HSPCs while OE has the opposite effect of accelerating the disease. Additional clinical correlates of MSI2 and AML patient survival have come from histological examination of blast cells in patient bone marrow and finding elevated protein levels and in particular rare cells with high amounts within in the nucleus as negative prognostic indication of disease outcome (Byers et al., 2011). These studies collectively show MSI2 as a central regulator in acute leukemia progression across multiple types of myeloid leukemias.

1.8.4 Post transcriptional regulation by Musashi family RBPs

Post transcriptional regulation by RNA binding proteins (RBP) is emerging as a vital mechanism for regulating complex genetic networks and establishing cellular diversity (Cassar and Stanford, 2012). These proteins function at multiple levels in mRNA metabolism including export, splicing, stability, degradation, and translation (Halbeisen et al., 2008). This allows for fine tuning of gene expression beyond transcription and therefore affects multiple levels of cellular physiology including proliferation and fate decisions in stem cells (Cassar and Stanford, 2012). Msi1 for instance binds the 3'untranslated region (3'UTR) of target transcripts (e.g. *Numb*) in neural stem cells to repress translation and maintain stem cell activity (Imai et al., 2001). Follow up work on Msi1 has suggested that *Numb* translation is inhibited by Msi1 competing with the eukaryotic translation initiation factor 4G (eIF4G) for poly-A binding protein (PABP) binding, which results in incomplete assembly of the mature ribosome (Kawahara et al., 2008) (Figure 4A). Msi1 shares 69% protein homology to Msi2 and 86% within their RNA binding domains (Ohyama et al., 2012). This has led to the hypothesis that the similarity between Musashi family proteins likely results in similar RNA consensus motifs and target transcripts for repression (Ohyama et al., 2012). Interestingly, studies in Xenopus oocytes have shown Msi1 and 2 can promote translation by promoting elongation of the poly-A tail (Cragle and MacNicol, 2014; MacNicol et al., 2011), a mechanism, however, that has not been tested yet in mammalian cells.

1.8.4 Msi2 mechanism of actions in normal and malignant hematopoiesis

Gene expression profiling in mouse HSPC populations after Msi2 knockdown/out or overexpression led to transcriptional changes in cell cycle regulators such as *p21* and *Cyclin D1* and several signaling pathways, including with overexpression, elevated Notch, Sonic Hedgehog, and Myc gene signatures (de Andrés-Aguayo et al., 2011; Hope et al., 2010; Kharas et al., 2010). Additional gene expression profiling performed in conditionally deleted Msi2 HSPCs as well as high-throughput sequencing of RNA isolated by crosslinking immunoprecipitation (HITS-CLIP) in a hematopoietic cell line revealed perturbed TGF-β signaling, a finding which was echoed in the non-responsiveness of knockout cells to TGF-β mediated HSPC expansion. Precise targets that were responsible for specifically mediating this response were not elucidated however (Park et al., 2014). In the context of MLL-AF9 driven leukemia, Msi2 stabilized and promoted translation of various oncogenes or cooperative oncogenes including *Hoxa9*, *Myc*, and *Ikzf2* mRNAs (Park et al., 2015). A similar Msi2-driven activating affect was seen with *Tspan3* mRNA in mouse models of leukemia, highlighting a novel post-transcriptionally driven leukemia promoting pathway (Kwon et al., 2015). Aside from regulating mRNA translation there is also evidence pointing to a role in controlling microRNA (miRNA) biogenesis, specifically at the stage primary miRNA (pri-miRNA) is cleaved by Drosha to precursor miRNA (pre-miRNA) (Choudhury et al., 2013). Msi2 was found to interact with HuR protein and bind and stabilize pri-miRNA stemloops leading to repression of the mature form of mir-7 (Figure 4B). Choudhury et al. used the Msi2 gene-trap mouse constructed by Thomas Graf's group (de Andrés-Aguayo et al., 2011) and went on to show that mir-7 was consequently upregulated in various whole tissue lysates. These studies, and previous work with Msi1, demonstrate Musashi proteins target multiple RNA species and interact with many protein binding partners resulting in promiscuous molecular mechanisms where they can promote or inhibit translation as well as affect miRNA development.

Finding Msi2 has pleiotropic effects on multiple RNA species is a common theme among RBPs. This has led to theories that RBPs govern specific cell phenotypes by working combinatorially with other RBPs to regulate subsets of functionally related transcripts (Keene, 2007). This "regulon" model has large implications on how proteins are made to control gene regulatory networks in post-mitotic cells and during stem cell developmental programs (Blackinton and Keene, 2014). However, identification of regulons at work in mouse or human HSPCs has not been thoroughly investigated. The interplay of multiple RBPs coordinating cell phenotypes does appear frequently in more mature populations of blood cells. For instance, post-transcriptional control by RBPs mediate mature immune cell responses (Kafasla et al., 2014; Turner et al., 2014), late stages of erythropoiesis (Thiadens and von Lindern, 2015; Zhang et al., 2013), and in mediating cell cycle and proliferation in numerous other cellular contexts including leukemia (Blackinton and Keene, 2014; Perrotti and Neviani, 2007). It remains highly likely that there is complex post-transcriptional control occurring in HSPCs to control their finely tuned expression networks. Thus exploratory studies are needed to begin testing the regulon model in the primitive hematopoietic compartment as it represents an unexplored mechanism of gene regulation.

1.9 Summary of intent

HSCs have a formative role in the development and maintenance of the hematopoietic system from pre-natal stages to adolescence to old age (Orkin and Zon, 2008). The regenerative potential of HSCs allows for their transplantation in patients with congenital hematopoietic disease or to recover the immune system post chemotherapy and irradiation to treat leukemia. Restraint in their clinical use lies in the difficulty of obtaining perfectly matched allogeneic donors. CB has numerous advantages to bone marrow sources of HSCs, however, with reduced total nucleated cell counts and lower frequency of progenitors, their efficacy is often limited, particularly for transplantion in adults (Ballen et al., 2013). A means to enhance this cell therapy such as with ex vivo expansion protocols could create a new clinical paradigm to aide in the treatment of blood diseases. Especially with human HSCs, there is a desperate need to improve our overall understanding of the biology of these cells and more specifically what drives their decisions to self-renew, differentiate or remain quiescent (Doulatov et al., 2012) as control of these mechanisms will support their culture and growth for transplantation purposes and inform novel anti-leukemic strategies and chemotherapies to limit them upon oncogenic transformation (Dick, 2008; Rentas et al., 2013). The discovery of Msi2 as a novel positive regulator of mouse HSC self-renewal and as a cooperative driver of mouse models of leukemia provides the impetus to explore this gene in normal human hematopoiesis and leukemogenesis (Hope et al., 2010; Kharas et al., 2010). Furthermore, the heavy focus on transcription factors and transcriptional control within the HSC field as the chief operators of cell fate (Wilkinson and Gottgens, 2013) has provided a myopic view of the complex control of stem cell behavior. This further befits the study of Msi2 since it exerts its control over stem cells through post-transcriptional control of various RNA species, including stabilizing or inhibiting mRNA translation and affecting miRNA biogenesis.

The primary theme of this thesis can thus be described as testing the hypothesis that MSI2 imparts positive control over human HSC self-renewal through a novel post-transcriptional regulatory axis.

If this hypothesis holds true and MSI2 positively enforces self-renewal programs in human HSCs, then overexpression (OE) of MSI2 and activation or suppression of downstream signaling pathways it impinges on could facilitate the ex vivo or *in vivo* expansion of human HSCs. An additional prediction from this hypothesis is that knockdown (KD) may have the opposite effect of inhibiting HSC self-renewal and proliferation ex vivo and or *in vivo*. The experimental aims to test the primary hypothesis of this thesis are as follows:

1) *Test MSI2 KD and OE in human HSCs to explore the effects it may have on self-renewal, differentiation, and proliferation in vitro and upon in vivo transplantation.*
2) *Perform RNA-seq to identify differentially expressed genes with MSI2 KD and OE and use cross-linking immunoprecipitation sequencing (CLIP-seq) to identify MSI2 bound RNA targets.*
3) *Use the large RNA-seq data sets from Aim 2 for hypothesis-driven investigation of MSI2's mechanism of action.*

The design of these aims allows for proper testing of our primary hypothesis by shedding light on new regulatory information on human HSC self-renewal. This work provides a foundation and step forward on basic mechanisms of post-transcriptional control in human HSCs by RBPs, an area that has yet to be explored to our knowledge, and allows for future studies aimed at understanding how the activity of MSI2 can facilitate expansion of HSCs for clinical use.

The secondary goal of this thesis is to utilize a conditional Msi2 knockout mouse (cKO) model generated by our lab to cast a wider net in exploring Msi2's mechanism of action in mouse HSCs, as there remains a glaring discrepancy between the two published Msi2 loss of function mouse models and the specific affect it has on HSPCs. This discrepancy comes from Thomas Graf's group showing deletion of Msi2 leads to a loss of ST-HSCs and MPPs while LT-HSCs are maintained and Michael Kharas' group showing MPPs, ST-HSCs and LT-HSCs are depleted with Msi2 deletion. Thus it remains to be confirmed whether LT-HSCs are lost or not with Msi2 deletion. Additionally, previous work using conditional deletion of Msi2 in mouse HSCs implicated dysregulated TGF-β signaling as a component of the ensuing impaired HSC activity (Park et al., 2014), yet an examination of how it may be doing so is unknown. In general, there is a fundamental lapse of basic knowledge on the activity of Msi2 within HSPCs and much of what we do know is inferred from model cell lines. For instance, in HSPCs, it is unknown whether Msi2 is involved in mRNA decay pathways, translation control (promotion or inhibition), or miRNA biogenesis. Nor is it known what proteins or RNAs Msi2 is interacting with or to what compartments within the cell it is localizing to and if this changes depending on progenitor or HSC class. Answering these questions may help identify how Msi2 is differentially regulating distinct classes of mouse HSPCs. Therefore, **the secondary theme of this thesis is to explore how Msi2 is functioning within the earliest stem and progenitor cells of the mouse hematopoietic system and to begin testing the hypothesis that RNA binding proteins such as Msi2 direct regulons controlling HSPC function**.

The experimental aims to test this secondary theme are as follows:

1) Validate that our lab's conditional Msi2 knockout mouse has impaired HSPC activity through in vivo transplantation assays and identify the most likely primitive cell type(s) Msi2 is impacting.

2) Explore localization of Msi2 in highly purified subsets of HSCs, MPPs and progenitors with known centers of RNA metabolism.

The design of these aims will help provide an in depth view into the specific mechanism of action of Msi2 in mouse HSPCs. Specifically, competitive and non-competitive transplants with Msi2 knockout cells will determine what role Msi2 has in controlling repopulation and specifically what cells its deletion impacts the most. Exploration in to the basic mechanism of action of Msi2 in HSPCs will be achieved by using confocal fluorescence microscopy to assess its intracellular localization with known areas of RNA metabolism including RNA decay, translation inhibition, and miRNA biogenesis.

The second part of the theme stated above was to broach the concept of RNA binding proteins, such as Msi2, directing regulons that control HSPC function. Specifically, I detail in a perspective (Chapter 3) the need to generate direct evidence that RNA binding proteins work combinatorially with other RNA binding proteins to target distinct populations of mRNA to mediate a coordinated cellular phenotype and thus define an RNA regulon. To show that this is likely the case, this perspective includes novel bioinformatic analyses of RNA binding protein expression profiles across functionally distinct primitive human hematopoietic cell types. This chapter is placed between my work on human and mouse models of hematopoiesis as it brings to light important concepts of post-transcriptional control important to both of these systems.

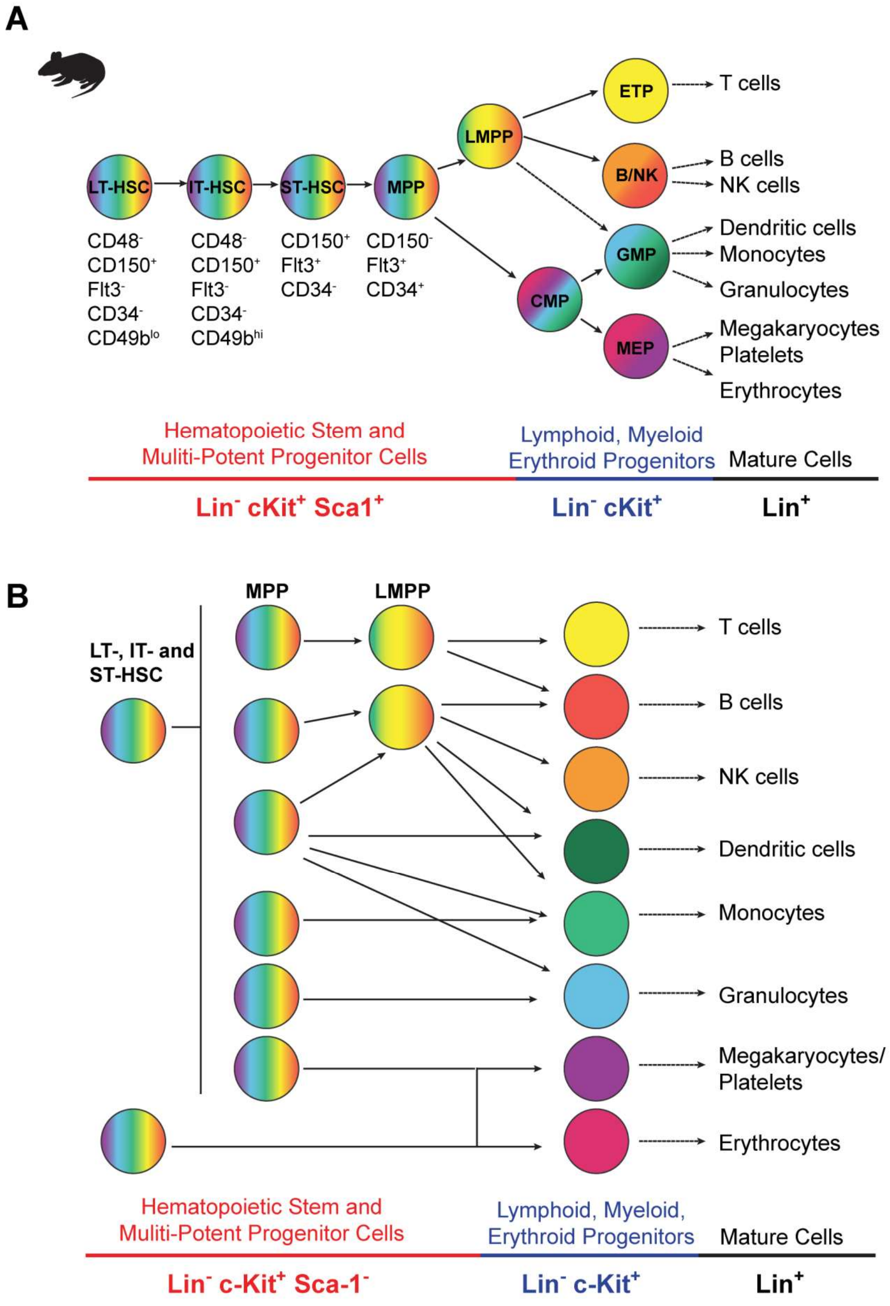
A
LT-HSC
IT-HSC
ST-HSC
MPP
LMPP
CMP
ETP
B/NK
GMP
MEP
CD48-
CD150+
Flt3-
CD34-
CD49blo
CD48-
CD150+
Flt3-
CD34-
CD49bhi
CD150+
Flt3+
CD34-
CD150-
Flt3+
CD34+
T cells
B cells
NK cells
Dendritic cells
Monocytes
Granulocytes
Megakaryocytes
Platelets
Erythrocytes
Hematopoietic Stem and
Muliti-Potent Progenitor Cells
Lymphoid, Myeloid
Erythroid Progenitors
Mature Cells
Lin- cKit+ Sca1+
Lin- cKit+
Lin+
B
LT-, IT- and
ST-HSC
MPP
LMPP
T cells
B cells
NK cells
Dendritic cells
Monocytes
Granulocytes
Megakaryocytes/
Platelets
Erythrocytes
Hematopoietic Stem and
Muliti-Potent Progenitor Cells
Lymphoid, Myeloid,
Erythroid Progenitors
Mature Cells
Lin- c-Kit+ Sca-1-
Lin- c-Kit+
Lin+

Figure 1. Classic and revised mouse hematopoietic hierarchy. (A) Schematic of the classic mouse hematopoietic hierarchy with corresponding cell surface markers used to isolate HSPCs. (B) Schematic of the revised mouse hematopoietic hierarchy showing lineage commitment occurs earlier.

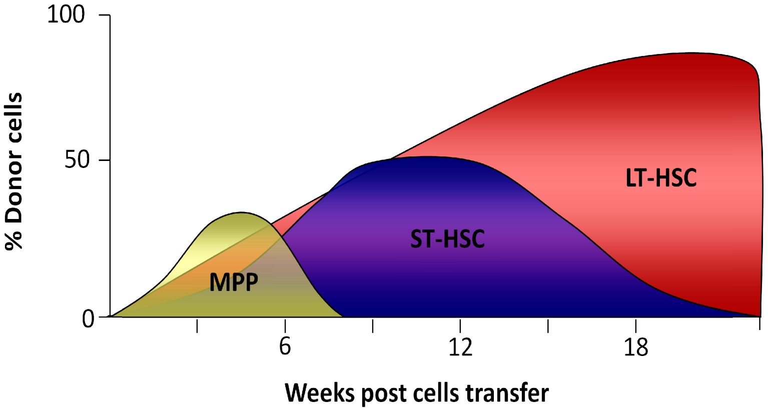
100
50
0
% Donor cells
6
12
18
Weeks post cells transfer
MPP
ST-HSC
LT-HSC

Figure 2. Transplantation kinetics of mouse HSPCS. Cartoon schematic of general engraftment kinetics of subsets of mouse HSPCs.

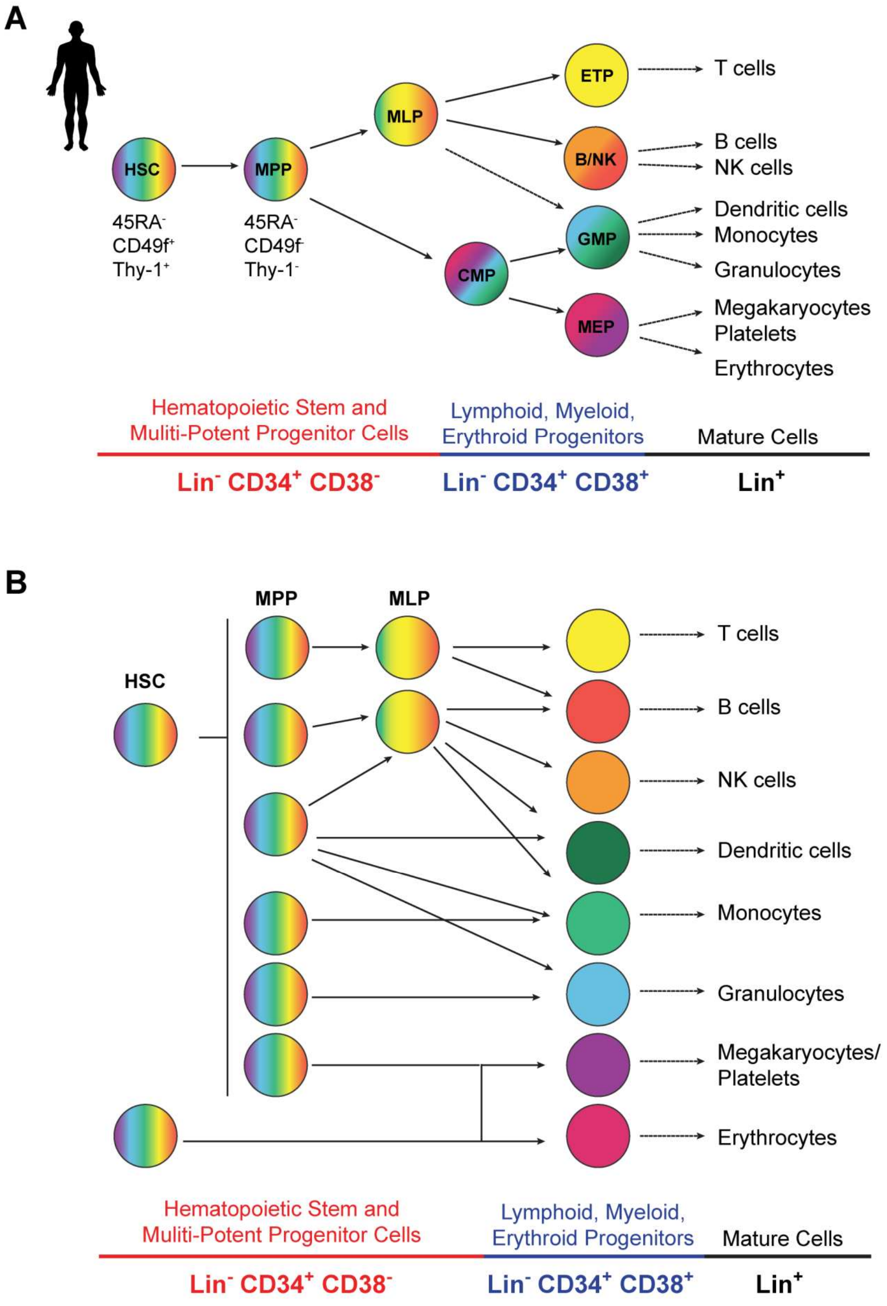
A
HSC
MPP
MLP
CMP
ETP
B/NK
GMP
MEP
45RA-
CD49f+
Thy-1+
45RA-
CD49f-
Thy-1-
T cells
B cells
NK cells
Dendritic cells
Monocytes
Granulocytes
Megakaryocytes
Platelets
Erythrocytes
Hematopoietic Stem and
Muliti-Potent Progenitor Cells
Lymphoid, Myeloid,
Erythroid Progenitors
Mature Cells
Lin- CD34+ CD38-
Lin- CD34+ CD38+
Lin+
B
HSC
MPP
MLP
T cells
B cells
NK cells
Dendritic cells
Monocytes
Granulocytes
Megakaryocytes/
Platelets
Erythrocytes
Hematopoietic Stem and
Muliti-Potent Progenitor Cells
Lymphoid, Myeloid,
Erythroid Progenitors
Mature Cells
Lin- CD34+ CD38-
Lin- CD34+ CD38+
Lin+

Figure 3. Classic and revised human hematopoietic hierarchy. (A) Schematic of the classic human hematopoietic hierarchy with corresponding cell surface markers used to isolate HSPCs. (B) Schematic of the revised human hematopoietic hierarchy showing lineage commitment occurs earlier.

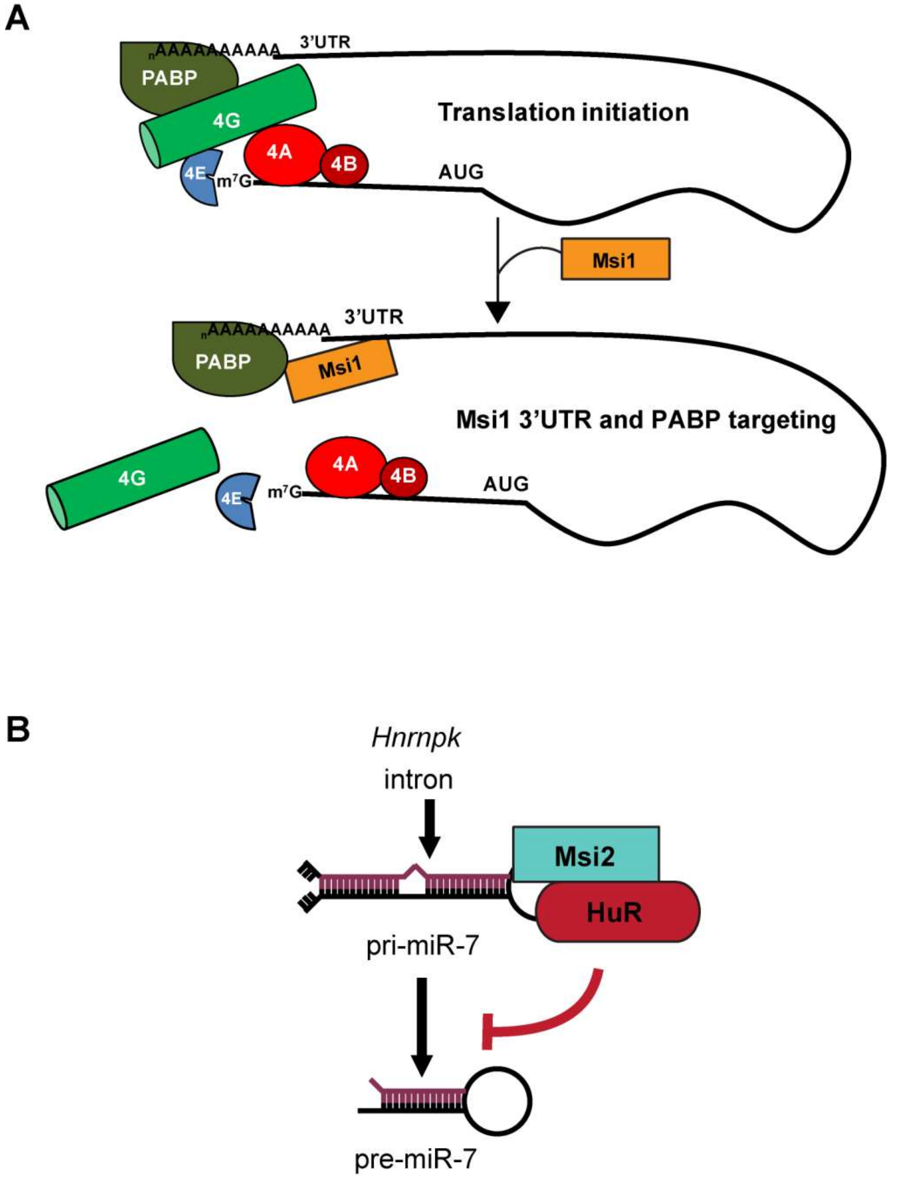
A
nAAAAAAAAAA
3'UTR
PABP
4G
Translation initiation
4A
4B
4E
m7G
AUG
Msi1
nAAAAAAAAAA
3'UTR
PABP
Msi1
Msi1 3'UTR and PABP targeting
4G
4A
4B
4E
m7G
AUG
B
Hnrnpk
intron
Msi2
HuR
pri-miR-7
pre-miR-7

Figure 4. Musashi RNA binding mechanisms. (A) Translational repression by Msi1 via binding target 3'UTR binding sites and PABP. This interaction prevents EIF4G from binding PABP inhibiting transcript circularization and efficient translation. (B) Inhibition of miRNA biogenesis by coordinated binding of Msi2 and HuR to target pri-miRNA stem-loops thus preventing cleavage by Drosha and pre-miRNA formation. Red strand represents guide strand.

CHAPTER 2

Musashi-2 Attenuates AHR Signaling to Expand Human Hematopoietic Stem Cells

Preamble

This chapter is an original published article and is presented in its final format.

“This research was originally published in Nature. Rentas S., Holzapfel N.T., Belew M.S., Pratt G., Voisin V., Wilhelm B.T., Bader G.T., Yeo G.W., Hope K.J. Musashi-2 Attenuates AHR Signaling to Expand Human Hematopoietic Stem Cells. April 28, 2016, 532, 508–511, doi:10.1038/nature17665. Copyright© Nature Publishing Group”

S.R. designed and performed experiments, analyzed data and wrote the manuscript. N.H. constructed CLIP-seq libraries. M.S.B. helped perform CB experiments. G.P. and G.W.Y advised CLIP-seq library construction, performed CLIP-seq bioinformatic analyses and wrote the manuscript. B.W. performed RNA-seq analyses. V.V and G.D.B performed RNA-seq bioinformatic analyses. K.H. conceived the project, supervised the study, analyzed data, interpreted results and wrote the manuscript.

To date there is very little research on what effect RBPs have in controlling self-renewal programs in mouse HSCs, let alone how they function in human HSCs. Therefore the aim of this work was to characterize the role of the RBP MSI2 in human HSCs, since previous findings showed its ortholog regulates HSC activity in mice (de Andrés-Aguayo et al., 2011; Hope et al., 2010; Kharas et al., 2010). Identifying novel regulators of self-renewal in human HSCs can help unlock the unmet clinical need of expanding human HSCs for transplantation therapy. That MSI2 could possibly enhance self-renewal activity was shown by Hope et al., where they provided evidence that overexpression of *Msi2* improved HSC self-renewal and resultant engraftment kinetics. In this work, we took the approach of knocking down and overexpressing *MSI2* and performing *in vitro* and *in vivo* assays to interrogate its self-renewal and differentiation capacity within CB HSPCs. Follow up experiments using next-generation sequencing technologies were then done to characterize its mechanism of action directly in HSPCs. Altogether this work identifies a novel post-transcriptional regulatory axis that facilitates the ex vivo expansion of human HSCs.

Musashi-2 Attenuates AHR Signaling to Expand Human Hematopoietic Stem Cells

Authors Stefan Rentas[1], Nicholas Holzapfel[1,7], Muluken S Belew[1,7], Gabriel Pratt[2,6,7], Veronique Voisin[4], Brian T Wilhelm[5], Gary D Bader[4], Gene W Yeo[2,3,6], Kristin J Hope[1]

Affiliations

[1] Department of Biochemistry and Biomedical Sciences, Stem Cell and Cancer Research Institute, McMaster University, Hamilton, ON, Canada

[2] Department of Cellular and Molecular Medicine, Institute for Genomic Medicine, University of California, San Diego, La Jolla, CA, USA

[3] Department of Physiology, National University of Singapore and Molecular Engineering Laboratory, A*STAR, Singapore

[4] The Donnelly Centre, University of Toronto, Toronto, ON, Canada.

[5] Institute for Research in Immunology and Cancer, University of Montreal, Montreal, QC, Canada

[6] Bioinformatics Graduate Program, University of California, San Diego, La Jolla, CA, USA

[7] Authors contributed equally

Umbilical cord blood (CB)-derived hematopoietic stem cells (HSCs) are essential in many life saving regenerative therapies, but their low number in CB units has

significantly restricted their clinical use despite the advantages they provide during transplantation[1]. Select small molecules that enhance hematopoietic stem and progenitor cell (HSPC) expansion in culture have been identified[2,3], however, in many cases their mechanisms of action or the nature of the pathways they impinge on are poorly understood. A greater understanding of the molecular pathways that underpin the unique human HSC self-renewal program will facilitate the development of targeted strategies that expand these critical cell types for regenerative therapies. Whereas transcription factor networks have been shown to influence the self-renewal and lineage decisions of human HSCs[4,5], the post-transcriptional mechanisms guiding HSC fate have not been closely investigated. Here we show that overexpression of the RNA-binding protein (RBP) Musashi-2 (MSI2) induces multiple pro-self-renewal phenotypes, including a 17-fold increase in short-term repopulating cells and a net 23-fold ex vivo expansion of long-term repopulating HSCs. By performing a global analysis of MSI2-RNA interactions, we determined that MSI2 directly attenuates aryl hydrocarbon receptor (AHR) signaling through post-transcriptional downregulation of canonical AHR pathway components in CB HSPCs. Our study provides new mechanistic insight into RBP-controlled RNA networks that underlie the self-renewal process and give evidence that manipulating such networks ex vivo can provide a novel means to enhance the regenerative potential of human HSCs.

Main

RBP-mediated control of translation in human HSCs and its potential to regulate HSC self-renewal remains underexplored. Here we investigated the role of MSI2 in post-transcriptionally controlling human HSPC self-renewal as it is known to regulate mouse HSCs[6-8], and is predicted to impact mRNA translation[9]. *MSI2* was present and elevated in primitive CB HSPCs and decreased during differentiation, whereas its paralog, *MSI1*, was not expressed (Extended Data Fig. 1a-f). Lentiviral overexpression (OE) of *MSI2* resulted in a 1.5-fold increase in colony forming units (CFU) relative to control, principally due to a 3.7-fold increase in the most primitive CFU-Granulocyte Erythrocyte Monocyte Megakaryocyte (GEMM) colony type (Extended Data Fig. 2a, Fig. 1a). Remarkably, 100% of MSI2 OE CFU-GEMMs generated secondary colonies compared to only 40% of controls. In addition, MSI2 OE yielded 3-fold more colonies per re-seeded CFU-GEMM (Fig. 1b, c, Extended Data Fig. 2b). During *in vitro* culture MSI2 OE resulted in 2.3- and 6-fold more cells relative to control at the 7 and 21-day time points, respectively (Extended Data Fig. 2c, d). Moreover after 7 days in culture MSI2 OE yielded a cumulative 9.3-fold increase in colony forming cells in the absence of changes in cell cycling or death (Extended Data Fig. 2e-h). Altogether, our data demonstrate that enforced expression of MSI2 has potent self-renewal effects on early progenitors and promotes their *in vitro* expansion.

Short-term repopulating cells (STRC) produce a transient multi-lineage graft in NOD-*scid*-*IL2Rγc*$^{-/-}$ (NSG) mice[10], and in patients reconstitute granulocytes and platelets critical for preventing post-transplant infection and bleeding[1]. STRCs overexpressing MSI2 exhibited 1.8-fold more primitive CD34^{+} cells post-infection and a dramatic 17-fold increase in functional STRCs relative to control as determined by limiting dilution analysis (LDA) of human chimerism at 3 weeks post-transplant (Fig. 1d-f, Extended Data Fig. 3a, b). Furthermore, at a protracted engraftment readout time of 6.5 weeks at non-limiting transplant doses, 100% of MSI2 OE STRC transplanted mice were engrafted compared to only 50% of controls, indicating MSI2 OE extended the duration of STRC-mediated engraftment (Extended Data Fig. 3c).

We next explored the effect of shRNA-induced MSI2 knockdown (KD) on HSPC function. MSI2 KD did not alter clonogenic potential but did decrease CFU replating 3-fold (Extended Data Fig. 4a-c). When effects on more primitive culture-initiating cells were explored we found MSI2 KD significantly decreased cell number over culture (Extended Data Fig. 4d, e) independent of increased death or altered cell cycling (data not shown). Upon transplantation, engrafted MSI2 KD GFP$^+$ cells showed no evidence of lineage skewing, yet were strikingly reduced relative to the percentage of GFP$^+$ cells initially transplanted (Extended Data Fig. 4f-h). Combined, our *in vitro* and *in vivo* data show that MSI2 KD reduces self-renewal in early progenitors and HSCs.

To characterize the earliest transcriptional changes induced by modulating MSI2 expression, we performed RNA-seq on CD34$^+$ MSI2 OE and KD cells immediately post-transduction (Supplementary Tables 1, 2). MSI2 OE-induced transcriptional changes anti-correlated with those of MSI2 KD, suggesting OE and KD have opposite effects (Extended Data Fig. 5a). When compared to transcriptome data from 38 human hematopoietic cell subpopulations[4], we observed that genes significantly upregulated upon MSI2 OE and downregulated upon MSI2 KD were exclusively enriched for those highly expressed in HSC and other primitive $CD34^+$ populations (Extended Data Fig. 5b).

Since MSI2 OE conferred an HSC gene expression program, we hypothesized that it could facilitate HSC expansion ex vivo. Remarkably, MSI2 OE induced a 4-fold increase in $CD34^+CD133^+$ phenotypic HSCs relative to control after 7 days of culture (Fig. 2a). We next performed an LDA to define functional HSC frequency before (day 3 post-transduction, D3) and after 7 days of ex vivo culture (day 10, D10; Extended Data Fig. 6a). D3 recipients displayed no altered engraftment as a result of MSI2 OE, however, recipients of MSI2 OE D10-expanded cells displayed multiple phenotypes of enhanced reconstitution relative to control, including a 2-fold increase in BM GFP^+ levels without changes to lineage output, proportionally more GFP^+ cells within the human graft relative to pre-transplant D10 levels, greater GFP mean fluorescence intensity and enrichment of CD34 expression in GFP^{high} cells (Fig. 2b, c, Extended Data Fig. 6b-h). As the lentiviral construct design ensures GFP levels mirror MSI2's, this indicates high levels of MSI2 impart enhanced competitiveness and are conducive to *in vivo* HSPC activity. Importantly, D10 MSI2 OE cultures contained more $CD34^+CD133^+$ cells prior to transplant (Extended Data Fig. 6i), and in accordance, the HSC frequency in D10 MSI2 OE cultures was increased 2-fold relative to the D3 culture time point, whereas control cultures displayed a 3-fold decrease. These results demonstrate that MSI2 OE facilitated an ex vivo net 6-fold increase in HSCs relative to control (Fig. 2g, h, Supplementary Tables 3, 4).

Secondary LDA transplants were performed to fully explore the effects of MSI2 OE and culturing has on self-renewal and long-term HSCs (LT-HSC). Robust engraftment with MSI2 OE did not display altered myelo-lymphopoiesis or leukemic development (Fig. 2e). Secondary LDA measurements revealed BM GFP$^+$ percentage increased 4.6-fold and LT-HSC frequency 3.5-fold with MSI2 OE compared to controls (Fig. 2d, e, f, Supplementary Table 5). This corresponds to MSI2 OE GFP$^+$ HSCs having expanded in primary mice 2.4-fold over input as compared to a decrease of 1.5-fold for control HSCs (Fig. 2g). The level of MSI2 OE-induced *in vivo* fold expansion reflects the behaviour of uncultured HSCs, which undergo similarly controlled expansion during passage in mice[3,11,12]. Finally, when accounting for the total change in GFP$^+$ HSCs upon ex vivo culture, MSI2 OE provided a cumulative 23-fold-expansion of secondary LT-HSC relative to control (Fig. 2g, h) indicating elevated MSI2 provides a significant self-renewal advantage to functional HSCs during ex vivo culture.

To gain mechanistic insights we examined MSI2 OE-induced differentially expressed genes and found Cytochrome P450 1B1 Oxidase (CYP1B1), an effector of AHR signaling[13], amongst the most repressed (Supplementary Table 1). Pathway analysis revealed many predicted AHR targets were enriched in MSI2 OE downregulated (Fig. 3a) and MSI2 KD upregulated gene sets (Extended Data Fig. 7a, b). Binding of the nuclear receptor transcription factor AHR with StemRegenin 1 (SR1) inhibits AHR target gene activation leading to human HSPC expansion in culture[2]. Gene set enrichment analysis (GSEA) revealed MSI2 OE downregulated genes significantly matched the SR1 downregulated gene set in an SR1 dose-dependent manner (Fig. 3b, c), whereas MSI2

KD induced the opposite expression profile (Extended Data Fig. 7c, d). We next examined the overlap of downregulated genes with ChIP-seq-identified AHR targets[14]. This comparison was extended to downregulated genes upon treatment with UM171, another compound that expands HSPCs, but independent of AHR[3]. Direct transcriptional targets of AHR were enriched in the MSI2 OE and SR1 downregulated gene sets by 3.8 and 5.6-fold, respectively, compared to UM171, an overrepresentation maintained for predicted AHR targets and one that suggests MSI2 OE expands HSPCs through AHR signaling attenuation (Fig. 3d, Extended Data Fig. 7e). Furthermore, SR1 treatment increased the percentage of $CD34^+$ cells 8-fold for control cultures compared to only 4-fold with MSI2 OE (Extended Data Fig. 8a, b), a finding that indicates a redundancy in SR1 and MSI2 OE activity on HSPCs, which suggests they act on the same pathway.

To further elucidate the AHR connection, MSI2 OE and control cultures were treated with the AHR agonist 6-Formylindolo(3,2-b)carbazole (FICZ), whose induction of canonical AHR targets in MSI2 OE cells, demonstrates that they remain competent for AHR activation (Extended Data Fig. 8c). FICZ induced a dramatic reversal of the MSI2 OE-mediated increases in primary CFU-GEMMs and their replating capacities (Fig. 3e, f). Furthermore, FICZ-treated MSI2 OE cultures displayed greater losses in phenotypic HSPCs compared to controls which showed no change (Extended Data Fig. 8d, e). Altogether, these results demonstrate agonist-induced restoration of AHR activity reduces MSI2 OE’s pro-self-renewal effects and strongly supports downregulation of AHR signaling as the mechanism through which MSI2 OE achieves HSPC expansion.

To identify key RNA targets underlying MSI2 function, we analyzed global MSI2 protein-RNA interactions using CLIP-seq (Extended Data Fig. 9a, b)[15]. Mapped reads identified highly correlated gene RPKMs and enrichment of significantly overlapping clusters within >6000 protein-coding genes from replicate experiments (Extended Data Fig. 9c, Fig. 4a, b). Within the top 40% of reproducible clusters, MSI2 bound predominantly to mature mRNA within their 3' untranslated regions (3'UTRs) (Fig. 4c). Importantly, 9% of annotated protein-coding genes were reproducible MSI2 targets, compared to 0.2% of long non-coding RNAs (Extended Data Fig. 9d), suggesting MSI2 controls stability or translation of coding mRNAs. Motif analyses identified a consensus pentamer (U/G)UAGU resembling the known mouse Msi1 binding sequence[9,16] within binding sites in all genic regions and significantly more conserved than background (Fig. 4d, Extended Data Fig. 9e-h). MSI2 binding sites within Msi1 targets[16] indicate Musashi proteins may bind the same genes through 3'UTR-embedded motifs (Extended Data Fig. 9i). Finally, target gene ontology analysis revealed 186 biological processes categories (Supplementary Table 6), among the most significant of which were electron transport, estrogen receptor signaling regulation and metabolism of small molecules, all processes known to be transcriptionally impacted by AHR signaling[17].

Strikingly, among the top 2% of enriched CLIP-seq targets (Supplementary Table 7) were the 3'UTRs of heat shock protein 90 (HSP90) and CYP1B1, two AHR pathway components. Each exhibited multiple MSI2 binding motifs correlating with overlapping clusters of CLIP-seq reads (Fig. 4e, Extended Data Fig. 10a). Querying MSI2's ability to post-transcriptionally regulate these genes during HSPC expansion, we looked for instances of uncoupled transcript and protein expression. HSP90 displayed uncoupling of transcript (1.6-fold up) and protein (1.6-fold down) early in culture, but at 7 days showed further upregulated transcript (2.5-fold) and variable protein levels (Fig. 4f, Extended Data Fig. 10b). Since AHR-HSP90 binding is critical for ligand-dependent transcriptional activity[13], downregulation of HSP90 protein at the outset of HSPC culture would be expected to reduce latent AHR complex formation and attenuate AHR signaling (Fig. 3a). Indeed, CYP1B1 transcript and protein displayed 2-fold reductions early in culture, consistent with decreased AHR pathway activity, however at day 7, CYP1B1 transcripts were upregulated 1.7-fold, uncoupled from 2-fold downregulated protein (Fig. 4g, Extended Data Fig. 10c). To test if MSI2 directly mediates post-transcriptional repression of these targets, *CYP1B1* and *HSP90* 3'UTR regions were coupled to luciferase. MSI2 OE induced significant reductions in luciferase signal from both reporters, an effect mitigated upon mutating the core CLIP-seq-identified UAG motifs (Extended Data Fig. 10d, e). Since MSI2 OE-mediated post-transcriptional downregulation of the AHR pathway converged on CYP1B1 protein repression throughout culture, we explored the effects of inhibiting CYP1B1 independently with (E)-2,3',4,5'-Tetramethoxystilbene (TMS) on HSPCs. During culture, TMS increased the frequency and total numbers of CD34$^+$ cells by 1.5- and 2-fold respectively (Fig. 4h, i), phenocopying the effects of MSI2 OE. Lastly, co-overexpression of 3'UTRless CYP1B1 with MSI2 decreased secondary CFU-GEMM replating efficiency (Extended Data Fig. 10f and g) suggesting that CYP1B1, while typically used to report on AHR signaling, promotes HSPC differentiation.

Our work identifies MSI2 as an important new mediator of human HSPC self-renewal and ex vivo expansion by coordinating the post-transcriptional regulation of proteins belonging to a shared self-renewal regulatory pathway (Extended Data Fig. 10h). We envision that manipulation of the post-transcriptional circuitry controlled by RBPs will provide a novel and powerful means by which to enhance the regenerative potential of not only human HSCs but other stem cell types as well.

References

1 Miller, P. H., Knapp, D. J. & Eaves, C. J. Heterogeneity in hematopoietic stem cell populations: implications for transplantation. *Curr Opin Hematol* **20**, 257-264 (2013).

2 Boitano, A. E. *et al.* Aryl hydrocarbon receptor antagonists promote the expansion of human hematopoietic stem cells. *Science* **329**, 1345-1348 (2010).

3 Fares, I. *et al.* Pyrimidoindole derivatives are agonists of human hematopoietic stem cell self-renewal. *Science* **345**, 1509-1512 (2014).

4 Novershtern, N. *et al.* Densely interconnected transcriptional circuits control cell states in human hematopoiesis. *Cell* **144**, 296-309 (2011).

5 Laurenti, E. *et al.* The transcriptional architecture of early human hematopoiesis identifies multilevel control of lymphoid commitment. *Nat Immunol* **14**, 756-763 (2013).

6 Hope, K. *et al.* An RNAi screen identifies Msi2 and Prox1 as having opposite roles in the regulation of hematopoietic stem cell activity. *Cell Stem Cell* **7**, 101-114 (2010).

7 de Andrés-Aguayo, L. *et al.* Musashi 2 is a regulator of the HSC compartment identified by a retroviral insertion screen and knockout mice. *Blood* **118**, 554-618 (2011).

8 Park, S. M. *et al.* Musashi-2 controls cell fate, lineage bias, and TGF-beta signaling in HSCs. *J Exp Med* **211**, 71-87 (2014).

9 Ohyama, T. *et al.* Structure of Musashi1 in a complex with target RNA: the role of aromatic stacking interactions. *Nucleic Acids Res* **40**, 3218-3231 (2012).

10 Glimm, H. *et al.* Previously undetected human hematopoietic cell populations with short-term repopulating activity selectively engraft NOD/SCID-beta2 microglobulin-null mice. *J Clin Invest* **107**, 199-206 (2001).

11 Cashman, J. D. & Eaves, C. J. Human growth factor-enhanced regeneration of transplantable human hematopoietic stem cells in nonobese diabetic/severe combined immunodeficient mice. *Blood* **93**, 481-487 (1999).

12 Holyoake, T. L., Nicolini, F. E. & Eaves, C. J. Functional differences between transplantable human hematopoietic stem cells from fetal liver, cord blood, and adult marrow. *Exp Hematol* **27**, 1418-1427 (1999).

13 Mimura, J. & Fujii-Kuriyama, Y. Functional role of AhR in the expression of toxic effects by TCDD. *Biochim Biophys Acta* **1619**, 263-268 (2003).

14 Lo, R. & Matthews, J. High-Resolution Genome-wide Mapping of AHR and ARNT Binding Sites by ChIP-Seq. *Toxicol Sci* **130**, 349-361 (2012).

15 Yeo, G. W. *et al.* An RNA code for the FOX2 splicing regulator revealed by mapping RNA-protein interactions in stem cells. *Nat Struct Mol Biol* **16**, 130-137 (2009).

16 Katz, Y. *et al.* Musashi proteins are post-transcriptional regulators of the epithelial-luminal cell state. *Elife* **3**, e03915 (2014).

17 Tijet, N. *et al.* Aryl hydrocarbon receptor regulates distinct dioxin-dependent and dioxin-independent gene batteries. *Mol Pharmacol* **69**, 140-153 (2006).

Methods

Mice

NOD-*scid*-*IL2Rγc*$^{-/-}$ (Jackson Laboratory) mice were bred and maintained in the Stem Cell Unit animal barrier facility at McMaster University. All procedures received the approval of the Animal Research Ethics Board at McMaster University.

Isolation of primitive human hematopoietic cells and flow cytometry

All patient samples were obtained with informed consent and with the approval of local human subject research ethics boards at McMaster University. Human umbilical cord blood mononuclear cells were collected by centrifugation with Ficoll-Paque Plus (GE), followed red blood cell lysis with ammonium chloride (Stemcell Technologies). Cells were then incubated with a cocktail of lineage specific antibodies (CD2, CD3, CD11b, CD11c, CD14, CD16, CD19, CD24, CD56, CD61, CD66b, and GlyA; Stemcell Technologies) for negative selection of Lin$^-$ cells using an EasySep immunomagnetic column (Stemcell Technologies). Live cells were discriminated on the basis of cell size, granularity and, as needed, absence of viability dye 7-AAD (BD Biosciences) uptake. All flow cytometry analysis was performed using a BD LSR II instrument (BD Biosciences). Data acquisition was conducted using BD FACSDiva software (BD Biosciences) and analysis was performed using FlowJo software (Tree Star).

HSPC sorting and qRT-PCR analysis

To quantify *MSI2* expression in human HSPCs, Lin$^-$ CB cells were stained with the appropriate antibody combinations to resolve HSC (CD34$^+$ CD38$^-$ CD45RA$^-$ CD90$^+$), MPP (CD34$^+$ CD38$^-$ CD45RA$^-$ CD90$^-$), CMP (CD34$^+$ CD38$^+$ CD71$^-$) and EP (CD34$^+$ CD38$^+$ CD71$^+$) fractions as similarly described previously[18,19] with all antibodies from BD Biosciences: CD45RA (HI100), CD90 (5E10), CD34 (581), CD38 (HB7) and CD71 (M-A712). Cell viability was assessed using the viability dye 7AAD (BD Biosciences). All cell subsets were isolated using a BD FACSAria II cell sorter (BD Biosciences) or a MoFlo XDP cell sorter (Beckman Coulter). HemaExplorer[20] analysis was used to confirm *MSI2* expression in human HSPCs and across the hierarchy. For all qRT-PCR determinations total cellular RNA was isolated with TRIzol LS reagent according to the manufacturer's instructions (Invitrogen) and cDNA was synthesized using the qScript cDNA Synthesis Kit (Quanta Biosciences). qRT-PCR was done in triplicate with PerfeCTa qPCR SuperMix Low ROX (Quanta Biosciences) with gene specific probes (Universal Probe Library, UPL, Roche) and primers: MSI2 UPL-26, Fggcagcaagaggatcagg, R-ccgtagagatcggcgaca; HSP90 UPL-46, F-gggcaacacctctacaagga, R-cttgggtctgggtttcctc; CYP1B1 UPL-20, F-acgtaccggccactatcact, R-ctcgagtctgcacatcagga; GAPDH UPL-60, F-agccacatcgctcagacac, R-gcccaatacgaccaaatcc; ACTB (UPL Set Reference Gene Assays, Roche). The mRNA content of samples compared by qRT-PCR was normalized based on the amplification of GAPDH or ACTB.

Lentivirus production and western blot validation

MSI2 shRNAs were designed with the Dharmacon algorithm (http://www.dharmacon.com). Predicted sequences were synthesized as complimentary oligonucleotides, annealed and cloned downstream of the H1 promoter of the modfied cppt-PGK-EGFP-IRES-PAC-WPRE lentiviral expression vector[18]. Sequences for the MSI2 targeting and control RFP targeting shRNAs were as follows: shMSI2, 5'-gagagatcccactacgaaa-3'; shRFP, 5'-gtgggagcgcgtgatgaac-3'. Human MSI2 cDNA (BC001526; Open Biosystems) was subcloned into the MA bi-directional lentiviral expression vector[21]. Human CYP1B1 cDNA (BC012049; Open Biosystems) was cloned in to psMALB[22]. All lentivirus was prepared by transient transfection of 293FT (Invitrogen) cells with pMD2.G and psPAX2 packaging plasmids (Addgene) to create VSV-G pseudotyped lentiviral particles. All viral preparations were titrated on HeLa cells before use on cord blood. Standard SDS-PAGE and western blotting procedures were performed to validate the effect of knockdown on transduced NB4 cells (DSMZ) and over expression on 293FT cells. Immunoblotting was performed with anti-MSI2 rabbit monoclonal IgG (EP1305Y, Epitomics) and β-actin mouse monoclonal IgG (ACTBD11B7, Santa Cruz Biotechnology) antibodies. Secondary antibodies used were

IRDye 680 goat anti-rabbit IgG and IRDye 800 goat anti-mouse IgG (LI-COR). 293FT and NB4 cell lines tested negative for mycoplasma. NB4 cells were authenticated by ATRA treatment prior to use.

CB transduction

CB transductions were conducted as described previously[18,23]. Briefly, thawed Lin^- CB, flow-sorted Lin^- $CD34^+$ $CD38^-$ or Lin^- $CD34^+$ $CD38^+$ cells were prestimulated for 8-12 hours in StemSpan medium (StemCell Technologies) supplemented with growth factors Interleukin 6 (IL-6; 20 ng/ml, Peprotech), Stem cell factor (SCF; 100 ng/ml, R&D Systems), Flt3 ligand (FLT3-L; 100 ng/ml, R&D Systems) and Thrombopoietin (TPO; 20 ng/ml, Peprotech). Lentivirus was then added in the same medium at a multiplicity of infection of 30–100 for 24 hours. Cells were then given 2 days post transduction before use in *in vitro* or *in vivo* assays. For *in vitro* CB studies biological (experimental) replicates were performed with three independent CB samples.

Clonogenic progenitor assays

Human clonogenic progenitor cell assays were done in semi-solid methylcellulose medium (Methocult H4434; Stem Cell Technologies) with flow-sorted GFP^+ cells post transduction (500 cells/ml) or from day seven cultured transduced cells (12000 cells/ml). Colony counts were carried out after 14 days of incubation. CFU-GEMMs can seed secondary colonies due to their limited self-renewal potential[24]. MSI2 OE and control CFU-GEMM replating for secondary CFU analysis was performed by picking single CFU-GEMMs at day 14 and disassociating colonies by vortexing. Cells were spun and resuspended in fresh methocult, mixed with a blunt end needle and syringe, and then plated into single wells of a 24-well plate. Secondary CFU analysis for shMSI2 and shControl expressing cells was performed by harvesting total colony growth from a single dish (since equivalent numbers of CFU-GEMMs), resuspending cells in fresh methocult by mixing vigorously with a blunt end needle and syringe and then plating into replicate 35 mm tissue culture dishes. In both protocols, secondary colony counts were done following incubation for 10 days. For primary and secondary colony forming assays performed with the AHR agonist 6-Formylindolo(3,2-b)carbazole (FICZ; Santa Cruz Biotechnology), 200 nM FICZ or 0.1% DMSO was added directly to H4434 methocult medium. 2-way ANOVA analysis was performed examining secondary CFU output and FICZ treatment for MSI2 OE or control conditions. Colonies were imaged with a Q-Colour3 digital camera (Olympus) mounted to an Olympus IX5 microscope with a 10X objective lens. Image-Pro Plus imaging software (Media Cybernetics) was used to acquire pictures and subsequent image processing was performed with ImageJ software (NIH).

Lin$^-$ CB and Lin$^-$ CD34$^+$ suspension cultures

Transduced human Lin$^-$ CB cells were sorted for GFP expression and seeded at a density of 1 x 10^5 cells/ml in IMDM 10% FBS supplemented with human growth factors IL-6 (10 ng/ml), SCF (50 ng/ml), FLT3-L (50 ng/ml), and TPO (20 ng/ml) as previously described[25]. To generate growth curves, every seven days cells were counted, washed, and resuspended in fresh medium with growth factors at a density of 1 x 10^5 cells/ml. Cells from suspension cultures were also used in clonogenic progenitor assays, cell cycle and apoptosis assays. Experiments performed on transduced Lin$^-$ CD34$^+$ CB cells used serum free conditions as described in the CB transduction subsection of the Methods. For *in vitro* CB studies biological (experimental) replicates were performed with three independent CB samples.

Cell cycle and apoptosis assays

Monitoring cell cycle progression was performed with the addition of BrdU to day 10 suspension cultures at a final concentration of 10 μM. After three hours of incubation, cells were assayed with the BrdU Flow Kit (BD Biosciences) according to the manufacture's protocol. Cell proliferation and quiescence was measured by Ki67 (BD Bioscience) and Hoechst 33342 (Sigma) on day 4 suspension cultures after fixing and permeabilizing cells with the Cytofix/Cytoperm kit (BD Biosciences). For apoptosis analysis, Annexin V (Invitrogen) and 7-AAD (BD Bioscience) staining on day 7 suspension cultures was performed according to the manufacture's protocol.

Intracellular flow cytometry

Lin$^-$ CB cells were initially stained with anti-CD34 PE (581) and anit-CD38 APC (HB7) antibodies (BD Biosciences) then fixed with the Cytofix/Cytoperm kit (BD Biosciences) according to the manufacturer's instructions. Fixed and permeabilized cells were immunostained with anti-MSI2 rabbit monoclonal IgG antibody (EP1305Y, Abcam) and detected by Alexa-488 goat anti-rabbit IgG antibody (Invitrogen).

RNA-Sequencing data processing

$CD34^+$ cells were transduced with MSI2 OE or KD lentivirus along with their corresponding controls and then sorted for GFP expression 3 days later. Transductions for MSI2 OE and KD were each performed on two independent CB samples. Total RNA from transduced cells ($>1x10^5$) was isolated using TRIzol LS as recommended by the manufacturer (Invitrogen), and then further purified using RNeasy columns (Qiagen). Sample quality was assessed using Bioanalyzer RNA Nano chips (Agilent). Paired-end, barcoded RNA-seq sequencing libraries were then generated using the TruSeq RNA Sample Prep Kit (v2) (Illumina) following the manufacturer's protocols starting from 1ug of total RNA. Quality of library generation was then assessed using a Bioanalyzer platform (Agilent) and Illumina MiSeq-QC run was performed or quantified by qPCR using KAPA quantification kit (KAPA Biosystems). Sequencing was performed using an Illumina HiSeq2000 using TruSeq SBS v3 chemistry at the Institute for Research in Immunology and Cancer's Genomics Platform (University of Montreal) with cluster density targeted at 750k clusters/mm2 and paired-end 2x100bp read lengths. For each sample, 90-95M reads were produced and mapped to the hg19 (GRCh37) human genome assembly using CASAVA (version 1.8). Read counts generated by CASAVA were processed in EdgeR (edgeR_3.12.0, R 3.2.2) using TMM normalization, paired design, and estimation of differential expression using a generalized linear model (glmFit). The false discovery rate (FDR) was calculated from the output p-values using the Benjamini-Hochberg method. The fold change of logarithm of base 2 of TMM normalized data (logFC) was used to rank the data from top up-regulated to top down-regulated genes and FDR (0.05) was used to define significantly differentially expressed genes. RNA-seq data has been deposited in NCBI's Gene Expression Omnibus and are accessible through GEO Series accession number GSE70685.

GSEA and iRegulon AHR target prediction

iRegulon[26] was used to retrieve the top 100 AHR predicted targets with a minimal occurrence count threshold of 5. The data were analyzed using GSEA[27] with ranked data as input with parameters set to 2000 gene-set permutations.

GSEA and StemRegenin 1 (SR1) gene-sets

The Gene Expression Omnibus (GEO) dataset GSE28359 that contains Affymetrix Human Genome U133 Plus 2.0 Array gene expression data of CD34$^+$ cells treated with SR1 at 30 nM, 100nM, 300nM and 1000nM was used to obtain lists of genes differentially expressed in the treated samples compared to the control ones (0 nM)[2]. Data were background corrected using Robust Multi-Array Average (RMA) and quantile normalized using the *expresso()* function of the affy Bioconductor package (affy_1.38.1 , R 3.0.1). Lists of genes were created from the 150 genes top upregulated and top downregulated by the SR1 treated samples at each dose compared to the non-treated samples (0 nM). The data were analyzed using GSEA with ranked data as input with parameters set to 2000 gene-set permutations. Normalized enrichment score (NES) and false discovery rate (FDR) were calculated for each comparison.

DMAP population comparisons

The GEO dataset GSE24759 that contains Affymetrix GeneChip HT-HG_U133A Early

Access Array gene expression data of 38 distinct hematopoietic cell states[4] was compared to the OE and KD data. GSE24759 data were background corrected using Robust Multi-Array Average (RMA), quantile normalized using the *expresso()* function of the affy Bioconductor package (affy_1.38.1 , R 3.0.1), batch corrected using the *ComBat()* function of the sva package (sva_3.6.0) and scaled using the standard score. Bar graphs were created by calculating for significantly differentially expressed genes the number of scaled data that were above (>0) or below (<0) the mean for each population. Percentages indicating time the observed value (set of up or downregulated genes) was better represented in that population than random values were calculated from 1000 trials.

AHR ChIP-seq comparison to downregulated gene sets

A unique list of genes closest to AHR bound regions previously identified from TCDD-treated MCF7 ChIP-seq data[14] was used to calculate the overlap with genes showing >1.5-fold down regulation with UM171 (35 nM) and SR1 (500 nM) relative to DMSO treated samples[3] as well as with genes significantly downregulated in MSI2 OE versus control treated samples (FDR<0.05). Percentage of downregulated genes with AHR bound regions was then graphed for each gene set. P-values were generated with Fisher's exact test between gene lists.

oPOSSUM analysis for promoter AHR binding sites in downregulated gene sets

AHR transcription factor binding sites in downregulated gene sets were identified with oPOSSUM-3[28]. Genes showing >1.5-fold down regulation with UM171 (35 nM) and SR1 (500 nM) relative to DMSO treated samples[3] were used along with significantly downregulated genes (FDR<0.05) with EdgeR analyzed MSI2 OE versus control treated samples. The three gene lists uploaded into oPOSSUM-3 and the AHR:ARNT transcription factor binding site profile was used with the matrix score threshold set at 80% and analyzing the region 1500 bp upstream and 1000 bp downstream of transcription start site. Percentage of downregulated genes with AHR binding sites in the promoter was then graphed for each gene set. Fisher's exact test was used to identify significant overrepresentation of AHR binding sites in gene lists relative to background.

Analysis for human chimerism

NSG mice were sublethally irradiated (315 cGy) one day prior to intrafemoral injection with transduced cells carried in IMDM 1% FBS at 25μl per mouse. Injected mice were analyzed for human hematopoietic engraftment at 12-14 weeks post transplantation or 3 and 6.5 weeks for STRC experiments. Mouse bones (femurs, tibiae and pelvis) and spleen were harvested and bones were crushed with a mortar and pestle then filtered in to single cell suspensions. Bone marrow and spleen cells were blocked with mouse Fc block (BD Biosciences) and human IgG (Sigma) and then stained with fluorochrome-conjugated antibodies specific to human hematopoietic cells. For multilineage engraftment analysis, cells from mice were stained with CD45 (HI30) (Invitrogen), CD33 (P67.6), CD15 (HI98), CD14 (MφP9), CD19 (HIB19), CD235a/GlyA (GA-R2), CD41a (HIP8) and CD34 (581) (BD Biosciences).

HSC and STRC xenotransplantations

For MSI2 KD in HSCs 5.0×10^4 and 2.5×10^4 sorted Lin^- $CD34^+$ $CD38^-$ cells were used per short-hairpin transduction experiment leading to transplantation of day zero equivalent cell doses of 10×10^3 and 6.25×10^3, respectively per mouse. For STRC LDA transplantation experiments 1×10^5 sorted $CD34^+CD38^+$ cells were used per control and MSI2 OE transduction. After assessing levels of gene transfer, day zero equivalent GFP^+ cell doses were calculated to perform the LDA. Recipients with greater than 0.1% $GFP^+CD45^{+/-}$ cells were considered to be repopulated. For STRC experiments that readout extended engraftment at 6.5 weeks, 2×10^5 $CD34^+$ $CD38^+$ cells were used per OE and control transduction allowing for non-limiting 5×10^4 day zero equivalent cell doses per mouse. For HSC expansion and LDA experiments $CD34^+CD38^-$ cells were sorted and transduced with MSI2 OE or control vectors (50,000 cells per condition) for three days and then analyzed for gene-transfer levels (% $GFP^{+/-}$) and primitive cell marker expression (% CD34 and CD133). To ensure equal numbers of GFP^+ cells were transplanted in both control and MSI2 OE mice, we added identically cultured GFP^- cells to the MSI2 culture to match % GFP^+ of the control culture (necessary due to the differing efficiency of transduction). The adjusted OE culture was recounted and aliquoted (63,000 cells) to match the output of half the control culture. Three day 0 equivalent GFP^+ cell doses (1000, 300 and 62) were then transplanted per mouse to perform the D3 primary LDA. A second aliquot of the adjusted OE culture was then taken and put in to culture in parallel with the remaining half of the control culture for performing another LDA after 7 days of growth (10 days total growth, D10 primary LDA). Altogether, 4 cell doses were transplanted, if converted back to day 0 equivalents these equaled approximately 1000, 250, 100, and 20 GFP^+ cells per mouse, respectively.

Pooled bone marrow from six engrafted primary mice that received D10 cultured control or MSI2 OE cells (from 2 highest doses transplanted) was aliquoted in to 4 cell doses of 15 million, 10 million, 6 million, 2 million and 1 million cells. Numbers of GFP$^+$ cells within primary mice was estimated from nucleated cell counts obtained from NSG femurs, tibias and pelvis and from Colvin et al.[29]. Actual numbers of GFP$^+$ cells used for determining numbers of GFP$^+$ HSCs and the number of mice transplanted for all LDA experiments is found in Supplementary Tables 3-5. The cutoff for HSC engraftment was a demonstration of multilineage reconstitution which was set at BM having >0.1% GFP$^+$ CD33$^+$ and >0.1% GFP$^+$ CD19$^+$ cells. Assessment of HSC and STRC frequency was carried out by using ELDA software[30]. For all mouse transplantation experiments, mice were aged (6-12wk) and sex matched. All transplanted mice were included for analysis unless mice died from radiation sickness before the experimental endpoint. No randomization or blinding was performed for animal experiments. Approximately 3-6 mice were used per cell dose for each CB transduction and transplantation experiment.

UV cross-linking immunoprecipitation sequencing (CLIP-seq) library preparation

CLIP-seq was performed as previously described[15]. Briefly, 25 million NB4 cells, a transformed human cell line of hematopoietic origin, were washed in PBS and UV-cross-linked at 400mJ/cm^2 on ice. Cells were pelleted, lysed in wash buffer (PBS, 0.1% SDS, 0.5% Na-Deoxycholate, 0.5% NP-40), DNAse treated, and supernatants from lysates were collected for immunoprecipitation. MSI2 was immunoprecipitated overnight using 5 μg of anti-MSI2 antibody (EP1305Y, Abcam) and Protein A Dynabeads (Invitrogen). Beads containing immunoprecipated RNA were washed twice with wash buffer, high-salt wash buffer (5X PBS, 0.1% SDS, 0.5% Na-Deoxycholate, 0.5% NP-40), and PNK buffer (50 mM Tris-Cl pH 7.4, 10 mM $MgCl_2$, 0.5% NP-40). Samples were then treated with 0.2 U MNase for 5 minutes at 37 degrees with shaking to trim immunopreciptated RNA. MNase inactivation was then carried out with PNK + EGTA buffer (50 mM Tris-Cl pH 7.4, 20 mM EGTA, 0.5% NP-40). The sample was dephosphorylated using alkaline phosphatase (CIP, NEB) at 37 degrees for 10 followed by washing with PNK+EGTA, PNK buffer, and then 0.1 mg/mL BSA in nuclease free water. 3' RNA linker ligation was performed at 16 degrees overnight with the following adapter: 5' P-UGGAAUUCUCGGGUGCCAAGG-puromycin. Samples were then washed with PNK buffer, radiolabelled using P32-y-ATP (Perkin Elmer), run on a 4-12% Bis-Tris gel and then transferred to a nitrocellulose membrane. The nitrocellulose membrane was developed via autoradiography and RNA-protein complexes 15-20 kDa above the molecular weight of MSI2 was extracted with Proteinase K followed by RNA extraction with acid phenol-chloroform. A 5' RNA linker (5' HO-GUUCAGAGUUCUACAGUCCGACGAUC-OH) was ligated to the extracted RNA using T4 RNA ligase (Fermentas) for two hours and the RNA was again purified using acid phenol-chloroform. Adapter ligated RNA was re-suspended in nuclease free water and reverse transcribed using Superscript III reverse transcriptase (Invitrogen). 20 cycles of PCR were performed using NEB Phusion Polymerase using a 3' PCR primer that contained a unique Illumina barcode sequence. PCR products were run on an 8% TBE gel. Products ranging between 150-200 bp were extracted using the QIAquick gel extraction kit (Qiagen) and re-suspended in nuclease free water. Two separate libraries were prepared and sent for single-end 50 bp Illumina sequencing at the Institute for Genomic Medicine at the University of California, San Diego. 47,098,127 reads from the first library passed quality filtering of which 73.83% mapped uniquely to the human genome. 57,970,220 reads from the second library passed quality filtering of which 69.53% mapped uniquely to the human genome. CLIP-data reproducibility was verified through high correlation between gene RPKMs and statistically significant overlaps in the clusters and genes within replicates. CLIP-seq data has been deposited in NCBI's Gene Expression Omnibus and are accessible through GEO Series accession number GSE69583.

CLIP-seq mapping and cluster identification

Before sequence alignment of CLIP-seq reads to the human genome was performed, sequencing reads from libraries were trimmed of poly-A tails, adapters, and low quality ends using Cutadapt with parameters --match-read-wildcards --times 2 -e 0 -O 5 --quality-cutoff' 6 -m 18 -b TCGTATGCCGTCTTCTGCTTG -b ATCTCGTATGCCGTCTTCTGCTTG -b CGACAGGTTCAGAGTTCTACAGTCCGACGATC -b TGGAATTCTCGGGTGCCAAGG -b AAAAAAAAAAAAAAAAAAAAAAAAAAAAAAAAAAAAAAAAAAAAAAAAA A -b TTTTTTTTTTTTTTTTTTTTTTTTTTTTTTTTTTTTTTTTTTTTTTTTTT. Reads were then mapped against a database of repetitive elements derived from RepBase (version 18.05). Bowtie (version 1.0.0) with parameters -S -q -p 16 -e 100 -l 20 was used to align reads against an index generated from Repbase sequences[31]. Reads not mapped to

Repbase sequences were aligned to the hg19 human genome (UCSC assembly) using STAR (version 2.3.0e)[32] with parameters --outSAMunmapped Within –outFilterMultimapNmax 1 –outFilterMultimapScoreRange 1. To identify clusters in the genome of significantly enriched CLIP-seq reads, reads that were PCR replicates were removed from each CLIP-seq library using a custom script of the same method as[33], otherwise reads were kept at each nucleotide position when more than one read's 5' end was mapped. Clusters were then assigned using the CLIPper software with parameters --bonferroni --superlocal --threshold-[34]. The ranked list of significant targets was calculated assuming a Poisson distribution, where the observed value is the number of reads in the cluster, and the background is the number of reads across the entire transcript and or across a window of 1000 bp +/- the predicted cluster.

Gene annotations for CLIP-seq

Transcriptomic regions and gene classes were defined using annotations found in gencode v17. Depending on the analysis clusters were either associated by the Gencode annotated 5' UTR, 3' UTR, CDS or intronic regions. If a cluster overlapped multiple regions, or a single part of a transcript was annotated as multiple regions, clusters were iteratively assigned first as CDS, then 3' UTR, 5' UTR and finally as proximal (<500 bases from an exon) and distal (>500 bases from an exon) introns. Overlapping peaks were calculated using bedtools and pybedtools[35,36].

Gene ontology analysis for CLIP-seq

Significantly enriched gene ontology (GO) terms were identified using a hypergeometric test that compared the number of genes that were MSI2 targets in each GO term to genes expressed in each GO term as the proper background. Expressed genes were identified by using the control samples in SRA study SRP012062. Mapping was performed identically to CLIP-seq mapping, without peak calling and changing the STAR parameter outFilterMultimapNmax to 10. Counts were calculated with featureCounts[37] and RPKMs were then computed. Only genes with a mean RPKM > 1 between the two samples were used in the background expressed set.

De-novo motif and conservation analysis for CLIP-seq

Randomly located clusters within the same genic regions as predicted MSI2 clusters were used to calculate a background distribution for motif and conservation analyses. Motif analysis was performed using the HOMER algorithm as in Lovci et al.[34]. For evolutionary sequence conservation analysis the mean (mammalian) phastCons score for each cluster was used.

Immunofluorescence

CD34$^+$ cells (>5x10^4) were transduced with MSI2 OE or control lentivirus, after 3 days GFP$^+$ cells were sorted and then put back in to StemSpan medium containing growth factors IL-6 (20 ng/ml), SCF (100 ng/ml), FLT3-L (100 ng/ml) and TPO (20 ng/ml). A minimum of 10,000 cells were used for immunostaining at culture days 3 and 7 post GFP-sort. Cells were fixed in 2% PFA for 10 minutes, washed with PBS and then cytospun on to glass slides. Cytospun cells were then permeabilized (PBS 0.2 % Triton X-100) for 20 minutes, blocked (PBS 0.1% saponin 10% donkey serum) for 30 minutes and stained with primary antibodies (anti-CYP1B1 antibody, EPR14972, Abcam; anti-HSP90 antibody, 68/hsp90, BD Biosciences) in PBS 10% donkey serum for 1 hour. Detection with secondary antibody was performed in PBS 10% donkey serum with Alexa-647 donkey anti-rabbit antibody or Alexa-647 donkey anti-mouse antibody for 45 minutes. Slides were mounted with Prolong Gold Antifade containing DAPI (Invitrogen). Several images (200-1000 cells total) were captured per slide at 20X magnification using an Operetta HCS Reader (Perkin Elmer) with epifluorescence illumination and standard filter sets. Columbus software (Perkin Elmer) was used to automate the identification of nuclei and cytoplasm boundaries in order quantify mean cell fluorescence.

Luciferase reporter gene assay

A 271 bp region of the *CYP1B1* 3'UTR that flanked CLIP-seq identified MSI2 blinding sites was cloned from human HEK293FT genomic DNA using the forward primer GTGACACAACTGTGTGATTAAAGG and reverse primer TGATTTTTATTATTTTGGT AATGGTG and placed downstream of renilla luciferase in the dual-luciferase reporter vector, pGL4 (Promega). A 271 bp geneblock (IDT) with 6 TAG>TCC mutations was cloned in to pGL4 using XbaI and NotI. The *HSP90* 3'UTR was amplified from HEK293FT genomic DNA with the forward primer TCTCTGGCTGAGGGATGACT and reverse primer TTTTAAGGCCAAGGAATTAAGTGA and cloned in pGL4. A geneblock of the *HSP90* 3'UTR (IDT) with 14 TAG>TCC mutations was cloned in to pGL4 using SfaAI and NotI. Co-transfection of wild type or mutant luciferase reporter (40 ng) and control or MSI2 OE lentiviral expression vector (100 ng) was performed in the non-Musashi1 and 2 expressing NIH-3T3 cell line. 50,000 cells were used per co-transfection. Reporter activity was measured using the Dual-Luciferase Reporter Assay System (Promega) 36-40 hours later.

MSI2 OE suspension cultures with AHR antagonist SR1 and agonist FICZ

For MSI2 OE cultures with the AHR antagonist SR1, Lin$^-$ CD34$^+$ cells were transduced with MSI2 OE or control lentivirus in medium supplemented with SR1 (750 nM; Abcam) or DMSO vehicle (0.1%). GFP$^+$ cells were isolated (20,000 cells per culture) and allowed to proliferate with or without SR1 for an additional 7 days at which point they were counted and immunophenotyped for CD34 and CD133 expression. For MSI2 OE cultures with the AHR agonist FICZ, Lin$^-$ CD34$^+$ cells were transduced with MSI2 OE or control lentivirus. GFP$^+$ cells were isolated (20,000 cells per culture) and allowed to proliferate with FICZ (200 nM; Santa Cruz Biotechnology) or DMSO (0.1%) for an additional 3 days at which point they were immunophenotyped for CD34 and CD133 expression.

HSPC expansion with (E)-2,3',4,5'-Tetramethoxystilbene (TMS)

Lin$^-$ CD34$^+$ cells were cultured for 72 hours (lentiviral treated but non-transduced flow-sorted GFP$^-$ cells) in StemSpan medium containing growth factors IL-6 (20 ng/ml), SCF (100 ng/ml), FLT3-L (100 ng/ml) and TPO (20 ng/ml) before the addition of the CYP1B1 inhibitor TMS (Abcam) at a concentration of 10 μM or mock treatment with 0.1% DMSO. Equal numbers of cells (12,000 per condition) were then allowed to proliferate for 7 days at which point they were counted and immunophenotyped for CD34 and CD133 expression.

Statistical analysis

Unless stated otherwise (i.e., analysis of RNA-seq and CLIP-seq data sets), all statistical analysis was performed using GraphPad Prism (GraphPad Software version 5.0). Unpaired student t-tests or Mann-Whitney tests were performed with $p < 0.05$ as the cut-off for statistical significance.

References

18 Doulatov, S. *et al.* PLZF is a regulator of homeostatic and cytokine-induced myeloid development. *Genes Dev* **23**, 2076-2163 (2009).

19 Majeti, R., Park, C. Y. & Weissman, I. L. Identification of a hierarchy of multipotent hematopoietic progenitors in human cord blood. *Cell Stem Cell* **1**, 635-645 (2007).

20 Bagger, F. O. *et al.* HemaExplorer: a database of mRNA expression profiles in normal and malignant haematopoiesis. *Nucleic Acids Res* **41**, D1034-1039 (2013).

21 Amendola, M., Venneri, M. A., Biffi, A., Vigna, E. & Naldini, L. Coordinate dual-gene transgenesis by lentiviral vectors carrying synthetic bidirectional promoters. *Nat Biotechnol* **23**, 108-116 (2005).

22 van Galen, P. *et al.* The unfolded protein response governs integrity of the haematopoietic stem-cell pool during stress. *Nature* **510**, 268-272 (2014).

23 Lechman, E. R. *et al.* Attenuation of miR-126 activity expands HSC *in vivo* without exhaustion. *Cell Stem Cell* **11**, 799-811 (2012).

24 Carow, C. E., Hangoc, G. & Broxmeyer, H. E. Human multipotential progenitor cells (CFU-GEMM) have extensive replating capacity for secondary CFU-GEMM: an effect enhanced by cord blood plasma. *Blood* **81**, 942-949 (1993).

25 Milyavsky, M. *et al.* A distinctive DNA damage response in human hematopoietic stem cells reveals an apoptosis-independent role for p53 in self-renewal. *Cell Stem Cell* **7**, 186-197 (2010).

26 Janky, R. *et al.* iRegulon: from a gene list to a gene regulatory network using large motif and track collections. *PLoS Comput Biol* **10**, e1003731 (2014).

27 Subramanian, A. *et al.* Gene set enrichment analysis: a knowledge-based approach for interpreting genome-wide expression profiles. *Proc Natl Acad Sci U S A* **102**, 15545-15550 (2005).

28 Kwon, A. T., Arenillas, D. J., Worsley Hunt, R. & Wasserman, W. W. oPOSSUM-3: advanced analysis of regulatory motif over-representation across genes or ChIP-Seq datasets. *G3 (Bethesda)* **2**, 987-1002 (2012).

29 Colvin, G. A. *et al.* Murine marrow cellularity and the concept of stem cell competition: geographic and quantitative determinants in stem cell biology. *Leukemia* **18**, 575-583 (2004).

30 Hu, Y. & Smyth, G. K. ELDA: extreme limiting dilution analysis for comparing depleted and enriched populations in stem cell and other assays. *J Immunol Methods* **347**, 70-78 (2009).

31 Langmead, B., Trapnell, C., Pop, M. & Salzberg, S. L. Ultrafast and memory-efficient alignment of short DNA sequences to the human genome. *Genome Biol* **10**, R25 (2009).

32 Dobin, A. *et al.* STAR: ultrafast universal RNA-seq aligner. *Bioinformatics* **29**, 15-21 (2013).

33 Darnell, R. CLIP (cross-linking and immunoprecipitation) identification of RNAs bound by a specific protein. *Cold Spring Harb Protoc* **2012**, 1146-1160 (2012).

34 Lovci, M. T. *et al.* Rbfox proteins regulate alternative mRNA splicing through evolutionarily conserved RNA bridges. *Nat Struct Mol Biol* **20**, 1434-1442 (2013).

35 Quinlan, A. R. & Hall, I. M. BEDTools: a flexible suite of utilities for comparing genomic features. *Bioinformatics* **26**, 841-842 (2010).

36 Dale, R. K., Pedersen, B. S. & Quinlan, A. R. Pybedtools: a flexible Python library for manipulating genomic datasets and annotations. *Bioinformatics* **27**, 3423-3424 (2011).

37 Liao, Y., Smyth, G. K. & Shi, W. featureCounts: an efficient general purpose program for assigning sequence reads to genomic features. *Bioinformatics* **30**, 923-930 (2014).

Supplementary Information

Supplementary Tables 1-7

Supplementary Figure 1

Acknowledgements

We thank Eric Lechman and Peter Van Galen for providing H1 and pSMALB vectors. The MA overexpression vector was provided as a gift by Luigi Naldini. We also thank the SCC-RI core flow cytometry staff, the Obstetrics and Gynecology Unit at McMaster Children's Hospital for cord blood, Brad Doble and Mick Bhatia for critical assessment of this work and all members of the Hope laboratory for experimental support and advice. This work was supported by an Ontario Institute for Cancer Research New Investigator Award (IA-033), an Ontario Institute for Cancer Research Cancer Stem Cell Program Team Grant (P.CSC.005) and a Canadian Institutes of Health Research (MOP-126030) grant to K.H. S.R. is supported by a Canadian Blood Services Graduate Fellowship and Health Canada. The views expressed herein do not necessarily represent the view of the federal government of Canada. This work was partially supported by grants from the National Institute of Health (HG004659 and NS075449) to G.W.Y. and from the California Institute of Regenerative Medicine (RB3-05219) to G.W.Y. G.P. was supported by a National Science Graduate Fellowship. G.W.Y. is an Alfred P. Sloan Research Fellow. We thank the UCSD Institute for Genomic Medicine's Genomics Center for providing access to high-throughput sequencing facilities.

Author Contributions

S.R. designed and performed experiments, analyzed data and wrote the manuscript. N.H. constructed CLIP-seq libraries. M.S.B. helped perform CB experiments. G.P. and G.W.Y advised CLIP-seq library construction, performed CLIP-seq bioinformatic analyses and wrote the manuscript. B.W. performed RNA-seq analyses. V.V and G.D.B performed RNA-seq bioinformatic analyses. K.H. conceived the project, supervised the study, analyzed data, interpreted results and wrote the manuscript.

Author Information

The authors declare no competing financial interests. Correspondence and requests for materials should be addressed to G.W.Y. (geneyeo@ucsd.edu), K.H. (kristin@mcmaster.ca).

Figures

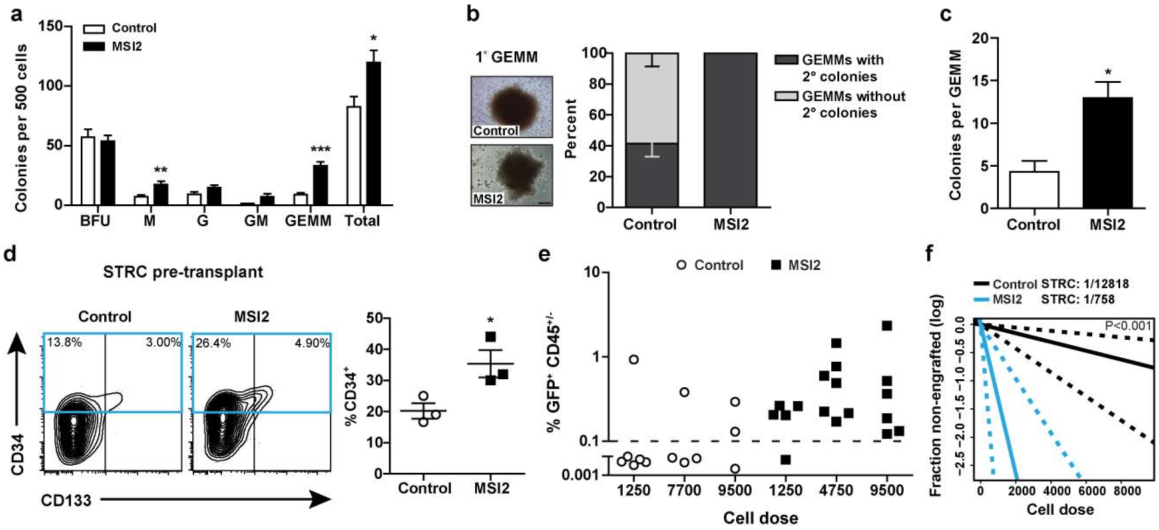
a
Control
MSI2
Colonies per 500 cells
150
100
50
0
**
***
*
BFU
M
G
GM
GEMM
Total
b
1° GEMM
Control
MSI2
Percent
100
80
60
40
20
0
Control
MSI2
GEMMs with 2° colonies
GEMMs without 2° colonies
c
Colonies per GEMM
20
15
10
5
0
*
Control
MSI2
d
STRC pre-transplant
Control
MSI2
13.8%
3.00%
26.4%
4.90%
CD34
CD133
% CD34+
50
40
30
20
10
0
*
Control
MSI2
e
Control
MSI2
% GFP+ CD45+/-
10
1
0.1
0.001
1250
7700
9500
1250
4750
9500
Cell dose
f
Control STRC: 1/12818
MSI2 STRC: 1/758
P<0.001
Fraction non-engrafted (log)
0.0
−0.5
−1.0
−1.5
−2.0
−2.5
0
2000
4000
6000
8000
Cell dose

Figure 1 | MSI2 OE enhances *in vitro* CB progenitor activity and increases numbers of STRCs. a, CFU output from transduced Lin$^-$ CB (n=9 control and 10 MSI2 OE cultures from 5 experiments). **b,** CFU-GEMM secondary CFU replating potential (n=24 control and 30 MSI2 OE from 2 experiments) and images of primary GEMMs (scale bar 200 μm). **c,** Number of secondary colonies per replated CFU-GEMM from **b**. **d,** CD34 expression in STRCs prior to transplant (n=3 experiments). **e,** Human chimerism at 3 weeks in mice transplanted with varying doses of transduced STRCs. Dashed line indicates engraftment cutoff (n=3 experiments). **f,** STRC frequency as determined by LDA from **e**. Dashed lines indicate 95% C.I. Data shown as mean ± SEM. *p<0.05; **p<0.01; ***p<0.001.

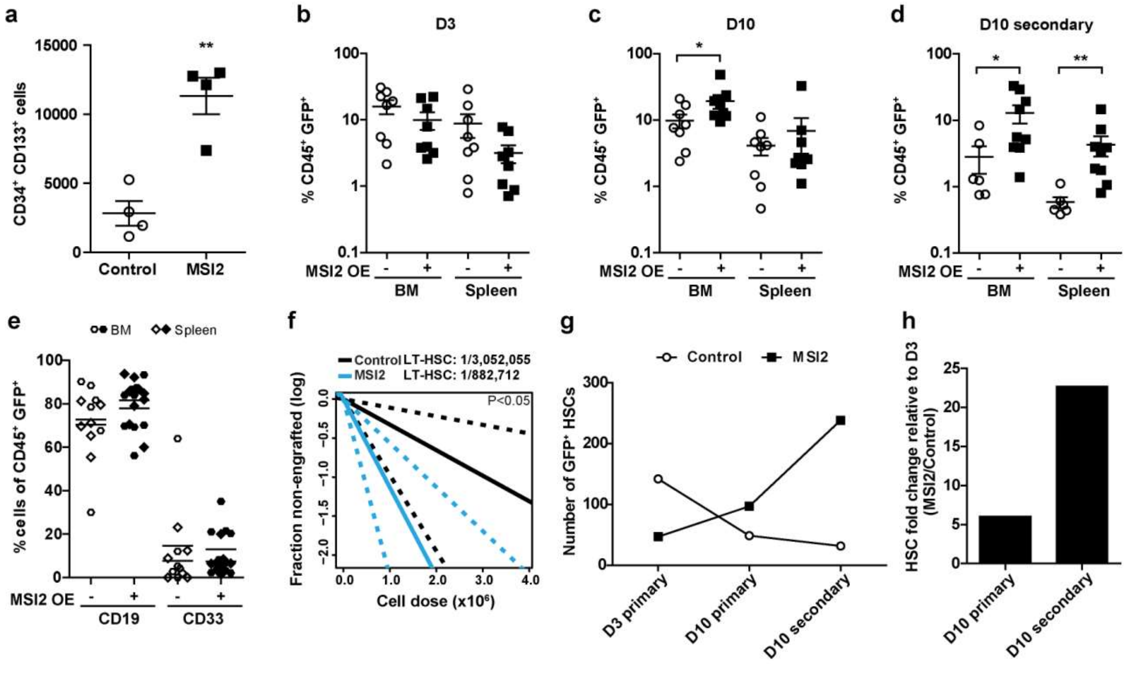
a
CD34⁺ CD133⁺ cells
15000
10000
5000
0
**
Control
MSI2
b
D3
% CD45⁺ GFP⁺
100
10
1
0.1
MSI2 OE
-
+
-
+
BM
Spleen
c
D10
*
% CD45⁺ GFP⁺
100
10
1
0.1
MSI2 OE
-
+
-
+
BM
Spleen
d
D10 secondary
*
**
% CD45⁺ GFP⁺
100
10
1
0.1
MSI2 OE
-
+
-
+
BM
Spleen
e
○● BM
◇◆ Spleen
% cells of CD45⁺ GFP⁺
100
80
60
40
20
0
MSI2 OE
-
+
-
+
CD19
CD33
f
Control LT-HSC: 1/3,052,055
MSI2 LT-HSC: 1/882,712
P<0.05
Fraction non-engrafted (log)
0.0
-0.5
-1.0
-1.5
-2.0
0.0
1.0
2.0
3.0
4.0
Cell dose (x10⁶)
g
Control
MSI2
Number of GFP⁺ HSCs
300
200
100
0
D3 primary
D10 primary
D10 secondary
h
HSC fold change relative to D3 (MSI2/Control)
25
20
15
10
5
0
D10 primary
D10 secondary

Figure 2 | MSI2 OE expands LT-HSCs with ex vivo culture. a, Transduced $CD34^+CD133^+$ cells after one week of culture (n=4 experiments, unpaired t-test). **b-d,** $CD45^+GFP^+$ engraftment from mice receiving the highest two cell doses for D3 and D10 (n=8 mice for both conditions) and the highest three doses for D10 secondary mice (n=6 control and 9 MSI2 OE mice, Mann-Whitney test). **e,** Myelo-lymphopoiesis in D10 secondary mice. **f,** Multi-lineage LT-HSC frequency in BM cells of D10 primary mice. Dashed lines indicate 95% C.I. **g,** Numbers of GFP^+ HSCs as evaluated by LDA. **h,** Cumulative fold change in MSI2 OE-transduced HSCs. Data shown as mean ± SEM. $^*p<0.05$; $^{**}p<0.01$.

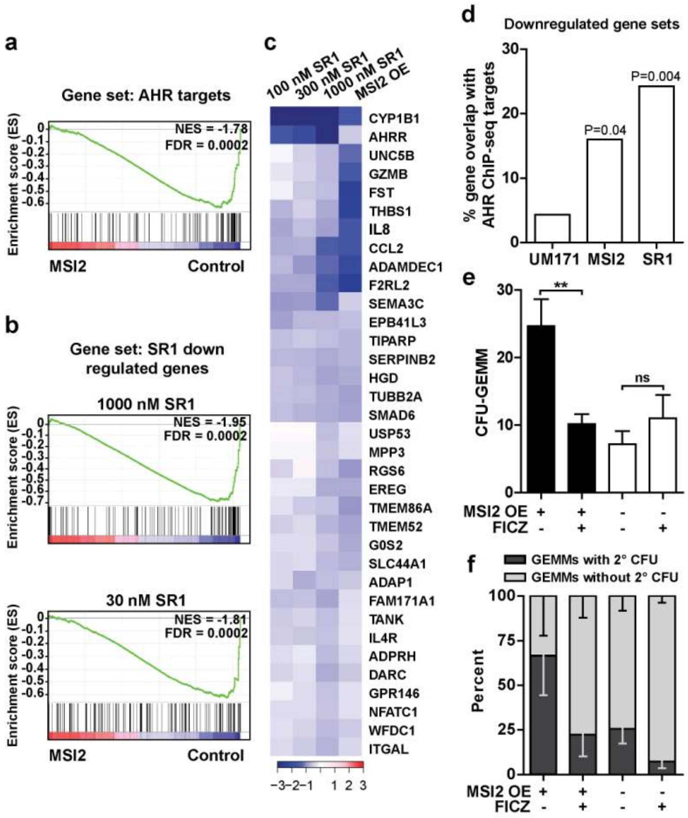
a
Gene set: AHR targets
Enrichment score (ES)
0
-0.1
-0.2
-0.3
-0.4
-0.5
-0.6
NES = -1.78
FDR = 0.0002
MSI2
Control
b
Gene set: SR1 down regulated genes
1000 nM SR1
Enrichment score (ES)
0
-0.1
-0.2
-0.3
-0.4
-0.5
-0.6
-0.7
NES = -1.95
FDR = 0.0002
30 nM SR1
Enrichment score (ES)
0
-0.1
-0.2
-0.3
-0.4
-0.5
-0.6
NES = -1.81
FDR = 0.0002
MSI2
Control
c
100 nM SR1
300 nM SR1
1000 nM SR1
MSI2 OE
CYP1B1
AHRR
UNC5B
GZMB
FST
THBS1
IL8
CCL2
ADAMDEC1
F2RL2
SEMA3C
EPB41L3
TIPARP
SERPINB2
HGD
TUBB2A
SMAD6
USP53
MPP3
RGS6
EREG
TMEM86A
TMEM52
G0S2
SLC44A1
ADAP1
FAM171A1
TANK
IL4R
ADPRH
DARC
GPR146
NFATC1
WFDC1
ITGAL
−3−2−1 1 2 3
d
Downregulated gene sets
% gene overlap with AHR ChIP-seq targets
0
10
20
30
P=0.04
P=0.004
UM171
MSI2
SR1
e
CFU-GEMM
0
10
20
30
**
ns
MSI2 OE + + - -
FICZ - + - +
f
GEMMs with 2° CFU
GEMMs without 2° CFU
Percent
0
25
50
75
100
MSI2 OE + + - -
FICZ - + - +

Figure 3 | MSI2 OE in human HSPCs attenuates AHR signaling. a, Predicted AHR targets compared by GSEA to genes downregulated with MSI2 OE. **b,** GSEA of SR1 and MSI2 OE downregulated gene sets. **c,** Log fold-change of MSI2 OE and SR1 GSEA leading edge genes. **d,** Percentage of gene overlap between UM171-, SR1-treated and MSI2 OE downregulated gene sets and AHR ChIP-seq-identified targets. **e,** Number of CFU-GEMMs generated from transduced cells grown in CFU medium containing FICZ or DMSO (n=3 experiments). **f,** CFU-GEMMs from **e** replated into CFU assays containing FICZ or DMSO (n=30 control and 29 MSI2 OE per treatment). Data are presented as mean ± SEM. $^{**}p<0.01$.

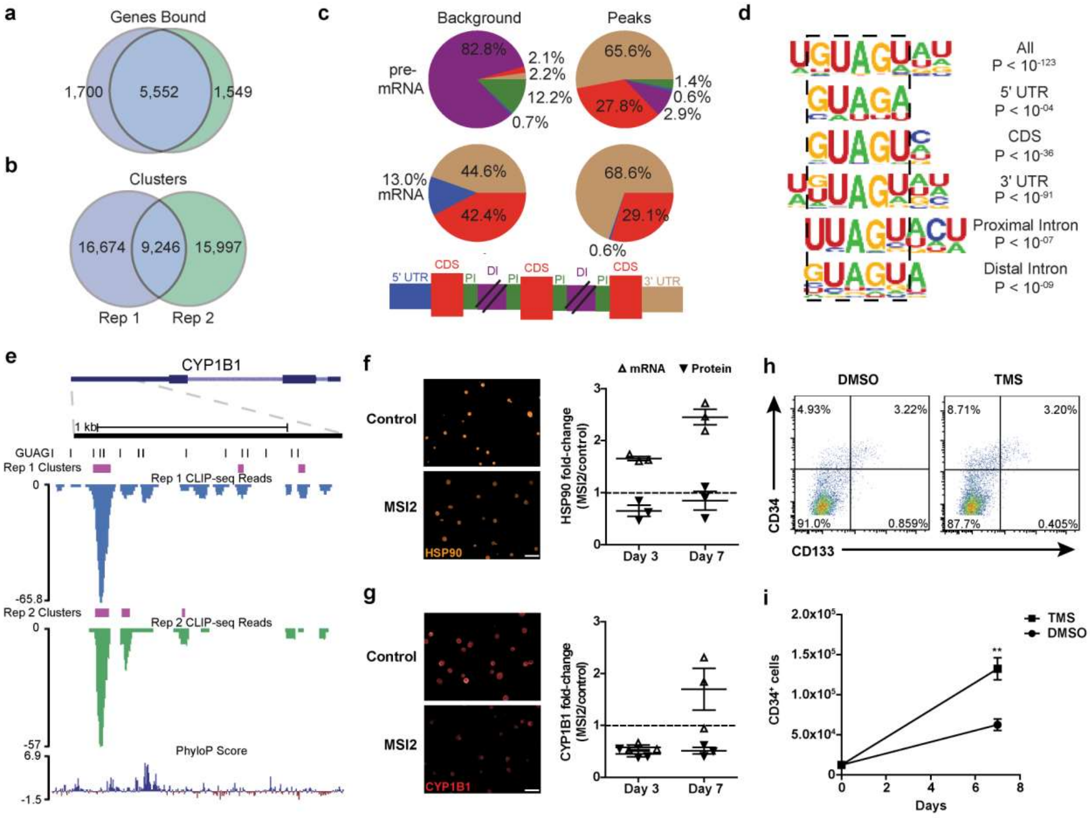
a
Genes Bound
1,700
5,552
1,549
b
Clusters
16,674
9,246
15,997
Rep 1
Rep 2
c
Background
Peaks
pre-mRNA
82.8%
2.1%
2.2%
12.2%
0.7%
65.6%
1.4%
0.6%
2.9%
27.8%
mRNA
13.0%
44.6%
42.4%
68.6%
29.1%
0.6%
5' UTR
CDS
PI
DI
3' UTR
d
All
P < 10-123
5' UTR
P < 10-04
CDS
P < 10-36
3' UTR
P < 10-91
Proximal Intron
P < 10-07
Distal Intron
P < 10-09
e
CYP1B1
1 kb
GUAGI
Rep 1 Clusters
Rep 1 CLIP-seq Reads
0
-65.8
Rep 2 Clusters
Rep 2 CLIP-seq Reads
0
-57
PhyloP Score
6.9
-1.5
f
Control
MSI2
HSP90
Δ mRNA
▼ Protein
HSP90 fold-change (MSI2/control)
Day 3
Day 7
g
Control
MSI2
CYP1B1
CYP1B1 fold-change (MSI2/control)
Day 3
Day 7
h
DMSO
TMS
4.93%
3.22%
91.0%
0.859%
8.71%
3.20%
87.7%
0.405%
CD34
CD133
i
TMS
DMSO
CD34+ cells
2.0x10⁵
1.5x10⁵
1.0x10⁵
5.0x10⁴
0
**
Days
0
2
4
6
8

Figure 4 | MSI2 OE post-transcriptionally downregulates AHR pathway components. a, Overlap between MSI2 target genes from separate CLIP-seq experiments. **b,** Statistically significant overlap ($p<0.0001$, hypergeometric test) of clusters between the replicates. **c,** Percent of CLIP-seq clusters in different genic regions. **d,** Consensus motifs within MSI2 clusters in different genic regions. P-values presented for the top 40% of clusters. **e,** CLIP-seq reads (replicate 1: blue, replicate 2: green) and clusters (purple) mapped to the 3'UTR of *CYP1B1*. Matches to the GUAG motif shown in black. **f and g,** Immunofluorescent images of HSP90 and CYP1B1 3 days after transduction and summary of fold-change in HSP90 and CYP1B1 protein and transcript levels with MSI2 OE at 3 and 7 days post transduction (scale bar 20 μm, dotted line indicates no change, n=3 experiments). **h,** HSPC marker expression by CD34$^+$ cells treated with TMS for 10 days. **i,** Absolute CD34$^+$ cell number with TMS (n=4 experiments). Data are presented as mean ± SEM. $^{**}p<0.01$.

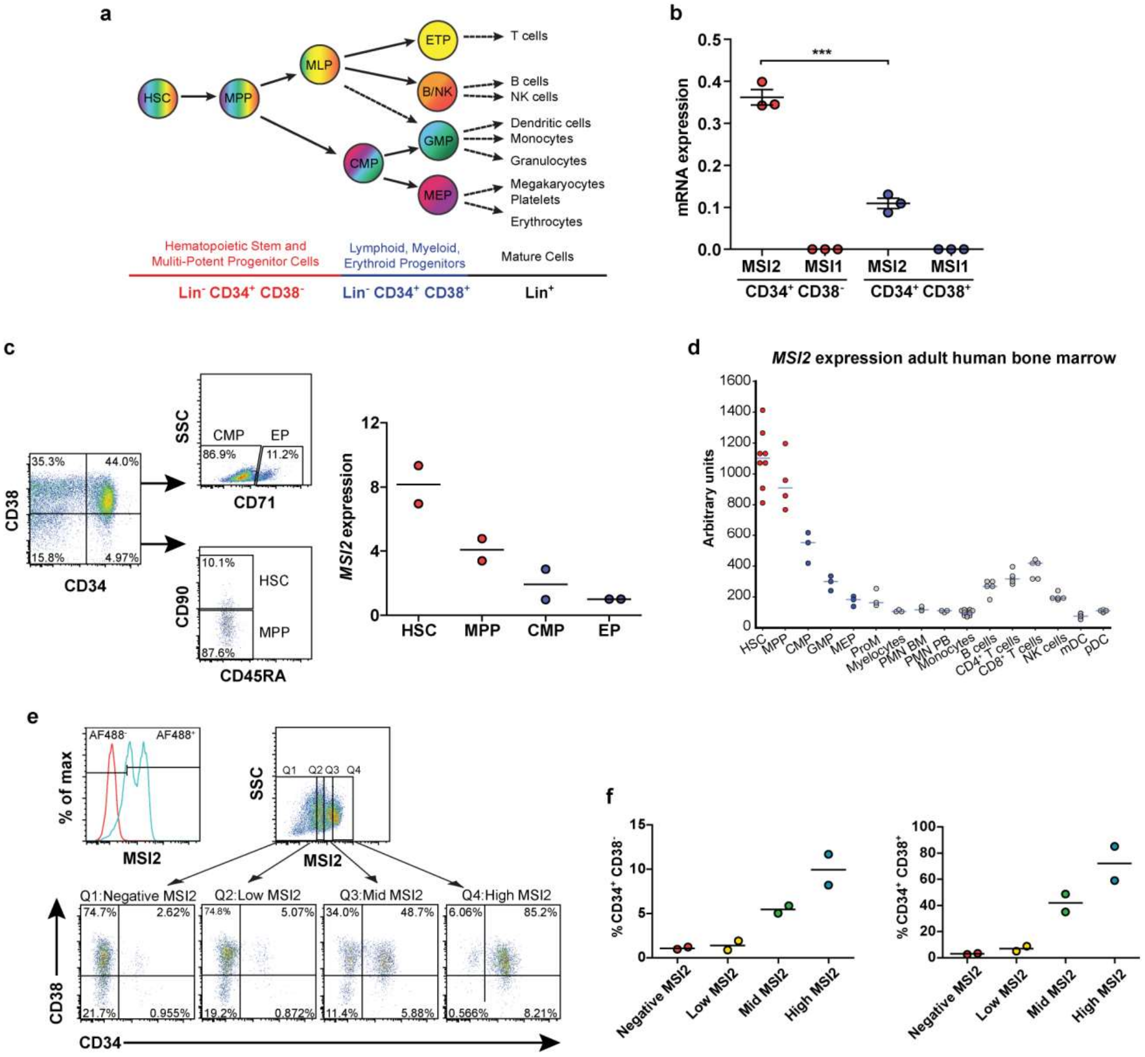
a
HSC
MPP
MLP
CMP
ETP
B/NK
GMP
MEP
T cells
B cells
NK cells
Dendritic cells
Monocytes
Granulocytes
Megakaryocytes
Platelets
Erythrocytes
Hematopoietic Stem and Muliti-Potent Progenitor Cells
Lymphoid, Myeloid, Erythroid Progenitors
Mature Cells
Lin- CD34+ CD38-
Lin- CD34+ CD38+
Lin+
b
mRNA expression
***
MSI2
MSI1
CD34+ CD38-
CD34+ CD38+
c
CD38
CD34
35.3%
44.0%
15.8%
4.97%
SSC
CD71
CMP
EP
86.9%
11.2%
CD90
CD45RA
10.1%
HSC
MPP
87.6%
MSI2 expression
d
MSI2 expression adult human bone marrow
Arbitrary units
HSC
MPP
CMP
GMP
MEP
ProM
Myelocytes
PMN BM
PMN PB
Monocytes
B cells
CD4+ T cells
CD8+ T cells
NK cells
mDC
pDC
e
AF488-
AF488+
% of max
MSI2
SSC
Q1
Q2
Q3
Q4
Q1:Negative MSI2
Q2:Low MSI2
Q3:Mid MSI2
Q4:High MSI2
74.7%
2.62%
21.7%
0.955%
74.8%
5.07%
19.2%
0.872%
34.0%
48.7%
11.4%
5.88%
6.06%
85.2%
0.566%
8.21%
CD38
CD34
f
% CD34+ CD38-
% CD34+ CD38+
Negative MSI2
Low MSI2
Mid MSI2
High MSI2

Extended Data Figure 1 | MSI2 is highly expressed in human hematopoietic stem and progenitor cell populations. a, Schematic of the human hematopoietic hierarchy showing key primitive cell populations and simplified surface marker expression. **b,** qRT-PCR analysis of *MSI1* and *MSI2* expression in Lin$^-$ CB cell populations (n=3 independent Lin- CB samples). **c,** Gating strategy used to sort sub-fractions of Lin$^-$ CB HSPCs for *MSI2* qRT-PCR expression analysis (n=2 independent pooled Lin$^-$ CB samples). **d,** *MSI2* expression across the human hematopoietic hierarchy. Each circle represents an independent gene expression dataset curated by HemaExplorer. **e,** Intracellular flow cytometry analysis of MSI2 protein levels in Lin$^-$ CB. Histograms show background staining with secondary antibody (red) and positive staining with anti-MSI2 antibody plus secondary in Lin$^-$ CB (blue). MSI2 fluorescence intensity was divided into quartiles of negative (Q1), low (Q2), mid (Q3) and high (Q4) level expression. **f,** Plots show cell percentage within each quartile from **e** that are CD34$^+$ CD38$^-$ (left) and CD34$^+$ CD38$^+$ (right) (n=2 independent Lin$^-$ CB samples). All data presented as mean ± SEM. *p<0.05; ***p<0.001.

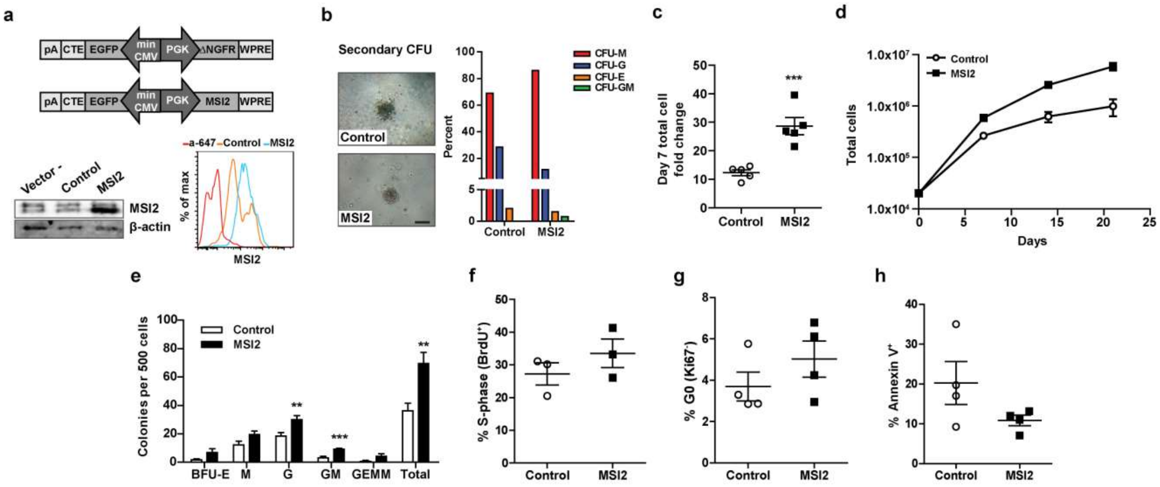
a
pA
CTE
EGFP
min CMV
PGK
ΔNGFR
WPRE
MSI2
Vector -
Control
MSI2
MSI2
β-actin
a-647
Control
MSI2
% of max
MSI2
b
Secondary CFU
Control
MSI2
CFU-M
CFU-G
CFU-E
CFU-GM
Percent
100
80
60
40
20
5
0
Control
MSI2
c
Day 7 total cell fold change
***
50
40
30
20
10
0
Control
MSI2
d
Control
MSI2
Total cells
$1.0x10^7$
$1.0x10^6$
$1.0x10^5$
$1.0x10^4$
0
5
10
15
20
25
Days
e
Colonies per 500 cells
Control
MSI2
100
80
60
40
20
0
**
***
**
BFU-E
M
G
GM
GEMM
Total
f
% S-phase (BrdU$^+$)
50
40
30
20
10
0
Control
MSI2
g
% G0 (Ki67$^-$)
8
6
4
2
0
Control
MSI2
h
% Annexin V$^+$
40
30
20
10
0
Control
MSI2

Extended Data Figure 2 | MSI2 OE enhances *in vitro* culture of primitive CB cells. a, Top: Schematic of bi-directional promoter lentivirus used to overexpress MSI2. Bottom: Western blot and histogram showing intracellular flow validation of enforced MSI2 expression in 293FT cells (left) and Lin$^-$ CB (right), respectively. **b,** Representative images of secondary CFU made from replated control and MSI2 OE CFU-GEMMs and types of colonies made, scale bar = 200 μm. **c,** Fold change in Lin$^-$ CB transduced cell number after 7 days in culture following transduction (n=5 experiments). **d,** 21 day growth curve of transduced Lin$^-$ CB cells (n=4 experiments). **e,** Colony output of transduced Lin$^-$ CB from day 7 cultures (n=8 cultures from 4 experiments). **f,** BrdU cell cycle analysis of transduced Lin$^-$ CB cells from day 10 cultures (n=3 experiments). **g,** Ki67 cell cycle analysis of transduced Lin$^-$ CB cells from day 4 cultures (n=4 experiments). **h,** Apoptotic and dead cells in day 7 cultures of transduced Lin$^-$ CB by Annexin V staining (n=3 experiments). Western blot source data in Supplementary Figure 1. All data presented as mean ± SEM. $^{**}p<0.01$; $^{***}p<0.001$.

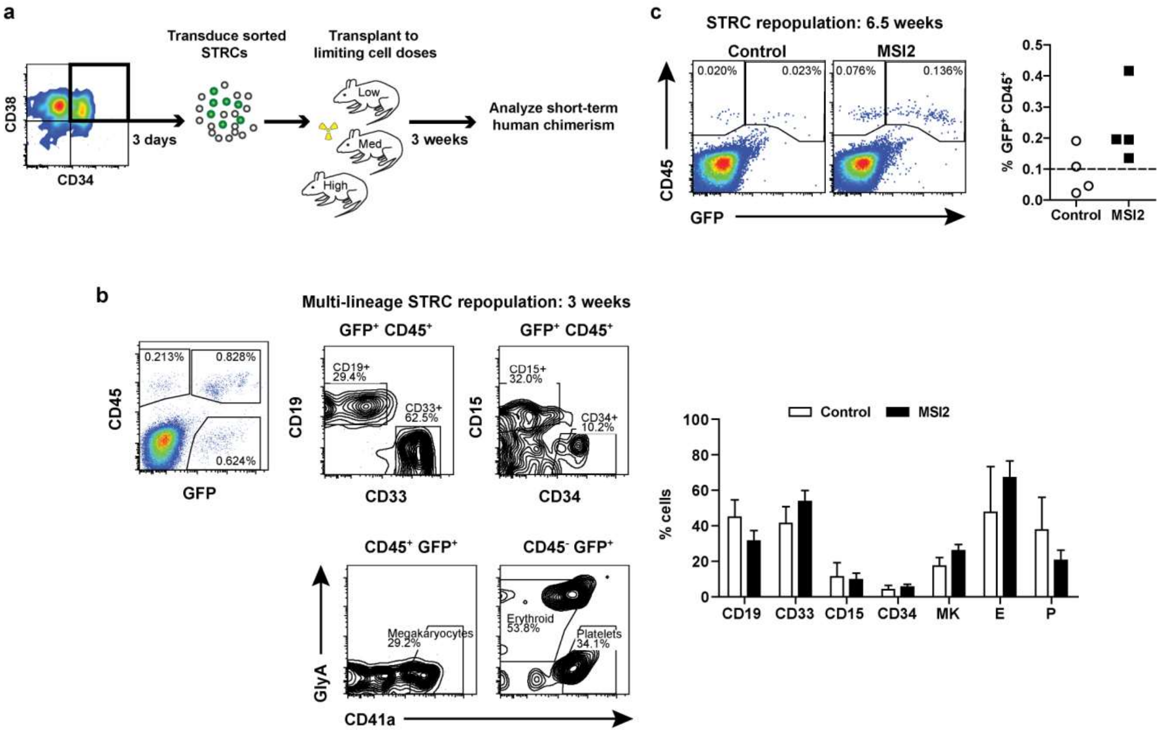
a
CD38
CD34
3 days
Transduce sorted STRCs
Transplant to limiting cell doses
Low
Med
High
3 weeks
Analyze short-term human chimerism
c
STRC repopulation: 6.5 weeks
Control
MSI2
0.020%
0.023%
0.076%
0.136%
CD45
GFP
% GFP+ CD45+
0.5
0.4
0.3
0.2
0.1
0.0
Control
MSI2
b
Multi-lineage STRC repopulation: 3 weeks
0.213%
0.828%
0.624%
CD45
GFP
GFP+ CD45+
CD19+ 29.4%
CD33+ 62.5%
CD19
CD33
GFP+ CD45+
CD15+ 32.0%
CD34+ 10.2%
CD15
CD34
CD45+ GFP+
Megakaryocytes 29.2%
CD45- GFP+
Erythroid 53.8%
Platelets 34.1%
GlyA
CD41a
Control
MSI2
% cells
100
80
60
40
20
0
CD19
CD33
CD15
CD34
MK
E
P

Extended Data Figure 3 | MSI2 OE does not affect STRC lineage output and extends STRC-mediated engraftment. a, Schematic of STRC LDA experimental setup. **b,** Left: Gating strategy to identify engrafted GFP$^+$ CD45$^+$ progenitor and myelo-lympho lineage positive cell types or GFP$^+$ CD45$^-$ erythroid cells and platelets. Right: Summary of lineage output in the injected femur at 3 weeks post-transplant (n=4 control and n=18 MSI2 OE mice). MK = Megakaryocyte, E = Erythroid cells, P = Platelets. **c,** Representative flow plots and summary of transduced STRCs read out for human CD45$^+$ engraftment at 6.5 weeks post-transplant (n=4 mice per condition). All data presented as mean ± SEM.

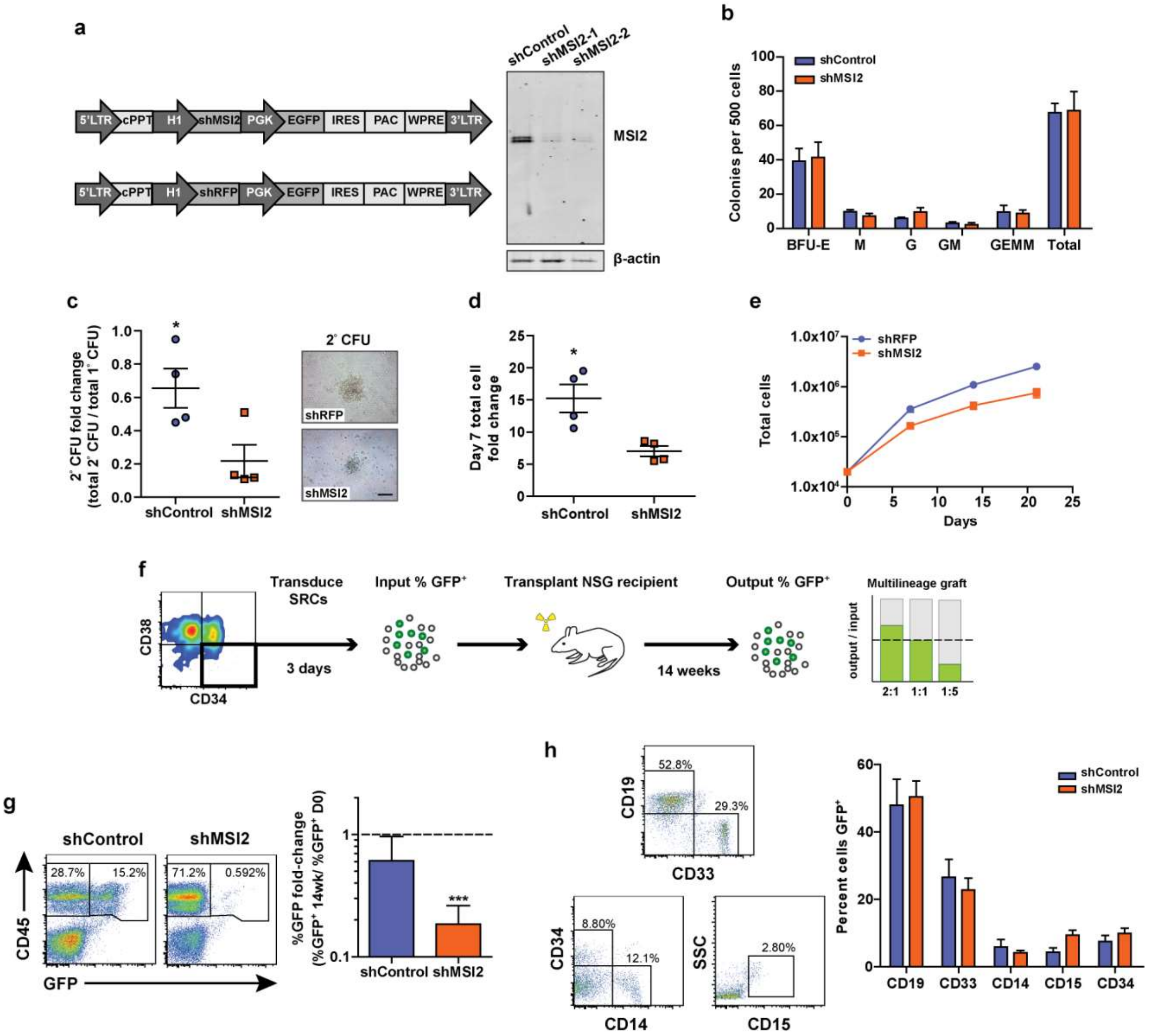
a
5'LTR
cPPT
H1
shMSI2
PGK
EGFP
IRES
PAC
WPRE
3'LTR
shRFP
shControl
shMSI2-1
shMSI2-2
MSI2
β-actin
b
Colonies per 500 cells
shControl
shMSI2
BFU-E
M
G
GM
GEMM
Total
c
2° CFU fold change (total 2° CFU / total 1° CFU)
2° CFU
shRFP
shMSI2
shControl
d
Day 7 total cell fold change
e
Total cells
shRFP
shMSI2
Days
f
Transduce SRCs
3 days
Input % GFP⁺
Transplant NSG recipient
14 weeks
Output % GFP⁺
Multilineage graft
output / input
2:1
1:1
1:5
CD38
CD34
g
shControl
shMSI2
28.7%
15.2%
71.2%
0.592%
CD45
GFP
%GFP fold-change (%GFP⁺ 14wk/ %GFP⁺ D0)
***
h
52.8%
29.3%
CD19
CD33
8.80%
12.1%
CD34
CD14
2.80%
SSC
CD15
Percent cells GFP⁺
CD19
CD33
CD14
CD15
CD34

Extended Data Figure 4 | MSI2 KD impairs secondary CFU replating potential and HSC engraftment capacity. a, Left: Schematic of MSI2- and control RFP-targeted shRNA lentiviruses. Right: Confirmation of MSI2 protein knockdown (both isoforms that can be detected by western blot) in transduced NB4 cells. **b,** CFU production by shMSI2 and shControl transduced Lin$^-$ CB (n=8 cultures from 4 experiments). **c,** Secondary CFU output from shMSI2 and images of representative secondary CFU (scale bar = 200 µm, performed on n=4 cultures from 2 experiments). **d,** Fold change in transduced cell number after 7 days in culture (n=4 experiments). **e,** Growth curves of cultures initiated with transduced Lin$^-$ CB cells (n=4 experiments). **f,** Experimental design to readout changes in HSC capacity with MSI2 KD. **g,** Left: Representative flow analysis of transduced CD34$^+$ CD38$^-$ derived human chimerism in NSG mouse BM. Right: Shown is the ratio of the percentage of GFP$^+$ cells in the CD45$^+$ population post-transplant to the initial pre-transplant GFP$^+$ cell percentage. Dotted line indicates the proportion of GFP$^+$ cells is unchanged relative to input. (One sample t-test, no change = 1, n = 6 shControl and n = 8 shMSI2 mice pooled from 2 experiments). **h,** Representative flow plots and summary of multilineage engraftment with shControl and shMSI2 (gated on GFP$^+$ cells). Western blot source data is shown in Supplementary Figure 1. Data presented as mean ± SEM. *p<0.05; ***p<0.001.

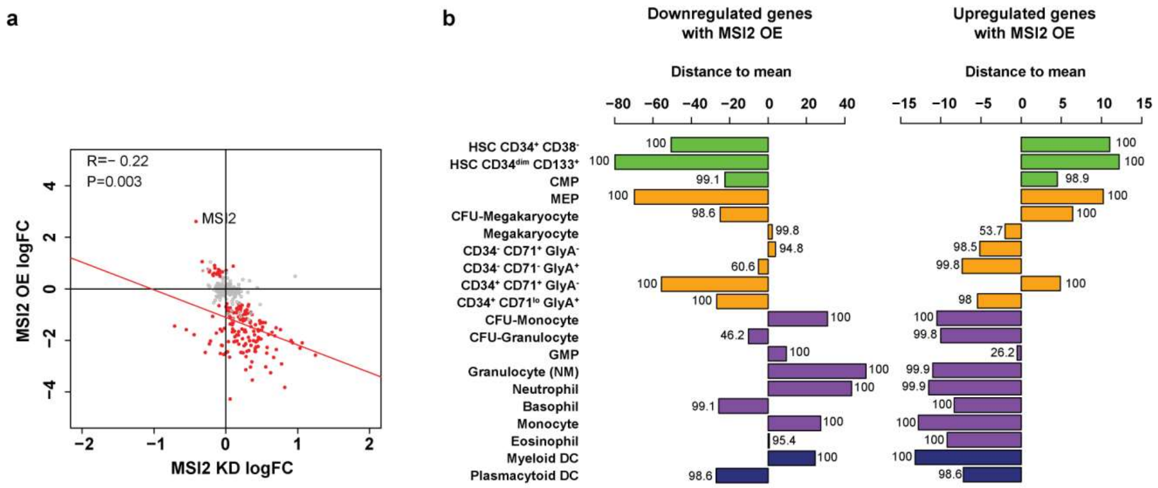
a
R=− 0.22
P=0.003
MSI2
MSI2 OE logFC
MSI2 KD logFC
−2
−1
0
1
2
4
2
0
−2
−4
b
Downregulated genes with MSI2 OE
Upregulated genes with MSI2 OE
Distance to mean
−80 −60 −40 −20 0 20 40
−15 −10 −5 0 5 10 15
HSC CD34⁺ CD38⁻
HSC CD34dim CD133⁺
CMP
MEP
CFU-Megakaryocyte
Megakaryocyte
CD34⁻ CD71⁺ GlyA⁻
CD34⁻ CD71⁻ GlyA⁺
CD34⁺ CD71⁺ GlyA⁻
CD34⁺ CD71lo GlyA⁺
CFU-Monocyte
CFU-Granulocyte
GMP
Granulocyte (NM)
Neutrophil
Basophil
Monocyte
Eosinophil
Myeloid DC
Plasmacytoid DC
100
100
99.1
100
98.6
99.8
94.8
60.6
100
100
100
46.2
100
100
100
99.1
100
95.4
100
98.6
100
100
98.9
100
100
53.7
98.5
99.8
100
98
100
99.8
26.2
99.9
99.9
100
100
100
100
98.6

Extended Data Figure 5 | MSI2 OE confers an HSC gene expression signature. a, Genes that are up in OE (21 genes, logFC>0) and down (156 genes, logFC<0) relative to control with a FDR<0.05 were compared to MSI2 KD normalized to shControl expression data. Red circles represent 177 significantly differentially expressed genes with OE. Gray outlined circles represent random genes (number of gray circles = number of red circles). Only genes that are significantly up or downregulated in OE have anti-correlation with KD. **b,** Differentially expressed genes between MSI2 OE and control cells (FDR <0.05) compared to DMAP populations. Numbers beside each bar indicate the percentage of the time the observed value (set of up or downregulated genes) was better represented in that population than random values (equal number of randomly selected genes based on 1000 trials).

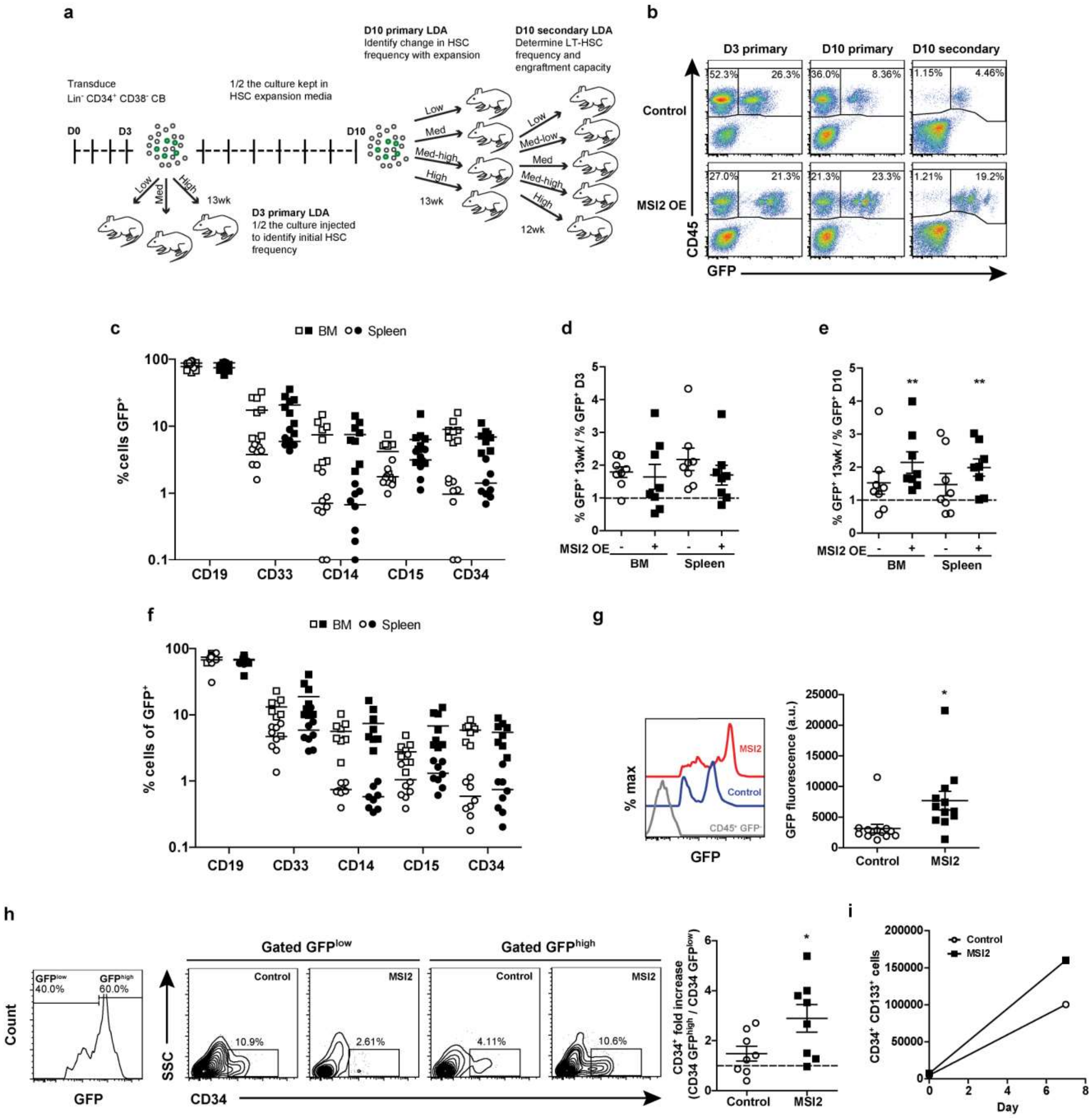
a
Transduce
Lin⁻ CD34⁺ CD38⁻ CB
D0
D3
Low
Med
High
13wk
D3 primary LDA
1/2 the culture injected to identify initial HSC frequency
1/2 the culture kept in HSC expansion media
D10
D10 primary LDA
Identify change in HSC frequency with expansion
Low
Med
Med-high
High
13wk
D10 secondary LDA
Determine LT-HSC frequency and engraftment capacity
Low
Med-low
Med
Med-high
High
12wk
b
D3 primary
D10 primary
D10 secondary
Control
52.3%
26.3%
36.0%
8.36%
1.15%
4.46%
MSI2 OE
27.0%
21.3%
21.3%
23.3%
1.21%
19.2%
CD45
GFP
c
BM
Spleen
% cells GFP⁺
100
10
1
0.1
CD19
CD33
CD14
CD15
CD34
d
% GFP⁺ 13wk / % GFP⁺ D3
MSI2 OE
BM
Spleen
e
% GFP⁺ 13wk / % GFP⁺ D10
**
**
MSI2 OE
BM
Spleen
f
BM
Spleen
% cells of GFP⁺
100
10
1
0.1
CD19
CD33
CD14
CD15
CD34
g
MSI2
Control
CD45⁺ GFP⁻
% max
GFP
GFP fluorescence (a.u.)
25000
20000
15000
10000
5000
0
*
Control
MSI2
h
GFPlow
40.0%
GFPhigh
60.0%
Count
GFP
Gated GFPlow
Gated GFPhigh
Control
MSI2
Control
MSI2
10.9%
2.61%
4.11%
10.6%
SSC
CD34
CD34⁺ fold increase (CD34 GFPhigh / CD34 GFPlow)
*
Control
MSI2
i
Control
MSI2
CD34⁺ CD133⁺ cells
200000
150000
100000
50000
0
Day
0
2
4
6
8

Extended Data Figure 6 | MSI2 OE enhances HSC activity after ex vivo culture. a, Experimental layout to measure changes in HSC engraftment capacity and frequency with ex vivo culture. **b,** Representative flow plots of $CD45^+$ GFP^+ reconstitution from mice receiving the highest cell dose transplanted per time point. **c,** Multilineage engraftment of mice injected with D3 cultures. **d,** Proportion of the human $CD45^+$ graft containing GFP^+ cells from D3 primary mice relative to pre-transplant levels of GFP^+ cells before expansion. Shown are mice transplanted at the two highest doses (n=8 mice for both conditions). **e,** Proportion of the human $CD45^+$ graft containing GFP^+ cells from D10 primary mice relative to pre-transplant levels of GFP^+ cells after expansion. Shown are mice transplanted at the two highest doses (n=8 mice for both conditions, one sample t-test, no change = 1). **f,** Summary of multilineage engraftment from mice in **c**. **g,** GFP mean fluoresence intensity (MFI) in D10 primary engrafted mice. Shown are mice transplanted with the highest three doses, n=11 control and 13 MSI2 mice. **h,** CD34 expression in GFP-high (top 60%) relative to GFP-low (bottom 40%) gated cells (set per mouse) from engrafted recipients in **c**. **i,** Number of transduced phenotyped HSCs after 7 days of culture from HSC expansion experiment described in **a**. Symbols represent individual mice and shaded symbols represent MSI2 OE. All data presented as mean ± SEM.

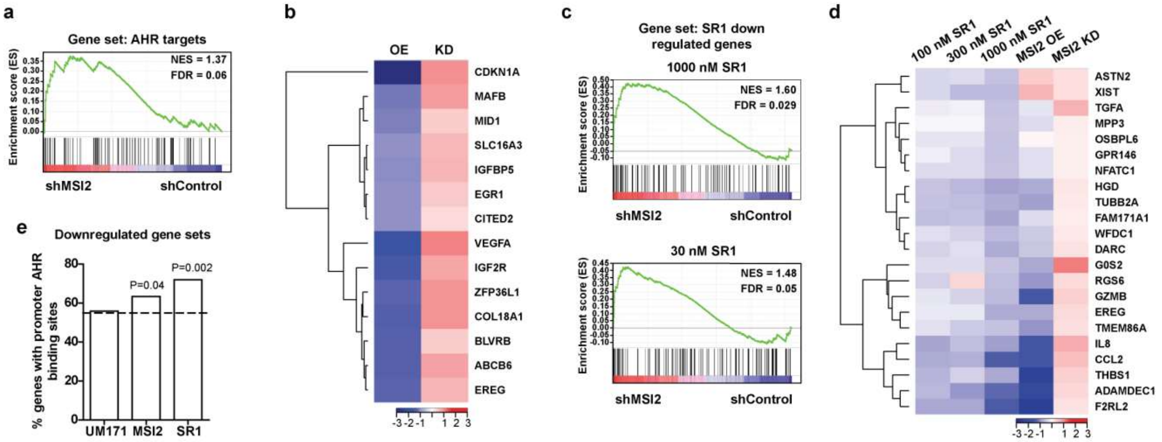
a
Gene set: AHR targets
Enrichment score (ES)
0.35
0.30
0.25
0.20
0.15
0.10
0.05
0.00
NES = 1.37
FDR = 0.06
shMSI2
shControl
b
OE
KD
CDKN1A
MAFB
MID1
SLC16A3
IGFBP5
EGR1
CITED2
VEGFA
IGF2R
ZFP36L1
COL18A1
BLVRB
ABCB6
EREG
-3 -2 -1 1 2 3
c
Gene set: SR1 down regulated genes
1000 nM SR1
Enrichment score (ES)
0.50
0.40
0.35
0.30
0.25
0.20
0.15
0.10
0.05
0.00
-0.05
-0.10
NES = 1.60
FDR = 0.029
shMSI2
shControl
30 nM SR1
Enrichment score (ES)
0.45
0.40
0.35
0.30
0.25
0.20
0.15
0.10
0.05
0.00
-0.05
-0.10
NES = 1.48
FDR = 0.05
shMSI2
shControl
d
100 nM SR1
300 nM SR1
1000 nM SR1
MSI2 OE
MSI2 KD
ASTN2
XIST
TGFA
MPP3
OSBPL6
GPR146
NFATC1
HGD
TUBB2A
FAM171A1
WFDC1
DARC
G0S2
RGS6
GZMB
EREG
TMEM86A
IL8
CCL2
THBS1
ADAMDEC1
F2RL2
-3 -2 -1 1 2 3
e
Downregulated gene sets
% genes with promoter AHR binding sites
80
60
40
20
0
P=0.04
P=0.002
UM171
MSI2
SR1

Extended Data Figure 7 | Predicted AHR targets and genes downregulated with SR1 and MSI2 OE are upregulated with MSI2 KD. a, Predicted AHR targets were identified with the iRegulon tool and compared with MSI2 KD normalized to shControl upregulated gene signature by GSEA. **b,** Heatmap of MSI2 OE and KD shared leading edge AHR target genes from GSEA. **c,** GSEA comparing SR1 high and low dose downregulated gene sets with the MSI2 KD upregulated gene signature. **d,** Heatmap shows list of shared leading edge genes identified by GSEA from MSI2 OE, KD and SR1 at varying doses. **e,** The percentage of downregulated genes from UM171-, SR1-treated and MSI2 OE data sets containing at least one AHR binding site 1500 bp upstream and downstream of transcription start site. Dotted line indicates the background percentage of genes with AHR binding sites. P-values were generated relative to background with Fisher's exact test.

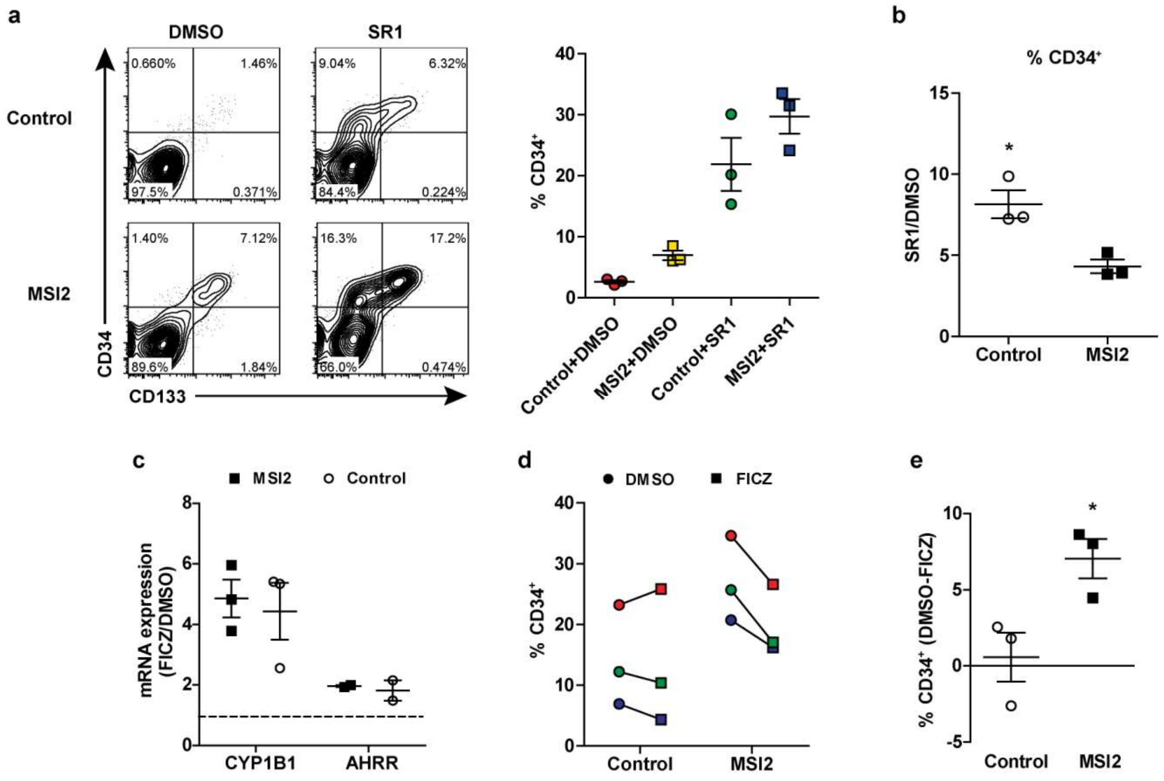
a
DMSO
SR1
Control
MSI2
CD34
CD133
0.660%
1.46%
97.5%
0.371%
9.04%
6.32%
84.4%
0.224%
1.40%
7.12%
89.6%
1.84%
16.3%
17.2%
66.0%
0.474%
% CD34+
40
30
20
10
0
Control+DMSO
MSI2+DMSO
Control+SR1
MSI2+SR1
b
% CD34+
SR1/DMSO
15
10
5
0
*
Control
MSI2
c
MSI2
Control
mRNA expression (FICZ/DMSO)
8
6
4
2
0
CYP1B1
AHRR
d
DMSO
FICZ
% CD34+
40
30
20
10
0
Control
MSI2
e
% CD34+ (DMSO-FICZ)
10
5
0
-5
*
Control
MSI2

Extended Data Figure 8 | AHR antagonism with SR1 has redundant effects with MSI2 OE, and AHR activation with MSI2 OE results in a loss of HSPCs. a, Representative flow plots and summary of CD34 expression with MSI2 OE and control transduced CD34^{+} CB cells grown for 10 days in medium containing SR1 or DMSO vehicle (n=3 experiments). **b,** Fold change in CD34 expression from results shown in **a**. **c,** Fold-increase in *CYP1B1* and *AHRR* transcript levels with FICZ in transduced cultures (n=3 experiments). **d,** Transduced CD34^{+} CB cells grown for 3 days in medium supplemented with FICZ and the corresponding change in CD34 expression. Each coloured pair (DMSO and FICZ) represents a matched CB sample (n=3 experiments). **e,** Differences in culture CD34 levels from **d**. All data presented as mean ± SEM. * $p<0.05$.

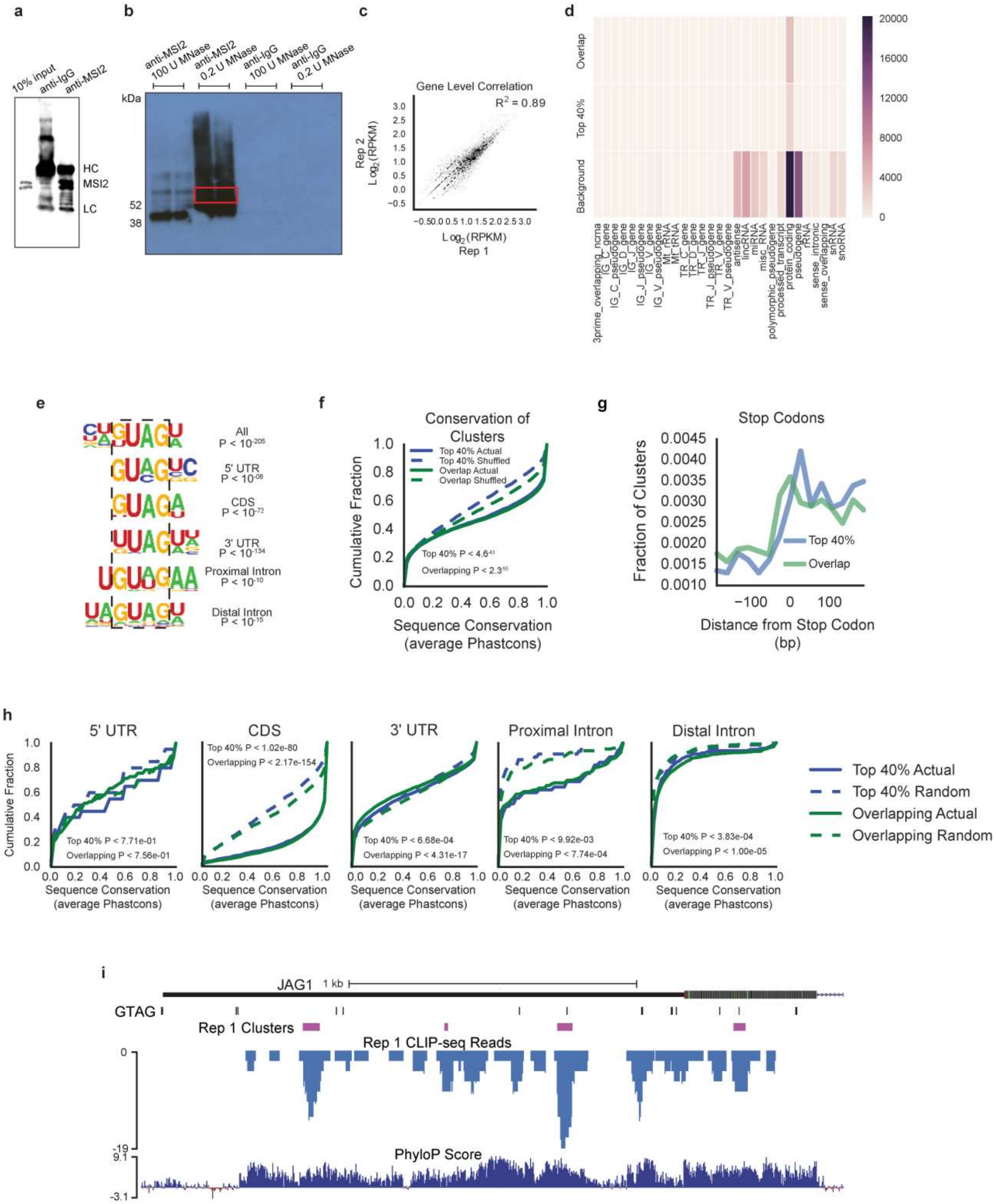
a
10% input
anti-IgG
anti-MSI2
HC
MSI2
LC
b
anti-MSI2 100 U MNase
anti-MSI2 0.2 U MNase
anti-IgG 100 U MNase
anti-IgG 0.2 U MNase
kDa
52
38
c
Gene Level Correlation
R² = 0.89
Rep 2 Log2(RPKM)
Log2(RPKM) Rep 1
d
Overlap
Top 40%
Background
20000
16000
12000
8000
4000
0
3prime_overlapping_ncrna
IG_C_gene
IG_C_pseudogene
IG_D_gene
IG_J_gene
IG_J_pseudogene
IG_V_gene
IG_V_pseudogene
Mt_rRNA
Mt_tRNA
TR_C_gene
TR_D_gene
TR_J_gene
TR_J_pseudogene
TR_V_gene
TR_V_pseudogene
antisense
lincRNA
miRNA
misc_RNA
polymorphic_pseudogene
processed_transcript
protein_coding
pseudogene
rRNA
sense_intronic
sense_overlapping
snRNA
snoRNA
e
All P < 10-205
5' UTR P < 10-08
CDS P < 10-72
3' UTR P < 10-134
Proximal Intron P < 10-10
Distal Intron P < 10-15
f
Conservation of Clusters
Top 40% Actual
Top 40% Shuffled
Overlap Actual
Overlap Shuffled
Top 40% P < 4.6-43
Overlapping P < 2.3-55
Cumulative Fraction
Sequence Conservation (average Phastcons)
g
Stop Codons
Top 40%
Overlap
Fraction of Clusters
Distance from Stop Codon (bp)
h
5' UTR
Top 40% P < 7.71e-01
Overlapping P < 7.56e-01
CDS
Top 40% P < 1.02e-80
Overlapping P < 2.17e-154
3' UTR
Top 40% P < 6.68e-04
Overlapping P < 4.31e-17
Proximal Intron
Top 40% P < 9.92e-03
Overlapping P < 7.74e-04
Distal Intron
Top 40% P < 3.83e-04
Overlapping P < 1.00e-05
Top 40% Actual
Top 40% Random
Overlapping Actual
Overlapping Random
Cumulative Fraction
Sequence Conservation (average Phastcons)
i
JAG1
1 kb
GTAG
Rep 1 Clusters
Rep 1 CLIP-seq Reads
0
-19
PhyloP Score
9.1
-3.1

Extended Data Figure 9 | MSI2 preferentially binds mature mRNA within the 3'UTR. a, Validation of the capacity of the anti-MSI2 antibody to immunoprecipitate MSI2 compared to IgG control pulldowns. **b,** Autoradiogram showing anti-MSI2 immunoprecipitated, MNase digested and radiolabelled RNA isolated for CLIP library construction and sequencing (red box). Low levels of MNase show a smearing pattern extending upwards from the modal weight of MSI2. **c,** Scatter plot of total number of uniquely mapped CLIP-seq reads for each gene, comparing both replicates. **d,** Heatmap indicating the number of different classes of Gencode annotated genes that contain at least one predicted MSI2 binding site. **e,** Consensus motifs within MSI2 clusters in the different genic regions. P-values for the most statistically significant enriched motif is presented for all overlapping clusters between replicates. **f,** Cumulative distribution function of mean conservation score (Phastcons) of MSI2 clusters, compared to a shuffled background control, computed for all overlapping clusters and the top 40% of overlapping clusters. P-values were obtained by a Kolgomorov-Smirnov two-tailed test comparing the distributions from actual and shuffled locations. **g,** Number of clusters within 200 bases of the annotated stop codon in known mRNA transcripts for all overlapping clusters between replicates and the top 40% of overlapping clusters. **h,** Cumulative distribution function of mean conservation score (Phastcons) of MSI2 clusters, compared to a shuffled background control, computed for overlapping clusters between the replicates and the top 40% of overlapping clusters found in different genic regions. Similarity in the 3'UTR conservation for the top 40% with the shuffled background control is likely due to MSI2 sites being small and not needing structural contexts for conservation. P-values were obtained by a Kolgomorov-Smirnov two-tailed test comparing the distributions from actual and shuffled locations. **i,** Genome browser views displaying CLIP-seq mapped reads from replicate 1 (blue), predicted clusters (purple), exact matches for the GUAG sequence (black) and mammal conservation scores (PhyloP) in the 3’ UTRs for a previously predicted Msi1 target.

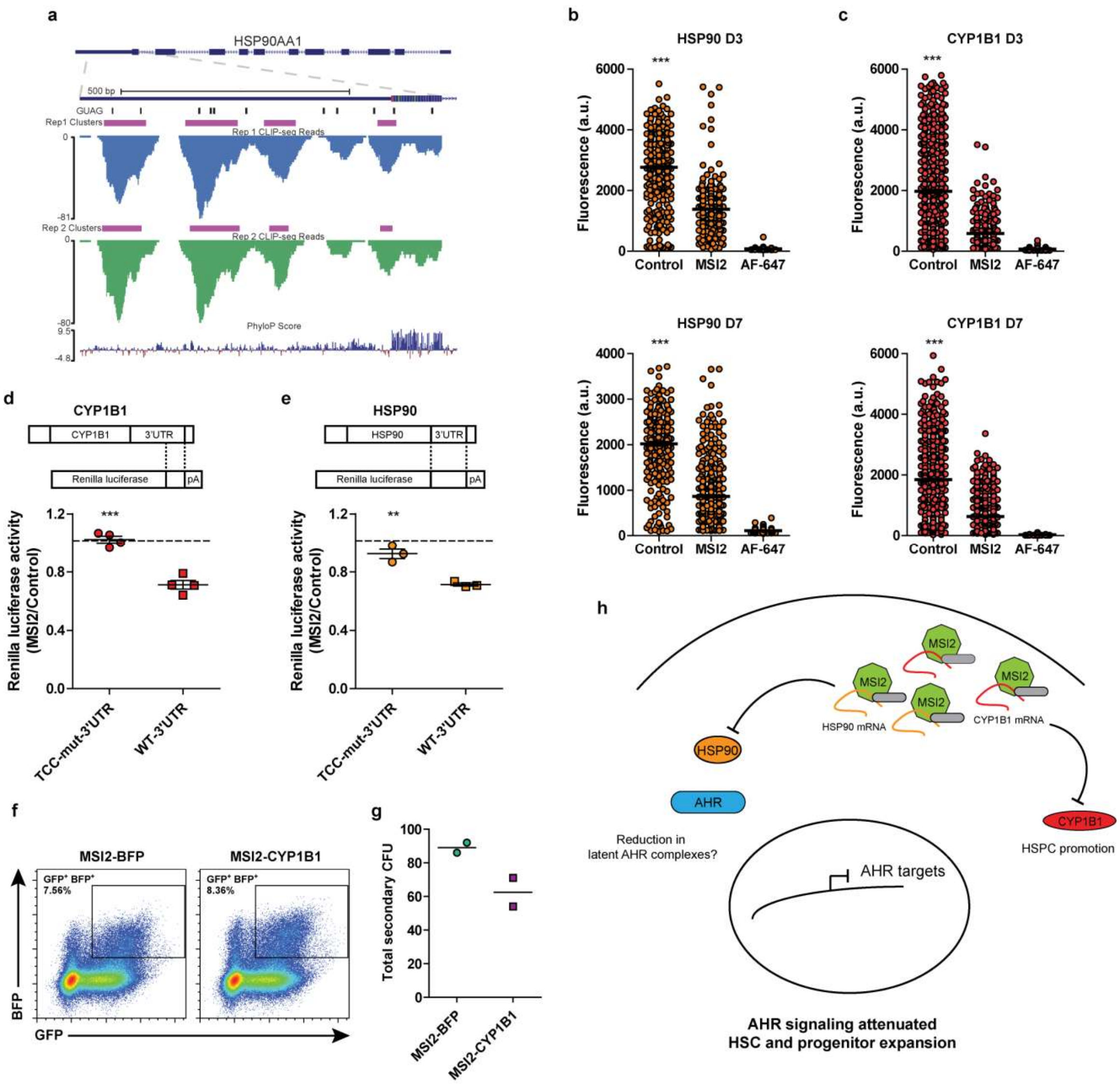
a
HSP90AA1
500 bp
GUAG
Rep1 Clusters
Rep 1 CLIP-seq Reads
0
-81
Rep 2 Clusters
Rep 2 CLIP-seq Reads
0
-80
9.5
PhyloP Score
-4.8
b
HSP90 D3
***
Fluorescence (a.u.)
6000
4000
2000
0
Control
MSI2
AF-647
c
CYP1B1 D3
***
HSP90 D7
CYP1B1 D7
4000
3000
1000
d
CYP1B1
CYP1B1
3'UTR
Renilla luciferase
pA
Renilla luciferase activity (MSI2/Control)
1.2
0.8
0.4
0.0
TCC-mut-3'UTR
WT-3'UTR
e
HSP90
**
HSP90
f
MSI2-BFP
MSI2-CYP1B1
GFP⁺ BFP⁺
7.56%
8.36%
BFP
GFP
g
Total secondary CFU
100
80
60
40
20
0
MSI2-BFP
MSI2-CYP1B1
h
MSI2
HSP90 mRNA
CYP1B1 mRNA
HSP90
AHR
Reduction in latent AHR complexes?
CYP1B1
HSPC promotion
AHR targets
AHR signaling attenuated
HSC and progenitor expansion

Extended Data Figure 10 | MSI2 OE represses CYP1B1 and HSP90 3'UTR Renilla Luciferase reporter activity. a, CLIP-seq reads (replicate 1 in blue and replicate 2 in green) and clusters (purple) mapped to the 3'UTR of HSP90. Matches to the GUAG motif are shown in black. Mammal PhyloP score listed in last track. **b and c,** Representative data of mean per cell fluoresence for HSP90 and CYP1B1 protein in transduced CD34$^+$ CB. Protein level in cells during *in vitro* culture was analyzed 3 days (D3) and 7 days (D7) after transduction and sorting for GFP. Corresponding secondary alone antibody staining is shown for each experiment. Each circle represents a cell, and greater than 200 cells were analyzed per condition. **d and e,** Levels of renilla luciferase activity in NIH-3T3 cells co-transfected with control or MSI2 OE vectors and the CYP1B1 or HSP90 wild type or TCC mutant 3'UTR luciferase reporter (dotted line indicates no change in renilla activity; n=4 CYP1B1 and n=3 HSP90 experiments). **f,** Flow plots of co-transduced CD34$^+$ CB cells with MSI2 (GFP) and CYP1B1 (BFP) lentivirus. **g,** GFP$^+$ BFP$^+$ CFU-GEMMs generated from **f** were replated in to secondary CFU assays and enumerated for total number of colonies formed. A total of 24 CFU-GEMMs from MSI2-BFP and MSI2-CYP1B1 were replated (n=2 experiments). Data presented as mean ± SEM. ***p<0.001, **p<0.01. **h,** A model for AHR pathway attenuation through MSI2 post-transcriptional processing. MSI2 mediates the post-transcriptional down regulation of HSP90 at the outset of culture and continuously represses the prominent AHR pathway effector CYP1B1 to facilitate HSPC expansion. The resultant MSI2-mediated repression of AHR signaling enforces a self-renewal program and allows HSPC expansion ex vivo.

CHAPTER 3

Post-transcriptional control by RNA binding proteins in hematopoietic stem cells

Preamble

This chapter is an original article in preparation for submission. It is presented in its pre-submission format.

"This article is currently in preparation for submission. Rentas S., DeRooij L.P., Hope K.J. **"***Regulon or off? Post-transcriptional control by RNA binding proteins in hematopoietic stem cells."*

S.R., prepared figures and wrote the manuscript, L.P.D, helped with data analysis and literature review and K.J.H. helped prepare and edit the manuscript.

This perspective is on the burgeoning role of RBPs and their capacity to regulate HSC self-renewal and differentiation. The thesis of this perspective is to address how little is known about post-transcriptional control by RBPs in HSCs and how concepts such as "regulons" (the coordinated control of functionally similar mRNA by multiple RBPs to mediate a cell response or phenotype) and their capacity to affect mRNA metabolism (synthesis, decay, translation promotion/inhibition) remains an intriguing theory, however has yet to be proved systematically in the context of HSPCs. The perspective addresses in detail a couple of recently studied RBPs that show significant control over HSC activity and ends with highlighting novel methodologies to study RBP-RNA interactions in rare primary cells. There are a few instances were sentences of my thesis introduction on the role of Msi2 in normal and malignant hematopoiesis were partially borrowed for this publication. Currently unpublished transcriptome data was used in this manuscript and I thank John Dick and members of his lab for providing us with curated RBP expression profiling data from multiple human hematopoietic stem cell populations, as this data helped strengthen the thesis of this manuscript.

Regulon or off? Post-transcriptional control by RNA binding proteins in hematopoietic stem cells

Authors Stefan Rentas, Laura P DeRooij and Kristin J Hope[1]

Affiliations

[1] Department of Biochemistry and Biomedical Sciences, Stem Cell and Cancer Research Institute, McMaster University, Hamilton, ON, Canada

Abstract

Continuing advances in methodologies to probe the interactions of protein and RNA has provided tremendous insight in to the world of post-transcriptional regulation. The important role of RNA binding proteins in controlling post-transcriptional mechanisms in many normal and malignant cellular contexts has led to the development of theories that RNA binding proteins work combinatorially with other RNA binding proteins and accessory factors to regulate subsets of functionally related RNAs to govern specific cellular responses or phenotypes. This “regulon” model has large implications on how proteins are made to control gene regulatory networks in post-mitotic cells and during coordinated stem cell developmental programs. While hematopoietic stem cells are often cited as the most well characterized adult stem cell population, specific examples and clear evidence of regulons at play in these cells is lacking. This perspective is designed to highlight emergent RBPs in hematopoietic stem cells and the very likelihood that regulons play integral roles in controlling their self-renewal and differentiation programs.

Introduction

Control of hematopoietic stem and progenitor cell (HSPC) function has coalesced around gene regulatory networks governed by transcription factors [1-5], however much less is known about the contribution of post-transcriptional mechanisms that guide mRNA stability and translation in these cells, even though these events dictate which gene products ultimately make the proteome. Post-transcriptional control encompasses all regulatory processes in the life-cycle of coding and non-coding RNA (ncRNA). This includes for protein coding transcripts, splicing, capping, poly-adenylation, export, translation initiation, and decay (decapping and deadenylation) [6-8]. Regulation of RNA through these processes is governed by the coordinated action of hundreds of RNA binding proteins (RBPs) [9]. Given the depth and complexity of RNA metabolism, this perspective will focus on the control of mRNA translation by RBPs and confine the discussion to their function in regulating mouse and human hematopoietic stem cell (HSC) behaviour, as there is little consensus to date on what role they provide in directing HSC quiescence, self-renewal, and differentiation. This is in contrary to the growing body of evidence on the essential role RBPs play in mature hematopoietic cells, in particular, mediating immune cell functions and their rapid response to stimuli [10,11] and promoting late-stages of erythropoiesis [12,13]. An important theme of this perspective is to highlight that RBPs have hundreds of targets, both predicted computationally [14] and tested experimentally [15,16], to coordinate control of functionally similar mRNA (i.e. coding for gene products that influence the same physiological process). This higher-level of control, termed “regulons” [17], allows RBPs to perform analogously to combinations of transcription factors binding multiple cis-elements in the genome to coordinate activation or repression of genes belonging to a shared gene program or pathway. To that end, we will touch on new methodologies to systematically characterize RBPs, their targets, and the outcome of these interactions in rare primitive hematopoietic cells, thus allowing testing of the regulon hypothesis in this context and in doing so yield a comprehensive understanding of how RBPs control HSC fate. This understanding may help improve the expansion of HSCs for transplantation therapies [18] or provide a basis for understanding how alterations in RBP controlled regulons promote leukemia [19].

Overview of RBPs and their control of translation

Translation proceeds through a step-wise progression of initiation, elongation, and termination stages. During translation initiation the eukaryotic initiation factor (eIF) 4F cap binding complex, along with eIF4B, interacts with mRNA that is bound to poly-A binding protein (PABP) to enable transcript activation and circularization – this essential step ensures transcripts are a suitable substrate for start codon scanning by 43S preinititation complexes [8]. Progression of the 43S complex to the 48S initiation complex allows 60S ribosome subunit loading to form a final translation elongation competent 80S complex. Regulation of translation by RBPs occurs early in the initiation phase and is generally repressive due to their direct interaction with transcripts and disrupting canonical eIF binding profiles which can lead to shuttling mRNAs to processing bodies to initiate cap-mediated decay or to RNP aggregates such as stress granules which prevent 40S ribosome maturation to elongation competent complexes (Figure 1) [20,21].

However many examples can be found of RBPs stabilizing transcripts and promoting translation, for instance during esinophil activation, GM-CSF cytokine expression and secretion is integral for immune cell survival and is dependent on Pin1 dephosphorylation reducing the binding affinity of the RBP AUF1 on GM-CSF mRNA which promotes its turnover and decay, this subsequently allows the RBP hnRNP C to bind instead and promote transcript stability and expression [22]. RBPs binding transcripts to mediate repressive or activating phenotypes do so via encoded RNA binding domains that are arranged in tandem configurations that provide high affinity and specificity to targeted RNAs [9,23]. The prevalence of recurring domains allows broad classification of RBPs and designates the likely species they interact with (i.e. mRNA vs. ncRNA) [24,25]. Aside from RNA binding domains, RBPs also contain various motifs that facilitate protein-protein interactions, thus increasing target diversity, including number and types of RNA, and versatility, for instance providing contextual binding under certain stimuli or stressors, such as the case with Pin1 [9,11,20]. There are two primary features of RNA molecules that yield specificity to the RBPs they attract: the first is short nucleotide binding sites which in the case of mRNA are typically found within its 3'untranslated region (3'UTR) [25]; the second feature is appropriate folding and secondary structure formation allowing the cis-binding site to be properly displayed for binding [26], for instance Staufen1 requires the region encompassing its binding site to have folded in to a double stranded RNA configuration [27]. Since 3'UTRs include important regulatory information, overall length increases with organismal complexity but still varies on a gene-by-gene basis [28]. This diversity in UTR structure allows for combinatorial binding by multiple RBPs and miRNAs to precisely control translation and coordinate dynamic cellular processes [29-31], such as with the long 3'UTRs and layered post-transcriptional control of many interleukins and cytokines in immune cells [11]. The multi-factorial nature of RBP-RNA targeting, including RNA binding domain structure, protein-protein interactions and physiological events to promote RNA binding, as well as RNA 3'UTR length, sequences it encodes and its conformation, allows for a high-level of nuanced complexity that is important for controlling gene expression, and sets the stage for understanding how these events can affect developmental processes in the hematopoietic stem cell compartment.

Distinct expression profiles of RBPs in normal human HSPCs

The role of RBPs as regulators of HSPC activity has gone largely untested. For instance, direct evidence of RBPs working combinatorially with other RBPs and targeting discrete populations of mRNA to elicit a coordinated cellular phenotype and therefore define an RNA regulon has not been rigorously shown in normal HSPCs (mouse or human). If RNA regulons are working in this context then there should be unique RBP expression profiles in primitive hematopoietic cell types, including within cells competent of self-renewal and establishing long-term hematopoiesis upon transplantation and unique expression profiles in progenitor populations that are shorter-lived but highly proliferative and necessary to maintain daily output of blood cells [32-34]. We explored this possibility here by analyzing the expression profiles of the approximately 1500 putative RBPs in the human genome [23] across the earliest stem and progenitor cell types of the human hierarchy [35] and found that there was indeed cell contextual RBP expression, particularly within the earliest identifiable stem cell type (Figure 2). For instance, the top 30 most highly abundant transcripts coding for RBPs in long-term HSC (LT-HSC), intermediate-term HSC (IT-HSC), short-term HSC (ST-HSC) and multipotent progenitors (MPP) were significantly correlated and comprised almost exclusively of genes involved in ribosome assembly and function (Figure 2A), however, despite this correlation, LT-HSCs maintain approximately 2-fold more transcripts in nearly all of these ribosome processing RBPs (Table 1, Figure 2B). Finding LT-HSCs more highly express RBPs mediating ribosome assembly may provide insight to the hematopoietic system's susceptibility to ribosomopathies, a class of diseases known by mutations causing defective ribosome biogenesis and development of bone marrow failure [36]. That LT-HSCs, a notably quiescent cell population, would have significantly more transcript across many of the proteins necessary to build ribosomes is somewhat paradoxical, particularly in light of recent evidence that protein synthesis is highly regulated and generally attenuated in LT-HSCs [37]. It may be the case then that human LT-HSCs are primed for rapid cell proliferation by expressing high-levels of these transcripts, such that upon commitment to differentiate or asymmetric division, the differentiating cell inherits sufficient transcripts to help create ribosomes and meet the demands of a rapid increase in protein synthesis. Principal component analysis (PCA) on the expression levels of the nearly 1500 expressed RBPs in the human hematopoietic stem cell compartment found LT-HSCs to have a distinct RBP expression profile (Figure 2C), which is in agreement with finding ribosomal associated RBPs to be differentially expressed in LT-HSCs. We further found among the most significantly upregulated RBPs in LT-HSCs a pattern of genes that displayed a step-wise decrease in expression down the hierarchy in proportion to self-renewal potential (Figure 2D). Finally, a literature search of the 153 upregulated RBPs in LT-HSCs relative to MPPs with the term "hematopoietic stem cell" or "leukemia" revealed only ~13% of genes having been studied in some capacity with regard to normal or malignant hematopoiesis, and very few functionally tested in mouse or human models of hematopoiesis. This analysis altogether shows HSPC populations with functionally distinct phenotypes have unique RBP expression profiles and demonstrates that a careful investigation in to how these RBPs coordinate the activity of these different primitive hematopoietic cell types as well as a systems level identification of their targets and corresponding protein level is necessary if progress is going to be made to map regulons at work in HSCs.

RBPs regulating mRNA in HSCs

Our brief analysis here of RBP expression in a published gene expression dataset outlines the interesting prospect that many RBPs are differentially expressed in the primitive hematopoietic compartment but remain largely unstudied. Progress in the field however has been made with a slew of recent work showcasing the role of dozens of RBPs that control HSPC behavior (Table 2) [18,38-60]. In particular, several studies have focused on Musashi-2 (Msi2) revealing it to be a critical regulator of both normal and malignant hematopoieis in mice and humans [18,40-47]. Musashi genes predominately regulate mRNA translation and were originally identified in *Drosophila* as regulators of asymmetric cell division and development of sensory bristles [61,62]. While mammals encode two Musashi paralogs (Msi1 and Msi2), only Msi2 is expressed in the hematopoietic system in both mice and humans and is specifically enriched within the HSPC compartment and decreases with progenitor commitment [18,41]. To demonstrate Msi2 is functional in mouse HSCs multiple groups have performed loss of function experiments using retroviral-mediated knockdown of Msi2 [41,42] and generated Msi2 gene-trap knockout and conditional deletion mice [44,47] to show significant impairment in long-term stem cell activity which appears to be due to altered transcriptional changes in cell cycle regulators and TFG-β signalling [41,42,44,47]. Similarly we found in the human system, lentiviral knockdown of MSI2 leads to losses in long-term repopulating capacity in xenotransplanted mice [18]. Msi2 overexpression in the mouse system has mostly been studied in the context of promoting leukemogenesis since knockdown/out of Msi2 in multiple models of oncogene driven leukemia significantly deters disease progression [40,43,45,46]. Whereas in the human system, MSI2 overexpression has only been functionally studied in normal HSCs where it profoundly enhanced the culture of HSCs and greatly facilitated their ex vivo expansion by attenuating aryl-hydrocarbon receptor (AHR) signalling [18]. Elevated levels of MSI2 have also been shown in human patient leukemias and are a prognostic indicator of increased disease burden and poor outcome [42,43,63]. Details in to Msi2 biochemical activity is largely inferred by its structural similarities to Msi1 [64], where Msi1 has been found to bind the 3'UTR of target transcripts (e.g. *Numb*) via its tandem RNA recognition domains to repress translation by binding PABP and outcompeting eIF4G which compromises assembly of the mature ribosome [65,66]. All evidence suggests that MSI2 also binds target 3'UTRs with greatest affinity over other genic regions as measured by cross-linking immunoprecipitation and high-throughput sequencing (CLIP-seq) or similar global RNA capture techniques [18,47,67,68]. These methods have also started to provide evidence of Msi2 nucleated regulons which is best represented so far in mouse models of leukemia and colon cancer [40,45,67] and human HSC expansion [18]. For instance, leukemogenesis brought on by MLL-AF9 overexpression is sustained by Msi2 driving stability and translation of multiple cooperative oncogenic transcripts such as *Hoxa9*, *Myc*, *Ikzf2*, and *Tspan3* [40,45], whereas with direct overexpression of MSI2 driving a colorectal cancer phenotype, MSI2 bound to *Lrig1*, *Bmpr1a* and *Pten* tumor suppressor transcripts, and at least for *Pten* yielded a reduction in protein levels [67] thus having an opposite effect to what was observed with leukemia. The RBP Igf2bp3 has also similarly been shown in a mouse model of B-acute lymphoblastic leukemia to promote *Myc* and *Cdk6* oncogene expression by binding to their 3'UTR [48]. In chronic myeloid leukemia multiple RBPs also facilitate disease progression [19], thus a common theme is emerging whereby RBPs in leukemias and other cancers may help promote oncogene addiction or tumor supressor repression to facilitate growth. In the normal human hematopoietic context, MSI2 overexpression during HSC ex vivo expansion showed attenuated AHR signalling which was traced back to direct binding and post-transcriptional repression (transcript upregulated or unchanged compared to downregulated protein) of *HSP90*, a necessary complex component for the AHR nuclear receptor transcription factor to bind ligands and activate downstream signaling, as well as post-transcriptional downregulation of the direct AHR effector *CYP1B1*, which in turn was found to help promote differentiation [18]. This stands as one of only a few known examples (see below) of an RBP controlling multiple elements of a self-renewal pathway in normal HSPCs, and the only example that's been shown in the context of human HSCPs. Important next steps to validating these emerging regulons will be to understand how Msi2 in these different contexts (malignant vs. normal, endogenous expression vs. ectopic, mouse vs. human) can post-transcriptionally support or repress target transcript protein levels, as these unique mechanisms likely involve support of uncharacterized RBPs or accessory proteins, such as alternative poly-adenylation enzymes [69], and/or the use of ncRNAs.

HSCs have tight regulation of mRNA translation and attenuated protein synthesis relative to progenitors since increasing or reducing levels of translation and protein synthesis by *Pten* loss or *Rpl24* haploinsufficiency, respectively, impair HSC activity [37]. A consequence of elevated translation is its taxing effect on the endoplasmic reticulum (ER) to fold-proteins bringing about ER stress [70]. This leads to activation of the unfolded protein response (UPR) which aims to restore protein homeostasis by turning on signaling pathways that lead to global translation attenuation, expression of chaperone proteins and apoptosis if the stress cannot be reversed, ultimately these events lower the self-renewal potential of HSCs [39,71]. UPR activation in HSCs occurs during standard *in vitro* culture [39] and is augmented with inclusion of compounds like tunicamycin in culture medium [71]. Thus levels of translation and global protein homeostasis are emerging paradigms that are critical for HSC function. One RBP that might be bridging the gap with a regulon mediating protein stress is developmental pluripotency-associated 5 (Dppa5) [39]. In this study by Stefan Karlsson's lab they found overexpression of Dppa5 in mouse HSCs significantly enhanced self-renewal during ex vivo culture by lowering ER stress, whereas knockdown reduced reconstitution capacity by elevating ER stress. To identify changes in the protein levels of genes involved in ER stress they transplanted mice after Dppa5 overexpression and allowed for months for repopulation to occur and then flow-sorted stem and progenitor cells from the marrow to perform 2D difference gel electrophoresis (2D DIGE) and mass spectrometry. Among the ER-stress genes they found downregulated were numerous stress chaperones (hsp90b1/GRP94, hspa5/GRP78, Txndc5, Pdia3, and Calreticulin), while some of the upregulated genes functioned in amino acid/protein-processing (Prosc, Ppp1cb, and Eif1ax) [39]. They went on to perform Dppa5 CLIP and targeted qPCR assays in a mouse bone marrow derived cell line to show Dppa5 could indeed bind directly to some of these targets, however a comprehensive CLIP-seq approach in these cells or primary cells was not performed. Thus it remains to be seen how Dppa5 precisely regulates ER stress in HSCs, but it is likely through its impact on the binding of potentially hundreds of transcripts [72] and nucleating regulons involved in mediating ER stress.

New methodologies to identify RBPs and their targets

To date there are approximately 1500 RBPs that have been annotated by global mRNA-protein and quantitative mass spectrometry methods [23,73]. By using UV crosslinking techniques to yield only highly specific interactions, the protein-mRNA interactomes created by Castello et al. and Baltz et al. identified many RBPs with common RNA-binding domains [9] as well as implicated hundreds of additional proteins without known

RNA-binding domains to have RNA binding affinity [74,75]. These newly uncovered RBPs has opened the flood gates to atypical RNA binding behaviour of hundreds of genes and as we showed here (Figure 2) necessitate following up in different cellular contexts such as in hematopoietic stem cells and cancer. The difficulty in assessing post-transcriptional regulation by RBPs lies in assessing changes in the proteome relative to the transcriptome. As mentioned above, the study by Miharada et al. performed 2D DIGE and mass spectrometry on primary mouse bone marrow cells enriched in HSPCs to get a complete overview of large-scale changes in the proteome with Dppa5 overexpression. More studies aimed at studying the post-transcriptional/translational effects of RBPs should pursue these methods, especially when analyzing mechanisms of action in bulk tumor samples, like in the case of oncogene driven mouse models of cancer as cell numbers should be less limiting in these situations to perform proteomic analyses. In circumstances where cell sample is increasingly limited, like with HSCs or leukemic stem cells (LSCs) [76], conventional mass spectrometry approaches are generally not feasible. To circumvent these limitations creation of single cell mass-cytometry methods have led to an unprecedented view of the molecular circuitry and unique proteomes that define cell types of the hematopoietic system [77] and modifications to the procedure to allow the co-assessment of transcript levels in single cells [78], as well other novel single cell transcriptome analyses [79], should prove to be critical new methodologies for assessing post-transcriptional gene regulation by RBPs in HSPCs. Additional improvements to CLIP-seq procedures that allow for reductions in cell input material, such as with the development of enhanced CLIP (eCLIP) [80], will also facilitate the identification of RBP-

RNA interactions directly in cells of interest instead of using model cell lines which may not replicate the cell contextual interactions which much of the regulon hypothesis impinges on. Systematic identification of RBP-protein complexes will also need to be explored to test the regulon hypothesis in HSPCs as it is likely the co-expression of ancillary proteins that help provide contextual regulation by RBPs. To that end, BioID and APEX genetic tagging methods [81,82] represent two methodologies to capture proteins that are in very close proximity to one another providing a powerful proteomics methods to capture RBPs in native multi-subunit complexes. Lastly, the development of ribosome profiling, a method for identifying actively translated transcripts [83] in combination with CLIP-seq, transcriptome and proteome analysis will allow researchers to map translation states of RBPs acting in a repressive versus activating manner and when combined with knowledge of the discrete complexes RBPs reside in, will bring about a complete understanding of RBP function and regulons they instruct.

The field of post-transcriptional regulation is rapidly expanding and reaching maturity in many cellular contexts but remains largely undefined in the study of HSPCs, and specifically hypotheses such as regulons need to be tested in HSPCs as they represent a level of control on gene regulatory networks on par with transcriptional activation and repression. The ongoing effort to define key RBPs that mediate HSPC function are necessary to test the regulon hypothesis and will be greatly aided by improvement in methods for probing the proteome and transcriptome at single cell resolution or small input cell numbers. Continued efforts are needed however for testing and identifying new RBP nucleated regulons in rare populations of cells such as mouse and human HSCs if we are to fully appreciate the depth of control they have on adult stem cell development and how during oncogenesis these post-transcriptional pathways are disrupted.

Materials and Methods

Statistical Analysis

LT-, IT-, ST-HSC and MPP gene expression data sets were provided by the Dick lab (Sazan et al., submitted) and the list of RBPs was obtained from Gerstberger et al. [23]. PCA analysis was performed using Excel add-in Multibase package. Plots were generated with GraphPad Prism version 5.0. Unpaired student t-tests were performed with $p < 0.05$ as the cut-off for statistical significance.

References

1 Paul, F. *et al.* Transcriptional Heterogeneity and Lineage Commitment in Myeloid Progenitors. *Cell* **163**, 1663-1677 (2015).

2 Heng, T. S. & Painter, M. W. The Immunological Genome Project: networks of gene expression in immune cells. *Nat Immunol* **9**, 1091-1094 (2008).

3 Novershtern, N. *et al.* Densely interconnected transcriptional circuits control cell states in human hematopoiesis. *Cell* **144**, 296-309 (2011).

4 Laurenti, E. *et al.* The transcriptional architecture of early human hematopoiesis identifies multilevel control of lymphoid commitment. *Nat Immunol* **14**, 756-763 (2013).

5 Wilkinson, A. C. & Gottgens, B. Transcriptional regulation of haematopoietic stem cells. *Adv Exp Med Biol* **786**, 187-212 (2013).

6 Kong, J. & Lasko, P. Translational control in cellular and developmental processes. *Nat Rev Genet* **13**, 383-394 (2012).

7 Reed, R. & Hurt, E. A conserved mRNA export machinery coupled to pre-mRNA splicing. *Cell* **108**, 523-531 (2002).

8 Sonenberg, N. & Hinnebusch, A. G. Regulation of translation initiation in eukaryotes: mechanisms and biological targets. *Cell* **136**, 731-745 (2009).

9 Lunde, B. M., Moore, C. & Varani, G. RNA-binding proteins: modular design for efficient function. *Nat Rev Mol Cell Biol* **8**, 479-490 (2007).

10 Kafasla, P., Skliris, A. & Kontoyiannis, D. L. Post-transcriptional coordination of immunological responses by RNA-binding proteins. *Nat Immunol* **15**, 492-502 (2014).

11 Turner, M., Galloway, A. & Vigorito, E. Noncoding RNA and its associated proteins as regulatory elements of the immune system. *Nat Immunol* **15**, 484-491 (2014).

12 Zhang, L. *et al.* ZFP36L2 is required for self-renewal of early burst-forming unit erythroid progenitors. *Nature* **499**, 92-96 (2013).

13 Thiadens, K. A. & von Lindern, M. Selective mRNA translation in erythropoiesis. *Biochem Soc Trans* **43**, 343-347 (2015).

14 Chushak, Y. G., Martin, J. A., Chavez, J. L., Kelley-Loughnane, N. & Stone, M. O. Computational design of RNA libraries for *in vitro* selection of aptamers. *Methods Mol Biol* **1111**, 1-15 (2014).

15 Kenan, D. J. & Keene, J. D. *In vitro* selection of aptamers from RNA libraries. *Methods Mol Biol* **118**, 217-231 (1999).

16 Darnell, R. CLIP (cross-linking and immunoprecipitation) identification of RNAs bound by a specific protein. *Cold Spring Harb Protoc* **2012**, 1146-1160 (2012).

17 Keene, J. D. RNA regulons: coordination of post-transcriptional events. *Nat Rev Genet* **8**, 533-543 (2007).

18 Rentas, S. *et al.* Musashi-2 attenuates AHR signalling to expand human haematopoietic stem cells. *Nature* **532**, 508-511 (2016).

19 Perrotti, D. & Neviani, P. From mRNA metabolism to cancer therapy: chronic myelogenous leukemia shows the way. *Clin Cancer Res* **13**, 1638-1642 (2007).

20 Buchan, J. R. & Parker, R. Eukaryotic stress granules: the ins and outs of translation. *Mol Cell* **36**, 932-941 (2009).

21 Jackson, R. J., Hellen, C. U. & Pestova, T. V. The mechanism of eukaryotic translation initiation and principles of its regulation. *Nat Rev Mol Cell Biol* **11**, 113-127 (2010).

22 Shen, Z. J., Esnault, S. & Malter, J. S. The peptidyl-prolyl isomerase Pin1 regulates the stability of granulocyte-macrophage colony-stimulating factor mRNA in activated eosinophils. *Nat Immunol* **6**, 1280-1287 (2005).

23 Gerstberger, S., Hafner, M. & Tuschl, T. A census of human RNA-binding proteins. *Nat Rev Genet* **15**, 829-845 (2014).

24 Meister, G. Argonaute proteins: functional insights and emerging roles. *Nat Rev Genet* **14**, 447-459 (2013).

25 Auweter, S. D., Oberstrass, F. C. & Allain, F. H. Sequence-specific binding of single-stranded RNA: is there a code for recognition? *Nucleic Acids Res* **34**, 4943-4959 (2006).

26 Wan, Y. *et al.* Landscape and variation of RNA secondary structure across the human transcriptome. *Nature* **505**, 706-709 (2014).

27 Park, E. & Maquat, L. E. Staufen-mediated mRNA decay. *Wiley Interdiscip Rev RNA* **4**, 423-435 (2013).

28 Chen, C. Y., Chen, S. T., Juan, H. F. & Huang, H. C. Lengthening of 3'UTR increases with morphological complexity in animal evolution. *Bioinformatics* **28**, 3178-3181 (2012).

29 Blackinton, J. G. & Keene, J. D. Post-transcriptional RNA regulons affecting cell cycle and proliferation. *Semin Cell Dev Biol* **34**, 44-54 (2014).

30 Fabian, M. R. & Sonenberg, N. The mechanics of miRNA-mediated gene silencing: a look under the hood of miRISC. *Nat Struct Mol Biol* **19**, 586-593 (2012).

31 Matoulkova, E., Michalova, E., Vojtesek, B. & Hrstka, R. The role of the 3' untranslated region in post-transcriptional regulation of protein expression in mammalian cells. *RNA Biol* **9**, 563-576 (2012).

32 Doulatov, S., Notta, F., Laurenti, E. & Dick, J. E. Hematopoiesis: a human perspective. *Cell Stem Cell* **10**, 120-136 (2012).

33 Orkin, S. H. & Zon, L. I. Hematopoiesis: an evolving paradigm for stem cell biology. *Cell* **132**, 631-644 (2008).

34 Seita, J. & Weissman, I. Hematopoietic stem cell: self-renewal versus differentiation. *Wiley Interdisciplinary Reviews Systems Biology and Medicine* **2**, 640-693 (2010).

35 Notta, F. *et al.* Isolation of single human hematopoietic stem cells capable of long-term multilineage engraftment. *Science* **333**, 218-239 (2011).

36 Raiser, D. M., Narla, A. & Ebert, B. L. The emerging importance of ribosomal dysfunction in the pathogenesis of hematologic disorders. *Leuk Lymphoma* **55**, 491-500 (2014).

37 Signer, R. A., Magee, J. A., Salic, A. & Morrison, S. J. Haematopoietic stem cells require a highly regulated protein synthesis rate. *Nature* **509**, 49-54 (2014).

38 Yuan, J., Nguyen, C. K., Liu, X., Kanellopoulou, C. & Muljo, S. A. Lin28b reprograms adult bone marrow hematopoietic progenitors to mediate fetal-like lymphopoiesis. *Science* **335**, 1195-1200 (2012).

39 Miharada, K., Sigurdsson, V. & Karlsson, S. Dppa5 improves hematopoietic stem cell activity by reducing endoplasmic reticulum stress. *Cell Rep* **7**, 1381-1392 (2014).

40 Kwon, H. Y. *et al.* Tetraspanin 3 Is Required for the Development and Propagation of Acute Myelogenous Leukemia. *Cell Stem Cell* **17**, 152-164 (2015).

41 Hope, K. *et al.* An RNAi screen identifies Msi2 and Prox1 as having opposite roles in the regulation of hematopoietic stem cell activity. *Cell Stem Cell* **7**, 101-114 (2010).

42 Kharas, M. *et al.* Musashi-2 regulates normal hematopoiesis and promotes aggressive myeloid leukemia. *Nature Medicine* **16**, 903-911 (2010).

43 Ito, T. *et al.* Regulation of myeloid leukaemia by the cell-fate determinant Musashi. *Nature* **466**, 765-773 (2010).

44 de Andrés-Aguayo, L. *et al.* Musashi 2 is a regulator of the HSC compartment identified by a retroviral insertion screen and knockout mice. *Blood* **118**, 554-618 (2011).

45 Park, S. M. *et al.* Musashi2 sustains the mixed-lineage leukemia-driven stem cell regulatory program. *J Clin Invest* **125**, 1286-1298 (2015).

46 Taggart, J. *et al.* MSI2 is required for maintaining activated myelodysplastic syndrome stem cells. *Nat Commun* **7**, 10739 (2016).

47 Park, S. M. *et al.* Musashi-2 controls cell fate, lineage bias, and TGF-beta signaling in HSCs. *J Exp Med* **211**, 71-87 (2014).

48 Palanichamy, J. K. *et al.* RNA-binding protein IGF2BP3 targeting of oncogenic transcripts promotes hematopoietic progenitor proliferation. *J Clin Invest* **126**, 1495-1511 (2016).

49 Ghosh, M. *et al.* Essential role of the RNA-binding protein HuR in progenitor cell survival in mice. *J Clin Invest* **119**, 3530-3543 (2009).

50 Stumpo, D. J. *et al.* Targeted disruption of Zfp36l2, encoding a CCCH tandem zinc finger RNA-binding protein, results in defective hematopoiesis. *Blood* **114**, 2401-2410 (2009).

51 Cho, J. *et al.* Ewing sarcoma gene Ews regulates hematopoietic stem cell senescence. *Blood* **117**, 1156-1166 (2011).

52 Gallardo, M. *et al.* hnRNP K Is a Haploinsufficient Tumor Suppressor that Regulates Proliferation and Differentiation Programs in Hematologic Malignancies. *Cancer Cell* **28**, 486-499 (2015).

53 Hartner, J. C., Walkley, C. R., Lu, J. & Orkin, S. H. ADAR1 is essential for the maintenance of hematopoiesis and suppression of interferon signaling. *Nat Immunol* **10**, 109-115 (2009).

54 Zipeto, M. A. *et al.* ADAR1 Activation Drives Leukemia Stem Cell Self-Renewal by Impairing Let-7 Biogenesis. *Cell Stem Cell* (2016).

55 Sugawara, T. *et al.* FET family proto-oncogene Fus contributes to self-renewal of hematopoietic stem cells. *Exp Hematol* **38**, 696-706 (2010).

56 Guo, S. *et al.* MicroRNA miR-125a controls hematopoietic stem cell number. *Proc Natl Acad Sci U S A* **107**, 14229-14234 (2010).

57 Gruber, J. J. *et al.* Ars2 links the nuclear cap-binding complex to RNA interference and cell proliferation. *Cell* **138**, 328-339 (2009).

58 Copley, M. R. *et al.* The Lin28b-let-7-Hmga2 axis determines the higher self-renewal potential of fetal haematopoietic stem cells. *Nat Cell Biol* **15**, 916-925 (2013).

59 Cheloufi, S., Dos Santos, C. O., Chong, M. M. & Hannon, G. J. A dicer-independent miRNA biogenesis pathway that requires Ago catalysis. *Nature* **465**, 584-589 (2010).

60 Lu, K., Nakagawa, M. M., Thummar, K. & Rathinam, C. V. Slicer Endonuclease Argonaute 2 Is a Negative Regulator of Hematopoietic Stem Cell Quiescence. *Stem Cells* **34**, 1343-1353 (2016).

61 Nakamura, M., Okano, H., Blendy, J. A. & Montell, C. Musashi, a neural RNA-binding protein required for Drosophila adult external sensory organ development. *Neuron* **13**, 67-81 (1994).

62 Okabe, M., Imai, T., Kurusu, M., Hiromi, Y. & Okano, H. Translational repression determines a neuronal potential in Drosophila asymmetric cell division. *Nature* **411**, 94-102 (2001).

63 Byers, R. J., Currie, T., Tholouli, E., Rodig, S. J. & Kutok, J. L. MSI2 protein expression predicts unfavorable outcome in acute myeloid leukemia. *Blood* **118**, 2857-2867 (2011).

64 Ohyama, T. *et al.* Structure of Musashi1 in a complex with target RNA: the role of aromatic stacking interactions. *Nucleic Acids Res* **40**, 3218-3231 (2012).

65 Imai, T. *et al.* The neural RNA-binding protein Musashi1 translationally regulates mammalian numb gene expression by interacting with its mRNA. *Mol Cell Biol* **21**, 3888-3900 (2001).

66 Kawahara, H. *et al.* Neural RNA-binding protein Musashi1 inhibits translation initiation by competing with eIF4G for PABP. *J Cell Biol* **181**, 639-653 (2008).

67 Wang, S. *et al.* Transformation of the intestinal epithelium by the MSI2 RNA-binding protein. *Nat Commun* **6**, 6517 (2015).

68 Katz, Y. *et al.* Musashi proteins are post-transcriptional regulators of the epithelial-luminal cell state. *Elife* **3**, e03915 (2014).

69 Cragle, C. & MacNicol, A. M. Musashi protein-directed translational activation of target mRNAs is mediated by the poly(A) polymerase, germ line development defective-2. *J Biol Chem* **289**, 14239-14251 (2014).

70 Walter, P. & Ron, D. The unfolded protein response: from stress pathway to homeostatic regulation. *Science* **334**, 1081-1086 (2011).

71 van Galen, P. *et al.* The unfolded protein response governs integrity of the haematopoietic stem-cell pool during stress. *Nature* **510**, 268-272 (2014).

72 Tanaka, T. S. *et al.* Esg1, expressed exclusively in preimplantation embryos, germline, and embryonic stem cells, is a putative RNA-binding protein with broad RNA targets. *Dev Growth Differ* **48**, 381-390 (2006).

73 Castello, A., Fischer, B., Hentze, M. W. & Preiss, T. RNA-binding proteins in Mendelian disease. *Trends Genet* **29**, 318-327 (2013).

74 Castello, A. *et al.* Insights into RNA biology from an atlas of mammalian mRNA-binding proteins. *Cell* **149**, 1393-1406 (2012).

75 Baltz, A. G. *et al.* The mRNA-bound proteome and its global occupancy profile on protein-coding transcripts. *Mol Cell* **46**, 674-690 (2012).

76 Dick, J. Stem cell concepts renew cancer research. *Blood* **112**, 4793-5600 (2008).

77 Bendall, S. C. *et al.* Single-cell mass cytometry of differential immune and drug responses across a human hematopoietic continuum. *Science* **332**, 687-696 (2011).

78 Frei, A. P. *et al.* Highly multiplexed simultaneous detection of RNAs and proteins in single cells. *Nat Methods* **13**, 269-275 (2016).

79 Macosko, E. Z. *et al.* Highly Parallel Genome-wide Expression Profiling of Individual Cells Using Nanoliter Droplets. *Cell* **161**, 1202-1214 (2015).

80 Van Nostrand, E. L. *et al.* Robust transcriptome-wide discovery of RNA-binding protein binding sites with enhanced CLIP (eCLIP). *Nat Methods* **13**, 508-514 (2016).

81 Rhee, H. W. *et al.* Proteomic mapping of mitochondria in living cells via spatially restricted enzymatic tagging. *Science* **339**, 1328-1331 (2013).

82 Roux, K. J., Kim, D. I., Raida, M. & Burke, B. A promiscuous biotin ligase fusion protein identifies proximal and interacting proteins in mammalian cells. *J Cell Biol* **196**, 801-810 (2012).

83 Ingolia, N. T. Ribosome Footprint Profiling of Translation throughout the Genome. *Cell* **165**, 22-33 (2016).

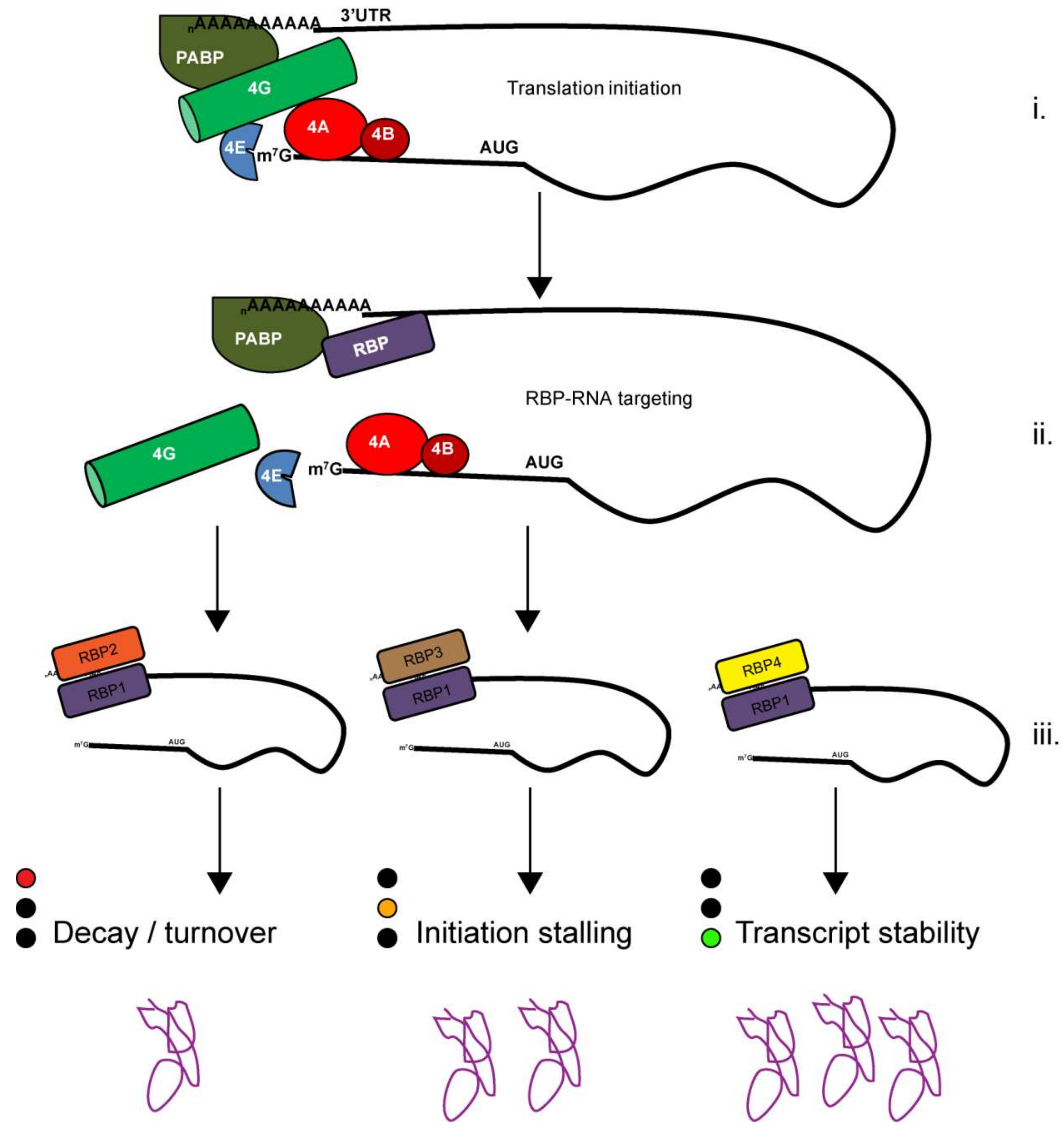
nAAAAAAAAAA
3'UTR
PABP
4G
4E
m7G
4A
4B
AUG
Translation initiation
i.
nAAAAAAAAAA
PABP
RBP
RBP-RNA targeting
4G
4E
m7G
4A
4B
AUG
ii.
RBP2
RBP1
m7G
AUG
RBP3
RBP1
m7G
AUG
RBP4
RBP1
m7G
AUG
iii.
Decay / turnover
Initiation stalling
Transcript stability

Figure 1. A general model of post-transcriptional control by RBPs. In this simplified schematic of RBP mediated post-transcriptional control, translation initiation is (i) depicted with activation and circularization of the transcript. (ii) RBP binding its target mRNA's 3'UTR can disrupt initiation events. (iii) Depending on presence of accessory RBPs or interacting proteins, bound transcripts can be shuttled to mRNA decay pathway resulting in substantially less protein (squiggly line) or continue to block initiation events yielding less protein production, alternatively RBP-RNA interactions can support transcript stability and promote translation producing increased levels of protein.

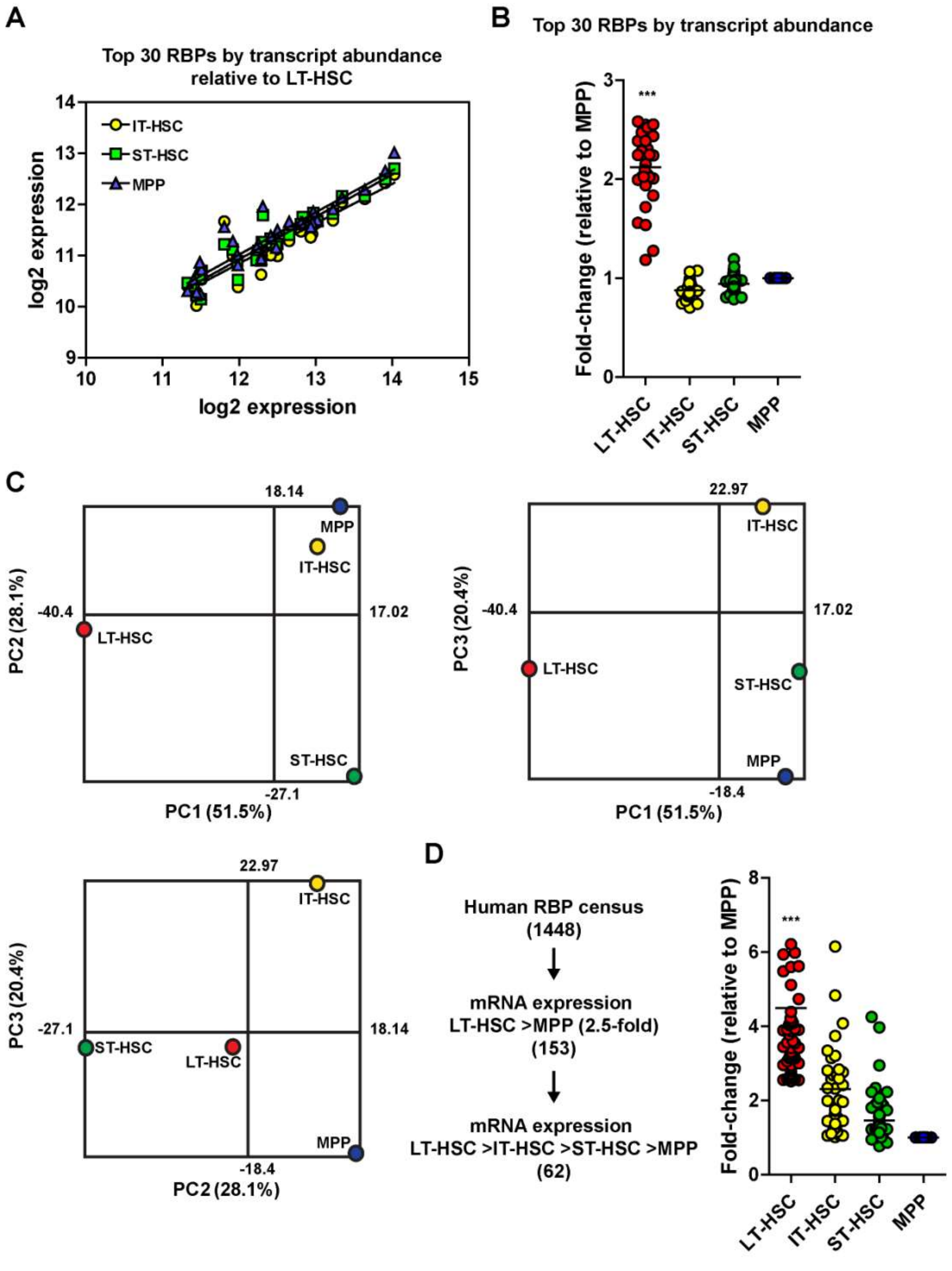
A
Top 30 RBPs by transcript abundance relative to LT-HSC
IT-HSC
ST-HSC
MPP
log2 expression
log2 expression
14
13
12
11
10
9
10
11
12
13
14
15
B
Top 30 RBPs by transcript abundance
Fold-change (relative to MPP)
***
3
2
1
0
LT-HSC
IT-HSC
ST-HSC
MPP
C
18.14
MPP
IT-HSC
-40.4
17.02
LT-HSC
ST-HSC
-27.1
PC2 (28.1%)
PC1 (51.5%)
22.97
IT-HSC
-40.4
17.02
LT-HSC
ST-HSC
MPP
-18.4
PC3 (20.4%)
PC1 (51.5%)
22.97
IT-HSC
-27.1
ST-HSC
LT-HSC
18.14
MPP
-18.4
PC3 (20.4%)
PC2 (28.1%)
D
Human RBP census
(1448)
mRNA expression
LT-HSC >MPP (2.5-fold)
(153)
mRNA expression
LT-HSC >IT-HSC >ST-HSC >MPP
(62)
Fold-change (relative to MPP)
***
8
6
4
2
0
LT-HSC
IT-HSC
ST-HSC
MPP

Figure 2. Differential expression of RBPs across human HSPCs. (A) Comparison of the top 30 RPBs ranked by transcript abundance in LT-HSCs (x-axis) to IT-, ST-HSCs and MPPs. (B) Top 30 RBP transcript level fold change relative to MPPs. (C) 1448 expressed and annotated RBPs in human HSPCs grouped by PCA. (D) Left: Bioinformatic pipeline to show RBPs with step-wisereductions in expression correlating with self-renewal potential. Right: Fold-change of the 62 RBPs with decreasing expression in HSCs to MPPs. Symbols represent individual genes. Data presented showing mean. *** $p < 0.001$.

Table 1. Top 30 RBPs in human HSPCs (Log2 expression)

RBP	LT-HSC	IT-HSC	ST-HSC	MPP
RPL37A	14.0	12.6	12.7	13.0
RPLP2	13.9	12.4	12.5	12.7
RPLP1	13.6	12.1	12.2	12.3
RPL36	13.3	12.0	12.2	12.1
RPL31	13.2	11.7	11.8	11.9
RPS19	13.0	11.6	11.7	11.7
RPL38	13.0	11.6	11.8	11.9
RPL11	13.0	11.4	11.7	11.6
RPL18	12.9	11.4	11.7	11.6
RPL8	12.8	11.6	11.8	11.6
RPS14	12.8	11.5	11.6	11.6
RPL35A	12.7	11.3	11.4	11.7
RPS29	12.5	11.0	11.2	11.5
RPS11	12.5	11.1	11.2	11.2
RPL30	12.4	11.0	11.3	11.4
RPS6	12.3	11.8	11.8	12.0
RPS9	12.3	11.0	11.3	11.0
RPS15	12.3	10.6	10.9	10.9
RPS21	12.3	11.0	11.1	11.2
RPL35	12.2	11.0	10.9	11.2
RPL27	12.0	10.4	10.5	10.8
RPS16	12.0	10.9	10.9	11.0
RPL19	11.9	11.0	11.1	11.3
GAPDH	11.8	11.7	11.2	11.6
RPL29	11.5	10.5	10.7	10.7
RPS8	11.5	10.2	10.1	10.2
RPS24	11.5	10.7	10.6	10.9
FAU	11.4	10.0	10.2	10.3
RPS13	11.4	10.3	10.4	10.5
HNRNPH1	11.3	10.4	10.5	10.3

Table 2. RBPs mediating HSC activity and leukemogenesis

Predominant target	Gene	RNA binding domain	Biochemical activity	HSC and or leukemia phenotype	References
mRNA	Msi2	RRM	transcript translation regulation	loss of HSC self-renewal with deletion and promotes leukemogenesis	18,40-47
	Dppa5	KH	unknown	overexpression positively regulates HSC self-renewal, suppresses ER-stress	39
	Igf2bp3	KH, RRM	transcript translation regulation	overexpression enhances HSC survival and proliferation, promotes B cell leukemia	48
	Elav1	RRM	transcript translation regulation	deletion results in progenitor apoptosis	49
	Zfp36l2	C3H1-type zinc fingers	transcript translation regulation	deletion embryonic lethal and abolshes fetal liver HSC repopulation capacity	50
	Ews	RRM	transcript translation regulation	deletion promotes HSC senescence	51
	hnRNP K	KH	transcript translation regulation	deletion embryonic lethal, haplosufficiency produces myeloproliferative disease	52
	Adar1	DRBM	A to I editase	ADAR1 deletion promotes HSC apoptosis, activated during blast crisis CML	53,54
	Fus	RRM	transcript translation regulation	deletion impairs long-term repopulating capacity	55
ncRNA	Ago2	piwi	pre-miRNA cleavage	embryonic lethal erythropoiesis deficiency with deletion, control HSC quiesence exit	59,60
	Lin28	CCHC zinc fingers	pri-miRNA processing	overexpression promotes adult HSC self-renewal	38,58
	Dicer	DRBM	pre-miRNA cleavage	loss of HSPC maintenance and survival with deletion	56
	Ars2	Nucleotide-bd a/b plait	miRNA processing	embryonic lethal and bone marrow failure with deletion	57

CHAPTER 4

Musashi-2 maintains early hematopoietic multipotent progenitor cells

Preamble

This chapter is an original article in preparation for submission. It is presented in its pre-submission format.

"This article is currently in preparation for submission. Rentas S., Ruzgar N.M, .Chan D., DeRooij L.P., Loo-Yong-Kee J., Belew M.S., Hope K.J. "Musashi-2 regulates miRNA biogenesis in HSPCs"

S.R. designed the project and experiments, performed experiments, analyzed data and wrote the manuscript. N.M.R., D.C., J.L, and L.P.D helped with mouse transplant experiments, including assisting with tamoxifen and cell injections, bleeding and harvesting tissues at experimental endpoints. M.S.B screened mouse embryonic stem cells for proper targeting and insertion of the floxed Msi2 exon 2 vector and initiated the mouse colony. K.J.H. supervised the study, interpreted results and edited the manuscript.

This project aims first and foremost to establish the use of our lab's conditional Msi2 knock out mouse model and examine the effects deletion has on HSPC activity. Interestingly, we observed results that differ in slight but meaningful ways from other Msi2 deletion models, specifically we observed that knocking out Msi2 leads to a loss of the earliest MPPs in the hematopoietic system without overt effects on LT-HSCs, which is in agreement with results by Thomas Graf's group (de Andrés-Aguayo et al., 2011), and differs from the LT-HSC loss observed by Michael Kharas' group (Park et al., 2014). Thus our study further supports that Msi2 plays a very significant role in the controlling early progenitors. Molecular and genetic regulatory control of MPPs to date has been less studied than HSCs, thus showing Msi2 as an important novel mediator of their maintenance and function is an important contribution to the field, especially now that there is a renewed interest in their biology since the discoveries that they are among the most important cells for maintaining both steady-state and stressed hematopoiesis. The second aim of this manuscript is to begin to explore the central theme presented in Chapter 3, which set out at length to describe the importance of identifying how RBPs work cooperatively or antagonistically in regulons within subsets of HSPCs in order to guide cell behaviour. The approach undertaken in this manuscript was to explore Msi2 colocalization with confocal microscopy with known centers of RNA metabolism in distinct populations of HSPCs. Exciting preliminary evidence would suggest that indeed RBPs can take on unique expression and localization features in distinct HSPC populations, which is an exciting prospect to formally testing the regulon hypothesis in HSPCs.

Musashi-2 maintains early hematopoietic multipotent progenitor cells

Authors Stefan Rentas, Laura P DeRooij, Derek Chan, Nensi M Ruzgar, Jessica Loo-Yong-Kee, Muluken S Belew, and Kristin J Hope[1*]

Affiliations

[1] Department of Biochemistry and Biomedical Sciences, Stem Cell and Cancer Research Institute, McMaster University, Hamilton, ON, L8S 4K1, Canada

* Correspondence to kristin@mcmaster.ca

Abstract

Post-transcriptional control of coding and non-coding RNA by RNA binding proteins (RBP) in hematopoietic stem and progenitor cells (HSPC) has not been closely investigated; this is in spite of the importance of these mechanisms in controlling RNA stability, processing, and expression to mediate stem cell regulatory programs. The RBP Musashi-2 (Msi2) plays a crucial role in murine HSC maintenance, however, its function within early multipotent progenitors (MPP) has not been investigated, despite its abundant expression therein. Here we used a conditional knock-out mouse model of Msi2 and found distinct losses in early MPP subsets upon transplantation stress and steady-state hematopoiesis, as well as myeloid biased reconstitution in competitive transplant experiments. To explore how Msi2 can distinctly impact both MPPs and HSCs, we explored Msi2 localization and expression in multiple populations of HSPCs with other putative interacting RBPs as well as proteins involved in known centers of RNA

metabolism and found evidence that RBPs can take on unique expression and localization features in distinct HSPC populations. This work highlights the prospect that Msi2 may have unique RBP interactions to coordinate the distinct activities of both stem and progenitor cells.

Introduction

Hematopoietic stem and progenitor cell (HSPC) self-renewal and differentiation maintains daily hematopoiesis over the course of an organism's lifespan [1]. Controlling HSPC fate decisions relies on the unique expression of protein encoding transcripts, such as transcription factors [2], and non-coding RNAs, including for example microRNA (miRNA) and long non-coding RNA (lncRNA) [3]. While the transcriptional programs that guide expression of coding and to some extent ncRNA have been investigated [2,4-9], post-transcriptional mechanisms controlling processing and stability of RNAs has gone largely unstudied in HSPCs, despite their critical importance in mediating the proteome or the production of functional and mature ncRNAs. To mediate post-transcriptional control, RNA binding proteins bind target RNAs by identifying encoded consensus motifs [10]. When the target is mRNA this typically leads to inhibitory or stabilizing effects on transcript translation by blocking assembly of eukaryotic initiation factor complexes and mature ribosomes or shuttling mRNA to decay pathways [11,12]. In the case of stabilizing, RBPs can have the opposite effect of preventing transcript decay or promoting interactions with core translation machinery [13]. With regards to ncRNA, and specifically miRNA, there are multiple steps during their maturation from primary-miRNA (pri-miRNA) to mature miRNA wherein RBPs can influence processing [14].

One candidate RBP that has pleiotropic effects on RNA metabolism and may affect both mRNA activity and miRNA biogenesis in HSPCs is Musashi-2 (Msi2). The Musashi gene family was originally identified in *Drosophila* as regulators of asymmetric cell division and sensory bristle development [15,16], and orthologs in mammals have been shown to regulate mRNA translation in various tissue stem cell populations, including for instance, promoting neural stem cell self renewal by maintaining Notch signaling through translational repression of *Numb* [17,18]. In this case, the Musashi paralog Msi1 inhibits *Numb* translation by competing with the eukaryotic translation initiation factor 4G (eIF4G) for poly-A binding protein (PABP) binding, which results in incomplete assembly of the mature ribosome [19]. Msi1 shares 69% protein homology to Msi2 and 86% within their RNA binding domains [20]. This has led to the hypothesis that the similarity between Musashi family proteins likely results in similar RNA consensus motifs and target RNAs [20]. In addition, Msi1 can bind to the RBP Lin28 in embryonic stem cells (ES) independent of RNA to significantly inhibit pri-mir-98 processing to pre-mir-98, thus reducing mature mir-98 levels [21]. Msi2 can also regulate translation and directly mediate miRNA biogenesis. For instance in the context of MLL-AF9 driven leukemia, Msi2 stabilizes and promotes translation of various oncogenic transcripts including *Hoxa9*, *Myc*, *Ikzf2*, and *Tspan3* [22,23], whereas during human HSC expansion, MSI2 overexpression represses translation of proteins in the AHR pathway to promote self-renewal [24]. While Msi1 interacts with Lin28 which in turn blocks miRNA maturation, the activity of MSI2 in various model cell lines shows its capacity to directly bind the stem-loop of target pri-miRNAs, like pri-mir-7, in cooperation with Hu antigen R (HuR, ELAV1) to prevent cleavage by Drosha and block maturation [25].

Msi2 has emerged as an important regulator of HSC self renewal since knockdown or deletion negatively affects transplantation outcomes, promotes loss of HSC quiescence and reduces numbers of LT-HSCs [26-29], however, as Msi2 remains abundantly expressed throughout all multipotent progenitor (MPP) and HSC populations in [27,28], it stands to reason some defects in repopulation are due in part to impaired MPP activity. Here we used a novel conditional knockout mouse model to show significant reductions to early MPP populations upon Msi2 deletion with competitive transplantation as well as during steady state hematopoiesis. Gene ablation was also found to promote a myeloid differentiation bias with transplantation to the detriment of the B cell lineage. We examined Msi2 localization in the cell in comparison to known centers of RNA metabolism and putative Msi2-interacting RBPs and show unique colocalization profiles across the primitive hierarchy. Our findings thus highlight the interesting prospect that Msi2 may have unique RBP-protein interactions to coordinate the distinct activities of both stem and progenitor cells.

Results

Conditional deletion of Msi2 significantly impairs competitive repopulation

To characterize the role of Msi2 in primitive hematopoiesis we generated a tamoxifen inducible conditional Msi2 knockout mouse (Figure 1A). Our strategy used targeting vectors that created a floxed exon 2 which encompasses an essential RNA recognition motif necessary for Msi2 biochemical activity [20]. To induce deletion we crossed Msi2$^{fl/fl}$ C57BL/6 mice with a congenic strain that ubiquitously expresses from the Rosa locus Cre recombinase fused to a triple mutant form of the human estrogen receptor (Rosa^{CreERT2}). In order to achieve highly penetrant Msi2 deletion across all cells in the hematopoietic system and to test that our model worked, we dosed Msi2$^{fl/fl}$ Rosa$^{CreERT2/+}$ conditional knockout mice and Msi2$^{fl/fl}$ Rosa$^{+/+}$ control mice with 6 doses of tamoxifen over 9 days (3 consecutive days followed by 3 days rest then 3 days of injections) and then harvested hematopoietic tissue 2 weeks later for genomic DNA extraction and protein analysis. We found excision of exon 2 and loss of Msi2 protein across all tamoxifen treated Msi2$^{fl/fl}$ Rosa$^{CreERT2/+}$ knockout mice while controls remained unaffected (Figure 1B). To further confirm robust deletion in the HSPC compartment, 6 weeks post tamoxifen injection LSK cells were sorted. Immunofluorescence detection showed nearly every cell analyzed lost its expression of MSI2 protein (Figure 1D).

To explore the function of Msi2 on HSPCs, we devised a competitive transplantation assay whereby upon tamoxifen induced deletion, CD45.2 expressing Msi2$^{\Delta/\Delta}$ Rosa$^{CreERT2/+}$ bone marrow is mixed at a 1:1 ratio with congenic competitor CD45.1 B6.SJL bone marrow (500,000 bone marrow cells each) or at a ratio of 7:3 with competitor marrow (700,000 knockout or control cells to 300,000 competitor cells), which yielded an approximately 2:1 ratio of CD45.2 to CD45.1 cells as validated by flow cytometry prior to transplantation (Figure 1C and E). Msi2$^{\Delta/\Delta}$ and similarly treated control Msi2$^{fl/fl}$ bone marrow cells were then transplanted into lethally irradiated B6.SJL mice and donor cell chimerism in peripheral blood was assessed at 7, 14 and 24 weeks (Figure 1C). Examining the repopulation capacity of Msi2$^{\Delta/\Delta}$ cells injected at a 1:1 ratio showed they were rapidly outcompeted by competitor cells at the earliest timepoint assayed, whereas Msi2$^{fl/fl}$ cells gradually increased and showed no sign of impairment at any time point (Figure 1F). Interestingly, even when Msi2$^{\Delta/\Delta}$ bone marrow cells were transplanted in excess relative to competitor cells, they were still unable to repopulate with any efficiency at early and late time points, indicating a significant impairment in their proliferative potential, this is contrast to control cells which were unaffected and able to fully reconstitute lethally irradiated recipients at higher proportions, as expected, with a 2:1 transplant ratio (Figure 1G).

Competitively transplanted mice were analyzed after 24 weeks for levels of engraftment and lineage output in the bone marrow, spleen and peripheral blood. In agreement with Msi2$^{\Delta/\Delta}$ inducing low levels of repopulation in the peripheral blood, we found reduced Msi2$^{\Delta/\Delta}$ CD45.2 marked donor cells in the bone marrow (2.5-fold) and significant reduction in the spleen (8.3-fold) relative to control Msi2$^{fl/fl}$ engrafted mice at the competitive 1:1 transplant ratio and that this phenotype was not rescued when cells were transplanted in 2:1 excess (2- and 4-fold less CD45.2 cells in the bone marrow and spleen respectively, Figure 2A). We next examined the contribution of lineage output from Msi2$^{\Delta/\Delta}$ and Msi2$^{fl/fl}$ donor cells as well as their CD45.1 competitively transplanted counterpart. Here we found that CD45.1 donor cells and CD45.2 Msi2$^{fl/fl}$ displayed similar myeloid lineage output across bone marrow, spleen and peripheral blood, whereas the Msi2$^{\Delta/\Delta}$ cells that remained in these tissues were highly biased to the myeloid lineage, particularly within the spleen and peripheral blood (8.3-fold increase relative control CD45.2 cells, Figure 2B). When taking into account however, reductions of total cells within the CD45.2 graft, actual numbers of myeloid cells decreased in the peripheral blood ($P<0.01$) and were unchanged in the bone marrow and spleen relative to Msi2$^{fl/fl}$ (data not shown). In agreement with increases to the proportion of the myeloid compartment within the remaining Msi2$^{\Delta/\Delta}$ graft, we found significant reductions in the proportion of donor B and T cells (gating on CD45.2^{+}, Figure 2C) and total numbers of these cells (Figure 2D). Altogether, this analysis shows Msi2$^{\Delta/\Delta}$ significantly restricts HSPC capacity to repopulate mice in competitive transplants yielding substantial reductions in circulating myeloid and lymphoid cell, and lymphoid cells across all hematopoietic tissues.

Msi2$^{\Delta/\Delta}$ in competitively transplanted mice have reduced numbers of MPPs

Two previous studies, one using an Mx1-Cre inducible Msi2 deletion system [29] and another using a gene trap Msi2 knockout model [28], showed differing results with respect to the effect Msi2 has on frequency and numbers of long-term and short-term HSC (LT-, ST-HSC) and multipotent progenitors such as lymphoid primed multipotent progenitors (LMPP). de Andres-Aguayo et al. found Msi2 deletion significantly reduced frequency and numbers of ST-HSC and LMPPs but had little effect on LT-HSC, whereas Park et al. showed that in addition to these MPP classes LT-HSCs were also reduced. Using a third strategy of tamoxifen inducible Msi2 deletion, we examined our competitively transplanted mouse bone marrow for the contribution of Msi2$^{\Delta/\Delta}$ and Msi2$^{fl/fl}$ cells to the

HSPC compartment. Within the committed progenitor faction of c-Kit^{+} Sca-1^{-} expressing CD45.2^{+} donor cells, fewer deleted cells contributed overall (1.3-fold) but the effect was not significant (Figure 3A). However, examining the lineage^{-} Sca-1^{+} c-Kit^{+} (LSK) fraction which contains all early MPP and HSC classes, we observed a significant 1.7-fold reduction with Msi2 loss (Figure 3B). Analysis of SLAM family marker expression within LSK cells allows the stratification of different MPP, ST-HSC, and LT-HSC populations based on their varying self-renewal and differentiation capacity [30-32]. We opted to label these populations as has been described by Pietras et al. [32] (Figure 3C). With Msi2 deletion we found, relative to Msi2$^{fl/fl}$ controls, increases in the frequency of LT-HSC and ST-HSC fractions (within LSK cells), but overall no significant change in the number of these cells within CD45.2 graft of bone marrow (Figure 3C-G). We observed that the increased frequency of ST- (3.5-fold) and LT-HSCs (3.8-fold) was due to a striking deficit in the proportion of the multipotent progenitor types MPP2 (3.4-fold) and MPP3 (1.5-fold), which also both demonstrated significantly lower numbers of cells in the grafts (4-fold MPP2 and 2-fold MPP3 loss, Figure 3H-K). Importantly, it has been recently shown that MPP2 and MPP3 cell types are integral for mediating repopulation upon transplantation [31,32], and their deficiency in the Msi2$^{\Delta/\Delta}$ setting may help account for the rapid loss in peripheral blood chimerism observed at the earliest timepoint analyzed (Figure 1F and G). Thus our analysis of the HSPC compartment shows Msi2$^{\Delta/\Delta}$ induces significant losses to multipotent progenitors but maintains numbers ST- and LT-HSCs.

Conditional deletion of Msi2 in non-competitively transplanted mice reduces bone marrow cellularity and depletes early MPPs

Having assessed the function of Msi2 deletion competitively under transplantation stress, we next aimed to test the role of Msi2 under steady-state conditions. Here we transplanted bone marrow from control mice (Msi2$^{fl/fl}$ Rosa$^{+/+}$), Msi2 heterozygous floxed (Msi2$^{fl/+}$ Rosa$^{CreERT2/+}$) and Msi2 homozygous floxed (Msi2$^{fl/fl}$ Rosa$^{CreERT2/+}$) mice into lethally irradiated BL6.SJL mice, allowed 6 weeks of unperturbed repopulation to occur, then treated with tamoxifen to induce deletion (Figure 4A). Resultant mice were analyzed 14 weeks later to assess changes in the hematopoietic system. Prior to inducing deletion we found similar levels in chimerism across the different genotypes transplanted (data not shown). Upon analysis 14 weeks post-Msi2 deletion (20 weeks total engraftment time), we found total bone marrow and spleen cellularity was reduced 1.6-fold and 1.4-fold, respectively, with Msi2$^{\Delta/\Delta}$ but one copy of Msi2 was sufficient to retain normal output of mature cells (Figure 4B and C), a finding consistent with other published data [29]. Next we examined the absolute numbers of LSK cells and found significant reductions in Msi2$^{\Delta/\Delta}$ (2.1-fold) and to a lesser extent Msi2$^{\Delta/+}$ (1.4-fold) transplanted mice relative to Msi2$^{fl/fl}$ controls (Figure 4D). Interestingly, in this post-repopulation deletion condition, we again observed increases in the frequency of LT-HSCs (2.2-fold) but actual numbers of cells within CD45.2 graft of bone marrow to be unchanged (Figure 4E-G), and the same again was observed for ST-HSC numbers being unchanged (Figure 4H-I). While the percentage of MPP2 cells was unchanged between the three genotypes (Figure 4J), numbers of MPP2 cells were significantly reduced with Msi2$^{\Delta/\Delta}$ (2.1-fold) and Msi2$^{\Delta/+}$ (2-fold) relative to Msi2$^{fl/fl}$ (Figure 4K). For MPP3 we found both the percentage (1.2-fold) and number (2.6-fold) of these cells to be significantly reduced with Msi2$^{\Delta/\Delta}$ relative to control cells and Msi2$^{\Delta/+}$ to be unchanged (Figure 4M). While under competitive transplant stress hematopoiesis we found a distinct myeloid bias and lymphoid cell depletion with Msi2$^{\Delta/\Delta}$, however this was not the case under steady state hematopoiesis as we found no changes in myelo/lymphoid proportions across the three genotypes in bone marrow or spleen (data not shown). Altogether this work highlights distinct defects in early MPP population maintenance under non-transplantation stress conditions as well as during competitive transplantation and supports the findings by both de Andres-Aguayo et al. and Park et al. that showed loss of these MPP cell types with Msi2 deletion, however we were unable to replicate the distinct loss of LT-HSCs as described only by Park et al.

Msi2 co-localization with RBPs and centers of RNA metabolism in HSPCs

Msi2 is abundantly and nearly equally expressed across all populations contained in the LSK HSPC fraction of bone marrow [26,28]. However data presented here as well as by others have shown Msi2 regulates discrete populations of HSPCs, including specific types of MPPs as well as LT-HSCs. To begin to test cell contextual activity of Msi2 in the primitive hematopoietic hierarchy we explored through the use of flow sorting, immunostaining, and confocal microscopy, Msi2's protein expression and localization with other RBPs and centers of RNA metabolism to identify if there are any distinguishing features between cell types (Figure 5A). Previous work with Msi1 has shown that it localizes to cytoplasm to mediate translation initiation repression [19] as well as to the nucleus in mouse ES cells to interact with the RBP Lin28 to inhibit pri-mir-98 processing [21]. We performed a sequence alignment with mouse and human Msi1 and 2 to show conservation in the nuclear localization signal (NLS) motifs across species and paralogs, therefore predictive of Msi2 also being competent to localize to the nucleus (Figure 5B). Next we profiled across Lineage depleted bone marrow committed progenitors c-Kit$^+$, MPP3, ST-HSC and LT-HSC populations, Msi2 protein expression and localization in combination with Edc3 which functions as an enhancer of mRNA decapping and assists in the formation ribonucleoprotein aggregates termed P-bodies [33], which act as centralized hubs for mRNA decay machinery in the cytoplasm [11]. Immunostaining analysis for Msi2 revealed a marked reduction in c-Kit$^+$ cells and preferential cytoplasmic localization relative to the high levels across the nucleus and cytoplasm (although higher in the cytoplasm/cell periphery) in MPP3, ST-HSC and LT-HSC populations (Figure 5C, 6A and 7A). Low levels of protein expression in c-Kit$^+$ cells relative to LSK derived subpopulations follows suit with its transcript expression pattern in these cell fractions [26]. Edc3 was found to stain diffusely throughout all cell types profiled and formed distinct, bright puncta indicative of P-body formation [33]. In thresholded images, we found 46% of c-Kit$^+$ cells profiled showed at least one bright staining granule, whereas proportions of cells having foci was higher in stem and multipotent progenitors including 64% of MPP3, 71% of ST-HSC and 55% of LT-HSC (Figure 5C). Interestingly, Edc3 foci in LT-HSCs were also not only less abundant compared to other LSK subpopulations but also tended to be smaller in size (Figure 5C). Msi2 was further unlikely to be highly abundant at the Edc3 foci as the magnitude in fluorescence intensity at the site of granules relative to the adjacent area increased only modestly with Msi2 (1.3-fold) compared to Edc3 (3.6-fold) (Figure 5D). Colocalization coefficients (R) for Msi2 with Edc3 across all populations was on average very low at 0.016 (scale 0.0 – 1.0), due to how much more abundantly expressed Msi2 is relative to Edc3 throughout the cell, whereas Edc3 colocalization with Msi2 was very high (R=0.8) in LSK subpopulations due to the presence of low level but positive Msi2 staining at P-bodies (Figure 5E and F). These results show that Msi2 likely has a limited role in processing transcripts for decay in HSPCs and also highlights the mRNA decay pathway as being differentially activated in HSPCs populations as based on the frequency and size of Edc3 foci.

We next explored Msi2 localization with Tia1, an RBP which functions to nucleate the assembly ribonucleoprotein aggregates of stalled translation initiation [11,34]. These sites of translationally stalled mRNAs, also termed stress granules, recruit multiple passenger RBPs, including Msi2, which was shown with heat shock to localize with Tia1to SGs [19]. While the HSPC populations sorted and stained for Tia1 and Msi2 were not "stressed" per se (i.e. treated with arsenite or heat shock), most evidence would point toward Tia1 functioning in a translation initiation repressive manner [34]. Thus Tia1expression and localization was used as a proxy for translation initiation repression, but not necessarily as evidence of bona fide stress granules, as additional markers were not used to validate this and Tia1's general expression throughout the nucleus and cytoplasm is in opposition to the discrete large puncta stress granules form with stress (Figure 6A) [11]. Comparing Tia1 expression and localization to Msi2 revealed Tia1 to be almost perfectly correlated

(R=0.92) with Msi2 in MPP3, ST-HSC, and LT-HSC, and high as well in c-Kit$^+$ (R=0.76), whereas the correlation coefficients of Msi2 expression with Tia1 was greater in the LSK compartment and decreased with self-renewal potential, and was overall lower in c-Kit$^+$ cells (Figure 6B and C). That Tia1 was abundantly expressed across the LSK compartment and highly correlated with Msi2 provides important evidence that Msi2 is mediating translational repression in normal HSPCs.

Lastly we examined Msi2 localization with HuR (Elav1), an RBP that is essential during hematopoietic development and supports the survival of hematopoietic progenitors by stabilizing Mdm2 mRNA thus blocking p53 mediated apoptosis [35]. HuR, like Msi2 has pleiotropic RNA activities as it not only binds mRNA but also directly interacts with pri-mir-7's stem-loop, in concert with Msi2, to repress mir-7 biogenesis [25]. Given this previous association we examined the protein expression and localization profiles of these two RBPs and found a unique pattern whereby the Msi2-HuR colocalization coefficient decreased with self-renewal potential (R=0.91 c-Kit$^+$, 0.61 MPP3, 0.38 ST-HSC, 0.29 LT-HSC), while HuR displayed a cell contextual colocalization phenotype, colocalizing more strongly in MPP3 (R=0.31) and LT-HSC (R=0.32) populations compared to c-Kit$^+$ (R=0.06) and ST-HSC (0.07) (Figure 7A-C). The inverse relationship seen in c-Kit$^+$ cells is likely because HuR is more highly expressed throughout the entire cell and Msi2 preferentially resides in the cell periphery (i.e. all Msi2 positive staining mapped to only a fraction of HuR positive staining). Interestingly, the HuR colocalization switch occurring from high to low in MPP3 to ST-HSC back to high in LT-HSC appears to be due to elevated Msi2 expression throughout the cell that occurs in LSK cells and an increasingly nuclear restricted staining profile for HuR (Figure 7A). In this staining experiment it would also appear then that ST-HSCs contain less positive Msi2 staining throughout the entire cell, although additional staining and microscopy experiments are needed to validate such an effect as this phenotype appears to be subtle based on the images acquired with Edc3 and Tia1. This analysis highlights along with the Tia1 and Edc3 imaging data that RBPs display different staining profiles across the primitive HSPC hierarchy yielding for the first time to our knowledge cell contextual RBP profiles relative to centres of RNA metabolism.

Discussion

Here we present evidence using a novel conditional Msi2 knockout mouse model that Msi2 specifically supports the maintenance and function of early hematopoietic MPPs. Competitive transplants revealed that loss of Msi2 dramatically impairs donor cell repopulation across multiple hematopoietic tissues and restricts engraftment in peripheral blood as early as 7 weeks post-transplant which was a phenotype maintained for 24 weeks and occurred regardless of the number of Msi2$^{\Delta/\Delta}$ cells transplanted (Figure 1F and G). We suggest this phenotype is indicative of defects occurring in progenitor populations that sustain robust levels of cell proliferation and persisting HSCs enabling the low-level graft to survive for 6 months. To corroborate this hypothesis, examination of the HSPC compartment revealed Msi2$^{\Delta/\Delta}$ induced significant depletion in MPP2 and MPP3 populations, while numbers of ST- and LT-HSC remained unaltered despite reductions in donor CD45.2^{+} bone marrow levels with Msi2 ablation (Figure 3E and G, Figure 2A).

The gating strategy used here did not include the Flt3 marker which separates lymphoid primed MPP (LMPP) subpopulation from LSK cells [36]. This multipotent progenitor which is biased to the lymphoid lineage and is competent to produce granulocytes (G) and monocytes (M) but has no megakaryocyte or erythroid (MK/E) potential, is classically identified by the markers Lin$^-$ c-Kit$^+$ Sca-1$^+$ Flt3$^+$, however the SLAM family markers used to delineate MPPs in this study has LMPPs falling within our MPP3 gate (Lin- c-Kit$^+$ Sca-1$^+$ CD150$^-$ CD48$^+$ Flt3$^{+/-}$), thus our MPP3s contain a mix of both myeloid GM primed Flt3$^-$ and LMPP Flt3$^+$ MPP cell types [32]. As MPP3s were consistently lost in both competitive transplant and steady-state settings with Msi2 deletion, we suspect this is due mainly to a specific reduction in LMPPs, as previous reports show specific depletion of LMPPs with Msi2 loss [28,29] and LMPPs comprise the majority of this population due to Flt3$^+$ cells being nearly entirely retained in the gated CD48$^+$ CD150$^-$ population [31,32]. This may also account for the distinct reductions in lymphoid cells across all tissues (Figure 2D) and a myeloid bias if Flt$^-$ MPPs remained less affected. We also observed loss of MPP2 cells in competitive and non-competitive transplants (Figure 3I and 4K). This population of MPPs has only recently been studied in depth and is found, like MPP3 cells, to be actively cycling [31], myeloid-biased MPPs that are competent to produce lymphoid cells and robustly but transiently produce Mks and platelets during repopulation [32]. It remains unreported however, if Msi2$^{\Delta/\Delta}$ yields any deficiencies in MK-platelet production. MPP2/LMPP and MPP3 populations undergo transient expansion during transplantation to replenish the myeloid and lymphoid compartments thus it remains in line that losses in these cells would impair output from donor grafts as we have demonstrated and result in reductions in recipient bone marrow and spleen cellularity during homeostasis (Figure 4B and C). Importantly, MPP2 and MPP3 cells are unable to regenerate themselves or other cells of the LSK compartment upon transplantation and therefore rely on the activity of HSCs to replenish the progenitor pool [31]. Thus we cannot rule out the reduction in these populations is due solely to intrinsic exhaustion/differentiation within the MPP compartment or a failure on behalf of the HSC pool to adequately proliferate and regenerate these cells. As such, we currently cannot rule out defects to LT-HSCs with Msi2 deletion and whether this manifests an inability to replenish MPPs.

To identify how Msi2 is mediating the biology of discrete self-renewing and non-renewing populations of HSPCs, we employed cell sorting and confocal imaging analysis of Msi2 with RNA metabolism related proteins, including Edc3 for mRNA decay pathway activity, Tia1 for translational repression, and HuR for RBP network correlations. To our knowledge, this represents the first attempts to map RBP associations and RNA metabolism networks within the HSPC compartment. While Msi2 did localize to Edc3 foci, primed areas for mRNA decapping [33], the magnitude of Msi2 at these locations was not substantial which makes Msi2's role in controlling mRNA decay or shuttling specific transcripts for decay unlikely. This is in agreement with work done by Taggart et al. where they found transcript abundance of MSI2 targets in a colorectal cancer model was not impacted with MSI2 binding but that their translation efficiency was [37]. Therefore, despite our evidence here and others suggesting Msi2 interacts with mRNA decapping machinery [19], this may be a byproduct of the complex cycling of transcripts and residual protein interactions that occur as mRNA moves through different processing events (e.g. decay, stalled translation initiation, or active translation) [11]. Interestingly we found Edc3 displayed cell type specific frequency in foci formation, indicating mRNA decay pathways are differentially utilized to meet the demands of different HSPC populations with LT-HSCs harboring the fewest Edc3 loci relative to other LSK subpopulations (Figure 5C). Examining Tia1 with Msi2 displayed nearly perfect correlation confirming that Msi2 likely functions in mediating translation repression in HSPCs, which is what has been described in earlier work concerning Musashi proteins [19,20]. The relationship between Msi2 and HuR revealed unexpected findings such as HuR appearing to become increasingly nuclear as self-renewal potential increases in the HSPC compartment while Msi2, although preferentially localized to the cell periphery, is abundantly expressed throughout the entire cell in all populations of LSK cells, indicating a likely function outside only translation repression. Obvious nuclear activities for Msi2 include working in concert with HuR to regulate pri-miRNA stability and mature miRNA biogenesis [25]. Altogether, this work highlights the unique role of Msi2 in maintaining MPPs and their proliferative potential to sustain high levels of mature blood cell production and provides direct evidence that RBPs can occupy distinct cellular localizations and interactions with centers of RNA metabolism and other RBPs in MPPs and HSCs. Ultimately, it remains to be seen how Msi2's distinct interactions within the HSPC compartment guides its role in regulating MPPs and possibly LT-HSCs.

Methods

Generation of the Msi2 conditional knock-out mouse

All procedures involving animals were carried out in accordance with and were approved by the Animal Research Ethics Board at McMaster University. Msi2 floxed exon 2 targeting vector (loxP site and a FRT-neo-FRT-loxP resistance) was homologously recombined in to the genome by multi-site Red/ET recombination of mouse embryonic stem cells of C57BL/6 background (Gene Bridges). Clones were then screened for correct integration by Southern blotting and offspring generated by diploid aggregation (The Centre for Phenogenomics) and heterozygous chimera mice bred to homozygosity, followed by breeding with FlpE mice (Jackson Laboratories) to excise the Neo cassette and finally Rosa-CreERT2 mice (Jackson Laboratories) to yield the conditional knock-out model for Msi2 in the C57BL/6 background. To induce deletion mice aged 8-12 weeks were given on 3 consecutive days, 1 mL intraperitoneal injections of 4-hydroxy tamoxifen (1 mg/mL dissolved in 100% ethanol) delivered in Phosphate Buffered Saline and 10% captizol (Sigma-Aldrich). This was followed by a 3-day wait period and then three additional daily injections.

Genotyping

Genotypes were confirmed by extracting genomic DNA from mouse tissues (tail snips or processed single-cell suspensions in PBS) with the Extract-N-Amp Tissue PCR kitTM (Sigma-Aldrich), followed by PCR using a BioRad ThermoCycler, as per manufacturer instructions.18 Forward-CTTGGCTTCTTTATTGCTCTTTG and Reverse-CAAAATCGAGAAGGGAATGC primers were used to confirm whether Msi2 allele was floxed, prior to tamoxifen-induced deletion of Exon 2. Forward-AAAGTCGCTCTGAGTTGTTAT), Reverse WT-GGAGCGGGAGAAATGGATATG and Reverse Cre-CCTGATCCTGGCAATTTCG primers were used to genotype the Rosa26 locus for the presence of the Cre sequence. After tamoxifen-injections, Cre-recombinase deletion of the floxed Exon 2 in the Msi2 locus of obtained tissues was confirmed using the primers: Forward-CACTCGCGCACCTTG and Reverse-CAAAATCGAGAAGGGAATGC.

Western blotting

The single-cell suspensions from mouse spleens, harvested at 5 weeks after tamoxifen induction, were lysed in radioimmunoprecipitation assay buffer (RIPA, Sigma-Aldrich) with 1X Protease Inhibitor Cocktail (Roche). Protein extracts were transferred into 1X NuPAGE LDS Sample Buffer (Thermo Fisher) with 0.1 mM B-mercaptoethanol, and were separated on 10% SDS-PAGE gels. The proteins were blotted with the monoclonal antibodies, rabbit anti-mouse-Msi2 (Abcam) and mouse anti-mouse B-actin (Santa Cruz Biotechnologies) at 4oC overnight; signals were detected using IR Dyes 680 goat anti-rabbit and 800CW goat anti-mouse IgGs (Li-COR), and visualized using the Licor-Odyssey imaging system with its associated software.

Competitive transplantation

8-12 week old Msi2$^{fl/fl}$ Rosa$^{+/+}$ or Msi2$^{fl/fl}$ Rosa^{CreERT2} mice were treated with tamoxifen as described above, sacrificed the following day and whole bone marrow was obtained from femurs, tibias and pelvis by crushing with a mortar and pestle. Bone marrow cells from competitor B6.SJL mice aged 8-12 weeks were processed identically. Cell suspensions were red blood cell lysed with ammonium choloride (Stem Cell Technologies), counted and mixed at ratios of 1:1 (500,000 cells each) and 7:3 (also referred to here as 2:1, 700,000 Msi2$^{fl/fl}$ or Msi2$^{\Delta/\Delta}$ cells with 300,000 SJL cells) and injected intravenously in to the tail vein of lethally irradiated (1050 rad) SJL mice. Mice were bled at 7, 14 and 24 weeks post transplant and sacrificed at 24 weeks for analysis.

Non-competitive transplants

8-12 week old Msi2$^{fl/fl}$ Rosa$^{+/+}$ or Msi2$^{fl/fl}$ Rosa^{CreERT2} mice were sacrificed and whole bone marrow was obtained from femurs, tibias and pelvis. Cell suspensions were red blood cell lysed with ammonium choloride (Stem Cell Technologies), counted and injected intravenously (1x10^{6} cells) in to the tail vein of lethally irradiated (1050 rad) SJL mice. 6 weeks post cell transplant, mice were treated with tamoxifen as described above and 14 weeks later analyzed for engraftment. Bone marrow obtained from femurs, tibias and pelvis and spleens were harvested, red blood cell lysed, counted and analyzed by flow cytometry.

Flow cytometry

The single-cell suspensions from bone marrow were blocked with mouse FC block (BD Biosciences) and stained with combinations of the following antibodies all from BD Biosciences unless otherwise stated: CD45.1 (A20), CD45.2 (104), CDllb (M1/70), Gr-1 (RB6-8C5), CD3 (17A2), B220 (RA3-6B2), Lineage cocktail (eBioscience), Sca-1 (E07354-217, eBioscience), c-Kit (2B8), CD48 (HM48-1), and CD150 (TC15-12F12.2, Biolegend). To sort for HSPCs for immunofluoresence, red blood cell lysed bone marrow from five 8-12 week old wild type C57BL/6 was pooled and lineage depleted using the

EasySep Mouse Hematopoietic Progenitor Cell Enrichment Kit (Stem Cell Technologies) according to manufacturer instructions. Cell populations used for sorting HSPCs include c-Kit$^+$ (Lin$^-$ c-Kit$^+$), LSK (Lin$^-$ Sca-1$^+$c-Kit$^+$), MPP3 (LSK CD150$^-$ CD48$^+$), ST-HSC (LSK CD150$^-$ CD48$^-$) and LT-HSC (LSK CD150$^+$ CD48$^-$) using the following antibody cocktail: Lineage cocktail-Pacific Blue, Sca-1-APC, c-Kit-PeCy7, CD150-PE and CD48-FITC. All cell sorts were completed using the BD FACSAria sorter and analysis was performed using the BD LSR II. Flow plot generation and analysis was performed using FlowJo software.

Immunofluorescence

Isolated populations of HSPCs were fixed with 2% PFA (Thermo Scientific) in PBS for 10 min and washed with PBS. At least 1000 cells were cyto-spun onto glass slides and were permeabilized with 0.2% Triton (Sigma-Aldrich) in PBS for 20 min. Cells were then blocked with 10% donkey serum and 0.1% saponin in PBS for 30 mins at room temperature, and then stained with the primary antibodies against Msi2 (EP1305Y, Abcam), HuR (ab28660, Abcam), Tia1 (sc-1751, Santa Cruz), or Edc3 (sc-365024, Santa Cruz) for an hour followed by an hour of secondary antibody staining with donkey anti-rabbit Alexa Fluor 488 for Msi2, donkey anti-mouse Alexa Fluor 647 for Edc3, or donkey anti-goat Alexa Fluor 647 for HuR (Invitrogen). Stained cells were mounted with DAPI Prolong Gold (Invitrogen). Images were acquired with a Zeiss LSM 800 laser scanning confocal microscope and Axiocam camera and Zen software. Co-localization analysis was performed using the Zen software feature and control secondary antibody alone stained c-Kit$^+$ cells to set gates for positive staining. Czi files were processed in

ImageJ (MBF plugin) for background subtraction, line plot analysis and foci counting using a threshold of 100.

Protein alignment

Mouse and human Msi1 and 2 amino acid sequences were obtained from Uniprot and aligned and visualized with Jalview.

Statistical analyses

All statistical analyses were performed using GraphPad Prism 5. Error bars reflect the SEM, unless otherwise stated, unpaired t-tests were used to compute p-values.

Acknowledgements

This work was supported by Canadian Institute of Health Research, Ontario Institute for Cancer Research, and Graduate Fellowship by Canadian Blood Services.

References

1 Orkin, S. H. & Zon, L. I. Hematopoiesis: an evolving paradigm for stem cell biology. *Cell* **132**, 631-644 (2008).

2 Wilkinson, A. C. & Gottgens, B. Transcriptional regulation of haematopoietic stem cells. *Adv Exp Med Biol* **786**, 187-212 (2013).

3 Jeong, M. & Goodell, M. A. Noncoding Regulatory RNAs in Hematopoiesis. *Curr Top Dev Biol* **118**, 245-270 (2016).

4 Arnold, C. P. *et al.* MicroRNA programs in normal and aberrant stem and progenitor cells. *Genome Res* **21**, 798-810 (2011).

5 Cabezas-Wallscheid, N. *et al.* Identification of regulatory networks in HSCs and their immediate progeny via integrated proteome, transcriptome, and DNA methylome analysis. *Cell Stem Cell* **15**, 507-522 (2014).

6 Paul, F. *et al.* Transcriptional Heterogeneity and Lineage Commitment in Myeloid Progenitors. *Cell* **163**, 1663-1677 (2015).

7 Heng, T. S. & Painter, M. W. The Immunological Genome Project: networks of gene expression in immune cells. *Nat Immunol* **9**, 1091-1094 (2008).

8 Novershtern, N. *et al.* Densely interconnected transcriptional circuits control cell states in human hematopoiesis. *Cell* **144**, 296-309 (2011).

9 Laurenti, E. *et al.* The transcriptional architecture of early human hematopoiesis identifies multilevel control of lymphoid commitment. *Nat Immunol* **14**, 756-763 (2013).

10 Lunde, B. M., Moore, C. & Varani, G. RNA-binding proteins: modular design for efficient function. *Nat Rev Mol Cell Biol* **8**, 479-490 (2007).

11 Buchan, J. R. & Parker, R. Eukaryotic stress granules: the ins and outs of translation. *Mol Cell* **36**, 932-941 (2009).

12 Jackson, R. J., Hellen, C. U. & Pestova, T. V. The mechanism of eukaryotic translation initiation and principles of its regulation. *Nat Rev Mol Cell Biol* **11**, 113-127 (2010).

13 Ray, D. *et al.* A compendium of RNA-binding motifs for decoding gene regulation. *Nature* **499**, 172-177 (2013).

14 Winter, J., Jung, S., Keller, S., Gregory, R. I. & Diederichs, S. Many roads to maturity: microRNA biogenesis pathways and their regulation. *Nat Cell Biol* **11**, 228-234 (2009).

15 Nakamura, M., Okano, H., Blendy, J. A. & Montell, C. Musashi, a neural RNA-binding protein required for Drosophila adult external sensory organ development. *Neuron* **13**, 67-81 (1994).

16 Okabe, M., Imai, T., Kurusu, M., Hiromi, Y. & Okano, H. Translational repression determines a neuronal potential in Drosophila asymmetric cell division. *Nature* **411**, 94-102 (2001).

17 Keyoung, H. *et al.* High-yield selection and extraction of two promoter-defined phenotypes of neural stem cells from the fetal human brain. *Nature Biotechnology* **19**, 843-893 (2001).

18 Imai, T. *et al.* The neural RNA-binding protein Musashi1 translationally regulates mammalian numb gene expression by interacting with its mRNA. *Mol Cell Biol* **21**, 3888-3900 (2001).

19 Kawahara, H. *et al.* Neural RNA-binding protein Musashi1 inhibits translation initiation by competing with eIF4G for PABP. *J Cell Biol* **181**, 639-653 (2008).

20 Ohyama, T. *et al.* Structure of Musashi1 in a complex with target RNA: the role of aromatic stacking interactions. *Nucleic Acids Res* **40**, 3218-3231 (2012).

21 Kawahara, H. *et al.* Musashi1 cooperates in abnormal cell lineage protein 28 (Lin28)-mediated let-7 family microRNA biogenesis in early neural differentiation. *J Biol Chem* **286**, 16121-16130 (2011).

22 Kwon, H. Y. *et al.* Tetraspanin 3 Is Required for the Development and Propagation of Acute Myelogenous Leukemia. *Cell Stem Cell* **17**, 152-164 (2015).

23 Park, S. M. *et al.* Musashi2 sustains the mixed-lineage leukemia-driven stem cell regulatory program. *J Clin Invest* **125**, 1286-1298 (2015).

24 Rentas, S. *et al.* Musashi-2 attenuates AHR signalling to expand human haematopoietic stem cells. *Nature* **532**, 508-511 (2016).

25 Choudhury, N. R. *et al.* Tissue-specific control of brain-enriched miR-7 biogenesis. *Genes Dev* **27**, 24-38 (2013).

26 Kharas, M. *et al.* Musashi-2 regulates normal hematopoiesis and promotes aggressive myeloid leukemia. *Nature Medicine* **16**, 903-911 (2010).

27 Hope, K. *et al.* An RNAi screen identifies Msi2 and Prox1 as having opposite roles in the regulation of hematopoietic stem cell activity. *Cell Stem Cell* **7**, 101-114 (2010).

28 de Andrés-Aguayo, L. *et al.* Musashi 2 is a regulator of the HSC compartment identified by a retroviral insertion screen and knockout mice. *Blood* **118**, 554-618 (2011).

29 Park, S. M. *et al.* Musashi-2 controls cell fate, lineage bias, and TGF-beta signaling in HSCs. *J Exp Med* **211**, 71-87 (2014).

30 Kiel, M. *et al.* SLAM family receptors distinguish hematopoietic stem and progenitor cells and reveal endothelial niches for stem cells. *Cell* **121**, 1109-1130 (2005).

31 Oguro, H., Ding, L. & Morrison, S. J. SLAM family markers resolve functionally distinct subpopulations of hematopoietic stem cells and multipotent progenitors. *Cell Stem Cell* **13**, 102-116 (2013).

32 Pietras, E. M. *et al.* Functionally Distinct Subsets of Lineage-Biased Multipotent Progenitors Control Blood Production in Normal and Regenerative Conditions. *Cell Stem Cell* **17**, 35-46 (2015).

33 Ling, S. H. *et al.* Crystal structure of human Edc3 and its functional implications. *Mol Cell Biol* **28**, 5965-5976 (2008).

34 Waris, S., Wilce, M. C. & Wilce, J. A. RNA recognition and stress granule formation by TIA proteins. *Int J Mol Sci* **15**, 23377-23388 (2014).

35 Ghosh, M. *et al.* Essential role of the RNA-binding protein HuR in progenitor cell survival in mice. *J Clin Invest* **119**, 3530-3543 (2009).

36 Adolfsson, J. *et al.* Identification of Flt3+ lympho-myeloid stem cells lacking erythro-megakaryocytic potential a revised road map for adult blood lineage commitment. *Cell* **121**, 295-306 (2005).

37 Taggart, J. *et al.* MSI2 is required for maintaining activated myelodysplastic syndrome stem cells. *Nat Commun* **7**, 10739 (2016).

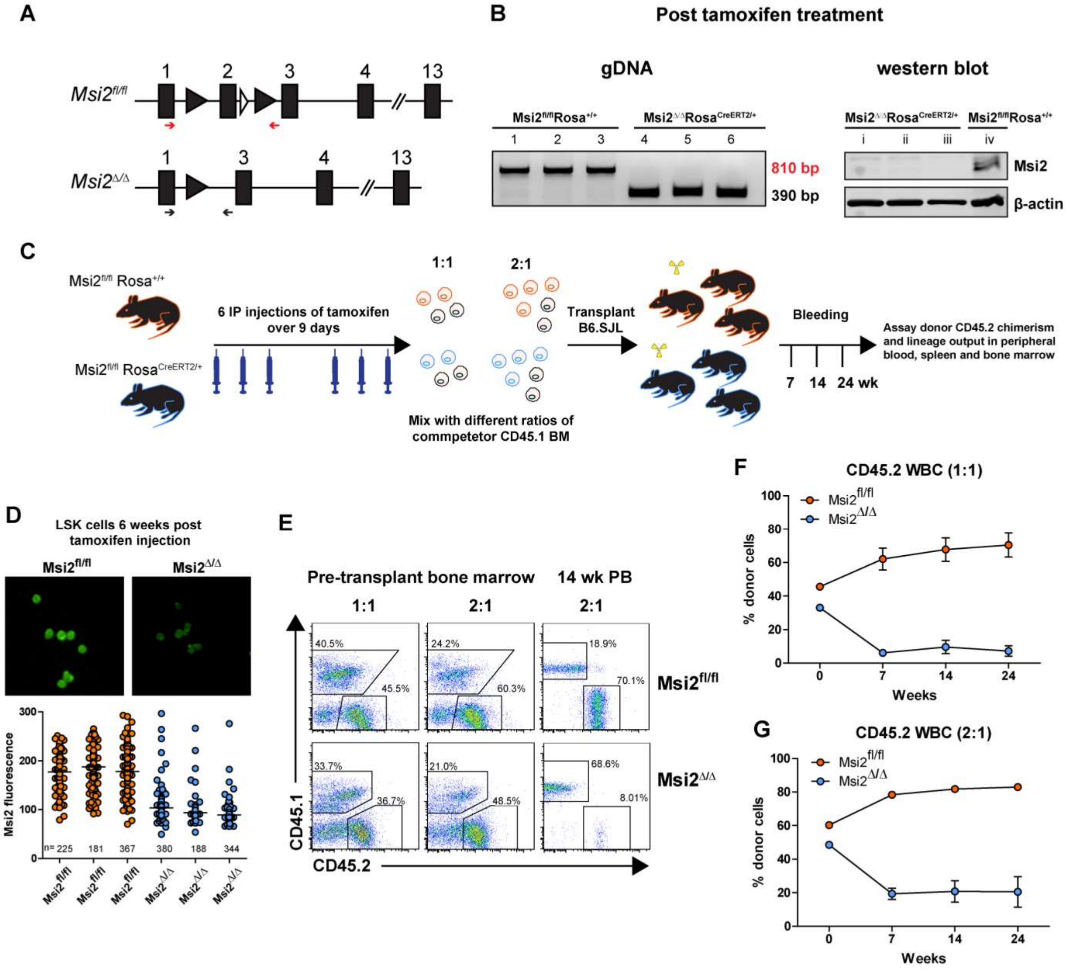
A
Msi2fl/fl
1
2
3
4
13
Msi2Δ/Δ
1
3
4
13
B
Post tamoxifen treatment
gDNA
Msi2fl/flRosa+/+
Msi2Δ/ΔRosaCreERT2/+
1
2
3
4
5
6
810 bp
390 bp
western blot
Msi2Δ/ΔRosaCreERT2/+
Msi2fl/flRosa+/+
i
ii
iii
iv
Msi2
β-actin
C
Msi2fl/fl Rosa+/+
Msi2fl/fl RosaCreERT2/+
6 IP injections of tamoxifen over 9 days
1:1
2:1
Mix with different ratios of commpetetor CD45.1 BM
Transplant B6.SJL
Bleeding
7
14
24 wk
Assay donor CD45.2 chimerism and lineage output in peripheral blood, spleen and bone marrow
D
LSK cells 6 weeks post tamoxifen injection
Msi2fl/fl
Msi2Δ/Δ
Msi2 fluorescence
300
200
100
0
n= 225
181
367
380
188
344
Msi2fl/fl
Msi2fl/fl
Msi2fl/fl
Msi2Δ/Δ
Msi2Δ/Δ
Msi2Δ/Δ
E
Pre-transplant bone marrow
14 wk PB
1:1
2:1
2:1
40.5%
45.5%
24.2%
60.3%
18.9%
70.1%
Msi2fl/fl
33.7%
36.7%
21.0%
48.5%
68.6%
8.01%
Msi2Δ/Δ
CD45.1
CD45.2
F
CD45.2 WBC (1:1)
Msi2fl/fl
Msi2Δ/Δ
% donor cells
100
80
60
40
20
0
0
7
14
24
Weeks
G
CD45.2 WBC (2:1)
Msi2fl/fl
Msi2Δ/Δ
% donor cells
100
80
60
40
20
0
0
7
14
24
Weeks

Figure 1. Conditional deletion of Msi2 significantly restricts HSPC reconstitution. (A) Schematic of Msi2 conditional knockout mouse model**.** Top: Msi2 locus is depicted with floxed (fl) exon 2 prior tamoxifen injection. Bottom: Homozygous deletion of exon 2 post tamoxifen. Arrows indicate primers used to assay deletionin B. (B) Confirmation of Msi2 deletion by genomic DNA PCR and subsequent loss of protein by western blot. Spleen lysates profiled for both assays 2 weeks after last tamoxifen injection. Numbers represent different mice. (C) Competitive transplant assay set up. (D) Confirmation of Msi2 deletion and protein reduction in LSK cells 6 weeks post tamoxifen. Number of cells quantified listed in each column. (E) Flow plots of pre-transplant bone marrow mixtures and 14 weeks peripheral blood chimerism. (F and G) Peripheral blood CD45.2 donor chimerism over 24 weeks with Msi2 deletion. n=3 Msi2$^{\Delta/\Delta}$ and Msi2$^{fl/fl}$ control mice transplanted at 1:1, and n=6 Msi2$^{\Delta/\Delta}$ and n=4 Msi2$^{fl/fl}$ control mice transplanted at 2:1. Results from are from 3 experiments.

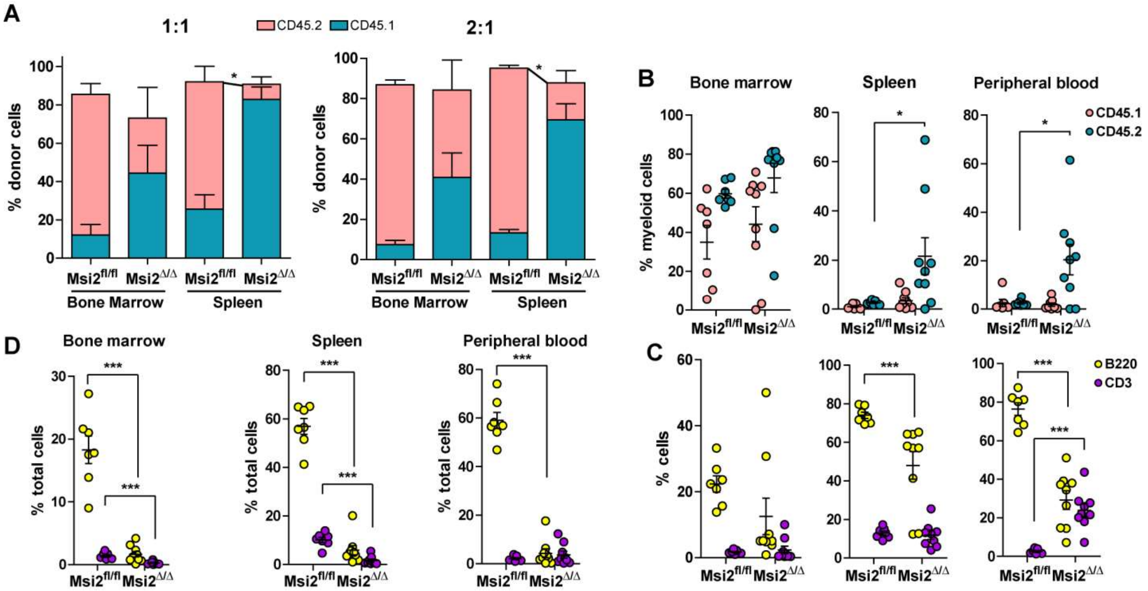
A
1:1
CD45.2
CD45.1
2:1
% donor cells
100
80
60
40
20
0
*
*
Msi2fl/fl
Msi2Δ/Δ
Msi2fl/fl
Msi2Δ/Δ
Bone Marrow
Spleen
B
Bone marrow
Spleen
Peripheral blood
% myeloid cells
CD45.1
CD45.2
*
*
C
% cells
B220
CD3
***
D
Bone marrow
Spleen
Peripheral blood
% total cells
***
Msi2fl/fl
Msi2Δ/Δ

Figure 2. Msi2 deletion promotes myeloid lineage bias and restricts lymphoid development. (A) CD45.2 and CD45.1 competitor donor cell chimerism at 21 weeks in bone marrow and spleen. (B). Myeloid lineage ($CD11b^+$ $Gr1^+$, gated on CD45.2 cells) analysis with Msi2 deletion across bone marrow, spleen and peripheral blood. 1:1 and 2:1 mice were pooled for analysis. (C and D) Frequency of lymphoid lineage analysis within CD45.2 cells (C) and within total bone marrow, spleen, or peripheral cells (D) with Msi2 deletion across bone marrow, spleen and peripheral blood from competitively transplanted mice. Data shown is from CD45.2 grafts. 1:1 and 2:1 mice were pooled for analysis. Data shown as mean ± SEM. Mann-Whitney test, *$p<0.05$; ***$p<0.001$.

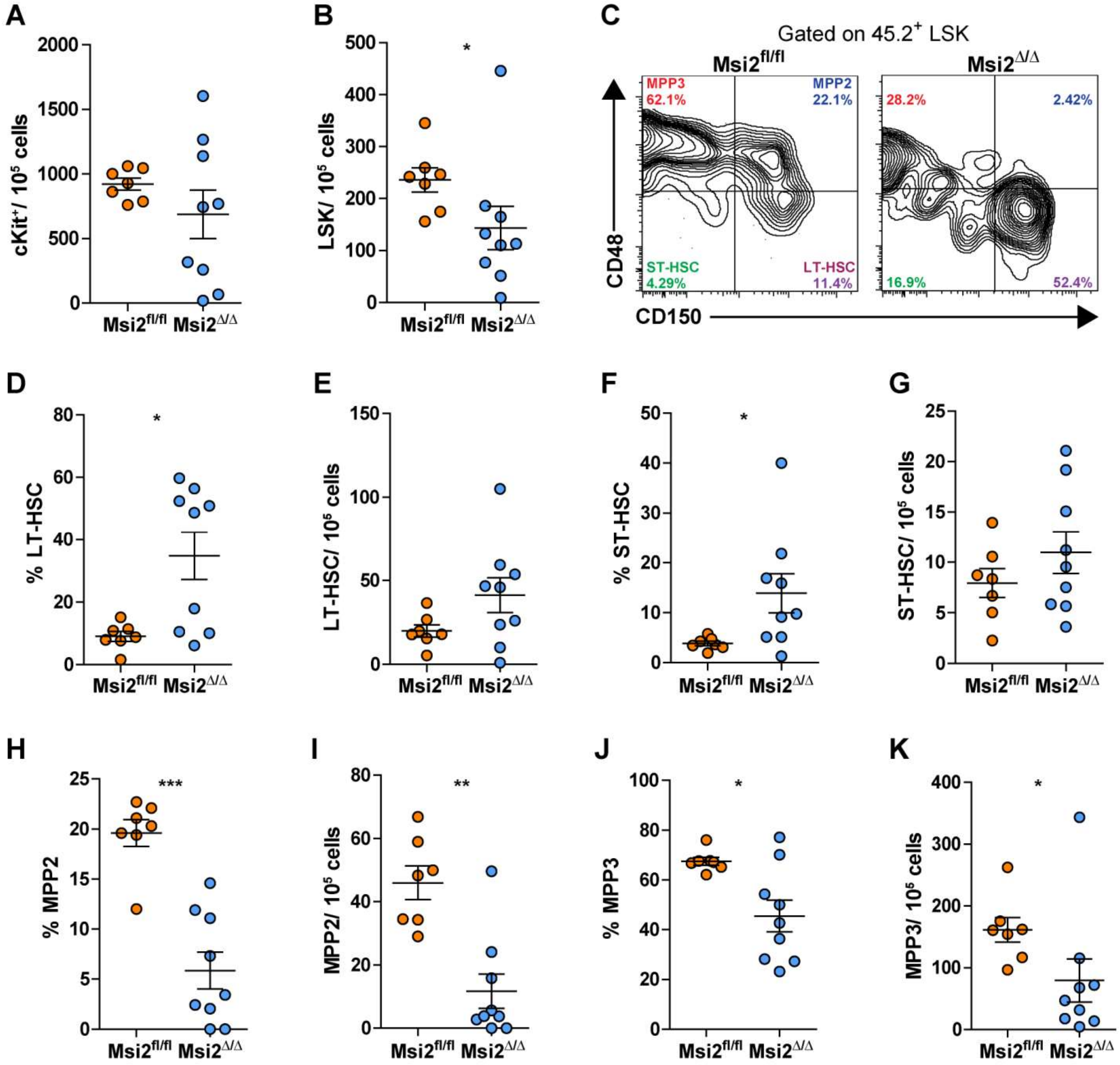
A
cKit⁺/ 10⁵ cells
Msi2fl/fl
Msi2Δ/Δ
B
LSK/ 10⁵ cells
*
C
Gated on 45.2⁺ LSK
Msi2fl/fl
Msi2Δ/Δ
MPP3 62.1%
MPP2 22.1%
ST-HSC 4.29%
LT-HSC 11.4%
28.2%
2.42%
16.9%
52.4%
CD48
CD150
D
% LT-HSC
*
E
LT-HSC/ 10⁵ cells
F
% ST-HSC
*
G
ST-HSC/ 10⁵ cells
H
% MPP2
***
I
MPP2/ 10⁵ cells
**
J
% MPP3
*
K
MPP3/ 10⁵ cells
*

Figure 3. Msi2 deletion depletes MPPs in competitively transplanted mice. (A) Number of c-Kit^{+} progenitors. (B) Number of LSK HSPCs. (C) Representative flow plots of HSC and MPP compartment in competitively transplanted mice at 24 weeks. (D and E) Frequency and number of LT-HSCs. (F and G) Frequency and number of ST-HSCs. (H and I) Frequency and number of MPP2. (J and K) Frequency and number of MPP3. All frequency plots are within gated LSK cells, all numbers of cells shown is representative of the CD45.2 bone marrow grafts. Data shown as mean ± SEM. Unpaired t-test, $*p<0.05$; $**p<0.01$; $***p<0.001$.

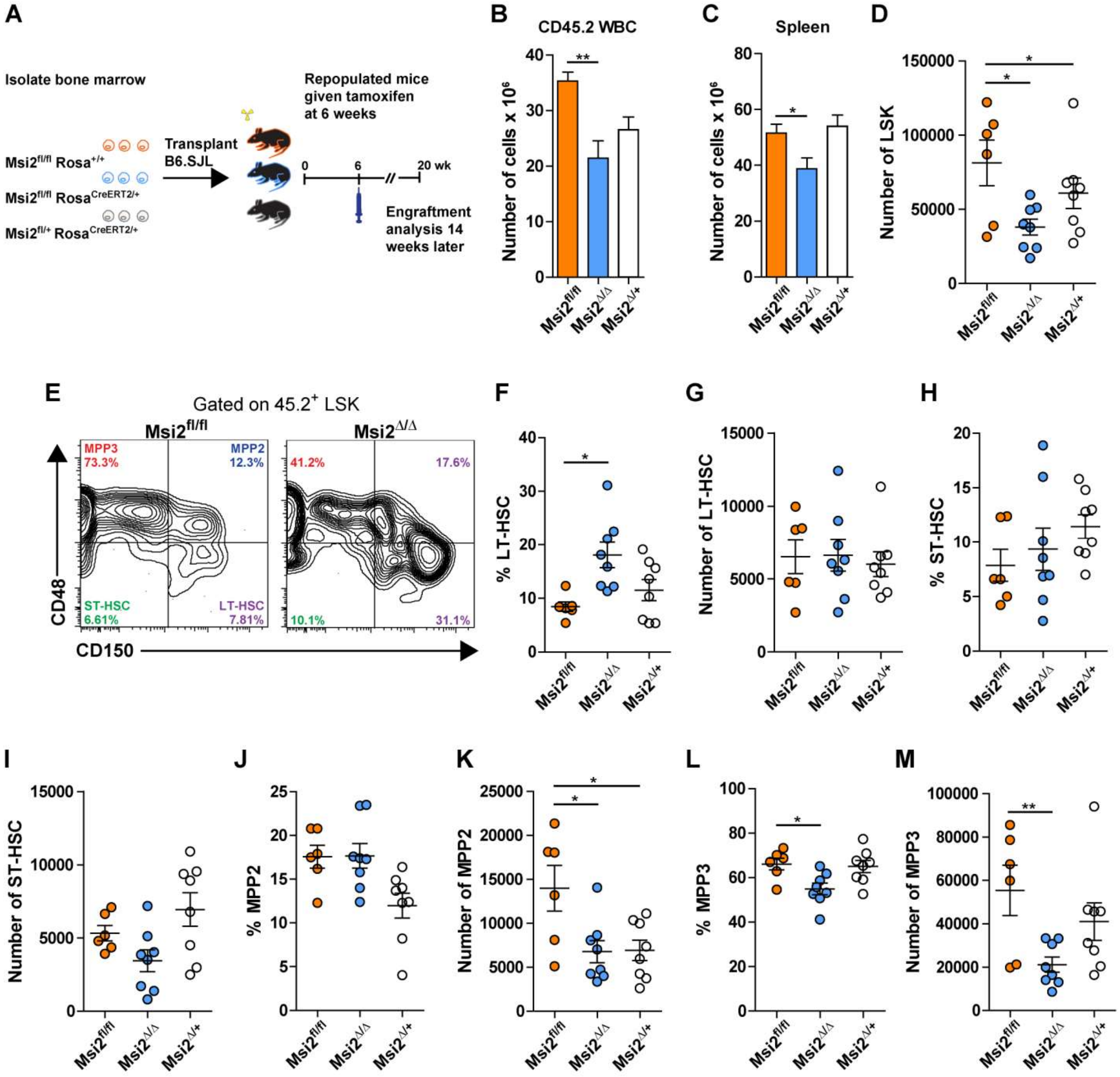
A
Isolate bone marrow
Msi2fl/fl Rosa+/+
Msi2fl/fl RosaCreERT2/+
Msi2fl/+ RosaCreERT2/+
Transplant B6.SJL
Repopulated mice given tamoxifen at 6 weeks
0
6
20 wk
Engraftment analysis 14 weeks later
B
CD45.2 WBC
Number of cells x 10^6
C
Spleen
D
Number of LSK
E
Gated on 45.2+ LSK
Msi2fl/fl
Msi2Δ/Δ
MPP3 73.3%
MPP2 12.3%
ST-HSC 6.61%
LT-HSC 7.81%
41.2%
17.6%
10.1%
31.1%
CD48
CD150
F
% LT-HSC
G
Number of LT-HSC
H
% ST-HSC
I
Number of ST-HSC
J
% MPP2
K
Number of MPP2
L
% MPP3
M
Number of MPP3
Msi2fl/fl
Msi2Δ/Δ
Msi2Δ/+
*
**

Figure 4. Conditional deletion of Msi2 in non-competitvely transplanted mice reduces bone marrow cellularity and depletes early MPPs. (A) Schematic for non-competitive transplant set up and tamoxifen dosing. (B-D) Absolute numbers of donor cells in bone marrow, spleen and HSPCs 14 weeks post tamoxifen induced Msi2 deletion (n= 8 Msi2$^{\Delta/\Delta}$, 6 Msi2$^{fl/fl}$, and 8 Msi2$^{\Delta/+}$). (E) Representative flow plots of HSC and MPP compartment in non-competitively transplanted mice at 14 weeks post tamoxifen induction. (F and G) Frequency and number of LT-HSCs. (H and I) Frequency and number of ST-HSCs. (J and K) Frequency and number of MPP2. (L and M) Frequency and number of MPP3. All frequency plots are within gated LSK cells, all numbers of cells shown is representative of the CD45.2 bone marrow grafts. Data shown as mean ± SEM. Unpaired t-test, *p<0.05; **p<0.01.

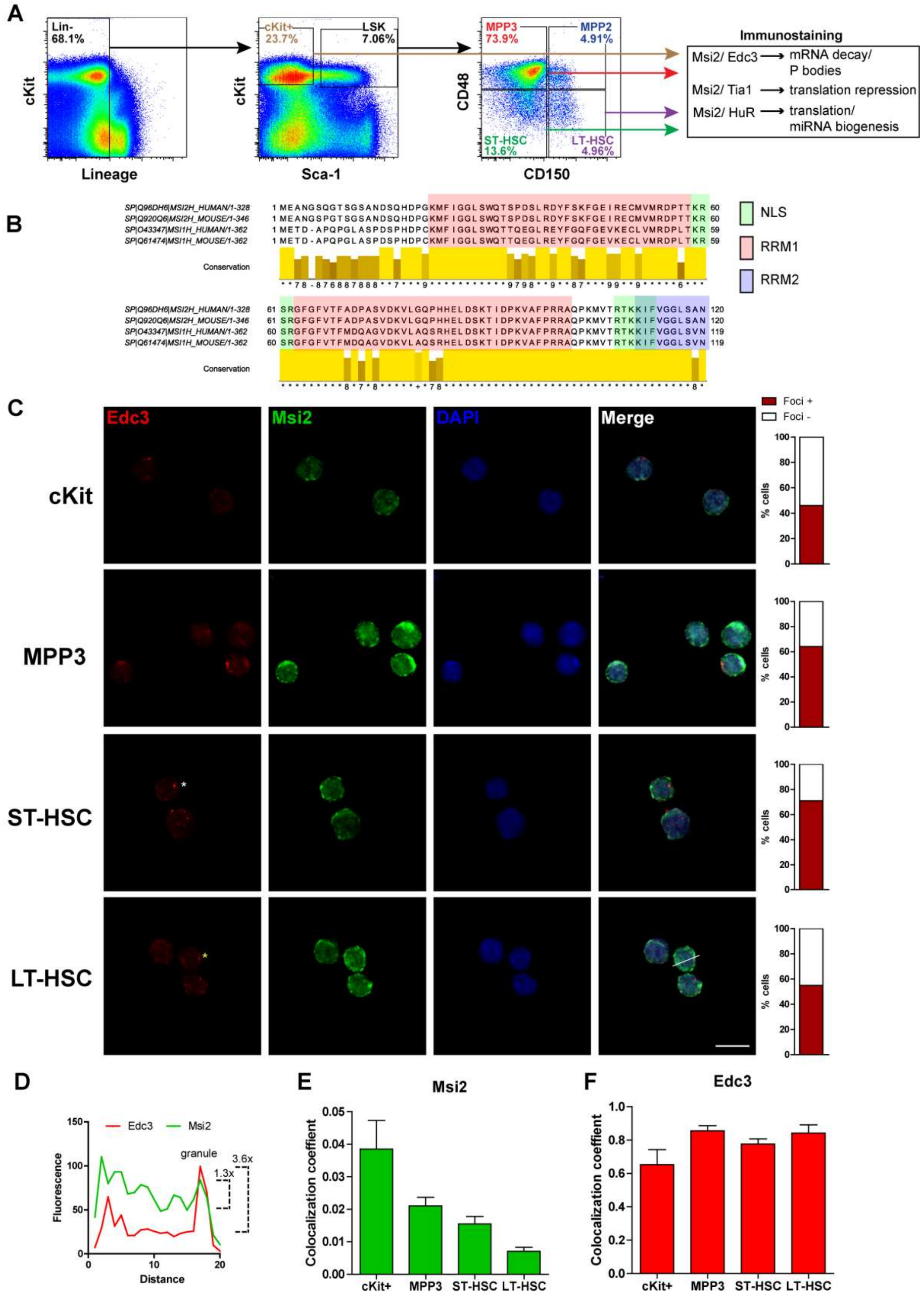
A
Lin-
68.1%
cKit
Lineage
cKit+
23.7%
LSK
7.06%
cKit
Sca-1
MPP3
73.9%
MPP2
4.91%
CD48
ST-HSC
13.6%
LT-HSC
4.96%
CD150
Immunostaining
Msi2/ Edc3 ⟶ mRNA decay/ P bodies
Msi2/ Tia1 ⟶ translation repression
Msi2/ HuR ⟶ translation/ miRNA biogenesis
B
SP|Q96DH6|MSI2H_HUMAN/1-328 1 MEANGSQGTSGSANDSQHDPGKMFIGGLSWQTSPDSLRDYFSKFGEIRECMVMRDPTTKR 60
SP|Q920Q6|MSI2H_MOUSE/1-346 1 MEANGSPGTSGSANDSQHDPGKMFIGGLSWQTSPDSLRDYFSKFGEIRECMVMRDPTTKR 60
SP|O43347|MSI1H_HUMAN/1-362 1 METD-APQPGLASPDSPHDPCKMFIGGLSWQTTQEGLREYFGQFGEVKECLVMRDPLTKR 59
SP|Q61474|MSI1H_MOUSE/1-362 1 METD-APQPGLASPDSPHDPCKMFIGGLSWQTTQEGLREYFGQFGEVKECLVMRDPLTKR 59
Conservation
78-8768878887***9***********9798**9**87***99**9*****6***
SP|Q96DH6|MSI2H_HUMAN/1-328 61 SRGFGFVTFADPASVDKVLGQPHHELDSKTIDPKVAFPRRAQPKMVTRTKKIFVGGLSAN 120
SP|Q920Q6|MSI2H_MOUSE/1-346 61 SRGFGFVTFADPASVDKVLGQPHHELDSKTIDPKVAFPRRAQPKMVTRTKKIFVGGLSAN 120
SP|O43347|MSI1H_HUMAN/1-362 60 SRGFGFVTFMDQAGVDKVLAQSRHELDSKTIDPKVAFPRRAQPKMVTRTKKIFVGGLSVN 119
SP|Q61474|MSI1H_MOUSE/1-362 60 SRGFGFVTFMDQAGVDKVLAQSRHELDSKTIDPKVAFPRRAQPKMVTRTKKIFVGGLSVN 119
Conservation
*********8*7*8*****+*78*******************************8*
NLS
RRM1
RRM2
C
Edc3
Msi2
DAPI
Merge
cKit
MPP3
ST-HSC
LT-HSC
Foci +
Foci -
% cells
0
20
40
60
80
100
D
Edc3
Msi2
granule
3.6x
1.3x
Fluorescence
0
50
100
150
0
10
20
Distance
E
Msi2
Colocalization coeffient
0.00
0.01
0.02
0.03
0.04
0.05
cKit+
MPP3
ST-HSC
LT-HSC
F
Edc3
Colocalization coeffient
0.0
0.2
0.4
0.6
0.8
1.0
cKit+
MPP3
ST-HSC
LT-HSC

Figure 5. Msi2 has nuclear and cytoplasmic localization in HSPCs and does not strongly localize to mRNA decapping machinery. (A) Gating strategy to sort distinct fractions of HSPCs from magnetic bead lineage depleted C57BL/6 mouse bone marrow for immunostaining with RBPs and centers for RNA regulation. (B) N-terminal alignment of human and mouse Msi1 and 2. (C) Immunofluorescence and confocal microscopy for Msi2 and Edc3. White asterisk designates representative Edc3 focus that was counted, yellow asterisk highlights smaller foci observed in LT-HSCs (numbers of cells tested for the presence of foci, n=43 c-Kit$^+$ cells, n=63 MPP3, n=34 ST-HSC, and n=38 LT-HSC). (D) Line plot through Edc3 granule and magnitude of fluorescence change for Msi2 and Edc3. (E and F) Summary of co-localization analysis with Msi2 relative to Edc3 (green) and Edc3 relative to Msi2 (red) (numbers of cells quantified for co-localization, n=43 c-Kit$^+$ cells, n=84 MPP3, n=70 ST-HSC, and n=50 LT-HSC). Scale bar 10 µm.

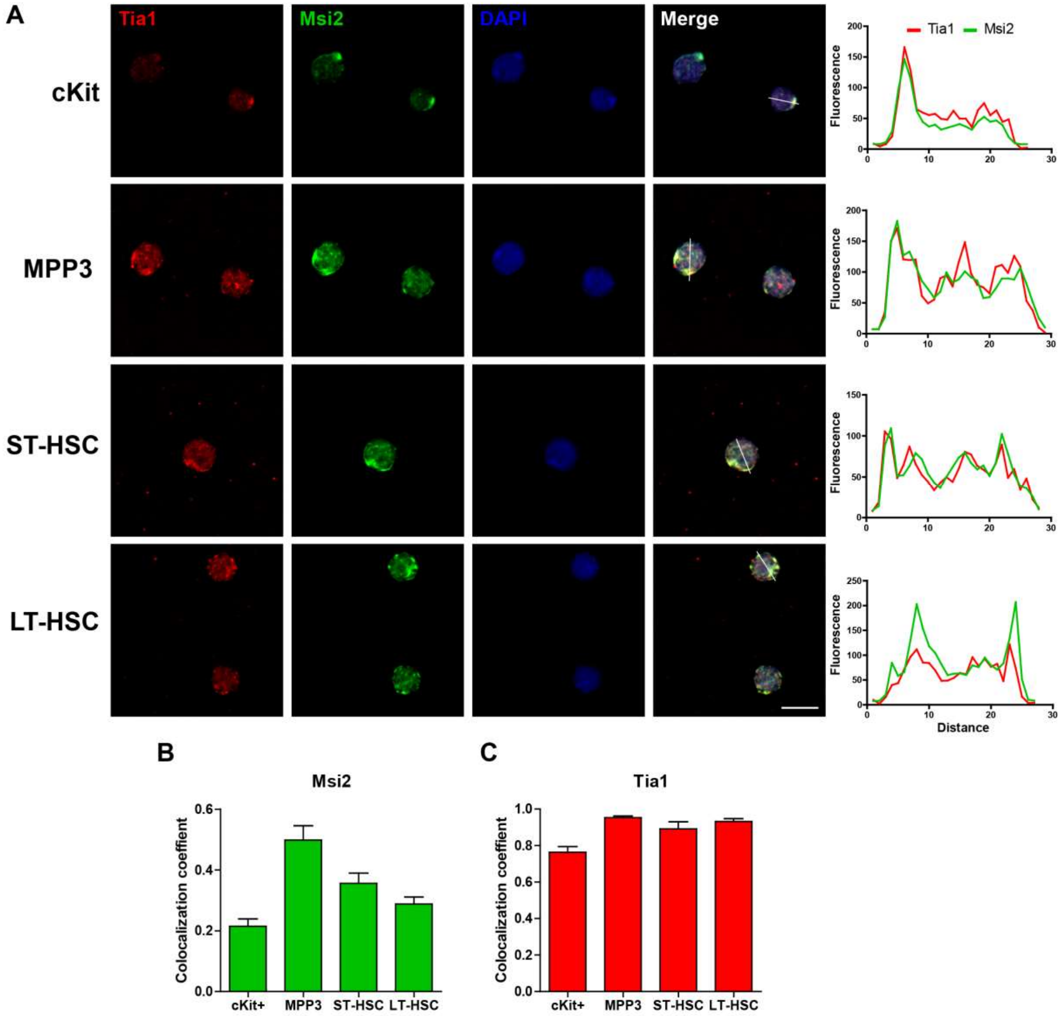
A
Tia1
Msi2
DAPI
Merge
cKit
MPP3
ST-HSC
LT-HSC
Tia1
Msi2
Fluorescence
Distance
0
10
20
30
B
Msi2
Colocalization coeffient
0.0
0.2
0.4
0.6
cKit+
MPP3
ST-HSC
LT-HSC
C
Tia1
Colocalization coeffient
0.0
0.2
0.4
0.6
0.8
1.0
cKit+
MPP3
ST-HSC
LT-HSC

Figure 6. Tia1 is highly colocalized with Msi2 in HSPCs. (A) Immunofluorescence and confocal microscopy for Msi2 and Tia1. Cell analyzed by line plot is shown in the merged image. (B and C) Summary of co-localization analysis with Msi2 relative to Tia1 (green) and Tia1 relative to Msi2 (red) (numbers of cells quantified for co-localization, n=89 c-Kit$^+$ cells, n=126 MPP3, n=49 ST-HSC, and n=49 LT-HSC). False yellow colour indicates overlapping fluoresence signal. Scale bar 10 μm.

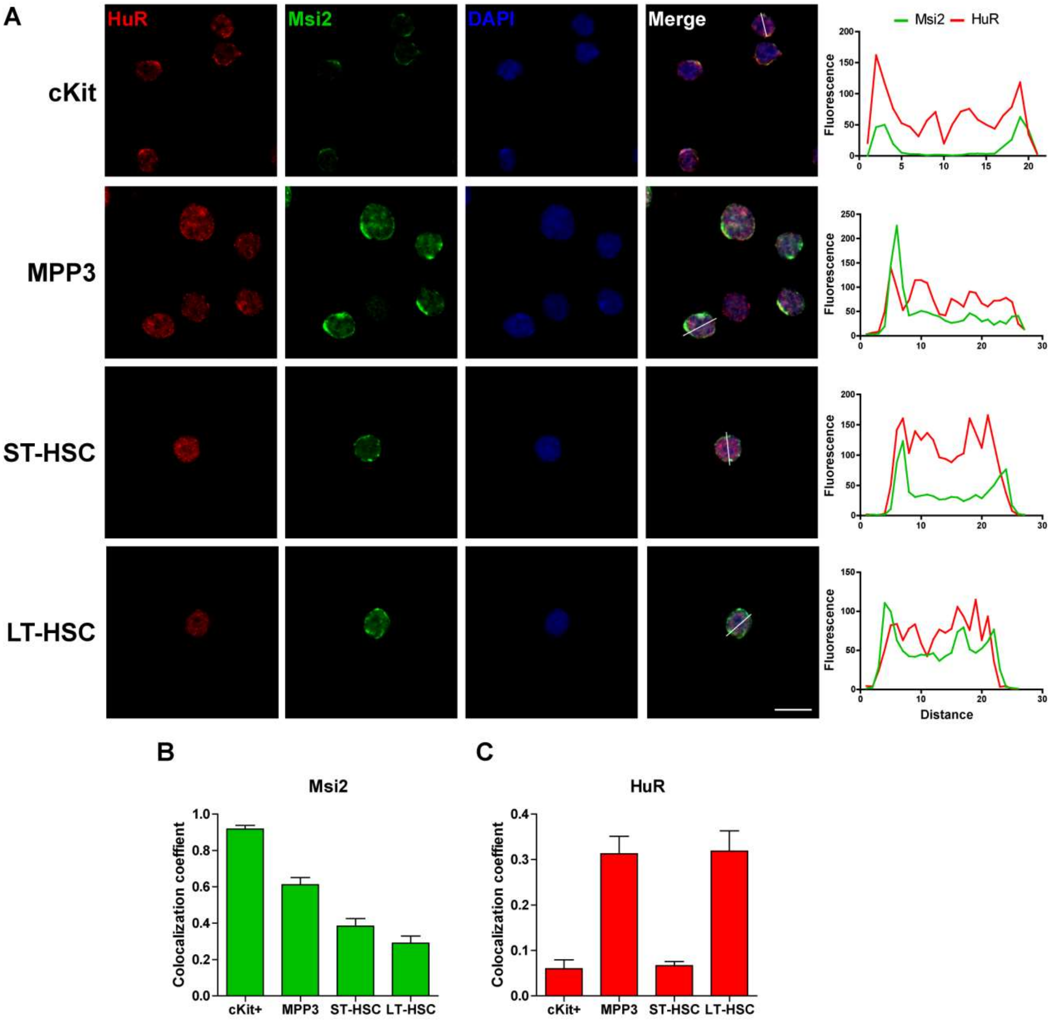
A
HuR
Msi2
DAPI
Merge
cKit
MPP3
ST-HSC
LT-HSC
Msi2
HuR
Fluorescence
Distance
B
Msi2
Colocalization coeffient
1.0
0.8
0.6
0.4
0.2
0.0
cKit+
MPP3
ST-HSC
LT-HSC
C
HuR
Colocalization coeffient
0.4
0.3
0.2
0.1
0.0
cKit+
MPP3
ST-HSC
LT-HSC

Figure 7. Msi2 and HuR are differentially colocalized in subsets of HSPCs. (A) Immunofluorescence and confocal microscopy for Msi2 and HuR. Cell analyzed by line plot is shown in the merged image. (B and C) Summary of co-localization analysis with Msi2 relative to HuR (green) and HuR relative to Msi2 (red) (numbers of cells quantified for co-localization, n=69 c-Kit$^+$ cells, n=90 MPP3, n=69 ST-HSC, and n=62 LT-HSC). False yellow colour indicates overlapping fluorescence signal. Scale bar 10 µm.

CHAPTER 5: DISCUSSION

5.0 Thesis overview

The identification of numerous intrinsic genetic regulators of mouse HSC activity and extrinsic niche signalling interactions has led to an increasingly comprehensive understanding of how these factors work in concert to control quiescence, self-renewal and differentiation fate decisions (Cabezas-Wallscheid et al., 2014; Heng and Painter, 2008; Morrison and Scadden, 2014; Orkin and Zon, 2008; Wilkinson and Gottgens, 2013), however there is a comparatively less thorough understanding of the molecular and genetic control of human HSC activity. This is due in large part to the difficulty in obtaining human HSCs for study (although access to CB has greatly helped), the inability to study them in their native environment and having to use immunocompromised mice as a proxy of their *in vivo* behaviour, and relying on viral gene-therapeutic techniques to characterise specific gene activity. These challenges aside, important advances have been made in human hematopoiesis leading to a surprising number of examples in which the mouse and human system are the same but also differ (Doulatov et al., 2012). For instance, at a high-level, mouse and human hematopoiesis show a hierarchal organization of highly self-renewing multipotent stem cells giving rise to increasingly limited self-renewing and lineage restricted progenitors, but there are many examples of the genes that direct cells through these developmental steps evolved to behave differently in subtle but meaningful ways in each system. This point perhaps is none more clearer then the evidence presented in this thesis of Msi2 regulating MPPs in the mouse system (Chapter

4) and LT-HSCs (and other progenitor classes) in the human (Chapter 2). As the discovery of Msi2 and its importance to the mouse system (Hope et al., 2010) led to central work performed in this thesis, it is clear that mouse models of hematopoiesis have and will continue to play a fundamental role in defining and refining our understanding of this complex developmental process, however there are nuanced differences between these systems that are to be appreciated (Chapter 1).

In the summary of intent (Chapter 1.9) I outlined the central aims of my graduate research. In the broadest sense, this thesis embarked on the exploration of the role of MSI2 in hematopoietic stem cells with the primary goal to *"test the hypothesis that MSI2 imparts positive control over human HSC self-renewal through a novel post-transcriptional regulatory axis"*. Delivering on the aims presented therein, I found MSI2 KD significantly impaired HSC repopulation whereas OE imparted multiple pro-self-renewal phenotypes, including increasing numbers of early multi-lineage colony types, increasing numbers of STRCs as readout at early transplant time points, and most impressively, facilitating the ex vivo expansion of HSCs as demonstrated by LDA and secondary LDA experiments. By using RNA-seq and CLIP-seq data sets, I traced these improved self-renewal and expansion phenotypes to suppression of the AHR signalling pathway, which when inhibited by small molecules expands HSCs (Boitano et al., 2010). My work showing that self-renewal can be significantly promoted by exogenous expression of an RBP and its downstream post-transcriptional regulatory effects has created a shift in the understanding of how gene regulatory networks behave in HSCs, as the field in both mouse and human systems has in large part centered on transcriptional, epigenetic and ncRNA control of self-renewal (Cabezas-Wallscheid et al., 2014; Greenblatt and Nimer, 2014; Jeong and Goodell, 2016; Novershtern et al., 2011).

Beyond testing the specific hypothesis that MSI2 exerts positive control over human HSCs, the prevailing theme of the research undertook in this thesis was to implicate on a larger scale the importance of its biochemical activity in binding functionally similar RNA targets to coordinate a specific phenotype. The path from gene to protein is complex and intervening regulatory steps are not well understood in specific cell HSPC types. Therefore, in Chapter 3 I highlight the regulon model (Keene, 2007), with my special attention to this mechanism of gene regulation in large part due to observing in my own work, multiple core AHR pathway genes as targets of MSI2.

For my last data chapter (Chapter 4), I set out to explore the fundamental role Msi2 has within mouse HSPCs. Here I began testing some of the ideas I put forth in Chapter 3 by using an immunofluoresence imaging approach and identifying patterns of Msi2 colocalization with RNA metabolism related proteins and other RPBs. These connections are crucial to demonstrating the regulon model of gene regulation in HSPCs since it identifies putative RBP-protein interactions that guide RNA processing of possibly functionally similar RNAs or species of RNA. This approach was further employed because I found strong evidence that Msi2 preferentially supports MPPs but not LT-HSCs, a phenotype that matches work performed by the Graf lab, but counters data recently published by Kharas' group where they showed loss of LT-HSCs with Msi2 deletion (de Andrés-Aguayo et al., 2011; Park et al., 2014). Therefore, driving my imaging and colocalization approach was an attempt to reconcile how Msi2 might differentially regulate subpopulations of HSPCs, despite being nearly equally expressed within them. That I was able to provide preliminary evidence that these centers of RNA metabolism and RBPs can indeed take on unique expression and colocalization profiles within subpopulations of HSPCs, provides initial support for the regulon model of gene regulation in early hematopoiesis.

5.1 Intersection of AHR, MSI2 and HSC self-renewal

Since AHR was originally discovered as the dioxin receptor and was found to be activated by numerous toxic aromatic hydrocarbons that all have an apparent man-made origin, our understanding of its function has generally been restricted to toxicology studies (Pohjanvirta, 2012). However, AHR existed long before humans were exposing themselves to chemical pollutants brought on by the industrial age, thus considerable recent effort has been made to identify its normal cell physiological functions (Beischlag et al., 2008; Mulero-Navarro and Fernandez-Salguero, 2016). Canonical AHR signaling involves ligand binding in the cytoplasm while AHR is complexed to HSP90, XAP2, and p23; AHR then proceeds to translocate to the nucleus and form a heterodimer complex with aryl hydrocarbon receptor nuclear translocator (ARNT) to bind xenobiotic response elements (XRE) in promoters of target genes to activate transcription (Mimura and Fujii-Kuriyama, 2003). There are numerous physiological processes affected by AHR activation, including cell proliferation, morphology, adhesion and migration (Mulero-Navarro and Fernandez-Salguero, 2016; Tijet et al., 2006). In particular, AHR has been found to mediate inflammation via control of adaptive and innate immune cell behaviour in tissues such as the gut and lungs (Gargaro et al., 2016; Stockinger et al., 2014). Outside these immunomodulatory effects, suppressing Ahr supports pluripotency in mouse embryonic stem cells (Ko et al., 2016), where as in drosophila, Ahr's ortholog Spineless has no known detoxifying enabling phenotypes, but instead facilitates antenna, leg, and bristle development (Duncan et al., 1998). Impaired development is also shared in mammals, as examination of Ahr null mice shows multiple organ defects, including in tissues of hepatic, cardiovascular, dermal, and hematopoietic origin (Fernandez-Salguero et al., 1995; Gasiewicz et al., 2014; Lahvis et al., 2000; Schmidt et al., 1996; van den Bogaard et al., 2015).

Defects in hematopoiesis with Ahr$^{-/-}$ mice include mainly a proliferative leukocyte phenotype, but not overt leukemia, and an increase in the LSK compartment due to loss of HSC quiescence leading to a decline in HSC function and repopulation capacity with aging (Gasiewicz et al., 2014). Whether this phenotype is evolutionarily conserved in human HSCs remains untested, since experiments knocking down AHR in human HSCs shows increased numbers of phenotypically marked HSPCs, but an assessment of their repopulation and self-renewal potential was not shown (Boitano et al., 2010). Despite this, there are important pieces of evidence that indicate AHR works differently in mice and humans. This was done by Novartis scientists Anthony Boitano and Michael Cooke, and chemist Peter Schultz from the Scripps Institute (Boitano et al., 2010). In this work by Boitano et al., they developed a high-content screen aimed to identify compounds that enable HSPCs to retain CD34 and CD133 cell surface marker expression with *in vitro* culture. Their top hit, SR1, showed with RNA-seq expression profiling that the most downregulated gene in CB HSPCs was *CYP1B1*, a canonical AHR target (Mimura and Fujii-Kuriyama, 2003). By using structure-activity relationship and *in vitro* binding assays they found SR1 antagonistically binds AHR preventing it to transcriptionally activate downstream genes. Importantly, they showed this effect was species specific such that SR1 had no effect on maintaining mouse HSCs during *in vitro* culture. Evidence presented in this thesis would also suggest the AHR suppression and HSC expansion phenotype is uniquely human. For instance, we show MSI2 OE downregulates AHR signalling since genes downregulated with MSI2 OE match gene sets from cells treated with SR1 (Chapter 2 Figure 3). Furthermore, MSI2 OE leads to expansion of normal functioning HSCs that robustly engraft primary and secondary mice without exhaustion or evidence of the onset of a myeloproliferative disease. Therefore suppression of AHR activity by chemical or genetic mechanisms shares the same phenotype of enhanced normal HSC function.

On the other hand, Ahr$^{-/-}$ mouse HSCs have increased numbers of HSCs due to a loss of quiescence and present with increases in total leukocyte numbers, but a reduction in stem cell activity during transplantation due to proliferative exhaustion (Gasiewicz et al., 2014). Interestingly, human MSI2 OE in a dox inducible mouse model shows HSC phenotypes that resemble many aspects of the Ahr$^{-/-}$ mouse. For instance, MSI2 OE promotes HSC cycling and loss of quiescence resulting in increased absolute numbers of LSK cells (like Ahr$^{-/-}$) but a decline in LT-HSC frequency indicating a push in their proliferation to lower self-renewing intermediates (Kharas et al., 2010). MSI2 OE also impairs engraftment in competitive transplants, again similar to what is observed in Ahr deleted mice (Singh et al., 2014). To help support this possible link between Msi2 and Ahr in mice it would be interesting to see if MSI2 OE in mouse HSCs also shows downregulation in Ahr target genes as we found when MSI2 was overexpressed in human HSCs, however this analysis has not been done yet. Given Ahr$^{-/-}$ mice yield a non-lethal myeloproliferative phenotype, pairing HSCs from this background with MDS or CML chronic phase oncogenic transformations could promote acute leukemia as previously shown with MSI2 OE cooperating with BCR-ABL oncogene (Ito et al., 2010; Kharas et al., 2010).

On this link between Ahr and Msi2 in leukemia, our lab has found in primary human leukemia samples that AHR signalling is inversely correlated with MSI2 expression in leukemia stem cell (LSC) enriched populations, but in non-self-renewing leukemic blasts, the phenotype switches to downregulated MSI2 and upregulated AHR signalling (Holzapfel et al. unpublished). Importantly, there is formal demonstration of AHR suppression by SR1 in primary human AML supporting *in vitro* growth and maintenance of LSCs (Pabst et al., 2014). Combining our findings and that of Pabst et al., the distinct possibility is presented that LSCs co-opt elevated MSI2 expression (Byers et al., 2011; Kharas et al., 2010) to repress AHR signalling which promotes LSC self-renewal and AML progression.

To summarize, there are many parallels within species (mouse or human) with MSI2 OE and AHR suppression, but the resultant HSC phenotypes differ, such that in humans there are pro-self-renewal effects without exhaustion compared to mice where there is loss of quiescence, increased numbers of HSPCs, reduced repopulation capacity and a preleukemic phenotype (Figure 1). It is important to note however that no formal demonstration has been made between mouse Ahr and Msi2, as I have shown in the human system, and that the MSI2 OE in mice discussed in this section was seen exclusively with a dox inducible human MSI2 overexpression mouse model. Altogether, my work revealing the novel MSI2-AHR signalling axis allows for multiple new avenues to pursue not only HSC expansion (described in the following section) but also exploration in to a novel pro-leukemic stem cell signalling axis, whereby elevated levels of MSI2 in LSCs reinforces leukemia through suppression of AHR.

5.2 MSI2 OE to novel CB HSC expansion protocols

The discovery of SR1 antagonizing AHR signalling to promote robust expansion of human HSPCs has since led to successful completion of phase I/II clinical trials which showed the safety and efficacy of SR1 in expanding CB HSPCs for transplant therapy (Wagner et al., 2016). Patients that received one of two CBs expanded with SR1 had significantly faster repopulation of neutrophils and platelets, which is a critical positive determinant of post-transplant survival, and maintained robust myelo-lymphopoiesis from expanded CB up until the last follow-up time point (median 271days and up to 688 days). Despite this success, an understanding of how suppression of AHR actually works to expand HSCs remains unknown (i.e. what is working downstream of AHR). In my work, I show that by inducing AHR repression by MSI2 OE, we can achieve significantly higher levels of early engraftment containing neutrophils and platelets in xenotransplanted mice due a 17-fold increase in STRCs (Chapter 2 Extended Data Figure

3). Furthermore, during CB ex vivo expansion, MSI2 OE enabled a net 23-fold expansion of LT-HSCs that had robust normal myelo-lymphopoiesis, thus phenocopying the expansion effects of SR1 (Chapter 2 Figure 2). Overall these phenotypes are unique not only because the effect was large, but because we achieved this level of expansion through overexpression of an RBP and its immediate post-transcription effects. Other attempts to promote human HSC growth through exogenous protein expression have typically focused on transcription factors (Buske et al., 2002; van Galen et al., 2014b), knockdown of map kinases (Baudet et al., 2012), and recently knockdown of cohesins, which appears promising despite being an unconventional target to enhance stem cell activity (Galeev et al., 2016).

To trace back how MSI2 attenuates AHR signalling, MSI2 was found to induce post-transcriptional down regulation of HSP90 and CYP1B1 protein (Chapter 2 Figure 4). By significantly reducing HSP90 at the outset of HSPC culture we concluded this impairs latent-AHR complex formation (Hughes et al., 2008; Mimura and Fujii-Kuriyama, 2003), thus disrupting ligand-dependent transcriptional activation of AHR and overall suppressing initiation of the pathway. After culturing cells for an additional week with MSI2 OE, *HSP90* transcript expression increases, and in most experiments, there is a return to normal HSP90 protein levels. Correspondingly, at this later time point, we see *CYP1B1* transcript levels increase, indicating AHR pathway activity is reactivated, but that CYP1B1 protein remains downregulated. From this observation we predicted MSI2 was maintaining post-transcriptional repression of CYP1B1 protein to help sustain HSPC growth, and confirmed this with luciferase reporter assays showing MSI2 can directly bind *CYP1B1* 3'UTR to lower luciferase levels, as well as used a chemical inhibitor of CYP1B1 to increase numbers of HSPCs during *in vitro* culture, and finally by performing co-overexpression of CYP1B1 protein with MSI2 OE to demonstrate it reduces one of its pro-self-renewal phenotypes (Chapter 2 Figure 4 and Extended Data Figure 10). We have further confirmed this interaction with RIP-PCR in another human cell line which showed significant MSI2 immunoprecitiation of *CYP1B1* transcript, and that knockdown of MSI2 in the cells we performed CLIP-seq on have upregulated CYP1B1 protein (data not shown). Additionally, in one experiment done by Boitano et al., they found lentiviral mediated downregulation of CYP1B1 promotes higher HSPC frequency (Boitano et al., 2010). These data altogether support that MSI2 post-transcriptionally regulates CYP1B1 and that CYP1B1 promotes HSPC differentiation. Despite identifying these interactions and a general role for CYP1B1 in early human HSPCs, it remains unknown how CYP1B1 is mediating this effect. The biochemical activity of CYP1B1 as a detoxifying enzyme is to use molecular oxygen at its heme center and electron flow from NADPH to hydroxylate substrates (Guengerich, 2007). The outcome of this enzymatic activity can induce reactive intermediates and oxidative stress, such as the case of CYP1B1 inducing 4-hydroxylation of endogenous estrogens (Zhu and Lee, 2005). In this case, CYP1B1 driving production of 4-hydroxyoestradiol leads to formation of oxidized derivatives like semiquinones and quinones. These carcinogenic metabolites drive hormone-related cancers like breast and ovarian by inducing depurination, DNA damage and mutation (Gajjar et al., 2012). Thus one possible explanation to how the AHR pathway is working to promote differentiation is activation of AHR leads to downstream CYP enzyme expression under normal culture conditions promoting oxidative stress in HSPCs thus impairing their self-renewal and driving differentiation. Recent evidence of the detriments caused by oxidative stress to human HSPCs was demonstrated by the Broxmeyer group where they showed maintaining HSPCs in hypoxia dramatically improved transplant outcome in mice (Mantel et al., 2015). Therefore when layering the effects of MSI2 OE in to this scenario, when MSI2 is over expressed there is early attenuation of the AHR pathway by reducing HSP90 levels and latent AHR complex formation, and at late culture time points, by continuing to post-transcriptionally repress CYP1B1, MSI2 may facilitate lowering oxidative stress levels helping to maintain/promote the culture of HSPCs. It would be interesting to stain MSI2 OE expanded CB HSPCs with probes for oxidative stress/reactive oxygen species to test this hypothesis.

Aside from the potential of CYP1B1 activating oxidative stress when AHR is active, there are also examples showing that $CD34^+$ cell *in vitro* differentiation to the myeloid lineage, and specifically to monocytes, yields activated AHR and elevated CYP1B1 (Platzer et al., 2009). Further support for this comes from examination of gene expression databases as well as qPCR in uncultured mononuclear cells (MNC) versus $CD34^+$ cells that show significant upregulation of *CYP1B1* during monocyte lineage commitment (data not shown) (Xu et al., 2014). Activation of AHR and *CYP1B1* expression has also been shown in iPS derived hematopoietic progenitors to massively expand erythroid lineage producing cells (Smith et al., 2013). Thus active AHR signalling and expression of CYP1B1 is conducive to multiple pro-differentiative phenotypes in the human blood system and given CYP1B1's unique and high expression under these circumstances it may help promote or reinforce these specific differentiation outcomes by providing pro-differentiation metabolites. This possibility is similar to CYP1B1 produced metabolites like 4-hydroxyestradiol promoting tumor growth outside of acting solely as a genotoxic agent (Kwon et al., 2016). Lastly, it may fruitful to explore the activities of other CYP enzymes in human HSPCs. For instance, a survey of transcript levels for 57 CYP enzymes in human CD34$^+$ HSPCs revealed 14 were expressed at moderate to high levels, and some having preferential expression in CD34$^+$ cells compared to MNCs and vice versa (Xu et al., 2014). As CD34 expression alone encompasses mostly non-self-renewing progenitor populations it is imperative to examine if CYP expression/activity promotes rare self-renewing HSCs to differentiate. Future work exploring broad chemical inhibitors of CYP enzymes, similar to the approach I took using TMS as specific inhibitor of CYP1B1, may help yield new small molecules that support HSC expansion.

One final outstanding question with regard to AHR promoting human HSPC differentiation is how is it getting activated in the first place? With no known canonical ligands added to the minimal serum-free cell culture medium, it would appear there is production of an unknown endogenous ligand(s) promoting its activation. Two supporting pieces of evidence for this include primary leukemia cells rapidly activating AHR pathway upon *in vitro* culture (Pabst et al., 2014), and in my own experiments (Chapter 2 Extended Data Figure 8) and others (Platzer et al., 2009), addition of agonists have little effect in promoting the loss of CD34 marker expression, likely due to sufficient endogenous activation in the pathway already. Identifying endogenously produced or natural ligands has been among the more challenging aspects of the study of AHR in normal physiological contexts, especially when historically the field was fixated on stimulation from potent environmental contaminants. The best characterized endogenously produced ligands of AHR are tryptophan metabolites (including FICZ as used in Chapter 2), indole containing structures, tetrapyroles such as bilirubin and biliverdin, 7-ketocholesterol, the metabolite lipoxin A4, and cAMP (Okey, 2007). Creating molecular probes that can distinguish the presence of these molecules in living cells would be an important step forward to allow assaying for their presence. If identification of these metabolites is possible or identifying enzymes producing metabolites stimulating AHR are found to be active, it may be possible then to develop potent inhibitors of them to generate a rival molecule to SR1. Alternatively, there may be enzymes at play that eliminate pro-differentiative metabolites or produce pro-self-renewal metabolites that are subsequently repressed with *in vitro* culture of HSPCs. Ultimately, what is necessary is a better understanding of human HSC metabolism if we are fully understand how endogenous AHR ligands, or other pro-differentiative metabolites are created. Improved knowledge here will no doubt leave to the development of novel strategies to expand HSCs for transplantation purposes.

This leads to my final point: it may be that we just scratched the surface with the MSI2 mechanism provided in Chapter 2 (and detailed again above). A comprehensive pathway analysis of genes differentially expressed with MSI2 OE and KD reveals numerous biological processes that are affected in CB HSPCs by MSI2 (Figure 2). Thus it may be an oversimplification if we attribute all these changes to AHR suppression alone. CLIP-sequencing found hundreds of highly significant targets of MSI2 of which we only followed up on two for this study as they were directly part of the core AHR signalling module. Additionally, there was a small number of lncRNA that were significantly bound to MSI2, and given MSI2's known role in regulating miRNA biogenesis (Choudhury et al., 2013), there is potential for ncRNA regulation by MSI2 in human HSCs as well. Finally, performing CLIP-seq, identifying protein-protein interactions, and determining changes to the proteome with MSI2 OE and KD all in CB HSPCs, as described in Chapter 3, will support a systems level understanding of MSI2 and help reveal the nature of RBP controlled expression networks in stem cells.

5.3 Msi2 regulation of MPPs mice

MPPs help maintain daily steady-state production of mature blood cells and are vital for proper hematopoietic recovery post-transplant (Adolfsson et al., 2005; Busch et al., 2015; Oguro et al., 2013; Pietras et al., 2015; Sun et al., 2014), yet the distinguishing molecular features that separate MPPs from other multipotent classes, such as self-renewing stem cells, is only beginning to be elucidated. For instance, among the major transcriptional changes that occur between MPPs and HSCs is the onset of lineage specific gene programs which are typically silenced in HSCs (Cabezas-Wallscheid et al., 2014; Pietras et al., 2015). The study of MPPs suffers through some confusion however, as consistencies in markers used to identify them changes between studies since the introduction of SLAM family markers (Kiel et al., 2005). Despite some of the challenges of sifting through flow gating strategies, the overwhelming consensus emerging is that there are many classes of MPPs (Chapter 1 Figure 1B) (Cabezas-Wallscheid et al., 2014; Naik et al., 2013; Pietras et al., 2015). These grab bags of cells with varying lineage potential found in the LSK fraction but cannot self-renew, are distinguished by their lymphoid lineage priming (LMPP), myeloid priming (e.g. MPP2, 3), and variability in the lengths of the transient grafts they make (Cabezas-Wallscheid et al., 2014; Pietras et al., 2015). This heterogeneity falls in line with different classes of LT- and ST-HSCs (Cabezas-Wallscheid et al., 2014; Christensen and Weissman, 2001; Oguro et al., 2013; Osawa et al., 1996) as well as the lineage biases they demonstrate at single cell level (Dykstra et al., 2007).

Two previous studies, one using Msi2 gene-trap knockout mice, and the other, Mx-1-Cre conditional Msi2 knockout mice, showed deletion induced significant impairments within the HSPC compartment, yet differed on describing what cells were affected most (de Andrés-Aguayo et al., 2011; Park et al., 2014). In the paper by de Andres-Aguayo et al., ST-HSCs and LMPPs were significantly reduced with Msi2 deletion, which coincided with significant impairments in competitive transplantation capacity. On the other hand, Park et al. found conditional deletion of Msi2 led to reductions across the whole primitive hierarchy, including LMPPs, ST-HSCs and LT-HSCs. These changes were complimented with loss of LT-HSC quiescence, myeloid biased grafts, and reductions in white blood cell counts after inducing deletion.

With our lab's generation of a tamoxifen inducible Msi2 knockout mouse, I was able to temporally ablate Msi2 from HSCs and test its function in HSPCs in similar fashion to the study by Park et al. Specifically, I found consistent reductions in distinct MPP classes of cells which I designated MPP3 and MPP2 based on previous work by the Morrison and Passegue labs (Oguro et al., 2013; Pietras et al., 2015). MPP2s have previously been shown to be a myeloid biased MPP subset with prevalent megakaryocyte lineage potential, whereas MPP3s, as I classified them, contain predominately LMPPs and a subpopulation of myeloid GM biased MPPs (Oguro et al., 2013; Pietras et al., 2015). Despite the losses in MPPs with Msi2 deletion, LT-HSC numbers remained unaffected under competitive transplant and steady-state hematopoiesis experiments which is in agreement with results performed with the Msi2 gene-trap knock mouse model (de Andrés-Aguayo et al., 2011) and counters data presented in the Mx1-Cre knockout mouse (Park et al., 2014). That our tamoxifen conditional deletion model falls in line with the germline deleted Msi2 gene-trap model and not the poly I:C Cre-induction method eliminates the discrepancy that the differing phenotype is due to cell ontogeny. Given the constitute deletion of Msi2 in the gene trap model, retention of LT-HSCs by this method precludes that there were surviving LT-HSCs that escaped and induction protocol, which was sometimes evident in the Mx1-Cre driven model. Currently I have not checked if this may be why LT-HSCs persist in our model but analysis of LSK cells post deletion at an extended time point suggests Msi2 is deleted in nearly every cell analyzed and no outgrowth of LSK cells that have retained Msi2 protein (Chapter 4 Figure 1D). As poly I:C and tamoxifen both induce HSC cycling and reduce self-renewal it is unlikely the induction regimen is the cause for discrepancy between my study and that of Park et al., especially since these effects are reversible (Frelin et al., 2013; Sanchez-Aguilera et al., 2014). An obvious difference between each model used was the nature of Msi2 deletion.

In our lab's model we have exon 2 floxed leading to a loss of Msi2 protein as assayed by western blot and immunofluoresence with an antibody that detects a C-terminal epitope. In the study by Park et al. they flox exons 1-4 to generate a null mutant, and in the work by de Andres-Aguayo et al. their β-galactosidase and neomycin resistance gene insertion mapped to intron 5 creating a truncated protein which they did not show was stable or not. It remains unlikely in at least the conditional knockout mouse models of a residual functional peptide remaining, but the case could be made in the gene-trap method of deletion.

One possible reason why LT-HSCs remained in our model after deletion may be because the steady-state experiments that were performed lasted for 14 weeks post deletion (20 weeks total engraftment time; Chapter 4 Figure 4), whereas Park et al. using the same experimental setup noted loss in LT-HSCs after 18 weeks, thus it may be that our endpoint was too early to read out an effect on LT-HSC numbers. Performing secondary transplants here would be a good measure for us to test LT-HSC capacity. Despite retaining LT-HSC in this experiment, it does not however explain why 24 week long competitive transplantation experiments do not show any loss of LT-HSCs, despite having significantly reduced repopulation levels overall (Chapter 4 Figure 1F and G). This phenotype, as argued in the Chapter 4, is likely due to the loss of MPPs that maintain robust levels of ongoing cell proliferation.

Interestingly, in my work and de Andres-Aguayo et al., the loss of MPPs and their proliferative capacity supports the observation found with MSI2 overexpression in a dox inducible model, which showed proliferation and expansion of LMPPs but not LT-HSCs

(Kharas et al., 2010). Additional support that the effect of Msi2 deletion spares some capacity of LT-HSCs is that deletion of Msi2 prior to transplanting cells non-competitively still leads to engraftment, albeit with lower white blood cell counts (data not shown) (de Andrés-Aguayo et al., 2011; Park et al., 2014). Park et al. however attributed this effect to non-deleted cells re-establishing a low-level late onset graft.

Lastly, Park et al. observed myeloid cells were decreased with Msi2 deletion due to a loss of myeloid biased LT-HSCs, while I observed lymphoid cells were reduced due to a loss of LMPPs. In the middle, is the work of de Andres-Aguayo et al. showing a general reduction in the output of all mature cells but no specific lineage biases with Msi2 deletion, which is likely due to the observed reduction in ST-HSCs. Thus all models generally show appropriate reductions in mature cell lineages based on the loss of the corresponding primitive cell type. An examination of other genes found in the literature to impact LMPPs but mostly spare LT-HSC showed their loss of function yielded similar phenotypes to my work and that of de Andres-Aguayo et al. For instance, deletion of the E2A transcription factor significantly reduces numbers of LMPPs leading to a reduction in lymphoid cells and compromised output in competitive transplantation experiments (Semerad et al., 2009; Yang et al., 2008). Similarly, loss of ssDNA-binding protein 2 reduces the frequency of LMPPs and diminishes HSPC capacity for repopulation (Li et al., 2014). Therefore, the results presented in Chapter 4 are in line with other work describing specific impairment in the MPP compartment.

Ultimately my work suggests that Msi2 is a critical determinant for maintaining MPPs, however, since the affected MPP populations are unable to regenerate themselves or other cells of the LSK compartment, particularly during transplantation, they require the activity of HSCs to replenish them (Oguro et al., 2013; Pietras et al., 2015). This means that the reduction in these populations could be due to intrinsic exhaustion/differentiation effects directly within the MPP compartment or a failure on behalf of the HSC pool to adequately proliferate and regenerate these cells. As such, it is difficult to completely rule out defects to LT-HSCs with Msi2 deletion at this time. One experiment that could help distinguish these two scenarios is to transplant sorted MPP populations and test if their transient engraftment kinetics is impacted by Msi2 deletion. If there is no change with deletion then we can likely conclude the defect is due to HSCs unable to properly sustain the MPP pool.

5.4 Post-transcriptional control in mouse HSPCs

An impressive study was recently published to characterize the transcriptome, proteome and methylome of several functionally distinct classes of mouse HSPCs (Cabezas-Wallscheid et al., 2014). To perform proteome analysis, which is generally unheard of with HSC populations, the researchers flow sorted 400,000 LT-HSCs and 400,000 ST-HSCs for electrospray ionization-tandem mass spectrometry. From this unbiased approach they found 47 differentially expressed proteins between these two populations. This relatively small number of differentially expressed proteins which apparently bestows LT-HSCs the ability to self-renew and propagate in secondary mice, included upregulated glutathione S-transferases which are involved in cell detoxification pathways, glycolytic enzymes, Hmga chromatin modulators and the Igf2bp2 RNA binding protein. Conversely, proteins downregulated in LT-HSCs relative to ST-HSCs were primarily involved in cell cycle and chromatin assembly/structure (Cabezas-Wallscheid et al., 2014). Interestingly, in this same study they found 479 transcripts were differentially expressed between these same two populations compared to the 47 proteins. From their analysis to correlate protein to transcript level they showed in the majority of cases transcript abundance matched protein level for the approximately 4000 reproducible proteins they could detect. Similarly, when looking at the 47 differentially expressed proteins, 15 had near perfect correlation in protein and transcript level fold-change from HSC:MPP. These 15 genes could be further classified by GO analysis and belonged to either cell cycle or cell response to cytokine stimulus classifications. On the other hand, many of the remaining genes showed discordant transcript and protein levels, for instance the glycolysis related genes had upregulated protein levels but largely unchanged transcript abundance in HSCs relative to MPPs. Conversely there were genes that had reduced transcript levels but protein levels were unaffected. This work provides the first unbiased report of post-transcriptional regulation occurring in very highly enriched stem cell fractions and this is despite the likely restrictions of the sensitivity of the proteomics analysis performed (i.e. only 47 proteins were significantly differentially expressed compared to 10-fold more coding transcripts).

With this formal demonstration of post-transcriptional control in mind, my approach to elucidate how the RBP activities of Msi2 could differentially regulate HSPCs was to look at different MPP and HSC populations and examine by confocal microscopy the location and expression pattern of Msi2 with other RBPs and RNA metabolising proteins. The proteins I choose for this analysis, Edc3, Tia1, and HuR, served two proposes: the first was they have already been shown to colocalize with Msi2 in the literature (Choudhury et al., 2013; Kawahara et al., 2008), and the second is that they each represent a different possible function for Msi2 to be cooperating in, including mRNA decay with Edc3, translation repression with Tia1, and translation activation and miRNA biogenesis control with HuR.

From this analysis I could deduce several intriguing patterns about Msi2 and these other proteins. For starters, Msi2 was not abundantly found at Edc3 foci across all cell types, indicating the unlikelihood its primary function is to funnel RNAs for decay. Edc3 foci also tended to be less abundant and not as pronounced in highly quiescent LT-HSC compared to other populations of LSK cells. This finding is intriguing as it suggests an attenuated mRNA decapping program in LT-HSCs and therefore reduced levels of ongoing mRNA decay. Indeed, analysis of Edc3 protein levels in the Cabezas-Wallscheid et al. data set also shows a reduction in LT-HSC compared to ST-HSC (Edc3 $\log_2$ ratio LT-HSC/ST-HSC = 0.075). This phenotype is reminiscent of the reduce protein synthesis and tight control of translation in LT-HSCs (Signer et al., 2014), whereby either decreasing or increasing rates of translation impairs HSC activity. It would be interesting to see here if increasing or decreasing mRNA decay rates by overexperssion or knockdown of decapping complex proteins similarly impairs HSC activity. Another interesting experiment to carry this work forward is treating mice with 5-Fluorouracil (5-FU) or similar stress agents to test if HSCs upregulate this machinery in response to cycling. Given that c-Kit$^+$ cells had fewer foci and are actively cycling cells, it may be a feature outside of cell proliferation. Finally, the Edc3 localized P-bodies represent a diverse set of RNP granules that share proteins involved in translation repression, nonsense-mediated mRNA decay, microRNA-mediated translational repression, and mRNA storage (Buchan and Parker, 2009). Thus these foci could be representing biochemical activity outside of 5’-to-3’ mRNA degradation.

Investigation in to Msi2 association with Tia1 revealed Tia1 to be nearly perfectly correlated with Msi2. Tia1is involved in many post-transcriptional activities including in the cytoplasm to control RNA location, stability and translation, and in the nucleus to regulate transcription and pre-mRNA splicing (Sanchez-Jimenez and Izquierdo, 2015). I found Tia1 to be abundantly expressed throughout the cell, but in general present at higher levels at the cell periphery/cytoplasm with Msi2, which coincides with their primary role in mediating translation repression. However, Tia1 has diverse molecular roles in the cytoplasm, which includes RRM binding T-rich ssDNA, interactions with the carboxy-terminal domain of RNA polymerase II during transcription, and being able to bind U-rich sequences proximal to pre-mRNA 5’splice acceptor sites (Sanchez-Jimenez and Izquierdo, 2015). In comparison, analysis of MSI2 targets from CLIP-seq studies would suggest a primary role in binding 3’UTR sequences (Katz et al., 2014; Rentas et al., 2016). However, from our data, MSI2 was also found binding coding sequence and to regions proximal to introns (Rentas et al., 2016). Thus similar to Tia1, Msi2 may have secondary RNA binding features outside mediating translation in the cytoplasm (although likely to be much less prevalent). The downstream effects that coincide with the diverse number and types of substrates Tia1 binds, include control over many physiological events, including cell cycle, apoptosis, stress responses and tumor suppression (Sanchez-

Jimenez and Izquierdo, 2015). Therefore, given its high and near ubiquitous expression across the early HSPC hierarchy, but Msi2's decreasing co-localization from MPP3 to LT-HSC, there may be cell contextual interactions and RNA binding preferences of Msi2 with Tia1 to control cell physiology. It will be important to determine if Msi2 just shares similar location to Tia1 or if they actually physically interact with one another in co-immunoprecipitation experiments.

The last protein I explored Msi2 colocalization with in mouse HSPCs was HuR. As an ongoing theme with RBPs, HuR has abundant RNA targets and species and can influence mRNA stability/translation in the cytoplasm, and in the nucleus target pre-mRNA splicing and nuclear export of mRNAs (Grammatikakis et al., 2016). HuR also has non-mRNA targets, including both pri-miRNA and mature miRNA (Choudhury et al., 2013; Mukherjee et al., 2016), and importantly, Msi2 was found to interact with HuR and cooperatively bind pri-miRNA to repress maturation. With this interaction in mind, I found HuR to have intriguing localization patterns in HSPCs, mainly a progressive nuclear accumulation in relation to increasing self-renewal potential. With Msi2 also having nuclear localization across all LSK populations, although appearing in some circumstances to be more cytoplasmic in ST-HSCs, highlights Msi2's possible nuclear activities with HuR, mainly suppressing miRNA biogenesis as previously described. To test this hypothesis, it will be important to perform global analysis of small RNA expression with tamoxifen induced Msi2 deletion to see if there are immediate changes to the miRNA programs of these cells. Finally, that HuR which is an RBP that is essential during hematopoietic development and supports the survival of hematopoietic progenitors by stabilizing Mdm2 mRNA thus blocking p53 mediated apoptosis (Ghosh et al., 2009), is largely cytoplasmic in c-Kit$^+$ progenitor cells, but appears to be progressively nuclear in self-renewing LSK cells, could be interpreted as a switch from an inactive or nuclear RNA processing role in HSCs and active translation control mechanism in progenitors where it plays an instrumental role in their function.

These results altogether show that indeed RBPs can take on unique expression and localization features in distinct HSPC populations, which is an exciting prospect to formally testing the regulon hypothesis in these cells. As far as I know, this is the first focused analysis of deciphering the interactions of RBPs with control centers of RNA metabolism in HSPCs. Expanding this approach to including proteomic methods in cell lines to further identify Msi2 interacting proteins is an important step forward to pushing this research along. Our lab has already begun this approach by using biotin-ligase tagging of Msi2 in mouse ES cells. Remarkably, the lab has generated preliminary evidence showing the RBP Igf2bp2 as a significant Msi2 interacting protein. As mentioned above, Igf2bp2 was the most abundantly expressed protein in LT-HSC from the study of Cabezas-Wallscheid et al. The role of Igf2bp2 in HSPCs has yet to be explored, however, the potential for the interfacing of these proteins to control RNA networks in LT-HSC seems promising. Finally, there are inherent challenges with imaging cells that are not much larger than the diameter of their nucleus, but I think I have still shown the utility of this approach, particularly with Edc3 staining, that it is possible to discern the features of RBP interactions. This is a critical step forward if we are to explore the combinatorial interactions and behaviours of these proteins in HSPCs.

5.5 Concluding remarks

This thesis represents a collection of work aimed at deciphering the regulatory control of Musashi-2 in hematopoietic stem cells of mouse and human origin. Through the varied use of primary cell cultures, lentiviral gene therapeutics, xenotransplant models, RNA-sequencing, transgenic mice and confocal imaging methods, I have been able to explore the multiple fascinating ways this protein controls stem and progenitor cell behaviour. As alluded to throughout this thesis, post-transcriptional control by RNA binding proteins remains a largely untapped area of research in hematopoietic stem and progenitor cells and it was the goal of this work to help bring to focus the importance of these mechanisms. This is none more apparent than my work showing Musashi-2 overexpression and its ensuing post-transcriptional effects can expand human hematopoietic stem cells. With ongoing efforts to map Musashi-2 protein-RNA and protein-protein interactions in stem and progenitor cells, future discoveries on this gene will no doubt yield unexpected and exciting results.

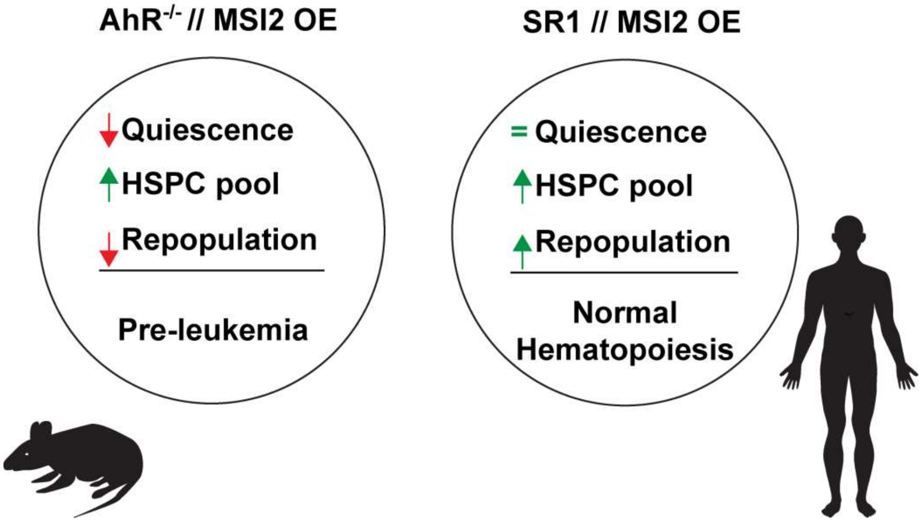
AhR$^{-/-}$ // MSI2 OE
↓ Quiescence
↑ HSPC pool
↓ Repopulation
Pre-leukemia
SR1 // MSI2 OE
= Quiescence
↑ HSPC pool
↑ Repopulation
Normal Hematopoiesis

Figure 1. Summary of hematopoietic phenotypes between mouse and human with MSI2 OE and AHR deletion or inhibition with SR1.

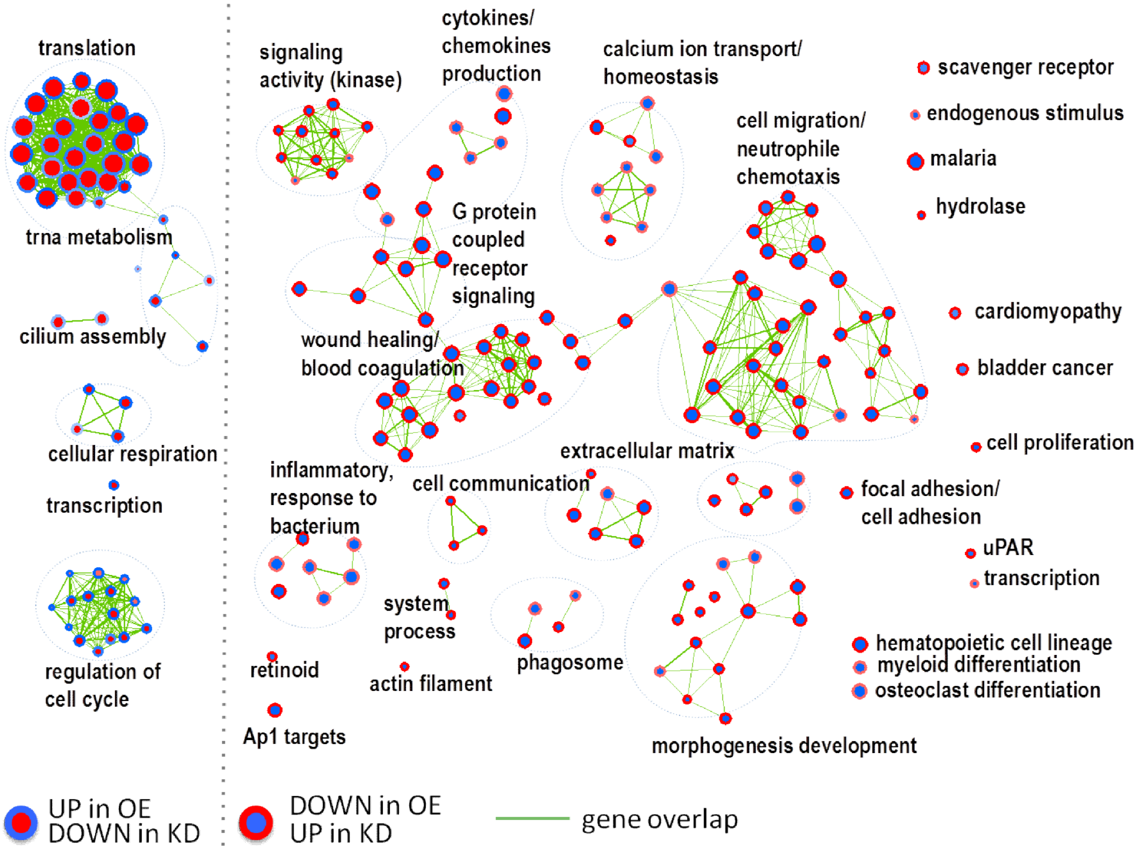
translation
trna metabolism
cilium assembly
cellular respiration
transcription
regulation of cell cycle
signaling activity (kinase)
cytokines/ chemokines production
calcium ion transport/ homeostasis
cell migration/ neutrophile chemotaxis
G protein coupled receptor signaling
wound healing/ blood coagulation
extracellular matrix
inflammatory, response to bacterium
cell communication
system process
phagosome
retinoid
actin filament
Ap1 targets
morphogenesis development
scavenger receptor
endogenous stimulus
malaria
hydrolase
cardiomyopathy
bladder cancer
cell proliferation
focal adhesion/ cell adhesion
uPAR
transcription
hematopoietic cell lineage
myeloid differentiation
osteoclast differentiation
UP in OE
DOWN in KD
DOWN in OE
UP in KD
gene overlap

Figure 2. Transcript pathway analysis in CB HSPCs with MSI2 OE and KD. Annotated map showing nodes derived from gene sets that are significantly enriched for both the OE and the KD condition. Node size is proportional to the NES (normalized enrichment score): the bigger the greater the enrichment. Node color is proportional to the p value. Here all the nodes are enriched with a p value equal or less than 0.05 for both OE (node center) and KD (node border) condition. 204 nodes are present on this map (from the 500 nodes that passed the threshold): they are the top 204 gene-sets and they have at 1 pvalue equal to 0.0005 (the smallest p value that can be obtained with 2000 permutations) in at least one of the condition.

BIBLIOGRAPHY

Acar, M., Kocherlakota, K. S., Murphy, M. M., Peyer, J. G., Oguro, H., Inra, C. N., Jaiyeola, C., Zhao, Z., Luby-Phelps, K., and Morrison, S. J. (2015). Deep imaging of bone marrow shows non-dividing stem cells are mainly perisinusoidal. Nature *526*, 126-130.

Adolfsson, J., Mansson, R., Buza-Vidas, N., Hultquist, A., Liuba, K., Jensen, C. T., Bryder, D., Yang, L., Borge, O. J., Thoren, L. A., *et al.* (2005). Identification of Flt3+ lympho-myeloid stem cells lacking erythro-megakaryocytic potential a revised road map for adult blood lineage commitment. Cell *121*, 295-306.

Aihara, Y., Buhring, H. J., Aihara, M., and Klein, J. (1986). An attempt to produce "pre-T" cell hybridomas and to identify their antigens. Eur J Immunol *16*, 1391-1399.

Antonchuk, J., Sauvageau, G., and Humphries, R. K. (2002). HOXB4-induced expansion of adult hematopoietic stem cells ex vivo. Cell *109*, 39-45.

Appelbaum, F. R. (2012). Pursuing the goal of a donor for everyone in need. N Engl J Med *367*, 1555-1556.

Baines, P., Mayani, H., Bains, M., Fisher, J., Hoy, T., and Jacobs, A. (1988). Enrichment of CD34 (My10)-positive myeloid and erythroid progenitors from human marrow and their growth in cultures supplemented with recombinant human granulocyte-macrophage colony-stimulating factor. Exp Hematol *16*, 785-789.

Ballen, K. K., Gluckman, E., and Broxmeyer, H. E. (2013). Umbilical cord blood transplantation: the first 25 years and beyond. Blood *122*, 491-498.

Barbouti, A., Höglund, M., Johansson, B., Lassen, C., Nilsson, P.-G., Hagemeijer, A., Mitelman, F., and Fioretos, T. (2003). A novel gene, MSI2, encoding a putative RNA-binding protein is recurrently rearranged at disease progression of chronic myeloid leukemia and forms a fusion gene with HOXA9 as a result of the cryptic t(7;17)(p15;q23). Cancer Research *63*, 1202-1208.

Barker, J. N., Weisdorf, D. J., DeFor, T. E., Blazar, B. R., Miller, J. S., and Wagner, J. E. (2003). Rapid and complete donor chimerism in adult recipients of unrelated donor umbilical cord blood transplantation after reduced-intensity conditioning. Blood *102*, 1915-1919.

Baudet, A., Karlsson, C., Safaee Talkhoncheh, M., Galeev, R., Magnusson, M., and Larsson, J. (2012). RNAi screen identifies MAPK14 as a druggable suppressor of human hematopoietic stem cell expansion. Blood *119*, 6255-6258.

Baum, C. M., Weissman, I. L., Tsukamoto, A. S., Buckle, A. M., and Peault, B. (1992). Isolation of a candidate human hematopoietic stem-cell population. Proc Natl Acad Sci U S A *89*, 2804-2808.

Becker, A. J., Mc, C. E., and Till, J. E. (1963). Cytological demonstration of the clonal nature of spleen colonies derived from transplanted mouse marrow cells. Nature *197*, 452-454.

Beckmann, J., Scheitza, S., Wernet, P., Fischer, J., and Giebel, B. (2007). Asymmetric cell division within the human hematopoietic stem and progenitor cell compartment: identification of asymmetrically segregating proteins. Blood *109*, 5494-5995.

Beerman, I., Seita, J., Inlay, M. A., Weissman, I. L., and Rossi, D. J. (2014). Quiescent hematopoietic stem cells accumulate DNA damage during aging that is repaired upon entry into cell cycle. Cell Stem Cell *15*, 37-50.

Beischlag, T. V., Luis Morales, J., Hollingshead, B. D., and Perdew, G. H. (2008). The aryl hydrocarbon receptor complex and the control of gene expression. Crit Rev Eukaryot Gene Expr *18*, 207-250.

Benveniste, P., Frelin, C., Janmohamed, S., Barbara, M., Herrington, R., Hyam, D., and Iscove, N. N. (2010). Intermediate-term hematopoietic stem cells with extended but time-limited reconstitution potential. Cell Stem Cell *6*, 48-58.

Bhatia, M., Wang, J. C., Kapp, U., Bonnet, D., and Dick, J. E. (1997). Purification of primitive human hematopoietic cells capable of repopulating immune-deficient mice. Proc Natl Acad Sci U S A *94*, 5320-5325.

Biasco, L., Pellin, D., Scala, S., Dionisio, F., Basso-Ricci, L., Leonardelli, L., Scaramuzza, S., Baricordi, C., Ferrua, F., Cicalese, M. P.*, et al.* (2016). *In Vivo* Tracking of Human Hematopoiesis Reveals Patterns of Clonal Dynamics during Early and Steady-State Reconstitution Phases. Cell Stem Cell.

Blackinton, J. G., and Keene, J. D. (2014). Post-transcriptional RNA regulons affecting cell cycle and proliferation. Semin Cell Dev Biol *34*, 44-54.

Boitano, A. E., Wang, J., Romeo, R., Bouchez, L. C., Parker, A. E., Sutton, S. E., Walker, J. R., Flaveny, C. A., Perdew, G. H., Denison, M. S.*, et al.* (2010). Aryl hydrocarbon receptor antagonists promote the expansion of human hematopoietic stem cells. Science *329*, 1345-1348.

Bosma, G. C., Custer, R. P., and Bosma, M. J. (1983). A severe combined immunodeficiency mutation in the mouse. Nature *301*, 527-530.

Boulais, P. E., and Frenette, P. S. (2015). Making sense of hematopoietic stem cell niches. Blood *125*, 2621-2629.

Brosh, R. M., Jr., Bellani, M., Liu, Y., and Seidman, M. M. (2016). Fanconi Anemia: A DNA repair disorder characterized by accelerated decline of the hematopoietic stem cell compartment and other features of aging. Ageing Res Rev.

Broxmeyer, H. E. (1984). Colony assays of hematopoietic progenitor cells and correlations to clinical situations. Crit Rev Oncol Hematol *1*, 227-257.

Broxmeyer, H. E., Douglas, G. W., Hangoc, G., Cooper, S., Bard, J., English, D., Arny, M., Thomas, L., and Boyse, E. A. (1989). Human umbilical cord blood as a potential source of transplantable hematopoietic stem/progenitor cells. Proc Natl Acad Sci U S A *86*, 3828-3832.

Buchan, J. R., and Parker, R. (2009). Eukaryotic stress granules: the ins and outs of translation. Mol Cell *36*, 932-941.

Busch, K., Klapproth, K., Barile, M., Flossdorf, M., Holland-Letz, T., Schlenner, S. M., Reth, M., Hofer, T., and Rodewald, H. R. (2015). Fundamental properties of unperturbed haematopoiesis from stem cells *in vivo*. Nature *518*, 542-546.

Buske, C., Feuring-Buske, M., Abramovich, C., Spiekermann, K., Eaves, C. J., Coulombel, L., Sauvageau, G., Hogge, D. E., and Humphries, R. K. (2002). Deregulated expression of HOXB4 enhances the primitive growth activity of human hematopoietic cells. Blood *100*, 862-868.

Buszczak, M., Signer, R. A., and Morrison, S. J. (2014). Cellular differences in protein synthesis regulate tissue homeostasis. Cell *159*, 242-251.

Byers, R. J., Currie, T., Tholouli, E., Rodig, S. J., and Kutok, J. L. (2011). MSI2 protein expression predicts unfavorable outcome in acute myeloid leukemia. Blood *118*, 2857-2867.

Cabezas-Wallscheid, N., Klimmeck, D., Hansson, J., Lipka, D. B., Reyes, A., Wang, Q., Weichenhan, D., Lier, A., von Paleske, L., Renders, S., *et al.* (2014). Identification of regulatory networks in HSCs and their immediate progeny via integrated proteome, transcriptome, and DNA methylome analysis. Cell Stem Cell *15*, 507-522.

Calvi, L. M., Adams, G. B., Weibrecht, K. W., Weber, J. M., Olson, D. P., Knight, M. C., Martin, R. P., Schipani, E., Divieti, P., Bringhurst, F. R., *et al.* (2003). Osteoblastic cells regulate the haematopoietic stem cell niche. Nature *425*, 841-846.

Capecchi, M. R. (1989). Altering the genome by homologous recombination. Science *244*, 1288-1292.

Cassar, P. A., and Stanford, W. L. (2012). Integrating post-transcriptional regulation into the embryonic stem cell gene regulatory network. J Cell Physiol *227*, 439-449.

Chen, J. Y., Miyanishi, M., Wang, S. K., Yamazaki, S., Sinha, R., Kao, K. S., Seita, J., Sahoo, D., Nakauchi, H., and Weissman, I. L. (2016). Hoxb5 marks long-term haematopoietic stem cells and reveals a homogenous perivascular niche. Nature *530*, 223-227.

Cheng, T., Rodrigues, N., Shen, H., Yang, Y., Dombkowski, D., Sykes, M., and Scadden, D. T. (2000). Hematopoietic stem cell quiescence maintained by p21cip1/waf1. Science *287*, 1804-1808.

Cheshier, S. H., Morrison, S. J., Liao, X., and Weissman, I. L. (1999). *In vivo* proliferation and cell cycle kinetics of long-term self-renewing hematopoietic stem cells. Proc Natl Acad Sci U S A *96*, 3120-3125.

Choudhury, N. R., de Lima Alves, F., de Andres-Aguayo, L., Graf, T., Caceres, J. F., Rappsilber, J., and Michlewski, G. (2013). Tissue-specific control of brain-enriched miR-7 biogenesis. Genes Dev *27*, 24-38.

Christensen, J., and Weissman, I. (2001). Flk-2 is a marker in hematopoietic stem cell differentiation: a simple method to isolate long-term stem cells. Proceedings of the National Academy of Sciences of the United States of America *98*, 14541-14547.

Civin, C. I., Strauss, L. C., Brovall, C., Fackler, M. J., Schwartz, J. F., and Shaper, J. H. (1984). Antigenic analysis of hematopoiesis. III. A hematopoietic progenitor cell surface antigen defined by a monoclonal antibody raised against KG-1a cells. J Immunol *133*, 157-165.

Conneally, E., Cashman, J., Petzer, A., and Eaves, C. (1997). Expansion *in vitro* of transplantable human cord blood stem cells demonstrated using a quantitative assay of their lympho-myeloid repopulating activity in nonobese diabetic-scid/scid mice. Proc Natl Acad Sci U S A *94*, 9836-9841.

Coulombel, L. (2004). Identification of hematopoietic stem/progenitor cells: strength and drawbacks of functional assays. Oncogene *23*, 7210-7222.

Cragle, C., and MacNicol, A. M. (2014). Musashi protein-directed translational activation of target mRNAs is mediated by the poly(A) polymerase, germ line development defective-2. J Biol Chem *289*, 14239-14251.

Csaszar, E., Kirouac, D. C., Yu, M., Wang, W., Qiao, W., Cooke, M. P., Boitano, A. E., Ito, C., and Zandstra, P. W. (2012). Rapid expansion of human hematopoietic stem cells by automated control of inhibitory feedback signaling. Cell Stem Cell *10*, 218-229.

Cutler, C., Multani, P., Robbins, D., Kim, H. T., Le, T., Hoggatt, J., Pelus, L. M., Desponts, C., Chen, Y. B., Rezner, B., *et al.* (2013). Prostaglandin-modulated umbilical cord blood hematopoietic stem cell transplantation. Blood *122*, 3074-3081.

de Andrés-Aguayo, L., Varas, F., Kallin, E., Infante, J., Wurst, W., Floss, T., and Graf, T. (2011). Musashi 2 is a regulator of the HSC compartment identified by a retroviral insertion screen and knockout mice. Blood *118*, 554-618.

Delaney, C., Heimfeld, S., Brashem-Stein, C., Voorhies, H., Manger, R. L., and Bernstein, I. D. (2010). Notch-mediated expansion of human cord blood progenitor cells capable of rapid myeloid reconstitution. Nat Med *16*, 232-236.

Dexter, T. M., Allen, T. D., and Lajtha, L. G. (1977). Conditions controlling the proliferation of haemopoietic stem cells *in vitro*. J Cell Physiol *91*, 335-344.

Dick, J. (2008). Stem cell concepts renew cancer research. Blood *112*, 4793-5600.

Dick, J. E., Magli, M. C., Huszar, D., Phillips, R. A., and Bernstein, A. (1985). Introduction of a selectable gene into primitive stem cells capable of long-term reconstitution of the hemopoietic system of W/Wv mice. Cell *42*, 71-79.

Ding, L., and Morrison, S. J. (2013). Haematopoietic stem cells and early lymphoid progenitors occupy distinct bone marrow niches. Nature *495*, 231-235.

Ding, L., Saunders, T. L., Enikolopov, G., and Morrison, S. J. (2012). Endothelial and perivascular cells maintain haematopoietic stem cells. Nature *481*, 457-462.

Dodt, H. U., Leischner, U., Schierloh, A., Jahrling, N., Mauch, C. P., Deininger, K., Deussing, J. M., Eder, M., Zieglgansberger, W., and Becker, K. (2007). Ultramicroscopy: three-dimensional visualization of neuronal networks in the whole mouse brain. Nat Methods *4*, 331-336.

Domashenko, A. D., Danet-Desnoyers, G., Aron, A., Carroll, M. P., and Emerson, S. G. (2010). TAT-mediated transduction of NF-Ya peptide induces the ex vivo proliferation and engraftment potential of human hematopoietic progenitor cells. Blood *116*, 2676-2683.

Doulatov, S., Notta, F., Eppert, K., Nguyen, L. T., Ohashi, P. S., and Dick, J. E. (2010). Revised map of the human progenitor hierarchy shows the origin of macrophages and dendritic cells in early lymphoid development. Nat Immunol *11*, 585-593.

Doulatov, S., Notta, F., Laurenti, E., and Dick, J. E. (2012). Hematopoiesis: a human perspective. Cell Stem Cell *10*, 120-136.

Duncan, D. M., Burgess, E. A., and Duncan, I. (1998). Control of distal antennal identity and tarsal development in Drosophila by spineless-aristapedia, a homolog of the mammalian dioxin receptor. Genes Dev *12*, 1290-1303.

Dykstra, B., Kent, D., Bowie, M., McCaffrey, L., Hamilton, M., Lyons, K., Lee, S.-J., Brinkman, R., and Eaves, C. (2007). Long-term propagation of distinct hematopoietic differentiation programs *in vivo*. Cell Stem Cell *1*, 218-247.

Fares, I., Chagraoui, J., Gareau, Y., Gingras, S., Ruel, R., Mayotte, N., Csaszar, E., Knapp, D. J., Miller, P., Ngom, M*., et al.* (2014). Pyrimidoindole derivatives are agonists of human hematopoietic stem cell self-renewal. Science *345*, 1509-1512.

Fernandez-Salguero, P., Pineau, T., Hilbert, D. M., McPhail, T., Lee, S. S., Kimura, S., Nebert, D. W., Rudikoff, S., Ward, J. M., and Gonzalez, F. J. (1995). Immune system impairment and hepatic fibrosis in mice lacking the dioxin-binding Ah receptor. science *268*, 722-726.

Flach, J., Bakker, S. T., Mohrin, M., Conroy, P. C., Pietras, E. M., Reynaud, D., Alvarez, S., Diolaiti, M. E., Ugarte, F., Forsberg, E. C*., et al.* (2014). Replication stress is a potent driver of functional decline in ageing haematopoietic stem cells. Nature *512*, 198-202.

Ford, C. E., Hamerton, J. L., Barnes, D. W., and Loutit, J. F. (1956). Cytological identification of radiation-chimaeras. Nature *177*, 452-454.

Foudi, A., Hochedlinger, K., Van Buren, D., Schindler, J. W., Jaenisch, R., Carey, V., and Hock, H. (2009). Analysis of histone 2B-GFP retention reveals slowly cycling hematopoietic stem cells. Nat Biotechnol *27*, 84-90.

Frelin, C., Herrington, R., Janmohamed, S., Barbara, M., Tran, G., Paige, C. J., Benveniste, P., Zuniga-Pflucker, J. C., Souabni, A., Busslinger, M., and Iscove, N. N. (2013). GATA-3 regulates the self-renewal of long-term hematopoietic stem cells. Nat Immunol *14*, 1037-1044.

Fulop, G. M., and Phillips, R. A. (1990). The scid mutation in mice causes a general defect in DNA repair. Nature *347*, 479-482.

Gajjar, K., Martin-Hirsch, P. L., and Martin, F. L. (2012). CYP1B1 and hormone-induced cancer. Cancer Lett *324*, 13-30.

Galeev, R., Baudet, A., Kumar, P., Rundberg Nilsson, A., Nilsson, B., Soneji, S., Torngren, T., Borg, A., Kvist, A., and Larsson, J. (2016). Genome-wide RNAi Screen Identifies Cohesin Genes as Modifiers of Renewal and Differentiation in Human HSCs. Cell Rep *14*, 2988-3000.

Gargaro, M., Pirro, M., Romani, R., Zelante, T., and Fallarino, F. (2016). AhR-dependent pathways in immune regulation. Am J Transplant.

Gasiewicz, T. A., Singh, K. P., and Bennett, J. A. (2014). The Ah receptor in stem cell cycling, regulation, and quiescence. Ann N Y Acad Sci *1310*, 44-50.

Genovese, G., Jaiswal, S., Ebert, B. L., and McCarroll, S. A. (2015). Clonal hematopoiesis and blood-cancer risk. N Engl J Med *372*, 1071-1072.

Ghosh, M., Aguila, H. L., Michaud, J., Ai, Y., Wu, M. T., Hemmes, A., Ristimaki, A., Guo, C., Furneaux, H., and Hla, T. (2009). Essential role of the RNA-binding protein HuR in progenitor cell survival in mice. J Clin Invest *119*, 3530-3543.

Glimm, H., Eisterer, W., Lee, K., Cashman, J., Holyoake, T. L., Nicolini, F., Shultz, L. D., von Kalle, C., and Eaves, C. J. (2001). Previously undetected human hematopoietic cell populations with short-term repopulating activity selectively engraft NOD/SCID-beta2 microglobulin-null mice. J Clin Invest *107*, 199-206.

Gluckman, E., Broxmeyer, H. A., Auerbach, A. D., Friedman, H. S., Douglas, G. W., Devergie, A., Esperou, H., Thierry, D., Socie, G., Lehn, P., and et al. (1989). Hematopoietic reconstitution in a patient with Fanconi's anemia by means of umbilical-cord blood from an HLA-identical sibling. N Engl J Med *321*, 1174-1178.

Gonczy, P. (2008). Mechanisms of asymmetric cell division: flies and worms pave the way. Nat Rev Mol Cell Biol *9*, 355-366.

Gorgens, A., Ludwig, A. K., Mollmann, M., Krawczyk, A., Durig, J., Hanenberg, H., Horn, P. A., and Giebel, B. (2014). Multipotent hematopoietic progenitors divide asymmetrically to create progenitors of the lymphomyeloid and erythromyeloid lineages. Stem Cell Reports *3*, 1058-1072.

Grammatikakis, I., Abdelmohsen, K., and Gorospe, M. (2016). Posttranslational control of HuR function. Wiley Interdiscip Rev RNA.

Gratwohl, A., Baldomero, H., Aljurf, M., Pasquini, M. C., Bouzas, L. F., Yoshimi, A., Szer, J., Lipton, J., Schwendener, A., Gratwohl, M., *et al.* (2010). Hematopoietic stem cell transplantation: a global perspective. JAMA *303*, 1617-1624.

Greaves, M., and Maley, C. C. (2012). Clonal evolution in cancer. Nature *481*, 306-313.

Greenbaum, A., Hsu, Y. M., Day, R. B., Schuettpelz, L. G., Christopher, M. J., Borgerding, J. N., Nagasawa, T., and Link, D. C. (2013). CXCL12 in early mesenchymal progenitors is required for haematopoietic stem-cell maintenance. Nature *495*, 227-230.

Greenblatt, S. M., and Nimer, S. D. (2014). Chromatin modifiers and the promise of epigenetic therapy in acute leukemia. Leukemia *28*, 1396-1406.

Guengerich, F. P. (2007). Mechanisms of cytochrome P450 substrate oxidation: MiniReview. J Biochem Mol Toxicol *21*, 163-168.

Halbeisen, R. E., Galgano, A., Scherrer, T., and Gerber, A. P. (2008). Post-transcriptional gene regulation: from genome-wide studies to principles. Cell Mol Life Sci *65*, 798-813.

Heng, T. S., and Painter, M. W. (2008). The Immunological Genome Project: networks of gene expression in immune cells. Nat Immunol *9*, 1091-1094.

Hock, H., Hamblen, M. J., Rooke, H. M., Schindler, J. W., Saleque, S., Fujiwara, Y., and Orkin, S. H. (2004). Gfi-1 restricts proliferation and preserves functional integrity of haematopoietic stem cells. Nature *431*, 1002-1007.

Hope, K., Cellot, S., Ting, S., MacRae, T., Mayotte, N., Iscove, N., and Sauvageau, G. (2010). An RNAi screen identifies Msi2 and Prox1 as having opposite roles in the regulation of hematopoietic stem cell activity. Cell Stem Cell *7*, 101-114.

Hu, Y., and Smyth, G. K. (2009). ELDA: extreme limiting dilution analysis for comparing depleted and enriched populations in stem cell and other assays. J Immunol Methods *347*, 70-78.

Huang, C. H., Chen, P. M., Lu, T. C., Kung, W. M., Chiou, T. J., Yang, M. H., Kao, J. Y., and Wu, K. J. (2010). Purified recombinant TAT-homeobox B4 expands CD34(+) umbilical cord blood and peripheral blood progenitor cells ex vivo. Tissue Eng Part C Methods *16*, 487-496.

Huang, G. P., Pan, Z. J., Jia, B. B., Zheng, Q., Xie, C. G., Gu, J. H., McNiece, I. K., and Wang, J. F. (2007). Ex vivo expansion and transplantation of hematopoietic stem/progenitor cells supported by mesenchymal stem cells from human umbilical cord blood. Cell Transplant *16*, 579-585.

Hughes, D., Guttenplan, J. B., Marcus, C. B., Subbaramaiah, K., and Dannenberg, A. J. (2008). Heat shock protein 90 inhibitors suppress aryl hydrocarbon receptor-mediated activation of CYP1A1 and CYP1B1 transcription and DNA adduct formation. Cancer Prev Res (Phila) *1*, 485-493.

Hulett, H. R., Bonner, W. A., Barrett, J., and Herzenberg, L. A. (1969). Cell sorting: automated separation of mammalian cells as a function of intracellular fluorescence. Science *166*, 747-749.

Humphries, R. K., Eaves, A. C., and Eaves, C. J. (1979). Characterization of a primitive erythropoietic progenitor found in mouse marrow before and after several weeks in culture. Blood *53*, 746-763.

Imai, T., Tokunaga, A., Yoshida, T., Hashimoto, M., Mikoshiba, K., Weinmaster, G., Nakafuku, M., and Okano, H. (2001). The neural RNA-binding protein Musashi1 translationally regulates mammalian numb gene expression by interacting with its mRNA. Mol Cell Biol *21*, 3888-3900.

Ito, K., Hirao, A., Arai, F., Takubo, K., Matsuoka, S., Miyamoto, K., Ohmura, M., Naka, K., Hosokawa, K., Ikeda, Y., and Suda, T. (2006). Reactive oxygen species act through p38 MAPK to limit the lifespan of hematopoietic stem cells. Nat Med *12*, 446-451.

Ito, T., Kwon, H., Zimdahl, B., Congdon, K., Blum, J., Lento, W., Zhao, C., Lagoo, A., Gerrard, G., Foroni, L.*, et al.* (2010). Regulation of myeloid leukaemia by the cell-fate determinant Musashi. Nature *466*, 765-773.

Jacobson, L. O., Simmons, E. L., Marks, E. K., and Eldredge, J. H. (1951). Recovery from radiation injury. Science *113*, 510-511.

Jeong, M., and Goodell, M. A. (2016). Noncoding Regulatory RNAs in Hematopoiesis. Curr Top Dev Biol *118*, 245-270.

Jung, J., Buisman, S., and de Haan, G. (2016). Hematopoiesis during development, aging and disease. Exp Hematol.

Kafasla, P., Skliris, A., and Kontoyiannis, D. L. (2014). Post-transcriptional coordination of immunological responses by RNA-binding proteins. Nat Immunol *15*, 492-502.

Kamel-Reid, S., and Dick, J. E. (1988). Engraftment of immune-deficient mice with human hematopoietic stem cells. science *242*, 1706-1709.

Katz, Y., Li, F., Lambert, N. J., Sokol, E. S., Tam, W. L., Cheng, A. W., Airoldi, E. M., Lengner, C. J., Gupta, P. B., Yu, Z*., et al.* (2014). Musashi proteins are post-transcriptional regulators of the epithelial-luminal cell state. Elife *3*, e03915.

Kawahara, H., Imai, T., Imataka, H., Tsujimoto, M., Matsumoto, K., and Okano, H. (2008). Neural RNA-binding protein Musashi1 inhibits translation initiation by competing with eIF4G for PABP. J Cell Biol *181*, 639-653.

Keene, J. D. (2007). RNA regulons: coordination of post-transcriptional events. Nat Rev Genet *8*, 533-543.

Kennedy, J. C., Till, J. E., Siminovitch, L., and McCulloch, E. A. (1966). The proliferative capacity of antigen-sensitive precursors of hemolytic plaque-forming cells. J Immunol *96*, 973-980.

Keyoung, H., Roy, N., Benraiss, A., Louissaint, A., Suzuki, A., Hashimoto, M., Rashbaum, W., Okano, H., and Goldman, S. (2001). High-yield selection and extraction of two promoter-defined phenotypes of neural stem cells from the fetal human brain. Nature Biotechnology *19*, 843-893.

Kharas, M., Lengner, C., Al-Shahrour, F., Bullinger, L., Ball, B., Zaidi, S., Morgan, K., Tam, W., Paktinat, M., Okabe, R., *et al.* (2010). Musashi-2 regulates normal hematopoiesis and promotes aggressive myeloid leukemia. Nature Medicine *16*, 903-911.

Kiel, M., Yilmaz, O., Iwashita, T., Yilmaz, O., Terhorst, C., and Morrison, S. (2005). SLAM family receptors distinguish hematopoietic stem and progenitor cells and reveal endothelial niches for stem cells. Cell *121*, 1109-1130.

Kiel, M. J., He, S., Ashkenazi, R., Gentry, S. N., Teta, M., Kushner, J. A., Jackson, T. L., and Morrison, S. J. (2007). Haematopoietic stem cells do not asymmetrically segregate chromosomes or retain BrdU. Nature *449*, 238-242.

Knoblich, J. A. (2008). Mechanisms of asymmetric stem cell division. Cell *132*, 583-597.

Ko, C. I., Fan, Y., de Gannes, M., Wang, Q., Xia, Y., and Puga, A. (2016). Repression of the Aryl Hydrocarbon Receptor is Required to Maintain Mitotic Progression and Prevent Loss of Pluripotency of Embryonic Stem Cells. Stem Cells.

Ko, K. H., Holmes, T., Palladinetti, P., Song, E., Nordon, R., O'Brien, T. A., and Dolnikov, A. (2011). GSK-3beta inhibition promotes engraftment of ex vivo-expanded hematopoietic stem cells and modulates gene expression. Stem Cells *29*, 108-118.

Kohler, G., and Milstein, C. (1975). Continuous cultures of fused cells secreting antibody of predefined specificity. Nature *256*, 495-497.

Kohli, L., and Passegue, E. (2014). Surviving change: the metabolic journey of hematopoietic stem cells. Trends Cell Biol *24*, 479-487.

Kowalczyk, M. S., Tirosh, I., Heckl, D., Rao, T. N., Dixit, A., Haas, B. J., Schneider, R. K., Wagers, A. J., Ebert, B. L., and Regev, A. (2015). Single-cell RNA-seq reveals changes in cell cycle and differentiation programs upon aging of hematopoietic stem cells. Genome Res *25*, 1860-1872.

Krivtsov, A. V., and Armstrong, S. A. (2007). MLL translocations, histone modifications and leukaemia stem-cell development. Nat Rev Cancer *7*, 823-833.

Kwon, H. Y., Bajaj, J., Ito, T., Blevins, A., Konuma, T., Weeks, J., Lytle, N. K., Koechlein, C. S., Rizzieri, D., Chuah, C*., et al.* (2015). Tetraspanin 3 Is Required for the Development and Propagation of Acute Myelogenous Leukemia. Cell Stem Cell *17*, 152-164.

Kwon, Y. J., Baek, H. S., Ye, D. J., Shin, S., Kim, D., and Chun, Y. J. (2016). CYP1B1 Enhances Cell Proliferation and Metastasis through Induction of EMT and Activation of Wnt/beta-Catenin Signaling via Sp1 Upregulation. PLoS One *11*, e0151598.

Lahvis, G. P., Lindell, S. L., Thomas, R. S., McCuskey, R. S., Murphy, C., Glover, E., Bentz, M., Southard, J., and Bradfield, C. A. (2000). Portosystemic shunting and persistent fetal vascular structures in aryl hydrocarbon receptor-deficient mice. Proc Natl Acad Sci U S A *97*, 10442-10447.

Lansdorp, P. M., Sutherland, H. J., and Eaves, C. J. (1990). Selective expression of CD45 isoforms on functional subpopulations of CD34+ hemopoietic cells from human bone marrow. J Exp Med *172*, 363-366.

Laurenti, E., Doulatov, S., Zandi, S., Plumb, I., Chen, J., April, C., Fan, J. B., and Dick, J. E. (2013). The transcriptional architecture of early human hematopoiesis identifies multilevel control of lymphoid commitment. Nat Immunol *14*, 756-763.

Lefkovits, I., and Waldmann, H. (1984). Limiting dilution analysis of the cells of immune system I. The clonal basis of the immune response. Immunol Today *5*, 265-268.

Lemieux, M. E., Rebel, V. I., Lansdorp, P. M., and Eaves, C. J. (1995). Characterization and purification of a primitive hematopoietic cell type in adult mouse marrow capable of lymphomyeloid differentiation in long-term marrow "switch" cultures. Blood *86*, 1339-1347.

Li, J., Kurasawa, Y., Wang, Y., Clise-Dwyer, K., Klumpp, S. A., Liang, H., Tailor, R. C., Raymond, A. C., Estrov, Z., Brandt, S. J.*, et al.* (2014). Requirement for ssbp2 in hematopoietic stem cell maintenance and stress response. J Immunol *193*, 4654-4662.

Lo Celso, C., Fleming, H., Wu, J., Zhao, C., Miake-Lye, S., Fujisaki, J., Côté, D., Rowe, D., Lin, C., and Scadden, D. (2008). Live-animal tracking of individual haematopoietic stem/progenitor cells in their niche. Nature *457*, 92-98.

Lorenz, E., Congdon, C., and Uphoff, D. (1952). Modification of acute irradiation injury in mice and guinea-pigs by bone marrow injections. Radiology *58*, 863-877.

Lu, R., Neff, N. F., Quake, S. R., and Weissman, I. L. (2011). Tracking single hematopoietic stem cells *in vivo* using high-throughput sequencing in conjunction with viral genetic barcoding. Nat Biotechnol *29*, 928-933.

MacNicol, M. C., Cragle, C. E., and MacNicol, A. M. (2011). Context-dependent regulation of Musashi-mediated mRNA translation and cell cycle regulation. Cell Cycle *10*, 39-44.

Majeti, R., Park, C. Y., and Weissman, I. L. (2007). Identification of a hierarchy of multipotent hematopoietic progenitors in human cord blood. Cell Stem Cell *1*, 635-645.

Mantel, C. R., O'Leary, H. A., Chitteti, B. R., Huang, X., Cooper, S., Hangoc, G., Brustovetsky, N., Srour, E. F., Lee, M. R., Messina-Graham, S., *et al.* (2015). Enhancing Hematopoietic Stem Cell Transplantation Efficacy by Mitigating Oxygen Shock. Cell *161*, 1553-1565.

Mayani, H., Dragowska, W., and Lansdorp, P. M. (1993). Cytokine-induced selective expansion and maturation of erythroid versus myeloid progenitors from purified cord blood precursor cells. Blood *81*, 3252-3258.

Mazurier, F., Doedens, M., Gan, O. I., and Dick, J. E. (2003). Rapid myeloerythroid repopulation after intrafemoral transplantation of NOD-SCID mice reveals a new class of human stem cells. Nat Med *9*, 959-963.

McCulloch, E. A., and Till, J. E. (1960). The radiation sensitivity of normal mouse bone marrow cells, determined by quantitative marrow transplantation into irradiated mice. Radiat Res *13*, 115-125.

McCune, J. M., Namikawa, R., Kaneshima, H., Shultz, L. D., Lieberman, M., and Weissman, I. L. (1988). The SCID-hu mouse: murine model for the analysis of human hematolymphoid differentiation and function. science *241*, 1632-1639.

Meldgaard Knudsen, L., Jensen, L., Jarlbaek, L., Hansen, P. G., Hansen, S. W., Drivsholm, L., Nikolaisen, K., Gaarsdal, E., and Johnsen, H. E. (1999). Subsets of CD34+ hematopoietic progenitors and platelet recovery after high dose chemotherapy and peripheral blood stem cell transplantation. Haematologica *84*, 517-524.

Milano, F., Heimfeld, S., Riffkin, I. B., Nicoud, I., Applebaum, F. R., Bernstein, I. D., and Delaney, C. (2014). Infusion of a Non HLA-Matched Off-the-Shelf Ex Vivo Expanded Cord Blood Progenitor Cell Product Following Myeloablative Cord Blood Transplantation Is Safe, Decreases the Time to Hematopoietic Recovery, and Results in Excellent Overall Survival. Blood *124*, 46-46.

Miller, P. H., Cheung, A. M., Beer, P. A., Knapp, D. J., Dhillon, K., Rabu, G., Rostamirad, S., Humphries, R. K., and Eaves, C. J. (2013a). Enhanced normal short-term human myelopoiesis in mice engineered to express human-specific myeloid growth factors. Blood *121*, e1-4.

Miller, P. H., Knapp, D. J., and Eaves, C. J. (2013b). Heterogeneity in hematopoietic stem cell populations: implications for transplantation. Curr Opin Hematol *20*, 257-264.

Milyavsky, M., Gan, O. I., Trottier, M., Komosa, M., Tabach, O., Notta, F., Lechman, E., Hermans, K. G., Eppert, K., Konovalova, Z., *et al.* (2010). A distinctive DNA damage response in human hematopoietic stem cells reveals an apoptosis-independent role for p53 in self-renewal. Cell Stem Cell *7*, 186-197.

Mimura, J., and Fujii-Kuriyama, Y. (2003). Functional role of AhR in the expression of toxic effects by TCDD. Biochim Biophys Acta *1619*, 263-268.

Miyamoto, T., Iwasaki, H., Reizis, B., Ye, M., Graf, T., Weissman, I. L., and Akashi, K. (2002). Myeloid or lymphoid promiscuity as a critical step in hematopoietic lineage commitment. Dev Cell *3*, 137-147.

Mohrin, M., Bourke, E., Alexander, D., Warr, M. R., Barry-Holson, K., Le Beau, M. M., Morrison, C. G., and Passegue, E. (2010). Hematopoietic stem cell quiescence promotes error-prone DNA repair and mutagenesis. Cell Stem Cell *7*, 174-185.

Morrison, S., and Weissman, I. (1994). The long-term repopulating subset of hematopoietic stem cells is deterministic and isolatable by phenotype. Immunity *1*, 661-734.

Morrison, S. J., and Scadden, D. T. (2014). The bone marrow niche for haematopoietic stem cells. Nature *505*, 327-334.

Mosier, D. E., Gulizia, R. J., Baird, S. M., and Wilson, D. B. (1988). Transfer of a functional human immune system to mice with severe combined immunodeficiency. Nature *335*, 256-259.

Mossadegh-Keller, N., Sarrazin, S., Kandalla, P. K., Espinosa, L., Stanley, E. R., Nutt, S. L., Moore, J., and Sieweke, M. H. (2013). M-CSF instructs myeloid lineage fate in single haematopoietic stem cells. Nature *497*, 239-243.

Mukherjee, K., Ghoshal, B., Ghosh, S., Chakrabarty, Y., Shwetha, S., Das, S., and Bhattacharyya, S. N. (2016). Reversible HuR-microRNA binding controls extracellular export of miR-122 and augments stress response. EMBO Rep.

Mulero-Navarro, S., and Fernandez-Salguero, P. M. (2016). New Trends in Aryl Hydrocarbon Receptor Biology. Front Cell Dev Biol *4*, 45.

Mulligan, R. C. (1993). The basic science of gene therapy. science *260*, 926-932.

Murray, L., Chen, B., Galy, A., Chen, S., Tushinski, R., Uchida, N., Negrin, R., Tricot, G., Jagannath, S., and Vesole, D. (1995). Enrichment of human hematopoietic stem cell activity in the CD34+Thy-1+Lin- subpopulation from mobilized peripheral blood. Blood *85*, 368-378.

Naik, S. H., Perie, L., Swart, E., Gerlach, C., van Rooij, N., de Boer, R. J., and Schumacher, T. N. (2013). Diverse and heritable lineage imprinting of early haematopoietic progenitors. Nature *496*, 229-232.

Nakamura, M., Okano, H., Blendy, J. A., and Montell, C. (1994). Musashi, a neural RNA-binding protein required for Drosophila adult external sensory organ development. Neuron *13*, 67-81.

Naldini, L., Blomer, U., Gallay, P., Ory, D., Mulligan, R., Gage, F. H., Verma, I. M., and Trono, D. (1996). *In vivo* gene delivery and stable transduction of nondividing cells by a lentiviral vector. Science *272*, 263-267.

Neumüller, R., and Knoblich, J. (2009). Dividing cellular asymmetry: asymmetric cell division and its implications for stem cells and cancer. Genes & Development *23*, 2675-2774.

Nishino, T., Miyaji, K., Ishiwata, N., Arai, K., Yui, M., Asai, Y., Nakauchi, H., and Iwama, A. (2009). Ex vivo expansion of human hematopoietic stem cells by a small-molecule agonist of c-MPL. Exp Hematol *37*, 1364-1377 e1364.

North, T. E., Goessling, W., Walkley, C. R., Lengerke, C., Kopani, K. R., Lord, A. M., Weber, G. J., Bowman, T. V., Jang, I. H., Grosser, T*., et al.* (2007). Prostaglandin E2 regulates vertebrate haematopoietic stem cell homeostasis. Nature *447*, 1007-1011.

Notta, F., Doulatov, S., Laurenti, E., Poeppl, A., Jurisica, I., and Dick, J. (2011). Isolation of single human hematopoietic stem cells capable of long-term multilineage engraftment. Science *333*, 218-239.

Notta, F., Zandi, S., Takayama, N., Dobson, S., Gan, O. I., Wilson, G., Kaufmann, K. B., McLeod, J., Laurenti, E., Dunant, C. F*., et al.* (2016). Distinct routes of lineage development reshape the human blood hierarchy across ontogeny. Science *351*, aab2116.

Novershtern, N., Subramanian, A., Lawton, L. N., Mak, R. H., Haining, W. N., McConkey, M. E., Habib, N., Yosef, N., Chang, C. Y., Shay, T*., et al.* (2011). Densely interconnected transcriptional circuits control cell states in human hematopoiesis. Cell *144*, 296-309.

Offner, F., Schoch, G., Fisher, L. D., Torok-Storb, B., and Martin, P. J. (1996). Mortality hazard functions as related to neutropenia at different times after marrow transplantation. Blood *88*, 4058-4062.

Ogawa, M., Matsuzaki, Y., Nishikawa, S., Hayashi, S., Kunisada, T., Sudo, T., Kina, T., and Nakauchi, H. (1991). Expression and function of c-kit in hemopoietic progenitor cells. J Exp Med *174*, 63-71.

Oguro, H., Ding, L., and Morrison, S. J. (2013). SLAM family markers resolve functionally distinct subpopulations of hematopoietic stem cells and multipotent progenitors. Cell Stem Cell *13*, 102-116.

Ohta, H., Sekulovic, S., Bakovic, S., Eaves, C. J., Pineault, N., Gasparetto, M., Smith, C., Sauvageau, G., and Humphries, R. K. (2007). Near-maximal expansions of hematopoietic stem cells in culture using NUP98-HOX fusions. Exp Hematol *35*, 817-830.

Ohyama, T., Nagata, T., Tsuda, K., Kobayashi, N., Imai, T., Okano, H., Yamazaki, T., and Katahira, M. (2012). Structure of Musashi1 in a complex with target RNA: the role of aromatic stacking interactions. Nucleic Acids Res *40*, 3218-3231.

Okabe, M., Imai, T., Kurusu, M., Hiromi, Y., and Okano, H. (2001). Translational repression determines a neuronal potential in Drosophila asymmetric cell division. Nature *411*, 94-102.

Okey, A. B. (2007). An aryl hydrocarbon receptor odyssey to the shores of toxicology: the Deichmann Lecture, International Congress of Toxicology-XI. Toxicol Sci *98*, 5-38.

Orkin, S. H. (2000). Diversification of haematopoietic stem cells to specific lineages. Nat Rev Genet *1*, 57-64.

Orkin, S. H., and Zon, L. I. (2008). Hematopoiesis: an evolving paradigm for stem cell biology. Cell *132*, 631-644.

Osawa, M., Hanada, K., Hamada, H., and Nakauchi, H. (1996). Long-term lymphohematopoietic reconstitution by a single CD34-low/negative hematopoietic stem cell. Science *273*, 242-245.

Pabst, C., Krosl, J., Fares, I., Boucher, G., Ruel, R., Marinier, A., Lemieux, S., Hebert, J., and Sauvageau, G. (2014). Identification of small molecules that support human leukemia stem cell activity ex vivo. Nat Methods *11*, 436-442.

Park, S. M., Deering, R. P., Lu, Y., Tivnan, P., Lianoglou, S., Al-Shahrour, F., Ebert, B. L., Hacohen, N., Leslie, C., Daley, G. Q., *et al.* (2014). Musashi-2 controls cell fate, lineage bias, and TGF-beta signaling in HSCs. J Exp Med *211*, 71-87.

Park, S. M., Gonen, M., Vu, L., Minuesa, G., Tivnan, P., Barlowe, T. S., Taggart, J., Lu, Y., Deering, R. P., Hacohen, N., *et al.* (2015). Musashi2 sustains the mixed-lineage leukemia-driven stem cell regulatory program. J Clin Invest *125*, 1286-1298.

Parmar, K., Mauch, P., Vergilio, J. A., Sackstein, R., and Down, J. D. (2007). Distribution of hematopoietic stem cells in the bone marrow according to regional hypoxia. Proc Natl Acad Sci U S A *104*, 5431-5436.

Passegue, E., Wagers, A. J., Giuriato, S., Anderson, W. C., and Weissman, I. L. (2005). Global analysis of proliferation and cell cycle gene expression in the regulation of hematopoietic stem and progenitor cell fates. J Exp Med *202*, 1599-1611.

Paul, F., Arkin, Y., Giladi, A., Jaitin, D. A., Kenigsberg, E., Keren-Shaul, H., Winter, D., Lara-Astiaso, D., Gury, M., Weiner, A., *et al.* (2015). Transcriptional Heterogeneity and Lineage Commitment in Myeloid Progenitors. Cell *163*, 1663-1677.

Peled, T., Glukhman, E., Hasson, N., Adi, S., Assor, H., Yudin, D., Landor, C., Mandel, J., Landau, E., Prus, E., *et al.* (2005). Chelatable cellular copper modulates differentiation and self-renewal of cord blood-derived hematopoietic progenitor cells. Exp Hematol *33*, 1092-1100.

Perie, L., Duffy, K. R., Kok, L., de Boer, R. J., and Schumacher, T. N. (2015). The Branching Point in Erythro-Myeloid Differentiation. Cell *163*, 1655-1662.

Perrotti, D., and Neviani, P. (2007). From mRNA metabolism to cancer therapy: chronic myelogenous leukemia shows the way. Clin Cancer Res *13*, 1638-1642.

Pietras, E. M., Mirantes-Barbeito, C., Fong, S., Loeffler, D., Kovtonyuk, L. V., Zhang, S., Lakshminarasimhan, R., Chin, C. P., Techner, J. M., Will, B.*, et al.* (2016). Chronic interleukin-1 exposure drives haematopoietic stem cells towards precocious myeloid differentiation at the expense of self-renewal. Nat Cell Biol *18*, 607-618.

Pietras, E. M., Reynaud, D., Kang, Y. A., Carlin, D., Calero-Nieto, F. J., Leavitt, A. D., Stuart, J. M., Gottgens, B., and Passegue, E. (2015). Functionally Distinct Subsets of Lineage-Biased Multipotent Progenitors Control Blood Production in Normal and Regenerative Conditions. Cell Stem Cell *17*, 35-46.

Platzer, B., Richter, S., Kneidinger, D., Waltenberger, D., Woisetschlager, M., and Strobl, H. (2009). Aryl hydrocarbon receptor activation inhibits *in vitro* differentiation of human monocytes and Langerhans dendritic cells. J Immunol *183*, 66-74.

Pohjanvirta, R. (2012). The AH Receptor in Biology and Toxicology, (New York: John Wiley & Sons).

Ramalho-Santos, M., and Willenbring, H. (2007). On the origin of the term "stem cell". Cell Stem Cell *1*, 35-38.

Rentas, S., Holzapfel, N., and Hope, K. (2013). Cancer Stem Cells: Prospective Isolation and Progress Toward Functional Biomarker Identification. Current Pathobiology Reports *1*, 81-90.

Rentas, S., Holzapfel, N. T., Belew, M. S., Pratt, G. A., Voisin, V., Wilhelm, B. T., Bader, G. D., Yeo, G. W., and Hope, K. J. (2016). Musashi-2 attenuates AHR signalling to expand human haematopoietic stem cells. Nature *532*, 508-511.

Rieger, M. A., Hoppe, P. S., Smejkal, B. M., Eitelhuber, A. C., and Schroeder, T. (2009). Hematopoietic cytokines can instruct lineage choice. Science *325*, 217-218.

Roeder, I., and Glauche, I. (2006). Towards an understanding of lineage specification in hematopoietic stem cells: a mathematical model for the interaction of transcription factors GATA-1 and PU.1. J Theor Biol *241*, 852-865.

Root, D. E., Hacohen, N., Hahn, W. C., Lander, E. S., and Sabatini, D. M. (2006). Genome-scale loss-of-function screening with a lentiviral RNAi library. Nat Methods *3*, 715-719.

Rossi, D. J., Bryder, D., Seita, J., Nussenzweig, A., Hoeijmakers, J., and Weissman, I. L. (2007). Deficiencies in DNA damage repair limit the function of haematopoietic stem cells with age. Nature *447*, 725-729.

Sacchetti, B., Funari, A., Michienzi, S., Di Cesare, S., Piersanti, S., Saggio, I., Tagliafico, E., Ferrari, S., Robey, P. G., Riminucci, M., and Bianco, P. (2007). Self-renewing osteoprogenitors in bone marrow sinusoids can organize a hematopoietic microenvironment. Cell *131*, 324-336.

Sanchez-Aguilera, A., Arranz, L., Martin-Perez, D., Garcia-Garcia, A., Stavropoulou, V., Kubovcakova, L., Isern, J., Martin-Salamanca, S., Langa, X., Skoda, R. C.*, et al.* (2014). Estrogen signaling selectively induces apoptosis of hematopoietic progenitors and myeloid neoplasms without harming steady-state hematopoiesis. Cell Stem Cell *15*, 791-804.

Sanchez-Jimenez, C., and Izquierdo, J. M. (2015). T-cell intracellular antigens in health and disease. Cell Cycle *14*, 2033-2043.

Schmidt, J. V., Su, G. H., Reddy, J. K., Simon, M. C., and Bradfield, C. A. (1996). Characterization of a murine Ahr null allele: involvement of the Ah receptor in hepatic growth and development. Proc Natl Acad Sci U S A *93*, 6731-6736.

Seita, J., and Weissman, I. (2010). Hematopoietic stem cell: self-renewal versus differentiation. Wiley Interdisciplinary Reviews Systems Biology and Medicine *2*, 640-693.

Semerad, C. L., Mercer, E. M., Inlay, M. A., Weissman, I. L., and Murre, C. (2009). E2A proteins maintain the hematopoietic stem cell pool and promote the maturation of myelolymphoid and myeloerythroid progenitors. Proc Natl Acad Sci U S A *106*, 1930-1935.

Shin, J. W., Buxboim, A., Spinler, K. R., Swift, J., Christian, D. A., Hunter, C. A., Leon, C., Gachet, C., Dingal, P. C., Ivanovska, I. L.*, et al.* (2014). Contractile forces sustain and polarize hematopoiesis from stem and progenitor cells. Cell Stem Cell *14*, 81-93.

Shpall, E. J., Quinones, R., Giller, R., Zeng, C., Baron, A. E., Jones, R. B., Bearman, S. I., Nieto, Y., Freed, B., Madinger, N.*, et al.* (2002). Transplantation of ex vivo expanded cord blood. Biol Blood Marrow Transplant *8*, 368-376.

Shultz, L. D., Ishikawa, F., and Greiner, D. L. (2007). Humanized mice in translational biomedical research. Nat Rev Immunol *7*, 118-130.

Shultz, L. D., Schweitzer, P. A., Christianson, S. W., Gott, B., Schweitzer, I. B., Tennent, B., McKenna, S., Mobraaten, L., Rajan, T. V., Greiner, D. L., and et al. (1995). Multiple defects in innate and adaptive immunologic function in NOD/LtSz-scid mice. J Immunol *154*, 180-191.

Signer, R. A., Magee, J. A., Salic, A., and Morrison, S. J. (2014). Haematopoietic stem cells require a highly regulated protein synthesis rate. Nature *509*, 49-54.

Siminovitch, L., Till, J., and McCulloch, E. (1964). Decline in colony-forming ability of marrow cells subjected to serial transplantation into irradiated mice. Journal of Cellular Physiology *64*, 23-54.

Singh, K. P., Bennett, J. A., Casado, F. L., Walrath, J. L., Welle, S. L., and Gasiewicz, T. A. (2014). Loss of aryl hydrocarbon receptor promotes gene changes associated with premature hematopoietic stem cell exhaustion and development of a myeloproliferative disorder in aging mice. Stem Cells Dev *23*, 95-106.

Smith, B. W., Rozelle, S. S., Leung, A., Ubellacker, J., Parks, A., Nah, S. K., French, D., Gadue, P., Monti, S., Chui, D. H*., et al.* (2013). The aryl hydrocarbon receptor directs hematopoietic progenitor cell expansion and differentiation. Blood *122*, 376-385.

Spangrude, G., Heimfeld, S., and Weissman, I. (1988). Purification and characterization of mouse hematopoietic stem cells. Science *241*, 58-120.

Spencer, J. A., Ferraro, F., Roussakis, E., Klein, A., Wu, J., Runnels, J. M., Zaher, W., Mortensen, L. J., Alt, C., Turcotte, R*., et al.* (2014). Direct measurement of local oxygen concentration in the bone marrow of live animals. Nature *508*, 269-273.

Spitzer, M. H., Gherardini, P. F., Fragiadakis, G. K., Bhattacharya, N., Yuan, R. T., Hotson, A. N., Finck, R., Carmi, Y., Zunder, E. R., Fantl, W. J*., et al.* (2015). An interactive reference framework for modeling a dynamic immune system. Science *349*, 1259425.

Stockinger, B., Di Meglio, P., Gialitakis, M., and Duarte, J. H. (2014). The aryl hydrocarbon receptor: multitasking in the immune system. Annu Rev Immunol *32*, 403-432.

Sun, J., Ramos, A., Chapman, B., Johnnidis, J. B., Le, L., Ho, Y. J., Klein, A., Hofmann, O., and Camargo, F. D. (2014). Clonal dynamics of native haematopoiesis. Nature *514*, 322-327.

Sutherland, H. J., Eaves, C. J., Eaves, A. C., Dragowska, W., and Lansdorp, P. M. (1989). Characterization and partial purification of human marrow cells capable of initiating long-term hematopoiesis *in vitro*. Blood *74*, 1563-1570.

Sutherland, H. J., Eaves, C. J., Lansdorp, P. M., Thacker, J. D., and Hogge, D. E. (1991). Differential regulation of primitive human hematopoietic cells in long-term cultures maintained on genetically engineered murine stromal cells. Blood *78*, 666-672.

Swierczek, S. I., Piterkova, L., Jelinek, J., Agarwal, N., Hammoud, S., Wilson, A., Hickman, K., Parker, C. J., Cairns, B. R., and Prchal, J. T. (2012). Methylation of AR locus does not always reflect X chromosome inactivation state. Blood *119*, e100-109.

Szilvassy, S., Humphries, R., Lansdorp, P., Eaves, A., and Eaves, C. (1990). Quantitative assay for totipotent reconstituting hematopoietic stem cells by a competitive repopulation strategy. Proceedings of the National Academy of Sciences of the United States of America *87*, 8736-8776.

Taggart, J., Ho, T. C., Amin, E., Xu, H., Barlowe, T. S., Perez, A. R., Durham, B. H., Tivnan, P., Okabe, R., Chow, A.*, et al.* (2016). MSI2 is required for maintaining activated myelodysplastic syndrome stem cells. Nat Commun *7*, 10739.

Takubo, K., Goda, N., Yamada, W., Iriuchishima, H., Ikeda, E., Kubota, Y., Shima, H., Johnson, R. S., Hirao, A., Suematsu, M., and Suda, T. (2010). Regulation of the HIF-1alpha level is essential for hematopoietic stem cells. Cell Stem Cell *7*, 391-402.

Taswell, C. (1981). Limiting dilution assays for the determination of immunocompetent cell frequencies. I. Data analysis. J Immunol *126*, 1614-1619.

Terstappen, L. W., Huang, S., Safford, M., Lansdorp, P. M., and Loken, M. R. (1991). Sequential generations of hematopoietic colonies derived from single nonlineage-committed CD34+CD38- progenitor cells. Blood *77*, 1218-1227.

Thiadens, K. A., and von Lindern, M. (2015). Selective mRNA translation in erythropoiesis. Biochem Soc Trans *43*, 343-347.

Tijet, N., Boutros, P. C., Moffat, I. D., Okey, A. B., Tuomisto, J., and Pohjanvirta, R. (2006). Aryl hydrocarbon receptor regulates distinct dioxin-dependent and dioxin-independent gene batteries. Mol Pharmacol *69*, 140-153.

Till, J., McCulloch, E., and Siminovitch, L. (1963). A stochastic model of stem cell proliferation, based on the growth of spleen colony-forming cells. Proceedings of the National Academy of Sciences of the United States of America *51*, 29-65.

Till, J. E., and McCulloch, E. A. (1961). A direct measurement of the radiation sensitivity of normal mouse bone marrow cells. Radiat Res *175*, 145-149.

Ting, S. B., Deneault, E., Hope, K., Cellot, S., Chagraoui, J., Mayotte, N., Dorn, J. F., Laverdure, J. P., Harvey, M., Hawkins, E. D.*, et al.* (2011). Asymmetrical segregation and self-renewal of hematopoietic stem and progenitor cells with endocytic Ap2a2. Blood.

Trumpp, A., Essers, M., and Wilson, A. (2010). Awakening dormant haematopoietic stem cells. Nat Rev Immuno *10*, 201-210.

Turner, M., Galloway, A., and Vigorito, E. (2014). Noncoding RNA and its associated proteins as regulatory elements of the immune system. Nat Immunol *15*, 484-491.

van den Bogaard, E. H., Podolsky, M. A., Smits, J. P., Cui, X., John, C., Gowda, K., Desai, D., Amin, S. G., Schalkwijk, J., Perdew, G. H., and Glick, A. B. (2015). Genetic and pharmacological analysis identifies a physiological role for the AHR in epidermal differentiation. J Invest Dermatol *135*, 1320-1328.

van Galen, P., Kreso, A., Mbong, N., Kent, D. G., Fitzmaurice, T., Chambers, J. E., Xie, S., Laurenti, E., Hermans, K., Eppert, K.*, et al.* (2014a). The unfolded protein response governs integrity of the haematopoietic stem-cell pool during stress. Nature *510*, 268-272.

van Galen, P., Kreso, A., Wienholds, E., Laurenti, E., Eppert, K., Lechman, E. R., Mbong, N., Hermans, K., Dobson, S., April, C.*, et al.* (2014b). Reduced lymphoid lineage priming promotes human hematopoietic stem cell expansion. Cell Stem Cell *14*, 94-106.

Wagner, J. E., Jr., Brunstein, C. G., Boitano, A. E., DeFor, T. E., McKenna, D., Sumstad, D., Blazar, B. R., Tolar, J., Le, C., Jones, J.*, et al.* (2016). Phase I/II Trial of StemRegenin-1 Expanded Umbilical Cord Blood Hematopoietic Stem Cells Supports Testing as a Stand-Alone Graft. Cell Stem Cell *18*, 144-155.

Walter, D., Lier, A., Geiselhart, A., Thalheimer, F. B., Huntscha, S., Sobotta, M. C., Moehrle, B., Brocks, D., Bayindir, I., Kaschutnig, P.*, et al.* (2015). Exit from dormancy provokes DNA-damage-induced attrition in haematopoietic stem cells. Nature *520*, 549-552.

Wilkinson, A. C., and Gottgens, B. (2013). Transcriptional regulation of haematopoietic stem cells. Adv Exp Med Biol *786*, 187-212.

Will, B., Vogler, T. O., Bartholdy, B., Garrett-Bakelman, F., Mayer, J., Barreyro, L., Pandolfi, A., Todorova, T. I., Okoye-Okafor, U. C., Stanley, R. F.*, et al.* (2013). Satb1 regulates the self-renewal of hematopoietic stem cells by promoting quiescence and repressing differentiation commitment. Nat Immunol *14*, 437-445.

Wilson, A., Ardiet, D. L., Saner, C., Vilain, N., Beermann, F., Aguet, M., Macdonald, H. R., and Zilian, O. (2007). Normal hemopoiesis and lymphopoiesis in the combined absence of numb and numblike. J Immunol *178*, 6746-6751.

Wilson, A., Laurenti, E., Oser, G., van der Wath, R., Blanco-Bose, W., Jaworski, M., Offner, S., Dunant, C., Eshkind, L., Bockamp, E.*, et al.* (2008). Hematopoietic stem cells reversibly switch from dormancy to self-renewal during homeostasis and repair. Cell *135*, 1118-1147.

Worton, R. G., McCulloch, E. A., and Till, J. E. (1969). Physical separation of hemopoietic stem cells differing in their capacity for self-renewal. J Exp Med *130*, 91-103.

Wu, M., Kwon, H., Rattis, F., Blum, J., Zhao, C., Ashkenazi, R., Jackson, T., Gaiano, N., Oliver, T., and Reya, T. (2007). Imaging hematopoietic precursor division in real time. Cell Stem Cell *1*, 541-595.

Xu, S., Ren, Z., Wang, Y., Ding, X., and Jiang, Y. (2014). Preferential expression of cytochrome CYP CYP2R1 but not CYP1B1 in human cord blood hematopoietic stem and progenitor cells. Acta Pharm Sin B *4*, 464-469.

Yang, L., Bryder, D., Adolfsson, J., Nygren, J., Månsson, R., Sigvardsson, M., and Jacobsen, S. (2005). Identification of Lin(-)Sca1(+)kit(+)CD34(+)Flt3- short-term hematopoietic stem cells capable of rapidly reconstituting and rescuing myeloablated transplant recipients. Blood *105*, 2717-2740.

Yang, Q., Kardava, L., St Leger, A., Martincic, K., Varnum-Finney, B., Bernstein, I. D., Milcarek, C., and Borghesi, L. (2008). E47 controls the developmental integrity and cell cycle quiescence of multipotential hematopoietic progenitors. J Immunol *181*, 5885-5894.

Yilmaz, O. H., Valdez, R., Theisen, B. K., Guo, W., Ferguson, D. O., Wu, H., and Morrison, S. J. (2006). Pten dependence distinguishes haematopoietic stem cells from leukaemia-initiating cells. Nature *441*, 475-482.

Yoshihara, H., Arai, F., Hosokawa, K., Hagiwara, T., Takubo, K., Nakamura, Y., Gomei, Y., Iwasaki, H., Matsuoka, S., Miyamoto, K., *et al.* (2007). Thrombopoietin/MPL signaling regulates hematopoietic stem cell quiescence and interaction with the osteoblastic niche. Cell Stem Cell *1*, 685-697.

Young, N. S. (2006). Pathophysiologic mechanisms in acquired aplastic anemia. Hematology Am Soc Hematol Educ Program, 72-77.

Zhang, H., Kozono, D. E., O'Connor, K. W., Vidal-Cardenas, S., Rousseau, A., Hamilton, A., Moreau, L., Gaudiano, E. F., Greenberger, J., Bagby, G.*, et al.* (2016). TGF-beta Inhibition Rescues Hematopoietic Stem Cell Defects and Bone Marrow Failure in Fanconi Anemia. Cell Stem Cell *18*, 668-681.

Zhang, J., Grindley, J. C., Yin, T., Jayasinghe, S., He, X. C., Ross, J. T., Haug, J. S., Rupp, D., Porter-Westpfahl, K. S., Wiedemann, L. M.*, et al.* (2006a). PTEN maintains haematopoietic stem cells and acts in lineage choice and leukaemia prevention. Nature *441*, 518-522.

Zhang, L., Prak, L., Rayon-Estrada, V., Thiru, P., Flygare, J., Lim, B., and Lodish, H. F. (2013). ZFP36L2 is required for self-renewal of early burst-forming unit erythroid progenitors. Nature *499*, 92-96.

Zhang, X. B., Beard, B. C., Beebe, K., Storer, B., Humphries, R. K., and Kiem, H. P. (2006b). Differential effects of HOXB4 on nonhuman primate short- and long-term repopulating cells. PLoS Med *3*, e173.

Zhou, B. O., Yue, R., Murphy, M. M., Peyer, J. G., and Morrison, S. J. (2014). Leptin-receptor-expressing mesenchymal stromal cells represent the main source of bone formed by adult bone marrow. Cell Stem Cell *15*, 154-168.

Zhu, B. T., and Lee, A. J. (2005). NADPH-dependent metabolism of 17beta-estradiol and estrone to polar and nonpolar metabolites by human tissues and cytochrome P450 isoforms. Steroids *70*, 225-244.

Zimdahl, B., Ito, T., Blevins, A., Bajaj, J., Konuma, T., Weeks, J., Koechlein, C. S., Kwon, H. Y., Arami, O., Rizzieri, D*., et al.* (2014). Lis1 regulates asymmetric division in hematopoietic stem cells and in leukemia. Nat Genet *46*, 245-252.